







2013 | Faculteit Wetenschappen



DOCTORAATSPROEFSCHRIFT

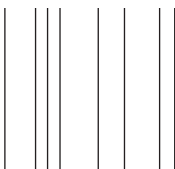


# Optimized Rieke zinc synthetic protocols toward polythiophene copolymers for organic photovoltaic applications

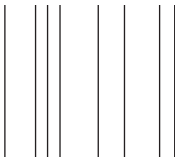
Proefschrift voorgelegd tot het behalen van de graad van doctor in de chemie, te verdedigen door

**Süleyman Kudret**

Promoter: prof. Wouter Maes  
Copromoter: prof. Dirk Vanderzande



D/2013/2451/52





Chairman	Prof. Dr. Karin Coninx, UHasselt
Promoter	Prof. Dr. Wouter Maes, UHasselt
Copromoter	Prof. Dr. Dirk Vanderzande, UHasselt
Members of the Jury	Dr. Laurence Lutsen, IMEC/IMOMECE Prof. Dr. Peter Adriaensens, UHasselt Prof. Dr. Thomas Junkers, UHasselt Prof. Dr. Bruno Van Mele, Vrije Universiteit Brussel Prof. Dr. Laurence Vignau, Institut Polytechnique de Bordeaux



## Table of Contents

<b>Chapter 1. Polythiophenes</b>	<b>1</b>
1.1. Introduction	2
1.2. Unsubstituted polythiophenes	3
1.3. Poly(3-alkylthiophenes)	4
1.4. Regioregular poly(3-alkylthiophenes)	6
1.4.1. The McCullough method	7
1.4.2. The Rieke method	8
1.4.3. The GRIM method	9
1.4.4. The Suzuki and Stille methods	10
1.5. Mechanism of the nickel-catalyzed polymerization	11
1.6. Side-chain functionalized regioregular poly(3-alkylthiophenes)	13
1.7. Polythiophene block copolymers	14
1.8. References	17
<b>Aim and Outline</b>	<b>27</b>
<b>Chapter 2. An efficient and reliable procedure for the preparation of highly reactive Rieke Zinc (Zn*)</b>	<b>31</b>
2.1. Introduction	32
2.2. Results and discussion	34
2.3. Conclusions	43
2.4. Experimental part	44
2.5. Acknowledgements	47
2.6. References	48

2.7. Supporting information	52
-----------------------------	----

<b>Chapter 3. Enhanced intrinsic stability of the bulk heterojunction active layer blend of polymer solar cells by varying the side chain pattern of the polythiophene donor polymer</b>	<b>55</b>
--	-----------

3.1. Introduction	56
3.2. Experimental section	61
3.3. Results and discussion	68
3.3.1. Synthesis and characterization	69
3.3.2. Bulk heterojunction polymer solar cells	77
3.3.3. Accelerated (thermal) ageing	78
3.4. Conclusions	88
3.5. Acknowledgments	89
3.6. References	90
3.7. Supporting information	97

<b>Chapter 4. Facile synthesis of 3-(<math>\omega</math>-acetoxyalkyl)thiophenes and derived copolythiophenes using Rieke zinc</b>	<b>103</b>
--	------------

4.1. Introduction	104
4.2. Results and discussion	106
4.3. Conclusions	117
4.4. Experimental	118
4.5. Acknowledgements	128
4.6. References	129
4.7. Supporting information	135



<b>Chapter 5.      Synthesis of ester side-chain functionalized diblock                          copolythiophenes via the Rieke method</b>	<b>145</b>
5.1. Introduction	146
5.2. Results and discussion	148
5.2.1. Living character of the Rieke polymerization	148
5.2.2. Block copolymer synthesis and characterization	151
5.3. Conclusions	159
5.4. Acknowledgements	159
5.5. Experimental section	160
5.6. References	168
5.7. Supporting information	173
<b>Chapter 6.      Applying the Rieke zinc method to the synthesis of                          alternative poly(hetero)arylenes</b>	<b>181</b>
6.1. Introduction	182
6.2. Results and discussion	183
6.2.1. Polyfluorenes	183
6.2.2. Thieno[3,4- <i>b</i> ]thiophenes	185
6.2.3. Benzo[ <i>b</i> ]thiophenes	188
6.3. Conclusions	190
6.4. Experimental part	191
6.5. References	194
<b>General conclusions</b>	<b>197</b>

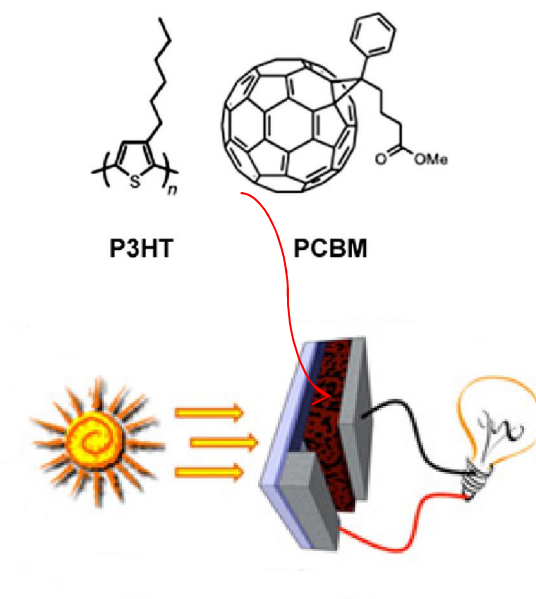
<b>List of publications</b>	<b>201</b>
<b>Acknowledgements</b>	<b>204</b>

---

# Chapter 1

## Polythiophenes

---



### 1.1. Introduction

Harvesting energy directly from sunlight using photovoltaic technology is considered as one of the most important ways to address the global energy needs using renewable resources.<sup>1</sup> For this purpose, organic photovoltaics (OPVs) based on light-harvesting conjugated polymers<sup>2,3</sup> have received considerable attention since the discovery of highly conductive polyacetylene by Shirakawa, MacDiarmid, and Heeger<sup>4</sup> over 30 years ago. Being cost effective and applicable to various flexible light-weight substrates by simple printing techniques,<sup>5-7</sup> polymer solar cells are obviously very attractive. Polythiophenes are the most important and widely studied conjugated polymer materials in organic electronics, especially in OPVs.<sup>8,9</sup> Bulk heterojunction (BHJ) organic solar cells with a polymer:fullerene blend as the active layer have extensively been studied for the benchmark P3HT:PC<sub>61</sub>BM combination.<sup>10-12</sup> Unsubstituted polythiophene is generally prepared via chemical<sup>13,14</sup> or oxidative<sup>15</sup> polymerizations. The material synthesized through these methods, although highly conductive and thermally stable, was only applied to a limited extent due to its insoluble nature. In the late 1980's, polythiophenes bearing flexible alkyl side chains - poly(3-alkylthiophenes) (P3ATs), with the prototype poly(3-hexylthiophene) (P3HT) - were prepared by similar methods.<sup>16-18</sup> However, these methods afford regioirregular P3ATs, which have a sterically twisted polymer backbone that gives rise to a diminished conductivity (along with other important material properties, polycrystallinity etc.). In 1992, the first regioregular (rr) P3ATs were synthesized by McCullough *et al.*,<sup>19</sup> shortly thereafter followed by Rieke.<sup>20</sup> Later on, the McCullough method was modified to a procedure generally depicted as the Grignard metathesis (GRIM) method.<sup>21</sup> All of these procedures give defect-free structurally homogeneous rr-P3ATs with greatly improved

---

electronic properties compared to their regiorandom analogues.<sup>22</sup> In many studies, it was shown that the regioregularity of P3HT has a strong effect on the efficiency of the BHJ solar cells based on this donor polymer.<sup>10,11,23-26</sup> This effect can be related to the enhanced optical absorption and charge transport resulting from the organization of the P3HT chains and domains in a more crystalline structure.<sup>9,27</sup>

The discovery of the synthesis of rr-P3ATs enabled the preparation of a variety of new functionalized polythiophenes.<sup>28,29</sup> On the other hand, the chain-growth mechanism along with the living nature of the polymerization protocols allows the synthesis of block copolymers via sequential addition of different 3-alkylthiophene monomers.<sup>30</sup>

In the paragraphs below, the synthetic protocols toward polythiophenes are summarized, focusing mainly on rr-P3ATs primarily used for electronic applications and block copolymers containing an rr-P3AT segment.

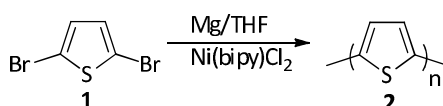
## 1.2. Unsubstituted polythiophenes

The first chemical syntheses of polythiophenes were reported in 1980, several years after the discovery of the first conducting polymer,<sup>4</sup> by the groups of Yamamoto<sup>13</sup> and Dudek<sup>14</sup> employing a metal-catalyzed polycondensation polymerization of 2,5-dibromothiophene (Scheme 1). In the Yamamoto method, 2,5-dibromothiophene (**1**) was treated with Mg in tetrahydrofuran (THF) to yield the mono-Grignard species, which was polymerized in the presence of Ni(bipy)Cl<sub>2</sub>, resulting in low molecular weight polymers.<sup>17</sup> Lin and Dudek<sup>14</sup> obtained the same results using metal acetylacetonate catalysts. An alternative method was introduced by Yoshino *et al.*, in which thiophene was treated with FeCl<sub>3</sub>.<sup>15</sup> A major disadvantage of this oxidative method is that, besides the formation of 2,5-coupled thiophenes, 2,4-coupled thiophenes

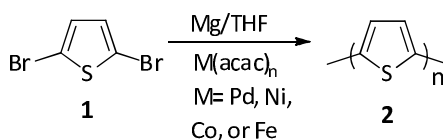
were observed as well, which results in reduced electrooptical properties due to the disturbance of conjugation.

**Scheme 1.** Syntheses of unsubstituted polythiophenes.

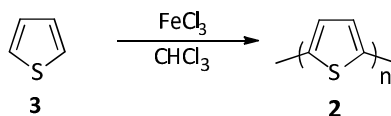
**Yamamoto route**



**Lin/Dudek route**



**Sugimoto/Yoshino Route**



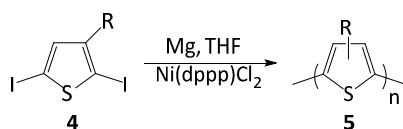
### 1.3. Poly(3-alkylthiophenes)

Starting from the mid 1980's, research toward the synthesis of P3ATs received more attention since the unsubstituted polythiophenes were found barely soluble and hence hardly applicable. Flexible alkyl side chains were introduced on the polymer backbone to enhance the solubility and processability. P3ATs with alkyl side chains longer than 4 carbon atoms are soluble in common organic solvents. At first, the same synthetic protocols as for unsubstituted polythiophene were applied to alkyl-substituted polythiophenes. The first chemical synthesis of environmentally stable and soluble poly(3-alkylthiophenes) (P3ATs) was reported by Elsenbaumer *et al.* using a Kumada-type cross-coupling reaction.<sup>16,31</sup> In this method, a mixture of regioisomeric

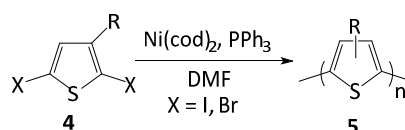
Grignard species was formed first by treating a 2,5-diiodo-3-alkylthiophene (**4**) with one equivalent of Mg in THF (Scheme 2). The polymerization was then performed by addition of a catalytic amount of Ni(dppp)Cl<sub>2</sub> to the Grignard intermediates. Although the molecular weights obtained by this procedure were originally not so high, later reports showed that high molecular weight P3ATs could be obtained in this way.<sup>32</sup> A second method to prepare P3ATs is the dehalogenation polymerization procedure known as the Yamamoto polycondensation, which uses a zero-valent Ni(cod)<sub>2</sub> catalyst (Scheme 2).<sup>17</sup> P3ATs can also be prepared through addition of FeCl<sub>3</sub> as reported by Sugimoto *et al.* (Scheme 2).<sup>18</sup> Materials prepared by this oxidative polymerization show molecular weights ranging from  $M_n = 30$  to 300 kD (PDI = 1.3 to 5).<sup>33,34</sup> Although all of the above methods produce soluble and processable P3ATs, one has to emphasize that in these methods the coupling of the 3-alkylthiophene occurs without strong regiochemical control and consequently structurally irregular polymers are produced.<sup>9,35</sup>

**Scheme 2.** Syntheses of poly(3-alkylthiophenes).

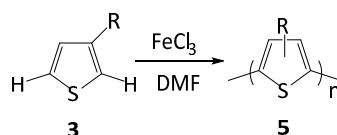
**Elsenbaumer**



**Yamamoto polycondensation**



**Sugimoto-Yoshino oxidative homocoupling**



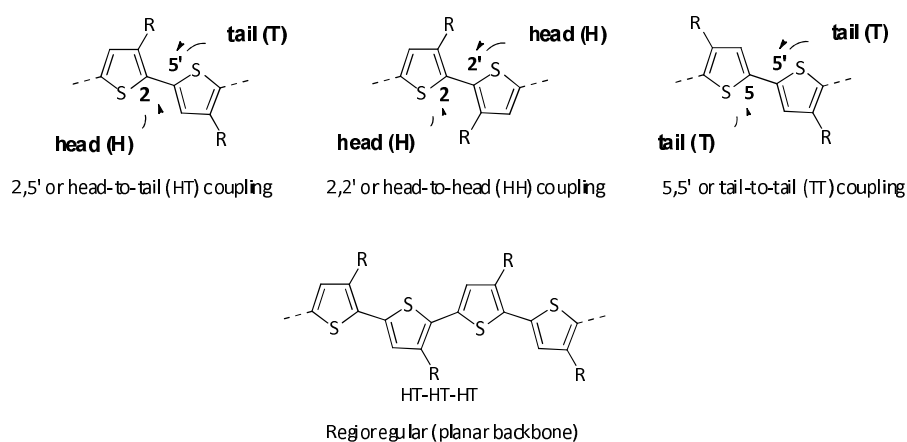
#### 1.4. Regioregular poly(3-alkylthiophenes)

In rr-P3ATs the incorporation of the alkyl substituents can occur in three different orientations due to the non-symmetrical structure of the 3-alkylthiophene monomer: a 2,5' or "head-to-tail" (HT) coupling, a 2,2' or "head-to-head" (HH) coupling, and a 5,5' or "tail-to-tail" (TT) coupling (Figure 1). The HT linkages result in a smaller steric congestion, which leads to a low energy planar conformation and highly conjugated materials, whereas the HH linkages cause steric interactions that diminish the planarity and conductivity of the polymer and result in larger band gaps. Due to the superior optoelectronic properties of the rr-P3ATs, further synthetic investigations were mainly devoted to this class of polymers.<sup>23-26</sup>

Regioregular poly(3-alkylthiophenes) are generally obtained by one out of three procedures, generally known as the McCullough (a Kumada (organomagnesium) coupling protocol),<sup>19</sup> the Rieke (a Negishi (organozinc) protocol),<sup>20</sup> and the GRIM (Grignard metathesis; a modified McCullough protocol)<sup>21</sup> method. These procedures use Ni- or Pd-catalyzed cross-coupling reactions and lead to polymers with comparable features. The Rieke method has the advantage over the other protocols that it tolerates a wider range of functional groups. Stille<sup>36</sup> (organotin) and Suzuki<sup>37</sup> (organoboron) methods were also employed. All of these methods are described below in somewhat more detail.

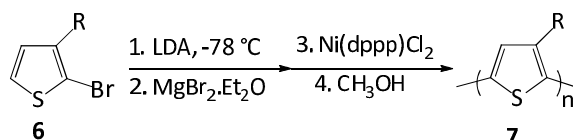


**Figure 1.** Regioisomeric coupling patterns for 3-alkylthiophenes (top) and rr-P3AT (bottom).



#### 1.4.1. The McCullough method

The first chemical synthesis of regioregular poly(3-alkylthiophenes) was reported by McCullough *et al.* in 1992 (Scheme 3).<sup>19</sup> The key step of this method is the regioselective deprotonation of 2-bromo-3-alkylthiophene (**6**) at the 5-position with lithium diisopropylamide (LDA) at  $-78\text{ }^{\circ}\text{C}$  to form the organolithium intermediate, which is stable at this temperature and does not undergo any metal-halogen exchange. This is followed by the addition of  $\text{MgBr}_2 \cdot \text{Et}_2\text{O}$  to the organolithium species to yield a Grignard reagent that remains stable at higher temperatures.<sup>38</sup> The addition of a catalytic amount of  $\text{Ni}(\text{dppp})\text{Cl}_2$  to the latter then affords the regioregular polymer (after quenching with methanol) in 44–66% yield.<sup>22,39</sup> According to NMR studies, the resulting polymers show a regioregularity above 98% and the number average molecular weights ( $M_n$ ) are typically 20–40 kD with polydispersities (PDI) of about 1.4.<sup>39</sup>

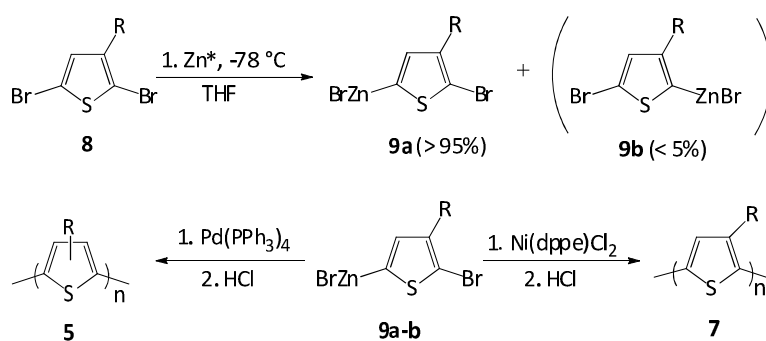
**Scheme 3.** The McCullough method for the synthesis of rr-P3ATs.

#### 1.4.2. The Rieke method

A second synthetic approach for preparing rr-P3ATs, reported soon after the McCullough method, was reported by Chen and Rieke.<sup>20,40</sup> This method differs in terms of the asymmetric organometallic intermediates. In the Rieke protocol, highly reactive Rieke zinc metal powder (Zn\*) undergoes oxidative addition to 2,5-dibromo-3-hexylthiophene (**8**) in a regiospecific manner, giving rise to 2-bromo-5-(bromozincio)-3-hexylthiophene (**9a**) as the major and 2-(bromozincio)-5-bromo-3-hexylthiophene (**9b**) as the minor regioisomer (Scheme 4).<sup>41,42</sup> The ratio between these two isomers is strongly affected by the reaction temperature; the lower the temperature, the more regioselective the oxidative addition of the Zn\* metal to the organic halide. Polymerization is performed by addition of a cross-coupling catalyst, either Ni(dppe)Cl<sub>2</sub> or Pd(PPh<sub>3</sub>)<sub>4</sub>. The regioregularity of the resulting polymer strongly depends upon the type of catalyst. Addition of Ni(dppe)Cl<sub>2</sub> yields regioregular poly(3-hexylthiophene), whereas addition of Pd(PPh<sub>3</sub>)<sub>4</sub> leads to formation of completely regiorandom poly(3-hexylthiophene).<sup>20,40</sup> The stereoregularity control is due to steric congestion during the transmetallation step and is related to both the metal (Ni vs Pd) and the ligands.<sup>20</sup> An alternative approach is the use of 2-bromo-3-alkyl-5-iodothiophene, which will react with Zn\* at room temperature to afford only 2-bromo-3-alkyl-5-(iodozincio)thiophene, thus eliminating the need for cryogenic temperature,<sup>43</sup> after precipitation and

soxhlet purification, the typical yield of a Rieke polymerization is 70–80%<sup>42,44</sup> and molecular weights are typically around  $M_n = 23\text{--}25\text{k}$  with  $\text{PDI} = 1.4\text{--}1.6$ .<sup>41,42</sup> As a major advantage, the Rieke method affords a functional group tolerant synthesis due to the usage of Rieke zinc, which is not reactive toward a variety of functional groups not compatible with Grignard reagents.<sup>45</sup>

**Scheme 4.** The Rieke method for regioregular polythiophenes.

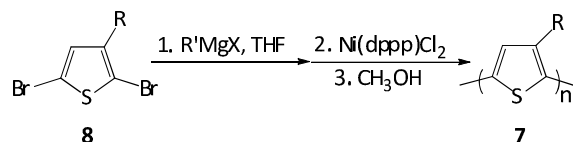


### 1.4.3. The GRIM method

In 1999, another method, nowadays generally known as the Grignard metathesis (GRIM) method, was reported, making modifications to the traditional McCullough method (Scheme 5).<sup>21</sup> This improved procedure eliminated the use of cryogenic temperatures and it enabled an easy and fast preparation of regioregular poly(3-alkylthiophenes) with high molecular weights. The GRIM method is based on treatment of 2,5-dibromo-3-alkylthiophene (**8**) with 1 equivalent of a Grignard reagent, which leads to the formation of a mixture of regioisomeric organomagnesium intermediates in a ratio of 85:15 to 75:25.<sup>46</sup> The ratio of these two regioisomers is independent of the reaction time, temperature and Grignard reagent used. In the final step, addition of catalytic amount of  $\text{Ni}(\text{dppp})\text{Cl}_2$  affords almost entirely regioregular (>99%) P3AT (catalyst dependent as for the Rieke method).<sup>46-48</sup>

The molecular weights of the polymers prepared via the original procedure were between 20–35 kD ( $M_n$ ) with low polydispersities (PDI = 1.2–1.4).<sup>21</sup>

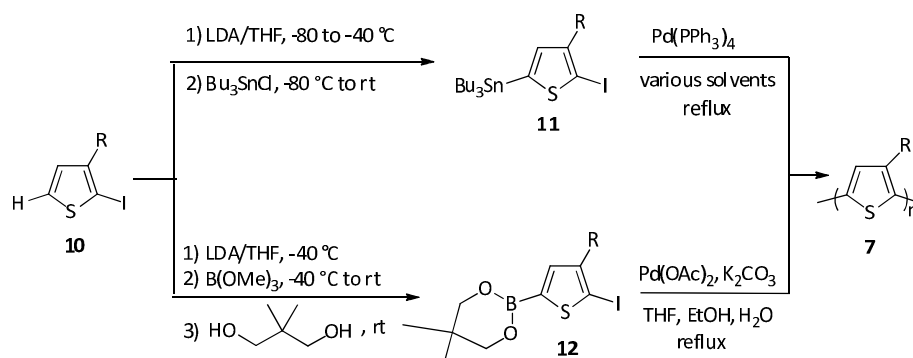
**Scheme 5.** Synthesis of regioregular poly(3-alkylthiophenes) via the GRIM method.



#### 1.4.4. The Suzuki and Stille methods

Other alternative methods employed to synthesize regioregular poly(3-alkylthiophenes) are Stille<sup>36</sup> and Suzuki<sup>37</sup> cross-coupling reactions (Scheme 6). The Pd-catalyzed cross-coupling of 3-hexyl-2-iodo-5-(tri-*n*-butylstannyl)thiophene (**11**) was studied by Iraqi *et al.* utilizing different solvents and catalysts.<sup>49</sup> The obtained polymers, regardless of the reaction conditions, had a regioregularity above 96% and average molecular weights ( $M_n = 10$ –16 kD with PDI = 1.2–1.4 after purification). The Stille method was also employed by McCullough and co-workers to prepare regioregular oxazoline-substituted polythiophene ( $M_n = 8$  kD, PDI = 1.2), which was later on converted to a water-soluble carboxylic acid derivative by a post-polymerization hydrolysis reaction.<sup>50</sup> The alternative Suzuki polycondensation reaction employing 3-octyl-2-iodo-5-boronatothiophene (**12**) yielded 96% regioregular P3AT with low molecular weight ( $M_w = 2.7$  kD, PDI = 1.5).<sup>51</sup> Although these methods afford more air and moisture stable intermediates, the preparation of the organometallic species **11** and **12** nevertheless requires cryogenic conditions. Furthermore, the organometallic stannyl and boronate derivatives have to be isolated and purified before the polymerization can proceed.

**Scheme 6.** Syntheses of rr-P3ATs by Stille (top) and Suzuki (bottom) cross-coupling reactions.



### 1.5. Mechanism of the nickel-catalyzed polymerization

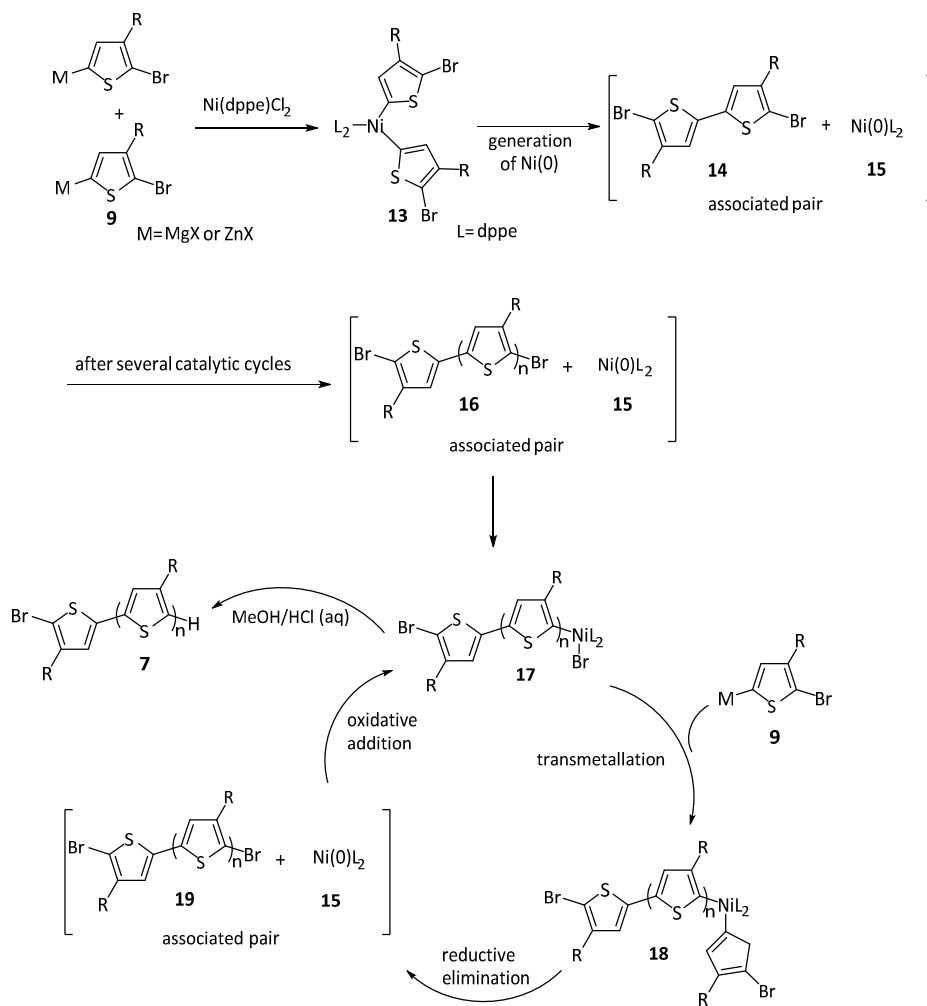
The synthetic methods toward rr-P3ATs are transition metal (Pd/Ni) catalyzed cross-coupling reactions, proceeding via a catalytic cycle of three sequential steps, i.e. oxidative addition, transmetalation, and reductive elimination.<sup>17,52</sup>

The polymerization follows a chain-growth mechanism as outlined in Scheme 7 for the Ni-initiated cross-coupling polymerization. The first step in the proposed mechanism is the formation of the organonickel compound **13** via reaction of 2 equivalents of an organometallic intermediate **9**, formed either by the Grignard or Rieke route, with  $\text{Ni}(\text{dppe})\text{Cl}_2$ . The “associated pair” of 2,2'-dibromo-3,3'-dialkyl-5,5'-bithiophene (**14**) (TT coupling) and  $\text{Ni}(0)$  is immediately formed upon reductive elimination. This formed dimer **14** undergoes fast oxidative addition to the  $\text{Ni}(0)$  species, giving rise to a new organonickel complex, which then adds a new monomer via transmetalation and subsequent reductive elimination. After several catalytic cycles, associated pairs of a polymer with  $n$  repeating units and the  $\text{Ni}(0)$  species are formed. As the nickel-catalyzed cross-coupling polymerization is a chain-

## Chapter 1

growth system, further growth of the polymer takes place by sequential insertion of monomer, as illustrated in the reaction cycle (**17-18-19-17**) (Scheme 7).<sup>30</sup> *rr*-P3ATs with a well-defined structure are obtained. After quenching the nickel-terminated *rr*-P3AT **17** with MeOH/HCl, the polymer chains have H/Br end groups.

**Scheme 7.** The chain-growth mechanism of the nickel-initiated cross-coupling polymerization.



---

### 1.6. Side-chain functionalized regioregular poly(3-alkylthiophenes)

Although the main idea of introducing alkyl side chains on the polythiophene backbone was to enhance polymer solubility, it has been realized later on that the side chains can also dramatically alter the optical and electrical properties of the polymers, especially when decorated with functional groups. *rr*-P3ATs functionalized with a heteroatom adjacent to the thiophene ring (O/S, i.e. alkoxy or alkylthio groups) show a decreased band gap by elevation of their highest occupied molecular orbital (HOMO) level, resulting in lower oxidation potentials and a more stable conducting state of the polymers. *rr*-P3ATs with pendant alkoxy groups were mainly synthesized through McCullough and GRIM polymerization protocols,<sup>27,53,54</sup> whereas alkylthio-functionalized *rr*-P3ATs were also obtained via the Rieke method.<sup>55</sup> *rr*-P3ATs bearing ester functional groups were prepared by the GRIM method as well.<sup>56-59</sup> The polymers showed a wider band gap, likely related to the electron withdrawing character of the carbonyl functionality. Fluoroalkyl<sup>60,61</sup> and chirally<sup>62-64</sup> substituted *rr*-P3ATs were also synthesized using McCullough, GRIM, or Rieke methods.

Functionalized *rr*-P3ATs can also be prepared by changing the terminal functional groups at the end of the alkyl side chains employing post-polymerization functionalization procedures, which is desirable with regard to tuning of the polymer properties. In many cases, the functional moieties at the end of the side chains are susceptible to react under the applied polymerization conditions. To alleviate such problems, protective groups have to be used. Tetrahydropyranyl-,<sup>65,66</sup> trimethylsilyl-,<sup>67</sup> and *tert*-butyldimethylsilyl-protected<sup>68</sup> *rr*-P3ATs were synthesized via McCullough and GRIM synthetic methods. In 2003, Stokes *et al.* reported the synthesis of *rr*-P3ATs bearing a phosphonic ester group by the Stille method.<sup>69</sup> Deprotection

of the ester gave rise to phosphonic acid functional groups. Recently, two other groups have also synthesized phosphonic ester-functionalized rr-P3ATs employing the Rieke method.<sup>70,71</sup> Within our own group, we have also used the Rieke polymerization protocol to prepare ester-functionalized rr-P3AT (co)polymers.<sup>72-75</sup> The ester moieties were subsequently hydrolyzed to hydroxyl groups and converted to photo-crosslinkable cinnamoyl entities. Some of the copolymers were applied as donor materials in BHJ organic solar cells and they were shown to improve the lifetime of the devices.<sup>28,76</sup>

In another approach, “reactive” functional groups, stable under the polymerization conditions, are introduced at the end of the alkyl side chains. rr-P3AT bearing (methylsulfanyl)hexyl side chains was synthesized by Lanzi *et al.* through the GRIM method.<sup>77</sup> The methylsulfanyl moieties were further converted to methylsulfinyl units. The most popular functionalized rr-P3ATs of this kind have a bromoalkyl reactive group. Iraqi and co-workers used the McCullough method and then substituted the bromine groups to carboxyanthraquinones.<sup>49</sup> The GRIM method was also utilized to prepare bromohexyl-functionalized rr-P3AT and the pendant groups were subsequently converted to different groups such as carboxylic acids, amines, thiols,<sup>29</sup> or cross-linkable vinyl moieties.<sup>78</sup> Finally, bromo- and chlorohexyl-substituted rr-P3ATs were also achieved via the Rieke method.<sup>71</sup>

### **1.7. Polythiophene block copolymers**

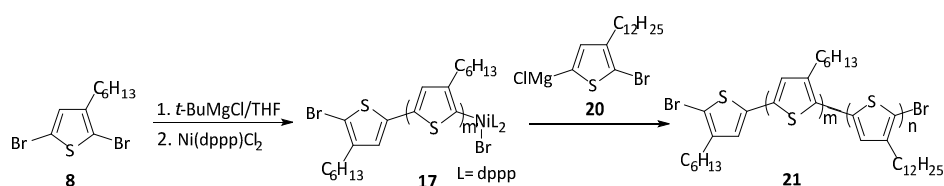
Block copolythiophenes have already been shown to allow control over the blend morphology of polymer-fullerene BHJ organic solar cells.<sup>79-82</sup> Since they incorporate different  $\pi$ -segments in a well-defined conjugated polymer structure, and each segment has different optical and electrical characteristics, block copolythiophenes are capable to self-assemble into



nanostructured morphologies with unique properties.<sup>83,84</sup> The synthetic methods used to synthesize P3AT homopolymers, namely the McCullough, GRIM, and Rieke protocols, are transition metal (Ni or Pd) catalyzed cross-coupling reactions (*vide supra*).<sup>17,52</sup> The catalytic reaction has been extensively studied and found to be affected by the ligand structure and the metal employed.<sup>20,40,46-48,85</sup> On the other hand, further studies revealed that this polymerization proceeds via a chain-growth mechanism and has a “living” character.<sup>30,86</sup> The living nature of the synthetic methodology opened up the possibility to prepare block copolythiophenes with well-defined molecular weights and narrow polydispersities through sequential addition of differently substituted thiophene monomers.

The first rr-P3AT block copolymer was synthesized by Iovu *et al.* (Scheme 8).<sup>30</sup> In this study, sequential addition of 2,5-dibromo-3-hexylthiophene (**8**) and 2,5-dibromo-3-dodecylthiophene (**20**) led to the formation of a diblock copolymer with  $M_n = 24$  kD. The polydispersity (PDI = 1.4) was slightly higher with regard to the homopolymer (PDI = 1.2), which was attributed to the formation of dead or inactive chains during the chain elongation process.

**Scheme 8.** Synthesis of poly(3-hexylthiophene)-*block*-poly(3-dodecylthiophene) (P3HT-*b*-P3DDT) by chain extension through sequential monomer addition.<sup>30</sup>



A diblock copolymer consisting of a hydrophobic 3-hexylthiophene and a hydrophilic 3-[2-(2-methoxyethoxy)ethoxy]methylthiophene segment was synthesized by a similar procedure as well.<sup>87</sup> Afterwards, using the same

## Chapter 1

---

methodology, a large number of rr-P3AT block copolythiophenes were synthesized and their microphase separation<sup>53,83,84,88-91</sup> along with their photovoltaic applications<sup>59,61,88,92-95</sup> were studied.

---

**1.8. References**

1. Irimia-Vladu, M.; Głowacki, E. D.; Voss, G.; Bauer, S.; Sariciftci, N. S. *Materials Today* **2012**, *15* (7–8), 340-346.
2. Günes, S.; Neugebauer, H.; Sariciftci, N. S. *Chemical Reviews* **2007**, *107* (4), 1324-1338.
3. Friend, R. H. *Pure Appl. Chem.* **2001**, *73* (3), 425-430.
4. Shirakawa, H.; Louis, E. J.; MacDiarmid, A. G.; Chiang, C. K.; Heeger, A. J. *Journal of the Chemical Society, Chemical Communications* **1977**, *0* (16), 578-580.
5. Krebs, F. C. *Solar Energy Materials and Solar Cells* **2009**, *93* (4), 394-412.
6. Alstrup, J.; Jørgensen, M.; Medford, A. J.; Krebs, F. C. *ACS Applied Materials & Interfaces* **2010**, *2* (10), 2819-2827.
7. Søndergaard, R. R.; Hösel, M.; Krebs, F. C. *Journal of Polymer Science Part B: Polymer Physics* **2013**, *51* (1), 16-34.
8. Roncali, J. *Chemical Reviews* **1992**, *92* (4), 711-738.
9. Osaka, I.; McCullough, R. D. *Accounts of Chemical Research* **2008**, *41* (9), 1202-1214.
10. Dang, M. T.; Hirsch, L.; Wantz, G. *Advanced Materials* **2011**, *23* (31), 3597-3602.
11. Marrocchi, A.; Lanari, D.; Facchetti, A.; Vaccaro, L. *Energy & Environmental Science* **2012**, *5*, 8457-8474.
12. Gadisa, A.; Oosterbaan, W. D.; Vandewal, K.; Bolsée, J.-C.; Bertho, S.; D'Haen, J.; Lutsen, L.; Vanderzande, D.; Manca, J. V. *Advanced Functional Materials* **2009**, *19* (20), 3300-3306.
13. Yamamoto, T.; Sanechika, K.; Yamamoto, A. *Journal of Polymer Science: Polymer Letters Edition* **1980**, *18* (1), 9-12.

## Chapter 1

---

14. Lin, J. W. P.; Dudek, L. P. *Journal of Polymer Science: Polymer Chemistry Edition* **1980**, *18* (9), 2869-2873.
15. Yoshino, K.; Hayashi, S.; Sugimoto, R.-I. *Japanese Journal of Applied Physics* **1984**, *23* (12), L899.
16. Elsenbaumer, R. L.; Jen, K. Y.; Oboodi, R. *Synthetic Metals* **1986**, *15* (2-3), 169-174.
17. Yamamoto, T.; Morita, A.; Miyazaki, Y.; Maruyama, T.; Wakayama, H.; Zhou, Z. H.; Nakamura, Y.; Kanbara, T.; Sasaki, S.; Kubota, K. *Macromolecules* **1992**, *25* (4), 1214-1223.
18. Sugimoto, R.; Takeda, S.; Gu, H. B.; Yoshino, K., *Chemistry Express* **1986**, *1*, 635.
19. McCullough, R. D.; Lowe, R. D. *Journal of the Chemical Society, Chemical Communications* **1992**, (1), 70-72.
20. Chen, T. A.; Rieke, R. D. *Journal of the American Chemical Society* **1992**, *114* (25), 10087-10088.
21. Loewe, R. S.; Khersonsky, S. M.; McCullough, R. D. *Advanced Materials* **1999**, *11* (3), 250-253.
22. McCullough, R. D.; Lowe, R. D.; Jayaraman, M.; Ewbank, P. C.; Anderson, D. L.; Tristram-Nagle, S. *Synthetic Metals* **1993**, *55* (2-3), 1198-1203.
23. Kim, Y.; Cook, S.; Tuladhar, S. M.; Choulis, S. A.; Nelson, J.; Durrant, J. R.; Bradley, D. D. C.; Giles, M.; McCulloch, I.; Ha, C.-S.; Ree, M. *Natur Materials* **2006**, *5* (3), 197-203.
24. Urien, M.; Bailly, L.; Vignau, L.; Cloutet, E.; de Cuendias, A.; Wantz, G.; Cramail, H.; Hirsch, L.; Parneix, J.-P. *Polymer International* **2008**, *57* (5), 764-769.

- 
25. Woo, C. H.; Thompson, B. C.; Kim, B. J.; Toney, M. F.; Fréchet, J. M. J. *Journal of the American Chemical Society* **2008**, *130* (48), 16324-16329.
26. Mauer, R.; Kastler, M.; Laquai, F. *Advanced Functional Materials* **2010**, *20* (13), 2085-2092.
27. McCullough, R. D.; Tristram-Nagle, S.; Williams, S. P.; Lowe, R. D.; Jayaraman, M. *Journal of the American Chemical Society* **1993**, *115* (11), 4910-4911.
28. Campo, B. J.; Bevk, D.; Kesters, J.; Gilot, J.; Bolink, H. J.; Zhao, J.; Bolsée, J.-C.; Oosterbaan, W. D.; Bertho, S.; D'Haen, J.; Manca, J.; Lutsen, L.; Van Assche, G.; Maes, W.; Janssen, R. A. J.; Vanderzande, D. *Organic Electronics* **2013**, *14* (2), 523-534.
29. Zhai, L.; Pilston, R. L.; Zaiger, K. L.; Stokes, K. K.; McCullough, R. D. *Macromolecules* **2002**, *36* (1), 61-64.
30. Iovu, M. C.; Sheina, E. E.; Gil, R. R.; McCullough, R. D. *Macromolecules* **2005**, *38* (21), 8649-8656.
31. Tamao, K.; Sumitani, K.; Kumada, M. *Journal of the American Chemical Society* **1972**, *94* (12), 4374-4376.
32. Chen, S. A.; Tsai, C. C. *Macromolecules* **1993**, *26* (9), 2234-2239.
33. Leclerc, M.; Diaz, F. M.; Wegner, G. *Die Makromolekulare Chemie* **1989**, *190* (12), 3105-3116.
34. Pomerantz, M.; Tseng, J. J.; Zhu, H.; Sproull, S. J.; Reynolds, J. R.; Uitz, R.; Arnott, H. J.; Haider, M. I. *Synthetic Metals* **1991**, *41* (3), 825-830.
35. McCullough, R. D. *Advanced Materials* **1998**, *10* (2), 93-116.
36. Stille, J. K. *Angewandte Chemie International Edition in English* **1986**, *25* (6), 508-524.
37. Suzuki, A. *Journal of Organometallic Chemistry* **1999**, *576* (1-2), 147-168.
-

## Chapter 1

---

38. McCullough, R. D.; Lowe, R. D.; Jayaraman, M.; Anderson, D. L. *The Journal of Organic Chemistry* **1993**, *58* (4), 904-912.
39. McCullough, R. D.; Williams, S. P.; Tristam-Nagle, S.; Jayaraman, M.; Ewbank, P. C.; Miller, L. *Synthetic Metals* **1995**, *69* (1-3), 279-282.
40. Chen, T. A.; O'Brien, R. A.; Rieke, R. D. *Macromolecules* **1993**, *26* (13), 3462-3463.
41. Chen, T.-A.; Wu, X.; Rieke, R. D. *Journal of the American Chemical Society* **1995**, *117* (1), 233-244.
42. Kudret, S.; D'Haen, J.; Oosterbaan, W.; Lutsen, L.; Vanderzande, D.; Maes, W. *Advanced Synthesis & Catalysis* **2013**, *355* (2-3), 569-575.
43. Kim, J.-G.; Kim, S.-H.; Rieke, R. *Macromolecular Research* **2011**, *19* (7), 749-752.
44. Wu, X.; Chen, T.-A.; Rieke, R. D. *Macromolecules* **1995**, *28* (6), 2101-2102.
45. Zhu, L.; Wehmeyer, R. M.; Rieke, R. D. *The Journal of Organic Chemistry* **1991**, *56* (4), 1445-1453.
46. Loewe, R. S.; Ewbank, P. C.; Liu, J.; Zhai, L.; McCullough, R. D. *Macromolecules* **2001**, *34* (13), 4324-4333.
47. Bolognesi, A.; Porzio, W.; Bajo, G.; Zannoni, G.; Fannig, L. *Acta Polymerica* **1999**, *50* (4), 151-155.
48. Mao, Y.; Wang, Y.; Lucht, B. L. *Journal of Polymer Science Part A: Polymer Chemistry* **2004**, *42* (21), 5538-5547.
49. Iraqi, A.; W. Barker, G. *Journal of Materials Chemistry* **1998**, *8* (1), 25-29.
50. McCullough, R. D.; Ewbank, P. C.; Loewe, R. S. *Journal of the American Chemical Society* **1997**, *119* (3), 633-634.
51. Guillerez, S.; Bidan, G. *Synthetic Metals* **1998**, *93* (2), 123-126.

- 
52. Negishi, E.; Takahashi, T.; Baba, S.; Van Horn, D. E.; Okukado, N. *Journal of the American Chemical Society* **1987**, *109* (8), 2393-2401.
53. Sheina, E. E.; Khersonsky, S. M.; Jones, E. G.; McCullough, R. D. *Chemistry of Materials* **2005**, *17* (13), 3317-3319.
54. Van den Bergh, K.; De Winter, J.; Gerbaux, P.; Verbiest, T.; Koeckelberghs, G. *Macromolecular Chemistry and Physics* **2011**, *212* (4), 328-335.
55. Wu, X.; Chen, T.-A.; Rieke, R. D. *Macromolecules* **1996**, *29* (24), 7671-7677.
56. Amarasekara, A. S.; Pomerantz, M. *Synthesis* **2003**, *2003* (14), 2255-2258.
57. Vallat, P.; Lamps, J. P.; Schosseler, F.; Rawiso, M.; Catala, J. M. *Macromolecules* **2007**, *40* (7), 2600-2602.
58. Ho, C.-C.; Liu, Y.-C.; Lin, S.-H.; Su, W.-F. *Macromolecules* **2011**, *45* (2), 813-820.
59. Suspene, C.; Miozzo, L.; Choi, J.; Gironda, R.; Geffroy, B.; Tondelier, D.; Bonnassieux, Y.; Horowitz, G.; Yassar, A. *Journal of Materials Chemistry* **2012**, *22* (10), 4511-4518.
60. Hong, X. M.; Collard, D. M. *Macromolecules* **2000**, *33* (19), 6916-6917.
61. Yamada, I.; Takagi, K.; Hayashi, Y.; Soga, T.; Shibata, N.; Toru, T. *International Journal of Molecular Sciences* **2010**, *11* (12), 5027-5039.
62. Goto, H.; Okamoto, Y.; Yashima, E. *Macromolecules* **2002**, *35* (12), 4590-4601.
63. Saito, F.; Takeoka, Y.; Rikukawa, M.; Sanui, K. *Synthetic Metals* **2005**, *153* (1-3), 125-128.
-

## Chapter 1

---

64. Bouman, M. M.; Havinga, E. E.; Janssen, R. A. J.; Meijer, E. W. *Molecular Crystals and Liquid Crystals Science and Technology. Section A. Molecular Crystals and Liquid Crystals* **1994**, *256* (1), 439-448.
65. Murray, K. A.; Holmes, A. B.; Moratti, S. C.; Rumbles, G. *Journal of Materials Chemistry* **1999**, *9* (9), 2109-2116.
66. Yu, J.; Holdcroft, S. *Macromolecules* **2000**, *33* (14), 5073-5079.
67. Lanzi, M.; Costa-Bizzarri, P.; Della-Casa, C.; Paganin, L.; Fraleoni, A. *Polymer* **2003**, *44* (3), 535-545.
68. Nam, C.-Y.; Qin, Y.; Park, Y. S.; Hlaing, H.; Lu, X.; Ocko, B. M.; Black, C. T.; Grubbs, R. B. *Macromolecules* **2012**, *45* (5), 2338-2347.
69. Stokes, K. K.; Heuzé, K.; McCullough, R. D. *Macromolecules* **2003**, *36* (19), 7114-7118.
70. Katagiri, M., *Advanced Materials Research* **2011**, *409*, 502-507.
71. Rieke, R. D.; Kim, S-H. *Bull. Korean Chem. Soc.* **2012**, *33* (6), 1-4.
72. Andreasen, B.; Tanenbaum, D. M.; Hermenau, M.; Voroshazi, E.; Lloyd, M. T.; Galagan, Y.; Zimmermann, B.; Kudret, S.; Maes, W.; Lutsen, L.; Vanderzande, D.; Wurfel, U.; Andriessen, R.; Rösch, R.; Hoppe, H.; Teran-Escobar, G.; Lira-Cantu, M.; Rivaton, A.; Uzunoglu, G. Y.; Germack, D. S.; Hosel, M.; Dam, H. F.; Jorgensen, M.; Gevorgyan, S. A.; Madsen, M. V.; Bundgaard, E.; Krebs, F. C.; Norrman, K. *Physical Chemistry Chemical Physics* **2012**, *14* (33), 11780-11799.
73. Rösch, R.; Tanenbaum, D. M.; Jorgensen, M.; Seeland, M.; Barenklau, M.; Hermenau, M.; Voroshazi, E.; Lloyd, M. T.; Galagan, Y.; Zimmermann, B.; Wurfel, U.; Hosel, M.; Dam, H. F.; Gevorgyan, S. A.; Kudret, S.; Maes, W.; Lutsen, L.; Vanderzande, D.; Andriessen, R.; Teran-Escobar, G.; Lira-Cantu, M.; Rivaton, A.; Uzunoglu, G. Y.; Germack, D.; Andreasen, B.; Madsen, M. V.;



---

Norrman, K.; Hoppe, H.; Krebs, F. C. *Energy & Environmental Science* **2012**, *5* (4), 6521-6540.

74. Tanenbaum, D. M.; Hermenau, M.; Voroshazi, E.; Lloyd, M. T.; Galagan, Y.; Zimmermann, B.; Hosel, M.; Dam, H. F.; Jorgensen, M.; Gevorgyan, S. A.; Kudret, S.; Maes, W.; Lutsen, L.; Vanderzande, D.; Wurfel, U.; Andriessen, R.; Rösch, R.; Hoppe, H.; Teran-Escobar, G.; Lira-Cantu, M.; Rivaton, A.; Uzunoglu, G. Y.; Germack, D.; Andreasen, B.; Madsen, M. V.; Norrman, K.; Krebs, F. C. *RSC Advances* **2012**, *2* (3), 882-893.

75. Teran-Escobar, G.; Tanenbaum, D. M.; Voroshazi, E.; Hermenau, M.; Norrman, K.; Lloyd, M. T.; Galagan, Y.; Zimmermann, B.; Hosel, M.; Dam, H. F.; Jorgensen, M.; Gevorgyan, S.; Kudret, S.; Maes, W.; Lutsen, L.; Vanderzande, D.; Wurfel, U.; Andriessen, R.; Rösch, R.; Hoppe, H.; Rivaton, A.; Uzunoglu, G. Y.; Germack, D.; Andreasen, B.; Madsen, M. V.; Bundgaard, E.; Krebs, F. C.; Lira-Cantu, M. *Physical Chemistry Chemical Physics* **2012**, *14* (33), 11824-11845.

76. Bertho, S.; Campo, B.; Piersimoni, F.; Spoltore, D.; D'Haen, J.; Lutsen, L.; Maes, W.; Vanderzande, D.; Manca, J. *Solar Energy Materials and Solar Cells* **2013**, *110* (0), 69-76.

77. Lanzi, M.; Paganin, L. *Reactive and Functional Polymers* **2010**, *70* (6), 346-360.

78. Miyanishi, S.; Tajima, K.; Hashimoto, K. *Macromolecules* **2009**, *42* (5), 1610-1618.

79. de Cuendias, A.; Hiorns, R. C.; Cloutet, E.; Vignau, L.; Cramail, H. *Polymer International* **2010**, *59* (11), 1452-1476.

80. Higashihara, T.; Ohshimizu, K.; Ryo, Y.; Sakurai, T.; Takahashi, A.; Nojima, S.; Ree, M.; Ueda, M. *Polymer* **2011**, *52* (17), 3687-3695.

## Chapter 1

---

81. Lin, Y.-H.; Smith, K. A.; Kempf, C. N.; Verduzco, R. *Polymer Chemistry* **2013**, *4*, 229-232.
82. Darling, S. B. *Energy & Environmental Science* **2009**, *2* (12), 1266-1273.
83. Zhang, Y.; Tajima, K.; Hirota, K.; Hashimoto, K. *Journal of the American Chemical Society* **2008**, *130* (25), 7812-7813.
84. Wu, P.-T.; Ren, G.; Li, C.; Mezzenga, R.; Jenekhe, S. A. *Macromolecules* **2009**, *42* (7), 2317-2320.
85. Verswyvel, M.; Verstappen, P.; De Cremer, L.; Verbiest, T.; Koeckelberghs, G. *Journal of Polymer Science Part A: Polymer Chemistry* **2011**, *49* (24), 5339-5349.
86. Yokoyama, A.; Miyakoshi, R.; Yokozawa, T. *Macromolecules* **2004**, *37* (4), 1169-1171.
87. Yokozawa, T.; Adachi, I.; Miyakoshi, R.; Yokoyama, A. *High Performance Polymers* **2007**, *19* (5-6), 684-699.
88. Wu, P.-T.; Ren, G.; Kim, F. S.; Li, C.; Mezzenga, R.; Jenekhe, S. A. *Journal of Polymer Science Part A: Polymer Chemistry* **2010**, *48* (3), 614-626.
89. Ohshimizu, K.; Ueda, M. *Macromolecules* **2008**, *41* (14), 5289-5294.
90. Lee, E.; Hammer, B.; Kim, J.-K.; Page, Z.; Emrick, T.; Hayward, R. C. *Journal of the American Chemical Society* **2011**, *133* (27), 10390-10393.
91. Hollinger, J.; DiCarmine, P. M.; Karl, D.; Seferos, D. S. *Macromolecules* **2012**, *45* (9), 3772-3778.
92. Chueh, C.-C.; Higashihara, T.; Tsai, J.-H.; Ueda, M.; Chen, W.-C. *Organic Electronics* **2009**, *10* (8), 1541-1548.
93. Lai, Y.-C.; Ohshimizu, K.; Lee, W.-Y.; Hsu, J.-C.; Higashihara, T.; Ueda, M.; Chen, W.-C. *Journal of Materials Chemistry* **2011**, *21* (38), 14502-14508.
94. Lin, Y.; Lim, J. A.; Wei, Q.; Mannsfeld, S. C. B.; Briseno, A. L.; Watkins, J. *Chemistry of Materials* **2012**, *24* (3), 622-632.

95. Ouhib, F.; Tomassetti, M.; Manca, J.; Piersimoni, F.; Spoltore, D.; Bertho, S.; Moons, H.; Lazzaroni, R.; Desbief, S.; Jerome, C.; Detrembleur, C. *Macromolecules* **2013**, *46* (3), 785-795.



### Aim and Outline

The rapid progress in the area of solution-processable organic photovoltaics requires constant development of new advanced light-harvesting materials, either small molecules or polymers, with defined properties. There are many synthetic methods for the preparation of conjugated polymers. The Rieke zinc protocol is one of these methods, which tolerates a wide range of functional groups (e.g esters, acids, etc.) in the side chains of the polymers. However, due to problems in the (reproducible) preparation of the active Rieke zinc (Zn\*) metal, giving rise to large batch to batch variations, its use has been limited. Only a few groups have actually used the method for a limited variation of semiconducting materials, mostly (co)polythiophenes. Therefore, the aim of this thesis was to render the preparation of the Rieke zinc (Zn\*) more reproducible and to optimize the Rieke protocol toward both small molecule precursors and side-chain functionalized block and random copolythiophenes. These copolymers could then be applied in bulk heterojunction organic solar cells to study the effects of side-chain functionalization on photovoltaic performance, and more in particular the donor-acceptor blend morphology and its evolution over time under thermal stress.

After a general **Introduction** on polythiophenes and the synthetic methods to obtain them, **Chapter 2** is dealing with the optimization of the preparation of the highly reactive Rieke zinc metal powder, the key reagent in the Rieke synthetic protocol. Commercially available naphthalene is analyzed by inductively coupled plasma-mass spectrometry (ICP-MS), high performance liquid chromatography (HPLC) coupled to a fluorescence detector and gas chromatography-mass spectrometry (GC-MS) to identify benzothiophene as

an important 'additive' leading to a more reliable preparation method. The optimized synthetic method – in which benzothiophene is deliberately added to the lithium naphthalenide solution used for the reduction of zinc chloride – is explained in detail and the newly prepared Rieke zinc is tested in the preparation of the well-known P3HT.

In **Chapter 3** ester side chain functionalized regioregular random copolythiophenes are prepared by the Rieke zinc protocol with varying percentages of functionalized side chains. Postpolymerization functionalization methods are utilized to further derivatize the resulting polymers. All materials are fully characterized by size exclusion chromatography (SEC), nuclear magnetic resonance (NMR), cyclic voltammetry (CV), UV-Vis absorption spectroscopy, thermogravimetric analysis (TGA) and differential scanning calorimetry (DSC). Bulk heterojunction organic solar cells are prepared by blending the copolymers with PCBM and accelerated life time measurements are done to study the impact of functionalization on the morphological stability of the active layer of the devices over time.

**Chapter 4** describes the preparation of a series of ester side chain functionalized 3-alkyl-2,5-dibromothiophenes and the random copolythiophenes made from these monomers by employing the optimized Rieke zinc synthetic protocol. The synthesized copolymers are again characterized by a combination of chromatographic, spectroscopic and thermal analysis techniques. Solar cells were made from all novel materials and the resulting power conversion efficiencies are in the same range as the parent P3HT:PC<sub>60</sub>BM.

In **Chapter 5** the synthesis of ester functionalized diblock copolythiophenes via the Rieke method is presented. The living nature of the Rieke polymerization

protocol is confirmed by end-capping the polymer with dimethylphenyl groups. Block copolymer formation is achieved by sequential addition of different organozinc monomers and confirmed by SEC, NMR and thermal analysis (via rapid heat-cool calorimetry, RHC).

Finally, **Chapter 6** explores the possibilities to extend the applicability of the Rieke polymerization protocol – with the advantages of short reaction times, low temperatures and compatibility with various functional groups compared to other polymerization methods (e.g Suzuki, Yamamoto, Stille) – toward alternative poly(hetero)arylenes. Studies conducted on the synthesis of polyfluorenes, thieno[3,4-*b*]thiophenes and benzo[*b*]thiophene are presented. The effect of adding LiCl on the oxidative addition of Rieke zinc to the carbon-halogen bond is reported as well.



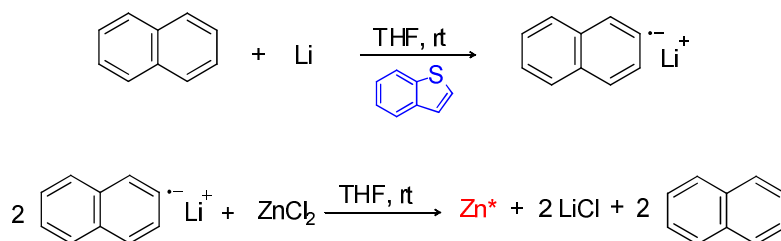


---

# Chapter 2

An efficient and reliable procedure for the preparation of highly reactive Rieke Zinc ( $Zn^*$ )

---



---

\* An efficient and reliable procedure for the preparation of highly reactive Rieke zinc ( $Zn^*$ ): Kudret, S.; D'haen, J.; Oosterbaan, W.; Lutsen, L.; Vanderzande, D.; Maes, W. *Adv. Synth. Catal.* **2013**, 355 (2-3), 569-575.

### 2.1. Introduction

Organozinc compounds are important synthetic intermediates as they exhibit excellent chemoselectivity and good functional group tolerance and stability.<sup>[1]</sup> However, due to their lower reactivity towards a broad range of electrophiles and moderate yields compared to Grignard reagents, they have received rather limited attention, mostly for Reformatsky<sup>[2]</sup> and Simmons-Smith reactions.<sup>[3]</sup> The first organozinc compound to be reported by Frankland in 1849 was prepared from the reaction of metallic Zn with ethyl iodide.<sup>[4]</sup> However, due to the lack of reactivity of the Zn metal, this reaction was quite limited in its scope. Several methods have been used to activate Zn, such as washing with a hydrochloric acid solution<sup>[5]</sup> or adding 1,2-dibromoethane to prevent passivation of the zinc surface.<sup>[6]</sup> Despite of these methods, direct oxidative addition of the Zn metal was only successful for relatively reactive alkyl iodides. Thus, metallic Zn did not generally allow preparation of organozinc reagents directly from organic halides. In the early 1970s, Rieke *et al.* introduced a new method which utilized potassium metal to reduce zinc salts, affording highly reactive Zn metal powder.<sup>[7]</sup> This active form of Zn was called “Rieke zinc (Zn\*)” and displayed excellent reactivity towards organic halides compared with bulk Zn metal, Zn dust or metallic Zn activated by entrainment methods. Later on, in 1991, the same group reported on an alternative method to prepare the active Zn species under milder and safer conditions by reduction of the zinc salt with lithium in the presence of naphthalene as an electron carrier, giving rise to even more reactive Zn\*.<sup>[8]</sup> Reduction of a zinc cyanide salt by the same method resulted in Rieke zinc which reacts at a synthetically useful rate with alkyl or aryl chlorides at r.t. to produce the corresponding organozinc halide reagents.<sup>[9]</sup> Liquid ammonia has also been used as an electron carrier to produce active Zn powder.<sup>[10]</sup> Since

---

then, Rieke zinc has found application in numerous organic syntheses, mostly for the preparation of organozinc reagents. Compared to Grignard and organolithium reagents, organozinc derivatives tolerate the presence of a wide range of functional groups, such as ketones, nitriles, esters and other halides, making it a very useful synthetic tool.<sup>[11]</sup> Rieke zinc has also been used as a reducing agent for common functional groups (conjugated aldehydes, alkynes, esters and nitro compounds).<sup>[12]</sup>

In polymer synthesis, the “Rieke method” - referring to the synthesis of regioregular (fully head-to-tail coupled) poly(3-hexylthiophene) (P3HT) (co)polymers by reaction of 2,5-dibromothiophene monomers with Rieke zinc - is of high relevance, as the resulting semiconducting conjugated polymer materials are of high importance in organic electronics, notably in organic photovoltaics.<sup>[13,14]</sup> Side chain functionalized poly(3-alkylthiophenes) were also prepared by the same protocol,<sup>[15]</sup> and the method was extended to a limited number of other polyarylenes such as poly(*p*-phenylene)<sup>[16]</sup> and poly(dialkylcyclopentadithiophene)<sup>[17]</sup>. Besides these notable exceptions, the Rieke polymerization protocol has been almost absent from literature. Thiophene-based homopolymers are generally prepared by the Grignard metathesis (GRIM) method,<sup>[14]</sup> although this procedure is not compatible with all desired functional side chain patterns (e.g. esters).<sup>[15]</sup>

Upon closer inspection of the available literature, one notices that the applicability of Rieke Zn seems mainly limited by obstacles in its preparation, which later on have a profound effect on the reactivity. Kharisov *et al.* have prepared the active Zn metal in a complicated and completely closed system.<sup>[18]</sup> Vyvyan *et al.* reported some difficulties in preparing large quantities of alkyl zinc reagents due to batch to batch variations in the reactivity of the Rieke zinc metal.<sup>[19]</sup> Zhou attempted to prepare alkylzinc

bromides from commercially available Rieke zinc (Aldrich), but this did not lead to high conversion of the primary alkylzinc bromides, even when a large excess of the active Zn metal was used.<sup>[20]</sup> He also tried to prepare the active Zn metal with Li and a stoichiometric amount of naphthalene, following the procedure from Rieke *et al.*,<sup>[8]</sup> which also gave no improvement.

In this paper, we report on a simple preparation method for highly reactive Rieke zinc under common laboratory conditions. As a proof of principle, the improved synthetic procedure was applied for both the preparation of 3-hexylthiophene and P3HT.

## 2.2. Results and discussion

The highly reactive form of metallic Zn, generally referred to as Rieke zinc (Zn\*), was first prepared in 1973.<sup>[7]</sup> The synthetic protocol involved reduction of a zinc salt in refluxing THF or DME utilizing either Na or K. These highly reactive Zn powders showed high reactivity towards organic halides in oxidative addition reactions. On the other hand, Rieke zinc prepared by this procedure was successfully implemented in Reformatsky reactions at r.t. or below, affording quantitative reaction yields.<sup>[21]</sup> Later on, a safer and milder procedure which uses Li and a catalytic amount of naphthalene (10 mol %) was introduced.<sup>[8,22]</sup> Initially it was believed that the use of an additional electron carrier would complicate purification of the final organic products, but actually the electron carrier can easily be removed by washing the reactive Zn powder with fresh THF or DME. Moreover, the preparation in THF or DME using either a stoichiometric amount of lithium naphthalenide<sup>[8]</sup> or Li and a catalytic amount of naphthalene even led to active Zn of higher reactivity. Reduction of the zinc salt with Li and naphthalene requires vigorous stirring for about 10 h to obtain the active Zn slurry, but also to prevent the

---

reduced Zn to coat the Li surface and thereby inhibit the reduction. The most convenient method actually involves reduction of the zinc salt with a stoichiometric amount of lithium naphthalenide, shortening the reduction time and eliminating the coating problem. The procedure is carried out in two steps. In the first step, the lithium naphthalenide/THF solution is prepared, which takes about 2 h. In the next step, the solution of the zinc salt in THF is transferred using a cannula into the lithium naphthalenide/THF solution over 10-15 minutes. When stirring is stopped, the very finely dispersed zinc particles settle out, leaving a clear colorless supernatant above the Zn powder. In some cases, the supernatant may appear more or less green due to the presence of some lithium naphthalenide. This method, with some improvements as mentioned below, was utilized for the preparation of the highly reactive Rieke zinc metal powder during this study.

In the standard preparation of highly reactive Rieke zinc, naphthalene is used as an electron carrier.<sup>[8]</sup> However, when we started to conduct Rieke polymerization reactions (towards P3HT) with new sources of naphthalene, the *in situ* formed Zn metal particles were found to strongly coagulate, yielding chunky metal clusters. On the other hand, the “old” naphthalene batch (Merck) still gave the desired Rieke zinc as a finely dispersed black slurry. Hence, it became clear that the old naphthalene had to be somehow different compared with the new one, and a number of analytical methods were applied to achieve insight on the properties (notably the impurities) of different naphthalene sources.

Commercially available naphthalene, produced from coal tar (of which it is the most important polycyclic aromatic hydrocarbon fraction),<sup>[23]</sup> contains small amounts of sulfur-containing aromatic compounds. The most abundant among these impurities is benzothiophene (BT), as previously also observed

---

by Hiyoshi *et al.*<sup>[24]</sup> In spite of the fact that the thia-heterocycles are normally eliminated by a desulfurization process, it is quite difficult to remove them to a full extent. Consequently, commercial naphthalene generally contains small amounts of thia-aromatic impurities.

The metallic trace elements in the naphthalene samples and in the Rieke zinc powder were initially analyzed by inductively coupled plasma-mass spectrometry (ICP-MS) for almost all the elements of the periodic table. Only a trace of sulfur was detected. In addition, high performance liquid chromatography (coupled to a fluorescence detector; HPLC-FLD) analysis of the old (Merck) and new (Acros) naphthalene was performed. The contaminant gave a signal around 230 nm. The HPLC results obtained for the two different naphthalene samples are summarized in Table 1. Analysis showed that both of samples contained the same contamination. The amount was, however, nine times higher in the old batch compared to the new naphthalene.

**Table 1.** Contaminant content in different naphthalene sources, as determined by HPLC (relative response).

Naphthalene	Purity (%)	Impurity content (%)	Exact purity (%)
Old (Merck)	99+%	5.6	94.4
New (Acros)	99+%	0.6	99.4

To identify the exact nature of the main contaminant, gas chromatography-mass spectrometry (GC-MS) analysis was performed on four different naphthalene batches (Table 2). According to this analysis, the main contaminant has a molar mass of 134 g/mol, which (as expected) corresponds

---

to BT. Additionally, the mass spectrum of the contaminant was in accordance with the spectrum of BT under the same conditions. The values obtained from GC-MS were somewhat lower than the HPLC-FLD ratios due to the difference in response factor.

**Table 2.** Benzothiophene content in different naphthalene sources, as determined by GC-MS (relative response).

Naphthalene	Purity (%)	BT content (%)
Old (Merck)	99+%	1.69
Merck	≥ 99%	0.06
Aldrich	≥ 99%	0.14
New (Acros)	99+%	0.20

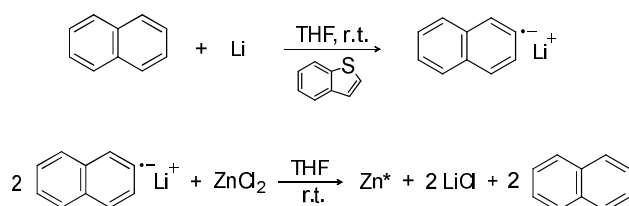
From the above, it is clear that the old (Merck) naphthalene was contaminated with BT to a larger extent and apparently this has an effect on the stabilization of the Zn particles in THF solution and hence on the success of the Rieke zinc preparation and reactivity. For this reason, we have pursued a convenient procedure for the preparation of Rieke zinc in highly active form by reducing the zinc chloride salt in THF with lithium-naphthalenide (prepared *in situ*) and deliberate addition of a catalytic amount of BT, as shown in Scheme 1.

It appears from our analysis that the presence of a catalytic amount of BT in the reducing lithium naphthalenide solution is crucial, affording a fine dispersion of the reactive metal powder. Without BT, coagulation of the Zn metal particles occurred, giving rise to unreactive chunky metal clusters. According to Rieke *et al.*, the appearance of the formed active Zn powder depends on the amount of zinc chloride salt added into the lithium

## Chapter 2

---

naphthalenide solution and on the addition speed.<sup>[8]</sup> With slow addition, i.e. 3 seconds per drop with no excess of Zn, a finely divided black slurry of the active Zn is formed, whereas in case of fast addition, i.e. ~1 second per drop, sponge-shaped active Zn is obtained. This effect was also observed by Bronk and discussed in his dissertation on C-C bond formation via intramolecular conjugate addition of organozinc compounds.<sup>[25]</sup> In our hands, however, it appeared that the reason of the coagulation of the highly reactive Zn particles was neither the addition of an excess of zinc chloride salt nor the addition speed, but the phenomenon could be attributed to the BT impurity, which is present in naphthalene in tiny but varying quantities.



**Scheme 1.** Optimized procedure for the preparation of Rieke zinc.

At this stage, a number of additional experiments were conducted to optimize the Rieke Zn formation. First, naphthalene with different purity grades from different companies was purchased and the reduction process was carried out in parallel with reactions employing the old (Merck) naphthalene to allow full comparison. All experiments that were performed with new naphthalene batches initially failed. Since the major difference between the naphthalene samples was the BT content, novel reactions were conducted with addition of some pure BT to the lithium naphthalenide mixture. Upon addition of the zinc chloride solution to lithium naphthalenide containing BT, a fine slurry of the highly reactive Rieke zinc metal powder was obtained. Further studies revealed that the amount of BT had a large effect on the physical properties of



---

the resulting reactive metal powder, which then later on affects the oxidative addition process of the Rieke zinc metal to organic halides. Thus, several experiments were carried to optimize the ratio BT/zinc chloride. It was found that the optimum amount of BT to be added is 3 mol% (with respect to  $\text{ZnCl}_2$ ). The limiting amount to prevent coagulation seems to be 1 mol%.

Scanning electron microscopy-energy disperse x-ray spectroscopy (SEM-EDX) studies were conducted on the Rieke metal powder prepared with the different methods to study the impact of the addition of BT on the formed Zn metal powder (Figure 1). In case of 1.5 mol% of BT (Figure 1b), the obtained Zn powder was not homogeneous and contained Zn particles of very different size compared with the ones prepared with either the old (Merck) naphthalene (Figure 1a) and the naphthalene containing 3 mol% of BT (Figure 1c).

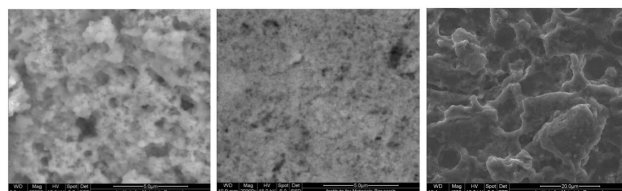


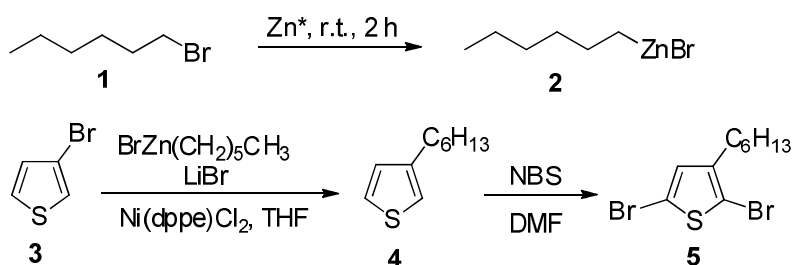
**Figure 1.** SEM-EDX pictures of the Rieke zinc powder prepared with old (Merck) naphthalene (left), 1.5 mol% BT (middle), and 3 mol% BT (right) (EDX Figures in SI).

The Zn metal powder obtained from the reaction with 1.5 mol% BT was implemented in a reaction with 2,5-dibromo-3-hexylthiophene (**5**) (towards the formation of P3HT). As expected, oxidative addition of the Rieke zinc did not proceed to a full extent (as analyzed by  $^1\text{H}$  NMR). This can be related to the decreased active surface of the reactive metal by agglomeration of the formed small particles, which gives rise to a loss of their reactivity towards

## Chapter 2

---

organic halides. However, when we prepared the Rieke zinc by adding at least 3 mol% of BT into the lithium naphthalenide solution, we always obtained a fine black slurry of Rieke Zn metal, showing excellent reactivity in the oxidative addition towards organic halides. Additionally, the active Zn powder kept its reactivity over several days and no further agglomeration of the particles (that could lead to loss of reactivity) was observed.<sup>[26]</sup> Despite of the fact that the mechanism of the stabilization of the Rieke zinc particles as a fine dispersion in THF supernatant is not fully understood, one could suggest a possible complex formation of BT with either Li or zerovalent Rieke Zn.<sup>[27,28]</sup> Following Rieke *et al.*, we then demonstrated the excellent reactivity of the Rieke zinc powder prepared through our optimized procedure by utilizing it in the well-known synthesis of P3HT.<sup>[14,29,30]</sup> The preparation of P3HT starts from the readily available reagents 3-bromothiophene (**3**) and hexyl bromide (**1**). Their conversion to 2,5-dibromohexylthiophene (**5**) is depicted in Scheme 2.

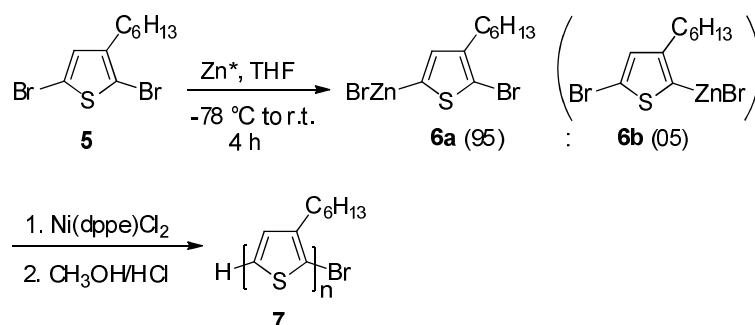


**Scheme 2.** Preparation of 2,5-dibromo-3-hexylthiophene (**5**) employing Rieke zinc.

First, hexyl bromide (**1**) was treated with an excess of Rieke  $Zn^*$ . The reactive Rieke Zn metal readily undergoes oxidative addition in a 1.0-1.2  $Zn^*/RX$  molar ratio at r.t. to afford hexylzinc bromide (**2**) within 2 h.<sup>[8]</sup> The hexylzinc bromide (**2**) solution was dark brown in color and stable under an argon (Ar)

---

atmosphere, and the conversion was estimated to be >99% GC-MS yield. The formation of the organozinc species was monitored by GC-MS and was based on the analysis of the reaction aliquot after quenching with iodine solution. The excess of the reactive metal powder could easily be separated from the solution by allowing the Zn to settle down for about 3 h. The hexylzinc bromide (**2**) solution was then transferred via cannula to another flask for the next reaction. In the latter, the coupling was conducted by reaction of *n*-hexylzinc bromide (**2**) with 3-bromothiophene (**3**) in the presence of 5 mol% of Ni(dppe)Cl<sub>2</sub> ([1,2-bis(diphenylphosphino)ethane] Nickel (II) chloride).<sup>[31]</sup> 3-Hexylthiophene is usually prepared via Kumada coupling of 3-bromothiophene using a Grignard instead of an organozinc reagent. To our knowledge, Rieke chemistry was employed here for the first time to prepare 3-hexylthiophene. The coupling reaction was performed at r.t. overnight. Additionally, when the coupling reaction was performed in the presence of LiBr the reaction time could be shortened from 2 days to 18 h and the yield was dramatically enhanced from 42 to 82% (close to the 87% reported for the Kumada coupling of the corresponding Grignard reagent).<sup>[31,32,33,34]</sup> Up until now, the role of the LiBr is not fully understood. Nonetheless, the beneficial effect of the addition of a Li salt in such reactions is well documented. Koszinowski and co-workers suggested that the Li salt forms complexes with the organozinc species, which increases their solubility and provides a clean metal surface. On the other hand, due to the electronegativity of the halogen atom, the organozinc gains nucleophilic character.<sup>[35]</sup> Subsequently, bromination of 3-hexylthiophene with *N*-bromosuccinimide (NBS) under mild conditions gave 2,5-dibromo-3-hexylthiophene (**5**).<sup>[34]</sup> Simple distillation of the crude product yielded the monomer in high purity.



**Scheme 3.** Regio-controlled synthesis of P3HT.

The synthesis of regioregular P3HT (**7**) is shown in Scheme 3. The highly reactive Rieke zinc ( $\text{Zn}^*$ ) metal powder undergoes oxidative addition to 2,5-dibromo-3-hexylthiophene in a regiospecific manner, yielding 2-bromo-5-(bromozincio)-3-hexylthiophene (**6a**) as the major (95%) and 2-(bromozincio)-5-bromo-3-hexylthiophene (**6b**) as the minor regioisomer (5%). The regioselectivity of the oxidative addition of  $\text{Zn}^*$  metal is higher at lower temperature.<sup>[29]</sup> In our case, the total yield for both regioisomers was >99%, as confirmed by GC-MS analysis after quenching the crude reaction mixture with a saturated ammonium chloride solution. After completion of the reaction, stirring was stopped and unreacted  $\text{Zn}^*$  particles were allowed to settle down. Removal of the excess  $\text{Zn}^*$  is crucial since it can further react with a bromine source and give rise to bis(organozinc) products, which lead to low molecular weight species. Polymerization of the resulting organozinc solution was carried out by adding a catalytic amount of  $\text{Ni}(\text{dppe})\text{Cl}_2$  catalyst to afford highly regioregular P3HT.<sup>[13]</sup>

After completion of the reaction the polymer was precipitated in a solution of 2M HCl/MeOH (2:1). The yield of the polymerization was over 90% at this point. The molecular weight and corresponding polydispersity were measured

---

by gel permeation chromatography (GPC) in THF. The polymer before extraction had  $M_w = 24.3 \times 10^3$  and  $M_n = 6.8 \times 10^3$  (corresponding to 41 repeating units per chain) with a polydispersity  $D = 3.6$ . The crude polymer was then purified by means of sequential soxhlet extractions with methanol and hexanes (24 h each), removing residual monomer and oligomer fractions. The yield was about 70% after soxhlet purification, and the molecular weight increased to  $M_w = 36.1 \times 10^3$ ,  $M_n = 22.9 \times 10^3$  (corresponding to 138 repeating units per chain), while the polydispersity narrowed down to 1.6. Therefore, one can conclude that the monomers were quantitatively cross-coupled in the polymerization reaction with at least 70% of the monomers incorporated in the polymer fraction.

The optimized Rieke procedure was later on also applied towards the preparation of a number of ester-functionalized P3AT copolymers, of particular interest for organic solar cell applications, and also there decent molecular weights were routinely obtained with high reproducibility.<sup>[15e-i]</sup>

### 2.3. Conclusions

In summary, we have developed a straightforward procedure to prepare Rieke zinc in highly reactive form under standard chemical laboratory conditions. The key to afford a highly reproducible protocol is the addition of a particular amount (3 mol%) of BT - which was identified as the main additive responsible for previously observed batch to batch variations - to the lithium naphthalenide solution employed for zinc chloride reduction. The reactivity of the newly prepared active Zn powder was demonstrated in the oxidative addition to hexyl bromide and 2,5-dibromo-3-hexylthiophene to give the corresponding organozinc reagents in excellent yields. The optimized method also readily enables the preparation of active Rieke Zn in large quantities with

high reproducibility. Accordingly, we believe that this optimized procedure can increase the synthetic scope of Rieke zinc in both general organic and polymer chemistry, as was already shown recently by the preparation of polythiophene-based conjugated (co)polymers for applications in organic photovoltaics.<sup>[15e-i]</sup>

## 2.4. Experimental Section

### Materials and methods

All manipulations were carried out with the aid of a dual manifold vacuum/Ar system. Lithium (granular, 99+%) from Acros was stored in a schlenk tube under Ar. Lithium, naphthalene and benzothiophene (Sigma-Aldrich, 98%) were weighed in air as needed and transferred to the schlenk tube under a stream of Ar. Naphthalene with different purity grade was purchased from different suppliers and it was stored in a separate dessicator together with BT over P<sub>2</sub>O<sub>5</sub>. Zinc chloride (Acros, analysis grade 98,5%) was transferred into small vials in the glove box and stored in a dessicator over P<sub>2</sub>O<sub>5</sub>. Zinc chloride was dried by treating it with thionyl chloride and heating with a Bunsen burner, and subsequently removed under a stream of Ar. THF was freshly distilled from Na/benzophenone under N<sub>2</sub> atmosphere at atmospheric pressure prior to use. Brass cannulas were stored at 110 °C and cleaned immediately after use with acetic acid (in the case of Zn\* remnant), acetone (to clean non-polymeric residues), or hot chloroform and/or chlorobenzene (for polymer-based contaminations).

HPLC analysis was carried out using an Agilent 1100 series system incorporating a chrompack 150 mm x 4.6 mm column and a spectra SYSTEM FL2000 type fluorescence detector. The mobile phase was MeCN/water (53/47 to 100/0 v/v) with a flow rate of 1.6 mL/min and an injection volume of

---

20  $\mu\text{L}$ . SEM was performed with a FEI Quanta 200 FEG-SEM in combination with EDX. ELAN DRC-e ICP-MS was employed to analyze the metallic trace elements in naphthalene. GC-MS analysis was carried out with a thermoquest TSQ7000, applying a DB-5MS 30 m x 0.25 mm column, in the temperature range 35-320  $^{\circ}\text{C}$ . Molecular weights and molecular weight distributions were determined relative to polystyrene standards by GPC. Chromatograms were recorded on a Spectra Series P100 (Spectra Physics) equipped with two mixed-B columns (10  $\mu\text{m}$ , 0.75 cm x 30 cm, Polymer labs) and a refractive index detector (Shodex) at 40  $^{\circ}\text{C}$ . THF was used as the eluent at a flow rate of 1.0 mL  $\text{min}^{-1}$ .

**Enhanced preparation method for highly reactive Rieke zinc ( $\text{Zn}^*$ ) metal powder**

Two 120 mL schlenk vessels, A and B, were dried by heating with a Bunsen burner under reduced pressure and cooled down to r.t. under a stream of Ar. Schlenk vessel A, filled with Ar, was weighed and then reassembled to the schlenk line. Under a stream of Ar,  $\text{ZnCl}_2$  was charged to the vessel. After three Ar/vacuum cycles,  $\text{ZnCl}_2$  was wetted with a small amount of  $\text{SOCl}_2$ . The schlenk was heated by a bunsen burner until the  $\text{ZnCl}_2$  salt melted and a white fume was released, and the schlenk was then cooled down under an Ar flow. Schlenk flask A was weighed again to determine the exact amount of  $\text{ZnCl}_2$  and a stirring bar was added. Dried  $\text{ZnCl}_2$  (1.1 equiv) was dissolved in freshly distilled THF (25 mL/g). Li pellets (2.2 equiv), naphthalene (2.25 equiv) and benzothiophene (0.04 equiv) were weighed in air and charged into schlenk B under an Ar stream. Dry THF (the same amount as added to dissolve  $\text{ZnCl}_2$ ) was added and the solution turned from colorless to dark green within less than 2 min. It was stirred further for 2 h to dissolve the Li pellets. The  $\text{ZnCl}_2$  solution was transferred dropwise via cannula to the lithium naphthalenide

solution over 10-15 min. The resulting black suspension might be stirred for 1 more h to consume the remaining Li or stirring can be stopped right after the addition. The highly reactive zinc powder was allowed to settle down for a couple of hours. The supernatant was siphoned off via cannula leaving the Zn\* powder. Thus prepared Rieke zinc was ready to use.

#### **Synthesis of 3-hexylthiophene (4)**

Hexyl bromide (4.7 mL, 28.1 mmol) was dissolved in dry THF (40 mL), it was added via a cannula to the active zinc powder (33.82 mmol) and the reaction mixture was stirred for 3 h at r.t.. Stirring was stopped and the solution was allowed to stand for a couple of hours to allow the excess of zinc to settle down from the dark brown organozinc bromide solution. In a 300 mL flame-dried schlenk vessel, LiBr (3.41 g, 39.25 mmol), Ni(dppe)Cl<sub>2</sub> (0.94 g, 1.784 mmol), and 3-bromothiophene (2.5 mL, 26.76 mmol) were dissolved in dry THF (150 mL). The organozinc bromide solution was then transferred via cannula over a period of 1 h to this mixture under continuous stirring at r.t. and the reaction mixture was allowed to stir overnight. The resulting mixture was then quenched with saturated NH<sub>4</sub>Cl, followed by extraction with diethyl ether, and simple distillation afforded 3-hexylthiophene (3.84 g, 82%) as a colorless liquid.

#### **Synthesis of 2,5-dibromo-3-hexylthiophene (5)**

2,5-Dibromo-3-hexylthiophene was obtained by bromination of 3-hexylthiophene following the literature procedure as reported by Bäuerle et al.<sup>[34]</sup>

#### **Synthesis of poly(3-hexylthiophene) (P3HT)**

A solution of 2,5-dibromo-3-hexylthiophene (4.08 g, 12.5 mmol) in THF (50 mL) was added via cannula to freshly prepared (according to the new procedure) Rieke Zn\* (13.79 mmol) at -78 °C. The mixture was stirred for 1 h



---

at this temperature and then allowed to warm to 0 °C gradually. The unreacted Zn\* was left to settle down overnight and the formed organozinc supernatant was then transferred by cannula via a 0.45 µm acrodisc filter into a flame-dried schlenk tube. Via a cannula, 0.2 mol% of Ni(dppe)Cl<sub>2</sub> (0.013 g, 0.025 mmol) suspended in THF (5 ml) was added to the ice-cooled organozinc solution. The schlenk vessel was immersed into a preheated oil bath at 60 °C and the mixture was stirred at this temperature overnight. It was then poured into a solution of MeOH:HCl (2M) and the resulting dark precipitate was filtered off and washed several times with MeOH. The crude polymer ( $M_w = 24.3 \times 10^3$ ,  $M_n = 6.8 \times 10^3$ ,  $D = 3.6$ ) was transferred into an extraction thimble and purification was performed by sequential soxhlet extractions with MeOH, acetone and hexanes. The polymer was collected with CHCl<sub>3</sub> and the solvent was removed under reduced pressure. The polymer was redissolved in CHCl<sub>3</sub> and precipitation was again performed upon addition of MeOH. Filtration and drying under high vacuum afforded the pure P3HT material (1.44 g, 70%;  $M_w = 36.1 \times 10^3$ ,  $M_n = 22.9 \times 10^3$ ,  $D = 1.6$ ).

## 2.5. Acknowledgements

*We thank IMEC for the PhD grant of S.K. We also acknowledge the OPV-Life project from the IWT (O&O 080368), the POLYSTAR project from PV ERA-NET and the IWT-SBO project POLYSPEC.*

## 2.6. References

- [1] a) *Organozinc Reagents, A Practical Approach* (Eds.: P. Knochel, P. Jones), Oxford University Press, New York, **1999**; b) *The Chemistry of Organozinc Compounds* (Eds: Z. Rappoport, I. Marek), John Wiley & Sons Ltd, West Sussex, England, **2006**; c) P. Knochel, M. A. Schade, S. Bernhardt, G. Manolikakes, A. Metzger, F. M. Piller, C. J. Rohbogner, M. Mosrin, *Beilstein J. Org. Chem.* **2011**, *7*, 1261; d) X.-F. Wu, *Chem. Asian J.* **2012**, *7*, 2505; e) X.-F. Wu, H. Neumann, *Adv. Synth. Catal.* **2012**, *354*, 3141.
- [2] S. Reformatsky, *Ber. Dtsch. Chem. Ges.* **1887**, *20*, 1210.
- [3] H. E. Simmons, R. D. Smith, *J. Am. Chem. Soc.* **1958**, *80*, 5323.
- [4] E. Frankland, *Justus Liebigs Ann. Chem.* **1849**, *71*, 171.
- [5] M. S. Newman, F. J. Evans, *J. Am. Chem. Soc.* **1955**, *77*, 946.
- [6] M. Bellassoued, M. Gaudemar, A. El Borgi, B. Baccar, *J. Organomet. Chem.* **1985**, *280*, 165.
- [7] R. D. Rieke, S. J. Uhm, P. M. Hudnall, *J. Chem. Soc., Chem. Commun.* **1973**, 269.
- [8] L. Zhu, R. M. Wehmeyer, R. D. Rieke, *J. Org. Chem.* **1991**, *56*, 1445.
- [9] M. Hanson, R. D. Rieke, *Synth. Commun.* **1995**, *25*, 101.
- [10] M. Mąkosza, K. Grela, *Tetrahedron Lett.* **1995**, *36*, 9225.
- [11] R. D. Rieke, *Science* **1989**, *246*, 1260.
- [12] a) W.-N. Chou, D. L. Clark, J. B. White, *Tetrahedron Lett.* **1991**, *32*, 299;  
b) J. Kroemer, C. Kirkpatrick, B. Maricle, R. Gawrych, M. D. Mosher, D. Kaufman, *Tetrahedron Lett.* **2006**, *47*, 6339.
- [13] T. A. Chen, R. D. Rieke, *J. Am. Chem. Soc.* **1992**, *114*, 10087.

- 
- [14] a) M. T. Dang, L. Hirsch, G. Wantz, *Adv. Mater.* **2011**, *23*, 3597; b) A. Smeets, K. Van den Bergh, J. De Winter, P. Gerbaux, T. Verbiest, G. Koeckelberghs, *Macromolecules* **2009**, *42*, 7638.
- [15] a) M. Pomerantz, Y. Cheng, R. K. Kasim, R. L. Elsenbaumer, *J. Mater. Chem.* **1999**, *9*, 2155; b) F. Saito, Y. Takeoka, M. Rikukawa, K. Sanui, *Synth. Met.* **2005**, *153*, 125; c) M. Katagiri, *Adv. Mater. Res.* **2011**, *409*, 502; d) R. D. Rieke, S.-H. Kim, *Bull. Korean Chem. Soc.* **2012**, *33*, 1; e) R. Rosch, D. M. Tanenbaum, M. Jorgensen, M. Seeland, M. Barenklau, M. Hermenau, E. Voroshazi, M. T. Lloyd, Y. Galagan, B. Zimmermann, U. Wurfel, M. Hosel, H. F. Dam, S. A. Gevorgyan, S. Kudret, W. Maes, L. Lutsen, D. Vanderzande, R. Andriessen, G. Teran-Escobar, M. Lira-Cantu, A. Rivaton, G. Y. Uzunoglu, D. Germack, B. Andreasen, M. V. Madsen, K. Norrman, H. Hoppe, F. C. Krebs, *Energy Environ. Sci.* **2012**, *5*, 6521; f) D. M. Tanenbaum, M. Hermenau, E. Voroshazi, M. T. Lloyd, Y. Galagan, B. Zimmermann, M. Hosel, H. F. Dam, M. Jorgensen, S. A. Gevorgyan, S. Kudret, W. Maes, L. Lutsen, D. Vanderzande, U. Wurfel, R. Andriessen, R. Rosch, H. Hoppe, G. Teran-Escobar, M. Lira-Cantu, A. Rivaton, G. Y. Uzunoglu, D. Germack, B. Andreasen, M. V. Madsen, K. Norrman, F. C. Krebs, *RSC Adv.* **2012**, *2*, 882.
- [16] T. A. Chen, R. A. O'Brien, R. D. Rieke, *Macromolecules* **1993**, *26*, 3462.
- [17] a) P. Coppo, H. Adams, D. C. Cupertino, S. G. Yeates, M. L. Turner, *Chem. Commun.* **2003**, 2548; b) P. Coppo, D. C. Cupertino, S. G. Yeates, M. L. Turner, *Macromolecules* **2003**, *36*, 2705.
- [18] B. I. Kharisov, L. A. Garza-Rodríguez, H. M. Leija Gutiérrez, U. Ortiz Méndez, R. García Caballero, A. Y. Tsivadze, *Synth. React. Inorg., Met.-Org., Nano-Met. Chem.* **2005**, *35*, 755.
-

## Chapter 2

---

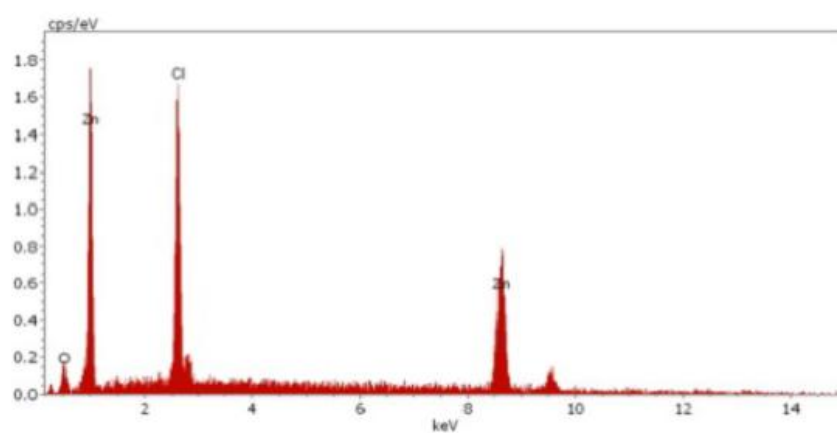
- [19] J. R. Vyvyan, C. Loitz, R. E. Looper, C. S. Mattingly, E. A. Peterson, S. T. Staben, *J. Org. Chem.* **2004**, *69*, 2461.
- [20] J. S. Zhou, *Dissertation*, Massachusetts Institute of Technology, **2005**.
- [21] a) R. D. Rieke, S. J. Uhm, *Synthesis* **1975**, 452; b) R. T. Arnold, S. T. Kulenovic, *Synth. Commun.* **1977**, *7*, 223.
- [22] R. D. Rieke, P. T.-J. Li, T. P. Burns, S. T. Uhm, *J. Org. Chem.* **1981**, *46*, 4323.
- [23] G. Azpíroz, C. G. Blanco, C. Banciella, *Fuel Process. Technol.* **2008**, *89*, 111.
- [24] N. Hiyoshi, R. Miura, C. V. Rode, O. Sato, M. Shirai, *Chem. Lett.* **2005**, *34*, 424.
- [25] B. S. Bronk, *Dissertation*, Massachusetts Institute of Technology, **1995**.
- [26] R. D. Rieke, M. S. Sell, W. R. Klein, T.-A. Chen, J. D. Brown, M. V. Hanson, in *Active Metals*, Wiley-VCH Verlag GmbH, **2007**, pp. 1-59.
- [27] S. Velu, X. Ma, C. Song, *Prepr. Pap. – Am. Chem. Soc., Div. Fuel Chem.* **2003**, *48*, 694.
- [28] L. A. Garza-Rodríguez, B. I. Kharisov, O. V. Kharissova, *Synth. React. Inorg., Met.-Org., Nano-Met. Chem.* **2009**, *39*, 270.
- [29] T.-A. Chen, X. Wu, R. D. Rieke, *J. Am. Chem. Soc.* **1995**, *117*, 233.
- [30] Y. Firdaus, A. Khetubol, S. Kudret, H. Diliën, W. Maes, L. Lutsen, D. Vanderzande, M. Van der Auweraer, *Proc. of SPIE* **2012**, *8438*, 84381G.
- [31] J. Dai, J. L. Sellers, R. E. Nofle, *Synth. Met.* **2003**, *139*, 81.
- [32] S.-H. Kim, J.-G. Kim, *Bull. Korean Chem. Soc.* **2009**, *30*, 2283.
- [33] G. T. Achonduh, N. Hadej, C. Valente, S. Avola, C. J. O'Brien, M. G. Organ, *Chem. Commun.* **2010**, *46*, 4109.

- 
- [34] P. Bäuerle, F. Pfau, H. Schlupp, F. Wurthner, K.-U. Gaudl, M. B. Caro, P. Fischer, *J. Chem. Soc., Perkin Trans. 2* **1993**, 489.
- [35] J. E. Fleckenstein, K. Koszinowski, *Organometallics* **2011**, *30*, 5018.

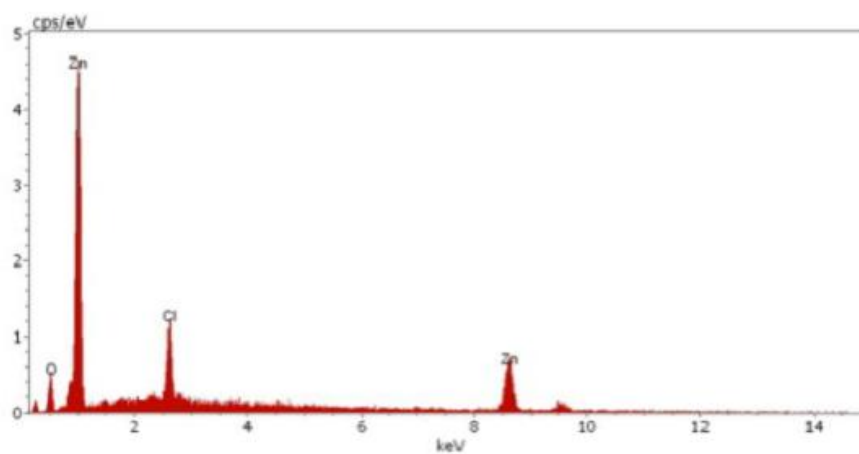
### 2.7. Supporting information

**Figure S1** EDX pictures of the Rieke zinc powder prepared with a) old (Merck) naphthalene, b) 1.5 mol% of benzothiophene, c) 3 mol% of benzothiophene

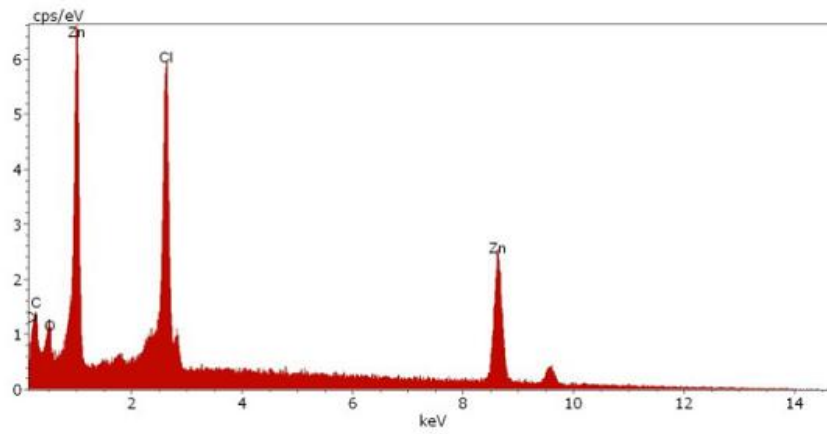
a)



b)



c)





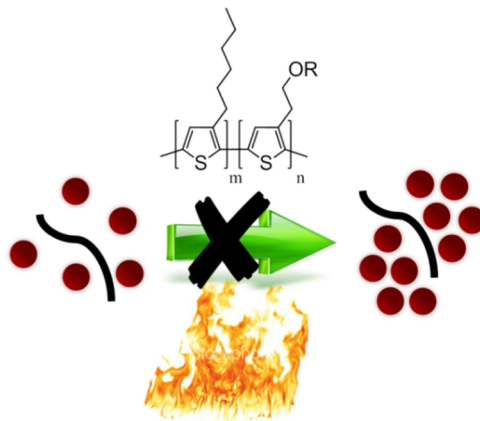


---

# Chapter 3

Enhanced intrinsic stability of the bulk heterojunction active layer blend of polymer solar cells by varying the side chain pattern of the polythiophene donor polymer

---



---

\* Enhanced intrinsic stability of bulk heterojunction polymer solar cells by varying the side chain pattern of the polythiophene donor polymer: Kesters, J.; Kudret, S.; Bertho, S.; Van den Brande, N.; Defour, M.; Van Mele, B.; Lutsen, L.; Manca, J.; Vanderzande, D.; Maes, W. to be submitted.

### 3.1. Introduction

As the introduction of alternative (non-fossil-based) abundant energy sources is becoming more and more important, organic/polymer bulk heterojunction (BHJ) solar cells have gained considerable interest as a means to produce green energy.<sup>1</sup> BHJ polymer solar cells show a number of desirable properties, as they combine unique features such as solution processability enabling low cost large-area thin film fabrication (by R2R printing), improved low-light performance, aesthetics, reduced weight and mechanical flexibility, making them ideal candidates for a multitude of (niche) applications, including portable/wearable chargers and building-integrated photovoltaics (BIPV). As record efficiencies are constantly being reported from various research facilities around the world,<sup>1,2</sup> the idea of commercialization is now becoming more and more realistic. However, additional to low production costs and high power conversion efficiencies (PCEs), it is obligatory for these solar cell devices to show a long-term stability, which is the current Achilles heel of state-of-the-art BHJ organic photovoltaics (OPVs).<sup>3</sup> Successful commercialization of OPV rests on 3 key parameters, i.e. cost, efficiency and lifetime (the 'Brabec triangle').<sup>4</sup> As moderate cost is a parameter rather inherent to this type of printable thin-layer (carbon-based) technology, and novel materials leading to increased performances are constantly on the horizon, it is OPV lifetime that urgently needs to be addressed.

At present, the most efficient light harvesting electron donor materials employed in BHJ organic solar cells all belong to the class of donor-acceptor or low bandgap copolymers.<sup>1,2,5</sup> These materials are combined in photoactive layer blends with a fullerene derivative, most often PC<sub>61</sub>BM ([6,6]-phenyl-C<sub>61</sub> butyric acid methyl ester), PC<sub>71</sub>BM ([6,6]-phenyl-C<sub>71</sub> butyric acid methyl ester) or ICBA (indene-C<sub>60</sub> bisadduct), as the electron accepting component.

---

Nevertheless, the well-established P3HT(poly-3-hexylthiophene):PC<sub>61</sub>BM blend is still a very successful and widely employed workhorse system, perfectly suitable for fundamental studies.<sup>6</sup> Solar cells based on these blends have afforded reasonably high efficiencies,<sup>6,7</sup> up to ~5%, and both materials are readily available in reproducible purity and/or molar mass (distribution) for everyone interested in studying and/or applying OPV blends, which is a serious drawback of the more recent low bandgap materials.

Degradation studies on the reference system P3HT:PC<sub>61</sub>BM have identified lifetimes of approximately 1500 hours when applying continuous illumination (under a sulphur plasma lamp with a light intensity of ca. 1000 W/m<sup>2</sup>), corresponding with lifetimes of ~1.5 years under exposure to direct sunlight.<sup>8,9</sup> Translating this to real-world applications, this will add up to lifetimes of 3-4 years, which is still not sufficient for many large-scale market applications. A number of degradation pathways are responsible for the moderate operational lifetime of OPV devices, acting on either the encapsulating materials, the electrodes, the interconnections or the photoactive layer,<sup>3</sup> and thorough understanding of the various failure mechanisms clearly provides the key to improve OPV reliability. Looking specifically at the photoactive layer blend, being the heart of the OPV device, the limited intrinsic stability of the intimately mixed BHJ donor:acceptor blend under light (photo-oxidation<sup>10</sup>) and heat (degradation and phase demixing<sup>11</sup>) stress are important drawbacks posing challenges to material chemists.<sup>3,12</sup> It is commonly known that the fullerene material diffuses into microcrystals upon heating the blend, leading to a near-to-complete phase separation of P3HT and PC<sub>61</sub>BM.<sup>3,13</sup> As a consequence, the total amount of contact area between donor and acceptor material decreases, charge separation will not occur optimally and less

favorable pathways for efficient charge transport to the electrodes are available.

Several strategies have been proposed to improve the thermal stability of BHJ polymer:fullerene blends, such as lowering the regioregularity of the polymer backbone, the use of compatibilizers, anchorage of the fullerene acceptor to the polymer backbone, the development of polymers with a higher glass transition temperature ( $T_g$ ), and crosslinkable fullerene and/or conjugated polymer derivatives.<sup>3,14</sup> An increase in  $T_g$  of the electron donor polymer hampers the demixing process by slowing down molecular diffusion<sup>11c,14j</sup> Another way to obtain a more stable blend is to build in a certain amount of functional groups in the donor polymer which can crosslink and ‘freeze in’ the ultimate morphology after a thermal or UV treatment. The photocrosslinking approach – which allows decoupling from the thermal annealing step<sup>14e</sup> – has successfully been demonstrated by Fréchet and co-workers based on bromine-functionalized poly(3-alkylthiophene) (P3AT) copolymers.<sup>14g</sup> Even though the photocrosslinked devices were much more stable, the effect of the rather harsh crosslinking process on the blend morphology is quite unpredictable and hence presents a serious drawback. In a similar way, an azide-functionalized P3HT copolymer was applied to suppress macroscale phase separation, attributed to the formation of an *in situ* compatibilizer at the polymer:PCBM interface.<sup>14m</sup> Choi *et al.* extended this approach to 4*H*-cyclopenta[2,1-*b*:3,4-*b'*]dithiophene-based copolymers with appended penta-1,4-diene moieties,<sup>14k</sup> one of the limited reports applying these principles to low bandgap materials. Fréchet and co-workers also extended their photocrosslinking work to thieno[3,4-*c*]pyrrole-4,6-dione (TPD) based donor-acceptor copolymers.<sup>14l</sup> Most degradation studies on low bandgap polymer solar cells have focused on PCDTBT (poly{[9-(1-octylnonyl)-9*H*-carbazole-2,7-

---

diyl]-2,5-thiophenediyl-2,1,3-benzothiadiazole-4,7-diyl-2,5-thiophene-diyl}}, for which lifetimes approaching seven years have been determined.<sup>15</sup> Although this is significantly longer than for P3HT-based devices, the initial ‘burn-in loss period’ – ascribed by the McGehee group to a photochemical reaction in the active layer<sup>15</sup> and analyzed in more detail by joint work of the Leclerc and Gardette groups<sup>16</sup> – is more important. McGehee *et al.* have also demonstrated that material purity of the low bandgap polymers is essential for long-term stability.<sup>17</sup> Very recently it has been shown that light exposure can enhance the thermal stability of polymer(PCDTBT):PC<sub>61</sub>BM solar cells, as independently reported by the Manca and Durrant groups.<sup>18</sup> The photostabilizing effect was linked to light-induced oligomerization of PC<sub>60</sub>BM, effectively hindering its diffusion and crystallization in the blend.

Previous work within our group has indicated that ester-functionalized random P3AT copolymers (with 10, 30 or 50% of functionalized side chains) can readily be synthesized by the Rieke polymerization protocol and that these materials show solar cell performances close to the reference P3HT material.<sup>19</sup> Moreover, the ester-functionalized copolymers were easily converted into the corresponding hydroxyl- and cinnamoyl-functionalized derivatives,<sup>20a</sup> and the absorption window was broadened by ‘click’ functionalization with phthalocyanines.<sup>20b</sup> Within the ISOS-3 inter-laboratory consortium, the stability of seven distinct sets of state-of-the-art OPV devices, degraded under well-defined conditions, was analyzed by different techniques at different research facilities.<sup>20d-g</sup> In this general study, the ester-functionalized P3AT copolymer showed better stability and reproducibility features as compared to regular P3HT in the same (semi-encapsulated, flexible and inverted) device setup, assigned to a more stable BHJ morphology within the photoactive layer. We have also shown that the morphology and

efficiency of hybrid ZnO:polythiophene solar cells can be effectively controlled via ester side chain functionalization.<sup>20c</sup> Evaluation of the efficiencies of BHJ solar cells composed of copolymer:PC<sub>61</sub>BM photoactive layers revealed that, despite their random structure, the performance of the ester-functionalized copolymers is comparable to regular P3HT, as far as the introduced side chains are not too long and the ratio of functionalized units is moderate (below 30%).<sup>20i</sup>

From our initial lifetime screening (9/1,7/3,1/1 ratios of the building blocks), the copolymers with 10% functionalized ester side chains seemed most promising in terms of both efficiency and stability.<sup>20i</sup> Hence, in this work, fine-tuning around this ratio was performed for a series of 4 copolymers (Figure 1) – for which a full description of the synthetic procedures and extensive characterization is provided – aiming to assess the impact of the density and chemical nature of the various side chains on OPV efficiency and stability. The evolution of the active layer morphology upon (artificial) accelerated aging under thermal stress was visualized by Transmission Electron Microscopy (TEM) with additional information from Selected Area Electron Diffraction (SAED) patterns, and the results were complemented with *in situ* I-V measurements at elevated temperatures.

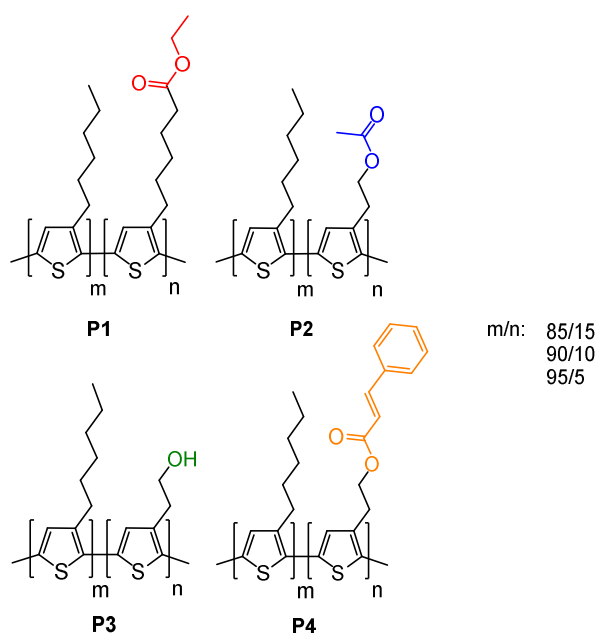


**Figure 1.** Chemical structures of functionalized P3AT random copolymers **P1-P4**.

### 3.2. Experimental section

#### Materials and methods

NMR chemical shifts ( $\delta$ , in ppm) were determined relative to the residual  $\text{CHCl}_3$  absorption (7.26 ppm) or the  $^{13}\text{C}$  resonance shift of  $\text{CDCl}_3$  (77.16 ppm). Gas chromatography-mass spectrometry (GC-MS) analyses were carried out applying Chrompack Cpsil5CB or Cpsil8CB capillary columns. Molar masses and distributions were determined relative to polystyrene standards (Polymer Labs) by analytical size exclusion chromatography (SEC). Chromatograms were recorded on a Spectra Series P100 (Spectra Physics) equipped with two mixed-B columns (10  $\mu\text{m}$ , 0.75 cm x 30 cm, Polymer Labs) and a refractive index detector (Shodex) at 40  $^\circ\text{C}$ . THF was used as the eluent at a flow rate of 1.0  $\text{mL min}^{-1}$ . UV-Vis absorption measurements were performed with a scan rate of

600 nm min<sup>-1</sup> in a continuous run from 200 to 800 nm. Thin film electrochemical measurements were performed with an Eco Chemie Autolab PGSTAT 30 Potentiostat/Galvanostat using a conventional three-electrode cell under N<sub>2</sub> atmosphere (electrolyte: 0.1 M TBAPF<sub>6</sub> in anhydrous CH<sub>3</sub>CN). For the measurements, a Ag/AgNO<sub>3</sub> reference electrode (0.01 M AgNO<sub>3</sub> and 0.1 M TBAPF<sub>6</sub> in anhydrous CH<sub>3</sub>CN), a platinum counter electrode and an indium tin oxide (ITO) coated glass substrate as working electrode were used. The polymers were deposited by drop-casting directly onto the ITO substrates. Cyclic voltammograms were recorded at 50 mV s<sup>-1</sup>. From the onset potentials of the oxidation and reduction the position of the energy levels could be estimated. All potentials were referenced using a known standard, ferrocene/ferrocenium, which in CH<sub>3</sub>CN solution is estimated to have an oxidation potential of -4.98 eV vs. vacuum. DSC measurements were performed at 20 K min<sup>-1</sup> in aluminum crucibles on a TA Instruments Q2000 Tzero DSC equipped with a refrigerated cooling system (RCS), using nitrogen (50 mL min<sup>-1</sup>) as purge gas. TGA experiments were performed at 20 K min<sup>-1</sup> in platinum crucibles on a TA Instruments Q5000 TGA using nitrogen (50 mL min<sup>-1</sup>) as purge gas.

### Synthesis

Monomer synthesis was performed according to the procedures previously reported in our manuscript focusing on ester-functionalized copolymers **P1** and **P2**.<sup>20i</sup>

### Preparation of highly reactive Rieke zinc metal (Zn\*)<sup>21</sup>

Two 120 mL schlenk vessels, A and B, were dried by heating with a bunsen burner under reduced pressure and cooled to rt under a stream of Ar. Schlenk vessel A, filled with Ar, was weighed and then reassembled to the schlenk line.



---

Under a stream of Ar, ZnCl<sub>2</sub> was charged to the vessel. After three Ar/vacuum cycles, ZnCl<sub>2</sub> was wetted with a small amount of SOCl<sub>2</sub>. The schlenk was heated by a bunsen burner until the ZnCl<sub>2</sub> salt melted and a white fume was released, and the schlenk was cooled down under an Ar flow. Schlenk flask A was weighed again to determine the exact amount of ZnCl<sub>2</sub> and a stirring bar was added. Dried ZnCl<sub>2</sub> (1.1 equiv) was dissolved in freshly distilled THF (25 mL/g). Li pellets (2.2 equiv), naphthalene (2.25 equiv) and benzothiophene (0.04 equiv) were weighted in air and charged into schlenk B under an Ar stream. Dry THF (the same amount as added to dissolve ZnCl<sub>2</sub>) was added (the solution turned from colorless to dark green within less than 2 min) and the mixture was stirred further for 2 h to dissolve the Li pellets. The ZnCl<sub>2</sub> solution was transferred dropwise via cannula to the lithium naphthalenide solution over 10-15 min. The resulting black suspension might be stirred for 1 more h to consume the Li that was not dissolved before or stirring can be stopped right after the addition. The highly reactive zinc was allowed to settle down for a couple of hours. The supernatant was siphoned off via cannula leaving the Zn\* powder. Thus prepared Rieke zinc was ready to use.

**Synthesis of copolymers P1 and P2 (poly{[3-hexylthiophene-2,5-diyl]-co-[3-(6-ethoxy-6-oxohexyl)thiophene-2,5-diyl]} or P[3HT-co-3(EOH)T] and poly{[3-hexylthiophene-2,5-diyl]-co-[3-(2-acetoxyethyl)thiophene-2,5-diyl]} or P[3HT-co-3(AE)T])<sup>20i</sup>**

The monomer mixture, 2,5-dibromo-3-hexylthiophene (**M1**) and either ethyl 6-(2,5-dibromothiophene-3-yl)hexanoate (**M2**) or 2-(2,5-dibromothiophene-3-yl)ethyl acetate (**M3**) (in the corresponding feed ratio: 95/5, 90/10 or 85/15), was added via cannula to freshly prepared Zn\*, as made by our modified Rieke method,<sup>21</sup> at -78 °C. The mixture was stirred for 1 h at this temperature and then allowed to warm to 0 °C gradually. Unreacted Zn\* was allowed to settle

---

down overnight and the organozinc supernatant was filtered via a 0.45  $\mu\text{m}$  microdisc filter into a flame-dried schlenk vessel. Via a cannula, 0.2 mol% of  $\text{Ni}(\text{dppe})\text{Cl}_2$  was added to the ice-cooled organozinc solution. The schlenk vessel was immersed into a preheated oil bath at 60  $^\circ\text{C}$  and the mixture was stirred at this temperature overnight. It was then poured into a solution of  $\text{MeOH}:\text{HCl}$  (2M) and the resulting dark precipitate was filtered off and washed several times with  $\text{MeOH}$ . The crude polymer was transferred into an extraction thimble and purification was performed by sequential soxhlet extractions with  $\text{MeOH}$ , acetone and hexanes. The polymer was then collected with chloroform and the solvent was removed under reduced pressure. The polymer was redissolved in chloroform and precipitation was again performed upon addition of  $\text{MeOH}$ . Filtration and drying under high vacuum afforded the pure polymer materials (~50-55% yield). **P1 85/15**: UV-Vis (film,  $\lambda_{\text{max}}$ , nm): 555, 602sh;  $^1\text{H}$  NMR (300 MHz,  $\text{CDCl}_3$ ,  $\delta$ , ppm): 6.96 (s), 4.10 (q), 2.79 (t), 2.56 (s), 2.31 (t), 1.69 (s), 1.48-1.20 (m), 0.90 (t); FT-IR (NaCl,  $\text{cm}^{-1}$ ):  $\nu_{\text{max}}$  = 3053, 2955, 2928, 2854, 1738, 1563, 1509, 1455, 1376, 1260, 1179, 820; SEC (THF):  $M_w$  =  $25.7 \times 10^3 \text{ g mol}^{-1}$ ,  $M_n$  =  $15.4 \times 10^3 \text{ g mol}^{-1}$ ,  $D$  = 1.67; **P1 90/10**: UV-Vis (film,  $\lambda_{\text{max}}$ , nm) 555, 602sh;  $^1\text{H}$  NMR (300 MHz,  $\text{CDCl}_3$ ,  $\delta$ , ppm): 6.96 (s), 4.11 (q), 2.79 (t), 2.55 (s), 2.31 (t), 1.68 (s), 1.48-1.20 (m), 0.90 (t); SEC (THF):  $M_w$  =  $29.0 \times 10^3 \text{ g mol}^{-1}$ ,  $M_n$  =  $x \times 10^3 \text{ g mol}^{-1}$ ,  $D$  = 1.67; **P1 95/5**: UV-Vis (film,  $\lambda_{\text{max}}$ , nm): 555, 602sh;  $^1\text{H}$  NMR (300 MHz,  $\text{CDCl}_3$ ,  $\delta$ , ppm): 6.96 (s), 4.10 (q), 2.79 (t), 2.56 (s), 2.31 (t), 1.69 (s), 1.48-1.20 (m), 0.90 (t); SEC (THF):  $M_w$  =  $29.0 \times 10^3 \text{ g mol}^{-1}$ ,  $M_n$  =  $17.9 \times 10^3 \text{ g mol}^{-1}$ ,  $D$  = 1.62. **P2 85/15**: UV-Vis (film,  $\lambda_{\text{max}}$ , nm): 551, 600sh;  $^1\text{H}$  NMR (300 MHz,  $\text{CDCl}_3$ ,  $\delta$ , ppm): 7.0 (s), 6.96 (s), 4.35 (t), 3.14 (t), 2.78 (t), 2.58 (t), 2.06 (s), 1.75-1.60 (m), 1.45-1.34 (m), 0.89 (t); FT-IR (NaCl,  $\text{cm}^{-1}$ ):  $\nu_{\text{max}}$  = 3055, 2954, 2926, 2856, 1744, 1509, 1455, 1378, 1236, 1036, 820; SEC (THF):  $M_w$  =  $37.0 \times 10^3 \text{ g mol}^{-1}$ ,  $M_n$  =  $22.0 \times 10^3 \text{ g mol}^{-1}$ ,  $D$  = 1.68; **P2 90/10**: UV-Vis

---

---

(film,  $\lambda_{\max}$ , nm): 551, 600sh;  $^1\text{H NMR}$  (300 MHz,  $\text{CDCl}_3$ ,  $\delta$ , ppm): 7.0 (s), 6.96 (s), 4.34 (t), 3.14 (t), 2.78 (t), 2.58 (t), 2.05 (s), 1.75-1.60 (m), 1.45-1.34 (m), 0.89 (t); SEC (THF):  $M_w = 29.4 \times 10^3 \text{ g mol}^{-1}$ ,  $M_n = 18.7 \times 10^3 \text{ g mol}^{-1}$ ,  $D = 1.57$ ; **P2 95/5**: UV-Vis (film,  $\lambda_{\max}$ , nm): 551, 600sh;  $^1\text{H NMR}$  (300 MHz,  $\text{CDCl}_3$ ,  $\delta$ , ppm): 7.0 (s), 6.96 (s), 4.35 (t), 3.14 (t), 2.78 (t), 2.58 (t), 2.05 (s), 1.75-1.61 (m), 1.48-1.34 (m), 0.9 (t); SEC (THF):  $M_w = 26.6 \times 10^3 \text{ g mol}^{-1}$ ,  $M_n = 17.3 \times 10^3 \text{ g mol}^{-1}$ ,  $D = 1.53$ .

**Synthesis of hydroxyl-functionalized copolymers P3 (poly{[3-hexylthiophen-2,5-diyl]-co-[3-(2-hydroxyethyl)thiophen-2,5-diyl]} or P[3HT-co-3(HE)T])**

Ester-functionalized copolymers **P2**, prepared with different monomer ratios, were dissolved in THF (1 g/100 mL) and a solution of KOH in  $\text{CH}_3\text{OH}$  (6% m/v, 1 g polymer/50 mL solution) was then added dropwise over a period of 1 h at rt. The reaction mixture was heated at reflux for 3 h, cooled down to rt and poured into  $\text{CH}_3\text{OH}$ . After neutralization, the precipitated polymers were recovered by filtration, rinsed with fresh  $\text{CH}_3\text{OH}$  and dried under high vacuum.

**P3 85/15**: UV-Vis (film,  $\lambda_{\max}$ , nm): 551, 600sh;  $^1\text{H NMR}$  (300 MHz,  $\text{CDCl}_3$ ,  $\delta$ , ppm): 7.03 (s), 6.96 (s), 3.94 (t), 3.11 (t), 2.77 (t), 1.65 (t), 1.45-1.25 (m), 0.87 (t); FT-IR (NaCl,  $\text{cm}^{-1}$ ):  $\nu_{\max} = 3055, 2954, 2926, 2856, 1509, 1455, 1377, 1046, 820$ ; SEC (THF):  $M_w = 29.3 \times 10^3 \text{ g mol}^{-1}$ ,  $M_n = 16.1 \times 10^3 \text{ g mol}^{-1}$ ,  $D = 1.82$ ; **P3 90/10**: UV-Vis (film,  $\lambda_{\max}$ , nm): 551, 600sh;  $^1\text{H NMR}$  (300 MHz,  $\text{CDCl}_3$ ,  $\delta$ , ppm): 7.03 (s), 6.96 (s), 3.93 (t), 3.09 (t), 2.78 (t), 1.67 (t), 1.45-1.25 (m), 0.89 (t); SEC (THF):  $M_w = 34.2 \times 10^3 \text{ g mol}^{-1}$ ,  $M_n = 19.7 \times 10^3 \text{ g mol}^{-1}$ ,  $D = 1.74$ ; **P3 95/5**: UV-Vis (film,  $\lambda_{\max}$ , nm): 551, 600sh;  $^1\text{H NMR}$  (300 MHz,  $\text{CDCl}_3$ ,  $\delta$ , ppm): 7.03 (s), 6.96 (s), 3.94 (t), 3.09 (t), 2.78 (t), 1.70 (t), 1.45-1.25 (m), 0.89 (t); SEC (THF):  $M_w = 31.7 \times 10^3 \text{ g mol}^{-1}$ ,  $M_n = 18.7 \times 10^3 \text{ g mol}^{-1}$ ,  $D = 1.69$ .

**Synthesis of copolymers P4 (poly{[3-hexylthiophen-2,5-diyl]-co-[3-(2-(Z)-(3-phenylacryloyloxy)ethyl)thiophen-2,5-diyl]} or P[3HT-co-3(PAOE)T])**

Hydroxyl-functionalized copolymers **P3** were dissolved in THF (1 g/100 mL) at 50 °C. The solutions were cooled down to rt and excess amounts of triethylamine and *trans*-cinnamoyl chloride (10 equiv with regard to the copolymer) were added. The reaction mixtures were warmed to 50 °C and stirred overnight. The mixtures were poured into CH<sub>3</sub>OH/HCl (2M) (2/1, v/v) and stirred for a 30 minutes. After neutralization, the precipitated polymers were filtered and rinsed with water and methanol intensively. The polymers were obtained in pure form after soxhlet extraction with acetone, followed by drying under high vacuum. **P4 85/15**: UV-Vis (film,  $\lambda_{\max}$ , nm): 553, 599sh; <sup>1</sup>H NMR (300 MHz, CDCl<sub>3</sub>,  $\delta$ , ppm): 7.67-7.05 (m), 6.96 (s), 6.42 (d), 4.49 (t), 3.23 (t), 2.79 (t), 1.75-1.61 (m), 1.49-1.25 (m), 0.9 (t); FT-IR (NaCl, cm<sup>-1</sup>):  $\nu_{\max}$  = SEC (THF):  $M_w = 35.2 \times 10^3 \text{ g mol}^{-1}$ ,  $M_n = 19.2 \times 10^3 \text{ g mol}^{-1}$ ,  $D = 1.83$ ; **P4 90/10**: UV-Vis (film,  $\lambda_{\max}$ , nm): 553, 599sh; <sup>1</sup>H NMR (300 MHz, CDCl<sub>3</sub>,  $\delta$ , ppm): 7.67-7.05 (m), 6.96 (s), 6.42 (d), 4.49 (t), 3.21 (t), 2.78 (t), 1.75-1.61 (m), 1.49-1.25 (m), 0.9 (t); SEC (THF):  $M_w = 31.7 \times 10^3 \text{ g mol}^{-1}$ ,  $M_n = 18.9 \times 10^3 \text{ g mol}^{-1}$ ,  $D = 1.67$ ; **P4 95/5**: UV-Vis (film,  $\lambda_{\max}$ , nm): 553, 599sh; <sup>1</sup>H NMR (300 MHz, CDCl<sub>3</sub>,  $\delta$ , ppm): 7.67 (d), 7.47-7.05 (m), 6.96 (s), 6.41 (d), 4.49 (t), 3.23 (t), 2.78 (t), 1.75-1.61 (m), 1.50-1.25 (m), 0.9 (t); SEC (THF):  $M_w = 33.9 \times 10^3 \text{ g mol}^{-1}$ ,  $M_n = 19.2 \times 10^3 \text{ g mol}^{-1}$ ,  $D = 1.76$ .

#### **BHJ OPV devices**

Bulk heterojunction solar cells were fabricated using the standard glass/ITO/polymer:PC<sub>61</sub>BM/Ca/Al device architecture. Before processing the devices, the ITO (100 nm) coated substrates (Kintec, sheet resistivity 20  $\Omega$ /sq) were exposed to a standard cleaning procedure using soap, demineralized water, acetone and isopropanol, followed by a UV/O<sub>3</sub>-treatment for 15 min. Afterwards, PEDOT-PSS (poly(3,4-ethylenedioxythiophene)-

---

poly(styrenesulfonic acid); Bayer)poly(styrenesulfonic acid); Bayer) was spin-coated on top with a thickness of  $\sim 30$  nm. The samples were placed under nitrogen atmosphere in a glove box and an annealing step was performed at  $130$  °C for 15 min to remove any residual water. This was followed by the deposition of the polymer:PC<sub>61</sub>BM (Solenne) active layer blends by spin-coating, aiming for a layer thickness of  $\sim 80$  nm. The solutions for the blends were prepared with  $10 \text{ mg mL}^{-1}$  of polymer in a 1:1 ratio with PC<sub>61</sub>BM, using chlorobenzene (CB) as a solvent. Subsequently, these layers were exposed to a post-process annealing at  $130$  °C for 10 min to optimize the layer morphology, and hence the initial efficiency. The devices were finalized by evaporating the top electrodes, Ca and Al, with layer thicknesses of  $\sim 20$  and  $80$  nm, respectively, at a pressure of  $1 \times 10^{-6}$  mbar. In this way, complete cells with an active area of  $25 \text{ mm}^2$  were obtained.

After device preparation, the initial efficiencies were measured using a Newport class A solar simulator (model 91195A), calibrated with a silicon solar cell to give an AM 1.5 spectrum. To investigate the thermal degradation behavior, the samples were exposed to an elevated temperature in a nitrogen atmosphere (glove box) for a certain amount of time, while measuring the *I-V* characteristics at particular time intervals, using a White 5500K LED (Lamina). Degradation experiments were always performed on a bulk of substrates. This means for example that the 3 most promising copolymers and the reference P3HT sample (always 4 solar cells at a time) were degraded at the same time in the same setup. Before performing the more detailed study, a rough screening experiment was performed utilizing a hotplate (280 x 200 mm, type PZ28-2ET, Harry Gestigkeit GmbH, with a PR5 programmer controller). To analyze the layer morphology more into detail, TEM (FEI Tecnai Spirit using an accelerating voltage of 120 kV) samples were prepared. To this end,

polymer:PC<sub>61</sub>BM layers were spin-coated directly on clean glass substrates. Subsequently, the active layers were removed from the substrates by etching in hydrofluoric acid.

### 3.3. Results and discussion

Up until recently, P3HT:PC<sub>61</sub>BM has always been the OPV workhorse system due to the material availability at a reasonable cost, the ease of processing and the relatively high efficiencies that can be obtained from this blend.<sup>6</sup> However, the intimately mixed donor:acceptor morphology of this heterogeneous blend is not thermodynamically stable over prolonged periods of time, a fact that is easily observable when it is exposed to higher temperatures. To evaluate the BHJ active layer intrinsic (thermal) stability – one of the key factors to improve general OPV stability – experiments monitoring the photovoltaic parameters are generally conducted at elevated temperatures ('accelerated aging' tests).

In previous work we have synthesized a series of regioregular functionalized random P3AT copolymers with different built-in ratios of the functionalized thiophene units (Figure 1).<sup>16</sup> From preliminary studies it is known that both the 'alcohol' and 'cinnamoyl'-substituted 9/1 copolymers (**P3** and **P4**, respectively) have a substantial effect on the thermal stability of the active layer blend morphology.<sup>20h</sup> For both copolymers, the short-circuit current density ( $J_{sc}$ ) remained above 90% of its initial value upon thermal annealing at 110 °C for 150 h. In this study, a more general screening of the stability features resulting from the introduction of functionalized side chains on a polythiophene backbone is presented, varying the amount of functional entities between 5 and 15%.

---

### 3.3.1. Synthesis and characterization

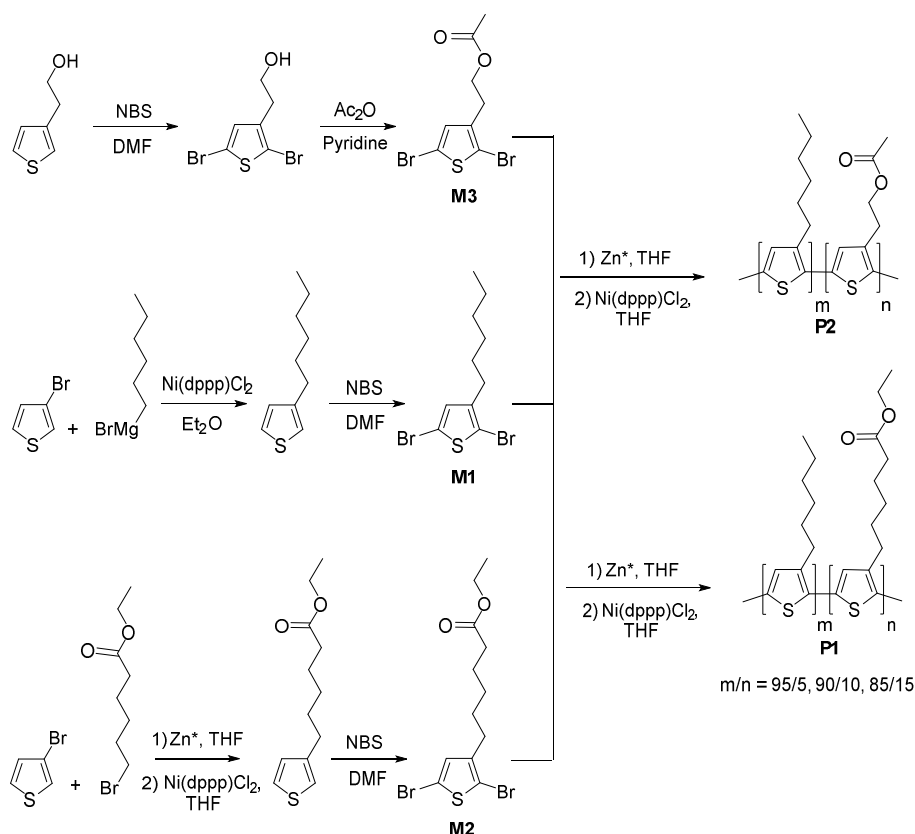
As the so-called 'Rieke zinc method' allows the preparation of regioregular polythiophenes with appended ester-functionalized side chains (in contrast to the widely employed GRIM method) directly from the prefunctionalized monomers, this procedure was adopted toward the desired side-chain functionalized random copolymers.<sup>6,22</sup> Despite the inherent advantages of this method – excellent chemoselectivity and high functional group tolerance and stability of the organozinc reagents<sup>23</sup> – it has only scarcely been used for the synthesis of conjugated polymer materials so far, and mostly for (co)polythiophenes.<sup>24,25</sup> The main reasons for this limited success are the rather unreliable synthesis of the active zinc species and the special precautions that had to be taken. To counter this, we have recently established an efficient and reproducible procedure for the preparation of highly reactive Rieke zinc under standard laboratory conditions.<sup>21</sup> Rieke zinc is commonly prepared by the reduction of zinc chloride with lithium using a stoichiometric amount of naphthalene. In our hands, it was observed that the reaction outcome was highly dependent on the naphthalene source and purity grade. The presence of benzothiophene seems crucial to avoid coagulation of the zinc particles and the amount of benzothiophene has a large effect on the physical properties and the reactivity of the resulting zinc powder. Accordingly, highly reactive Rieke zinc was easily prepared from zinc chloride by adding an optimum amount (3 mol% with regard to ZnCl<sub>2</sub>) of benzothiophene into the lithium naphthalenide solution (prepared *in situ*). The Rieke zinc obtained in this way was previously successfully employed in the synthesis of regioregular P3HT.<sup>21</sup>

The synthetic strategies applied for the requested 2,5-dibromothiophene monomers and ester-functionalized copolymers are shown in Scheme 1.<sup>20i</sup> 2,5-

Dibromo-3-hexylthiophene (**M1**) was prepared according to the literature procedure via Kumada coupling of 3-bromothiophene and hexylmagnesium bromide and subsequent dibromination with an excess of *N*-bromosuccinimide (NBS) in DMF.<sup>26</sup> 2-(Thiophene-3-yl)acetic acid was reduced with lithium aluminium hydride in diethyl ether to give 2-(thiophene-3-yl)ethanol, which was then dibrominated and finally reacted with acetic anhydride in pyridine yielding monomer **M3** in high yield. A similar route was followed to prepare ethyl 6-(2,5-dibromothiophene-3-yl)hexanoate (**M2**). Nevertheless, in the first step an organozinc reagent was employed instead of the standard organomagnesium reagent. Following the optimized procedure to prepare Rieke zinc in highly reactive form,<sup>21</sup> 6-bromohexanoate was treated with an excess of Rieke zinc at room temperature to afford (6-ethoxy-6-oxohexyl)zinc bromide (by oxidative addition) in excellent (>99%) yield. The coupling reaction with 3-bromothiophene was performed in the presence of 5 mol% of Ni(dppe)Cl<sub>2</sub> catalyst and LiBr salt to shorten the reaction time.<sup>27</sup>

The ester-functionalized copolymers **P1** and **P2** were then synthesized by the Rieke method (Scheme 1).<sup>20i,21</sup> Monomer mixtures of **M1**, **M2** and **M3**, in molar compositions 95/5, 85/15 and 90/10, were treated with freshly prepared Rieke zinc to form the corresponding organozinc solutions. Addition of 0.2 mol% of the Ni(dppe)Cl<sub>2</sub> catalyst then afforded the respective polymers in good yields (~50-55%) after successive purification by precipitation in methanol, soxhlet extractions (first with methanol to remove the catalyst, thereafter with hexanes to get rid of the low molecular weight species, and finally with acetone to narrow the polydispersity), and reprecipitation.



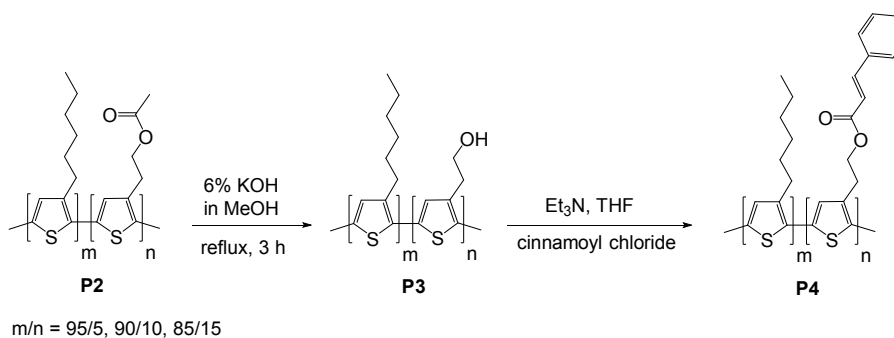


**Scheme 1.** Synthetic pathways toward ester-functionalized P3AT copolymers **P1** and **P2**.

The pendant ester moieties can easily be converted to other functionalities by applying post-polymerization protocols (Scheme 2). Hydrolysis was performed by refluxing the **P2** copolymers in methanolic potassium hydroxide.<sup>20h,28</sup> The success of the reaction was confirmed by the disappearance of the acetoxy singlet ( $\delta = 2.06$  ppm) in the <sup>1</sup>H NMR spectrum and the C=O vibration at  $\sim 1740$  cm<sup>-1</sup> in the FT-IR spectrum (Figure S3). Hydrolysis of the ester functions to alcohol moieties reduced the copolymer solubility. Further reaction of the

## Chapter 3

alcohol groups with cinnamoyl chloride in the presence of triethylamine afforded copolymer series **P4** (Scheme 2).<sup>20h,29</sup> Full conversion was proven by the appearance of the cinnamon-related signals in the aromatic region of the <sup>1</sup>H NMR spectrum ( $\delta = 6-7$  ppm) and reappearance of an ester-like C=O absorption ( $\sim 1716$  cm<sup>-1</sup>) in FT-IR (Figure S3).



**Scheme 2.** Post-polymerization hydrolysis and further functionalization of the **P2** ester copolymers.

Size exclusion chromatography (SEC) was used to determine the molar masses and polymer distributions (Table 1). All copolymers had reasonable average molecular weights ( $M_w = 26-37 \times 10^3$  g mol<sup>-1</sup> and  $M_n = 15-20 \times 10^3$  g mol<sup>-1</sup>) with polydispersity indices of 1.6-1.8. Compared with P3HT synthesized by the same procedure ( $M_w = 53.1$  kDa,  $M_n = 35.3$  kDa,  $D = 1.51$ ), the molecular weights of the copolymers are only slightly lower.

**Table 1.** Molar masses and distributions of copolymers **P1-P4**, as determined by SEC.

Polymer	$M_n$ ( $\times 10^3$ g mol <sup>-1</sup> )	<i>D</i>
P3HT	35.3	1.51
<b>P1</b> – 85/15	15.4	1.67
<b>P1</b> – 90/10	17.3	1.67
<b>P1</b> – 95/5	17.9	1.62
<b>P2</b> – 85/15	22.0	1.68
<b>P2</b> – 90/10	18.7	1.57
<b>P2</b> – 95/5	17.3	1.53
<b>P3</b> – 85/15	16.1	1.82
<b>P3</b> – 90/10	19.7	1.74
<b>P3</b> – 95/5	18.7	1.69
<b>P4</b> – 85/15	19.2	1.83
<b>P4</b> – 90/10	18.9	1.67
<b>P4</b> – 95/5	19.2	1.76

The UV-Vis absorption spectra of the side-chain functionalized copolymers were recorded both in solution and in thin film using chloroform as the (casting) solvent (Figure S1, S2). The solution UV-Vis spectra show that the four different regioregular copolymers all have a maximum absorption wavelength ( $\lambda_{\max}$ ) at approximately 450 nm. The solid-state UV-Vis spectra are red-shifted, suggesting molecular organization in the thin films. All copolymers showed a maximum absorption at ~550 nm with a shoulder at ~605 nm.<sup>30</sup> The absorption around 605 nm was in general slightly more intense compared to Rieke P3HT, pointing to a larger degree of ordering (crystallinity and/or supramolecular aggregation).

Cyclic voltammetry (CV) was employed to study the electrochemical characteristics of the polymers and to estimate their highest occupied molecular orbital (HOMO) and lowest unoccupied molecular orbital (LUMO) energy levels and bandgaps. The results obtained (for unannealed thin films of

the respective copolymers) are summarized in Table S1. Rieke P3HT showed a HOMO level of -5.25 eV, a LUMO level of -3.37 eV, and an optical band gap of 1.88 eV. The side-chain functionalized copolymers all showed comparable values with regard to the reference polymer, indicating that the functionalization does not lead to a noticeable impact on the electrochemical characteristics.

Thermogravimetric analysis (TGA) was performed on the 85/15 copolymers to evaluate the thermal stability as a result of the different side-chain functionalities introduced. From Figure 2, it can clearly be seen that all materials are stable up to a temperature of at least 300 °C.

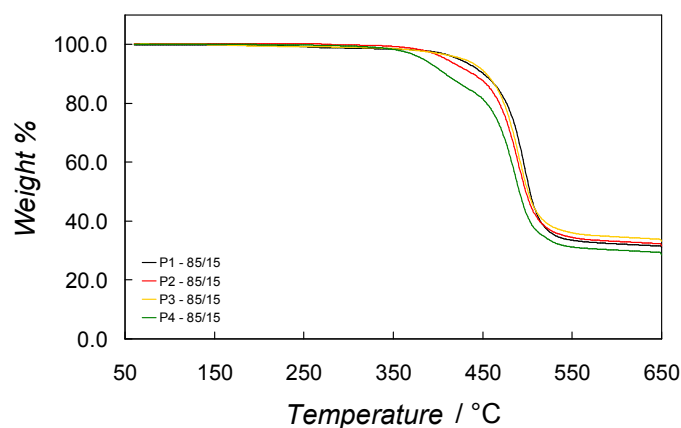


**Figure 2.** TGA (at 20 K min<sup>-1</sup>) of the **P1-P4 85/15** copolymers.

DSC thermograms for the different random copolymers are presented in Figure 3, and the values of the melting peak temperatures and enthalpies are gathered in Table 2. All the polymers analyzed show semi-crystalline behavior. The glass transition temperatures ( $T_g$ ) were hard to determine due to an unclear step in the heat capacity giving a broad transition. This is consistent with the high melting enthalpies detected in second heating, indicative for a

high degree of crystallinity. In all Figures, a thermogram of pure Rieke P3HT is included for comparison. For the **P2** copolymers, a higher amount of functionalized repeating units leads to higher melting points and higher crystallinity (higher  $\Delta H_m$ ). This trend does not hold for the other copolymers studied. In the case of the **P1**, **P3** and **P4** copolymers a maximum in both melting point and crystallinity is reached for the 95/5 composition. Further inclusion of functionalized repeating units in these systems probably disturbs crystal formation. These trends might be important for the respective functionalized P3HT:PC<sub>61</sub>BM state diagrams<sup>13</sup> and corresponding thermal annealing procedures toward an optimized nanomorphology and performance of the photoactive layer.

**Table 2.** Melting peak temperatures and enthalpies for all copolymers. Rieke-P3HT is included for comparison.

Polymer	$T_m$ (°C)	$\Delta H_m$ (J g <sup>-1</sup> )
<b>P1</b> – 95/5	221	24.6
<b>P1</b> – 90/10	214	19.4
<b>P1</b> – 85/15	207	19.8
<b>P2</b> – 95/5	226	17.0
<b>P2</b> – 90/10	232	21.0
<b>P2</b> – 85/15	233	21.0
<b>P3</b> – 95/5	228	23.0
<b>P3</b> – 90/10	224	18.7
<b>P3</b> – 85/15	218	14.4
<b>P4</b> – 95/5	224	21.9
<b>P4</b> – 90/10	215	18.0
<b>P4</b> – 85/15	205	14.1
P3HT (Rieke)	215	16.2

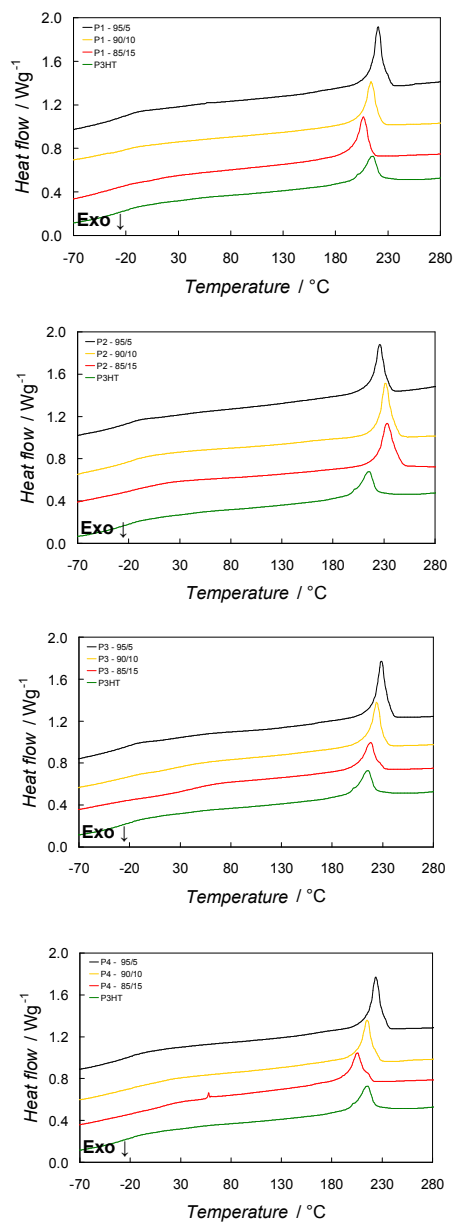


**Figure 3.** DSC thermograms of the second heating (at 20 K min<sup>-1</sup>) of the P1-P4 copolymers. Rieke P3HT was included for comparison. The curves were shifted vertically for clarity.

---

### 3.3.2. Bulk heterojunction polymer solar cells

Solar cells were produced using the glass/ITO/PEDOT-PSS/Active layer/Ca/Al architecture, with donor polymers P3HT and **P1-P4** blended in a 1:1 ratio with PC<sub>61</sub>BM and using chlorobenzene as the active layer spin-coating solvent. The incorporation of functional moieties on the side chains influences both the solubility and the crystallinity of the copolymers,<sup>20a,i</sup> which obviously have an effect on the P3AT:PC<sub>61</sub>BM blend film morphology, hence also strongly influencing the *I-V* characteristics (open circuit voltage  $V_{oc}$ , short-circuit current density  $J_{sc}$ , fill factor FF and efficiency  $\eta$ ). However, as can be observed in Figure 4 and Table 3, showing the optimized efficiencies of the copolymers with 5% of appended functionalized side chains, the power conversion efficiencies (PCEs) are only altered to a minor extent compared to regular P3HT if small amounts of the functionalized comonomers are introduced. In this case, dibromooctane (DBO) was used as an additive in a concentration of 2.5 w/v% to enhance the solar cell performance, rather than performing an annealing step as routinely done for P3HT-based blends.<sup>31</sup> Interestingly, the solar cell output parameters are in the same range as for regular P3HT for the copolymers in which the functionalized side chain is rather small (**P2** and **P3**), whereas the copolymers with larger side chains generally show a slightly lower performance (**P1** and **P4**), which is most notable in the  $J_{sc}$  (Table 3). In general,  $V_{oc}$ 's and fill factors are higher for all copolymer devices at the expense of the current (density). The (short) ester-functionalized copolymer **P2** shows even higher efficiency than regular P3HT. As previously shown, larger aberration on the side chains might result in a non-optimal configuration of the crystalline domains, hindering the efficiency of charge separation.<sup>20a,i</sup> The efficiencies of the 10% and 15% functionalized P3ATs were generally (slightly) lower (Table S2), but it has to be mentioned that the

processing parameters (solvent, concentration, additive, polymer:fullerene ratio) are not individually optimized and they might deviate more strongly from the standard P3HT processing conditions for larger functionalization degrees.

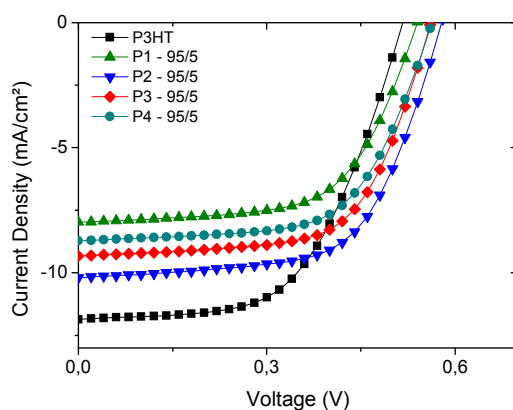


**Figure 4.** Optimum  $J$ - $V$  characteristics for the copolymer:PC<sub>61</sub>BM systems with a built-in ratio of 5%.

**Table 3.** Photovoltaic parameters of optimized solar cells based on P3HT and **P1-P4**.<sup>a</sup>

Donor materials	$V_{oc}$	$J_{sc}$	FF	$\eta$
P3HT <sup>b</sup>	0.52	11.86	0.56	3.48
<b>P1</b> – 95/5	0.54	7.97	0.62	2.67
<b>P2</b> – 95/5	0.58	10.20	0.62	3.69
<b>P3</b> – 95/5	0.56	9.33	0.64	3.34
<b>P4</b> – 95/5	0.56	8.72	0.63	3.07

<sup>a</sup> Glass/ITO/PEDOT-PSS/Active Layer/Ca/Al, using chlorobenzene as a solvent with 2.5 w/v% of DBO added. <sup>b</sup> In-house prepared.

### 3.3.3. Accelerated (thermal) ageing

Table 4 shows the initial efficiencies for the solar cell devices applied for the thermal degradation experiments. The devices were not annealed prior to the initial lifetime screening tests. However, the first data points, as shown in the



Table 4, are taken after 5 hours of exposure to a temperature of 85 °C. Moreover, the additive was not included to minimize the influence of additional components and/or parameters. It has to be noted that the optimal annealing times are actually different for the various copolymer systems, easily observable by a clear color shift from orange to purple. More in detail, one can observe this shift after 5 min for P3HT, whereas this occurs at slightly longer (15-20 min) for materials **P1-P4**. For these aging experiments, it should also be mentioned that the applied pristine P3HT material was synthesized in-house, by the same Rieke protocol, to allow optimal comparison with the various copolymer derivatives (enhancing the chances of the presence of similar ‘impurities’). This might explain the slightly inferior *I-V* characteristics obtained for the reference system in comparison with literature values.<sup>6</sup>

**Table 4.** Initial solar cells performance parameters for copolymer series **P1-P4** prior to the thermal degradation experiments.<sup>a</sup>

<b>Donor materials</b>	<b><math>V_{oc}</math></b>	<b><math>J_{sc}</math></b>	<b>FF</b>	<b><math>\eta</math></b>
P3HT	0.56	7.99	0.62	2.77
<b>P1 – 95/5</b>	0.54	5.70	0.61	1.88
<b>P1 – 90/10</b>	0.55	7.49	0.64	2.62
<b>P1 – 85/15</b>	0.54	7.5	0.63	2.55
<b>P2 – 95/5</b>	0.58	8.75	0.60	3.04
<b>P2 – 90/10</b>	0.56	8.38	0.65	3.06
<b>P2 – 85/15</b>	0.59	7.97	0.64	2.99
<b>P3 – 95/5</b>	0.56	8.47	0.65	3.08
<b>P3 – 90/10</b>	0.55	7.15	0.50	1.97
<b>P3 – 85/15</b>	0.60	6.79	0.58	2.33
<b>P4 – 95/5</b>	0.55	8.27	0.62	2.83
<b>P4 – 90/10</b>	0.56	7.91	0.44	1.96
<b>P4 – 85/15</b>	0.56	6.92	0.35	1.29

<sup>a</sup> Glass/ITO/PEDOT-PSS/Active Layer/Ca/Al, using chlorobenzene as a solvent. No annealing was performed. Data points were taken after 5 h exposure to 85 °C.

First of all, a preliminary screening experiment was performed to identify the most promising materials for the different copolymer series and conduct a more in-depth lifetime study (up to 700 h) on these derivatives only. Initially, a temperature stress of 85 °C was chosen, as this has become the standard degradation temperature for polymer:PC<sub>61</sub>BM solar cells (related to the maximum usage T).<sup>20d-g</sup> Additionally, the experiments were repeated at 100 °C. Solar cell devices of the various materials were prepared as indicated above and placed on a hotplate in the glove box at the specified temperature. At specifically chosen time intervals, the substrates were removed from the hotplate and the *I-V* characteristics were measured. Figure 5 gathers the data of the degradation study performed at 85 °C during 700 h (Figure S4 shows the results at 100 °C for 140 h). The long exposure times are chosen to reveal any possible additional degradation behavior, as it has been shown to be the case for past experiments.<sup>19,32</sup> The use of relative values (ratio of a value at time *t* and *t*<sub>0</sub>) is not to hide the lower performance of the copolymers, as the initial efficiencies are comparable to P3HT (as shown above), but to provide an accessible means of comparison between the different material systems. As can clearly be observed, copolymers **P2**, **P3** and **P4** lead to more stable blend systems in comparison with the system containing regular P3HT as the donor material. On the other hand, copolymers **P1** seem to give rise to less stable blends, for each of the three different built-in ratios. Closer inspection of Figures 5b and 5d, containing the degradation data on copolymers **P2** and **P4**, reveals a particular trend amongst the various functionalization degrees, i.e. an increased stability upon moving from 5% to 15% of functionalized (ester) side chains. On the other hand, for the alcohol-copolymer **P3** series (Figure 5c), the 10% functionalized copolymer seems to provide the most thermally stable blend. Even though the differences obtained are rather small, the

results of the degradation study at 100 °C confirm the observed phenomena (Figure S4).

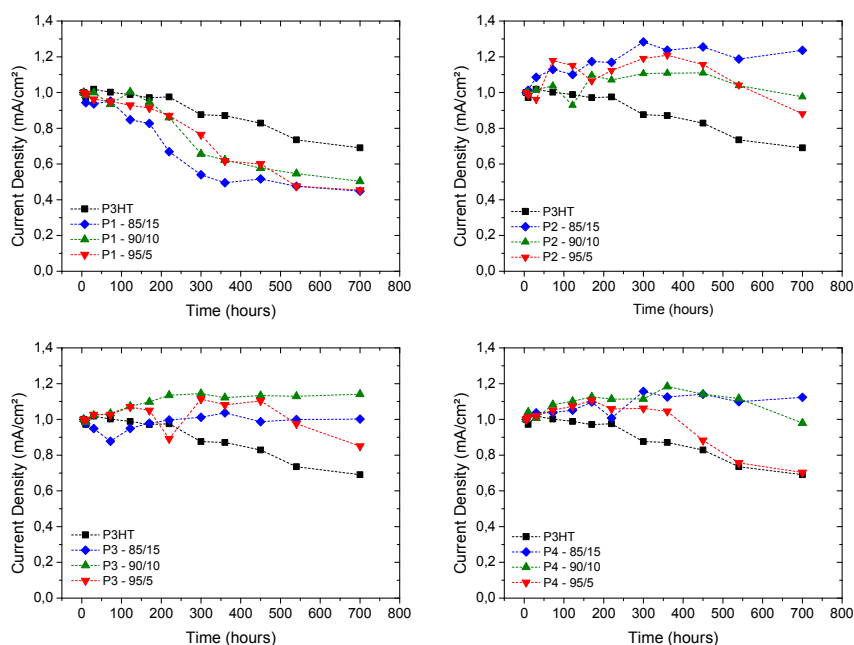


**Figure 5.** Initial screening of the degradation behavior for all P3AT:PC<sub>61</sub>BM-based systems at 85 °C. In all cases Rieke P3HT was included for comparison. Dashed lines serve as a guide to the eye only.

A possible explanation for the differences in stability in comparison with the standard P3HT:PC<sub>61</sub>BM system obviously has to focus on the presence of the functional groups. For copolymers **P4**, (spontaneous) crosslinking of the vinyl groups could possibly explain the increase in stability.<sup>19</sup> A simple test consisting of dipping the substrates in the applied spin-coating solvent (chlorobenzene) revealed, however, that the active layer dissolved in the solvent, so no crosslinking has occurred. For copolymers **P2-P4**, the increase in stability could be due to the presence of dipole-dipole interactions and/or

hydrogen bonds between the functionalities on different polymer strains or between the polymer chains and PC<sub>61</sub>BM. The reason why this is not the case for the **P1** copolymers remains unclear for now.

Following the initial screening of the large material set for the optimal comonomer ratios, a more thorough degradation study was performed in a more dedicated setup. Copolymers **P2** 85/15, **P3** 90/10 and **P4** 85/15 were subjected to a constant heating at 85 °C, and the *I-V* characteristics were measured *in situ* and compared against a reference P3HT:PC<sub>61</sub>BM solar cell. The results for these experiments are visualized in Figure 6.

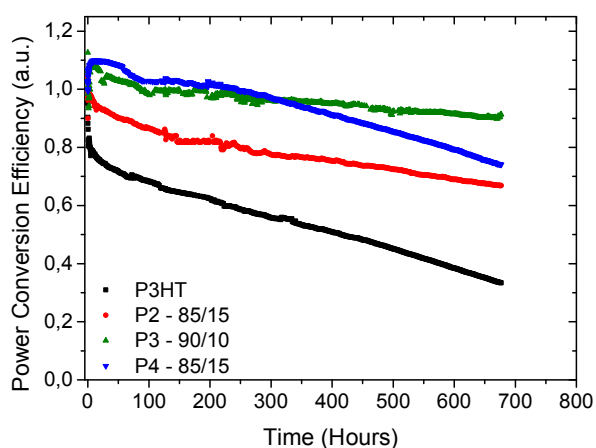


**Figure 6.** Degradation behavior of BHJ OPV devices with photoactive layers based on P3HT and the best-performing P3AT (**P2-P4**) copolymers. The curves were normalized to the first measurement point at 85 °C.

As can be observed, due to the constant monitoring of the efficiency, additional features come into play (separate degradation curves for the  $V_{oc}$ ,  $J_{sc}$  and FF are shown in Figure S5). For the **P3** – 90/10 and **P4** – 85/15 copolymers, an initial increase in efficiency (mainly due to  $J_{sc}$ , Figure S5) can be

---

seen, from which we can deduce that the annealing step (130 °C for 10 min) was not sufficient to afford an optimal nanocrystalline interpenetrating network. The most remarkable observation is the steep decrease in efficiency of the reference P3HT:PC<sub>61</sub>BM solar cell in less than a couple of hours, which has been identified in literature as the initial 'burn-in'.<sup>15a-b</sup> Afterwards, the efficiency remains more stable, although the decrease is still more pronounced for the reference system in comparison with the three copolymers. For the functionalized P3ATs the initial burn-in is almost absent and consequently the overall efficiency remains noticeably higher than for the P3HT:PC<sub>61</sub>BM reference solar cell. As the only different parameter compared to the reference system – assuming a similar purity of all materials, as they are made and purified by the same protocols – is the introduction of functional groups, we can conclude that the increase in stability has to be attributed to the presence of these functions. Among the different copolymers, the ester- and alcohol-functionalized derivatives look somewhat more promising, as a gradual efficiency decrease is noticed for the cinnamoyl derivative after ~300 hours. Obviously, one must note that the exposure of the devices to elevated temperatures for these prolonged periods of time will also have consequences for the electrodes and the interphases, which might lead to (minor) artifacts in the curves.

Optical microscopy images were taken to reveal preliminary information on the film morphology aging process. Figure 7 shows the films of P3HT:PC<sub>61</sub>BM and **P2-P4** - 90/10:PC<sub>61</sub>BM blends at 3 different stages upon exposure to a temperature of 125 °C. As can be observed, the P3HT:PC<sub>61</sub>BM film already contains a multitude of microcrystalline (fullerene) needles after only 15 minutes, whereas the other systems barely show any needle formation. After intense annealing for 24 hours at 125 °C, a small amount of crystallization has

occurred, giving a preliminary indication on the increased thermal stability of these BHJ blends in comparison to regular P3HT:PC<sub>61</sub>BM.

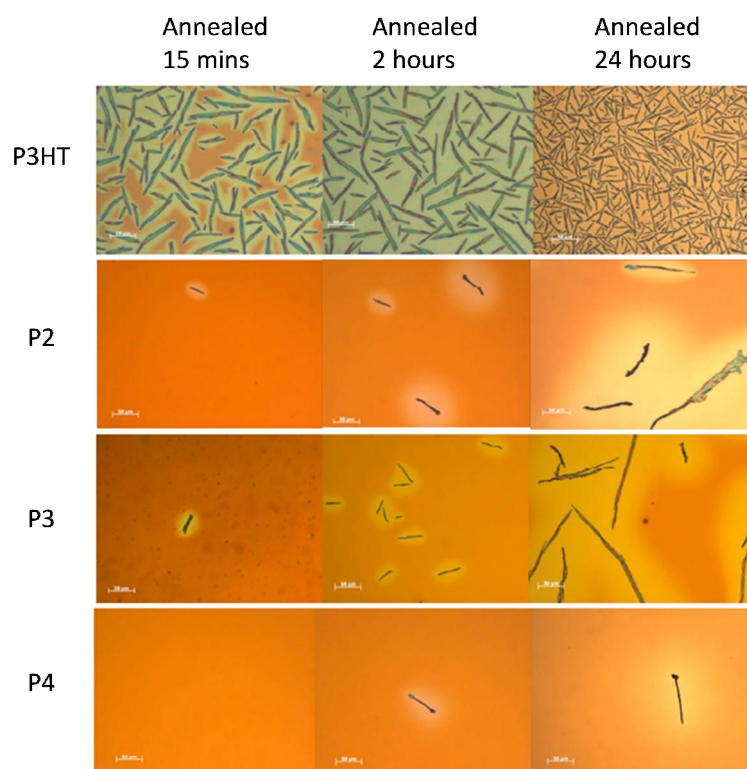


**Figure 7.** Optical microscopy images of P3HT and **P2-P4** - 90/10 films when blended with PC<sub>61</sub>BM, annealed at 125°C for 15 min, 2 h and 24 h.

To gain a more in-depth view, TEM images were taken to visualize the morphological changes occurring within the active layer blends during the thermal treatment at 85 °C in more detail (Figure 8). Based on the data obtained from the degradation study, it was opted to have the images taken directly after the post-process annealing step at 130 °C and after 15 and 700 hours of exposure to the thermal stress. TEM images were made at different

---

places within the samples and no differences in morphology were observed, which makes the images representative for the whole sample. After the initial annealing, some phase-separated needles can already be seen for the reference P3HT:PC<sub>61</sub>BM system. Lighter colored areas are visible around these needles. SAED patterns (also shown in Figure 8) at different locations reveal the content of the mixture. For the darker colored areas, the diffraction pattern shows two concentric rings, which can be ascribed to the presence of both P3HT (outer ring) and PC<sub>61</sub>BM (inner ring) in the blend. When moving toward the lighter area, the inner ring disappears, revealing that this area contains mostly P3HT. The needle-like structures are crystalline and the diffraction patterns show that these structures are indeed PC<sub>61</sub>BM microcrystals. In other words, once a PC<sub>61</sub>BM nucleus is formed, the PC<sub>61</sub>BM surrounding this point will diffuse toward this nucleus and the crystal needle will grow, leaving a depletion area of PC<sub>61</sub>BM-deficient P3HT around it.<sup>33</sup> The TEM image of the reference P3HT:PC<sub>61</sub>BM solar cell exposed to 85 °C for 15 hours shows a substantially higher amount of needles and larger depletion areas. From this, we can conclude that across this timeframe, the surrounding PC<sub>61</sub>BM has diffused even more toward the already formed crystals, leading to an enhanced phase separation and therefore a decrease in efficiency. Finally, after 700 hours of exposure to 85 °C, the phase separation is almost complete, leading to a system consisting mainly of PC<sub>61</sub>BM microcrystals embedded in a P3HT-rich layer.<sup>11c,13</sup> Moving on toward the **P3**:PC<sub>61</sub>BM and **P4**:PC<sub>61</sub>BM blends, we can observe that along the entire time range of 700 hours no PC<sub>61</sub>BM microcrystals are formed, which explains the increased thermal stability for these blends. For the copolymer **P2**:PC<sub>61</sub>BM blend, the TEM images reveal that exposure of the films to 85 °C for 15 hours does not lead to any microcrystal

formation. However, after 700 hours, the system is in a similar state as the reference P3HT:PC<sub>61</sub>BM layer after 15 hours.

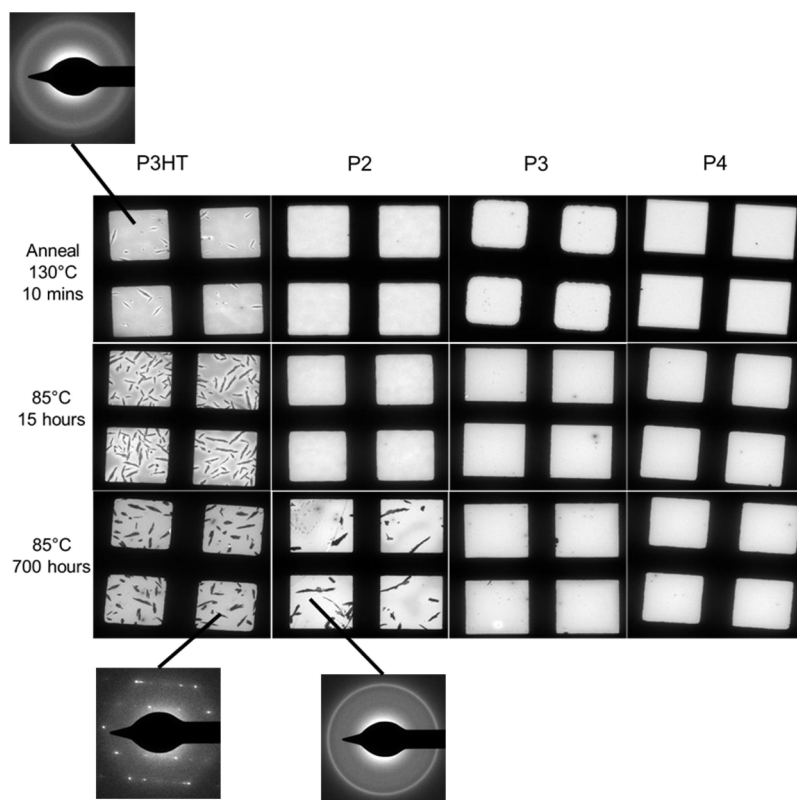


**Figure 8.** TEM images after annealing (10 min at 130 °C, 15 h at 85 °C, and 700 h at 85 °C) for blends of PC<sub>61</sub>BM and P3HT or the most stable P3AT copolymers **P2-P4**.

Integration of the SAED patterns of Figure 8 provides a more accurate picture of the amount of PC<sub>61</sub>BM left in the matrix in between of the needles after exposure to the thermal stress (Figure 9). As illustrated in Figure 9a, the peaks around 3.6 and 4.5 Å are related to P3HT and PC<sub>61</sub>BM, respectively. The more intense the peak at 4.5 Å, the higher the PC<sub>61</sub>BM content in the matrix. As can be observed from Figure 9a, prolonged exposure to 85 °C leads to a strong



decrease in PC<sub>61</sub>BM content for the P3HT:PC<sub>61</sub>BM reference system, proving that it is really PC<sub>61</sub>BM that is diffusing out of the mixture into needle-like structures. On the other hand, the SAED patterns for copolymer **P2** reveal the presence of considerable amounts of PC<sub>61</sub>BM remaining in the matrix, even after completion of the stability test (Figure 9b). The intensity of the PC<sub>61</sub>BM peak somewhat decreased, confirming the results from the TEM images. Finally, Figures 9c and d show that the PC<sub>61</sub>BM content in the matrix of the blends based on copolymers **P3** and **P4** remains practically constant, even after exposure to 85 °C for up to 700 hours.

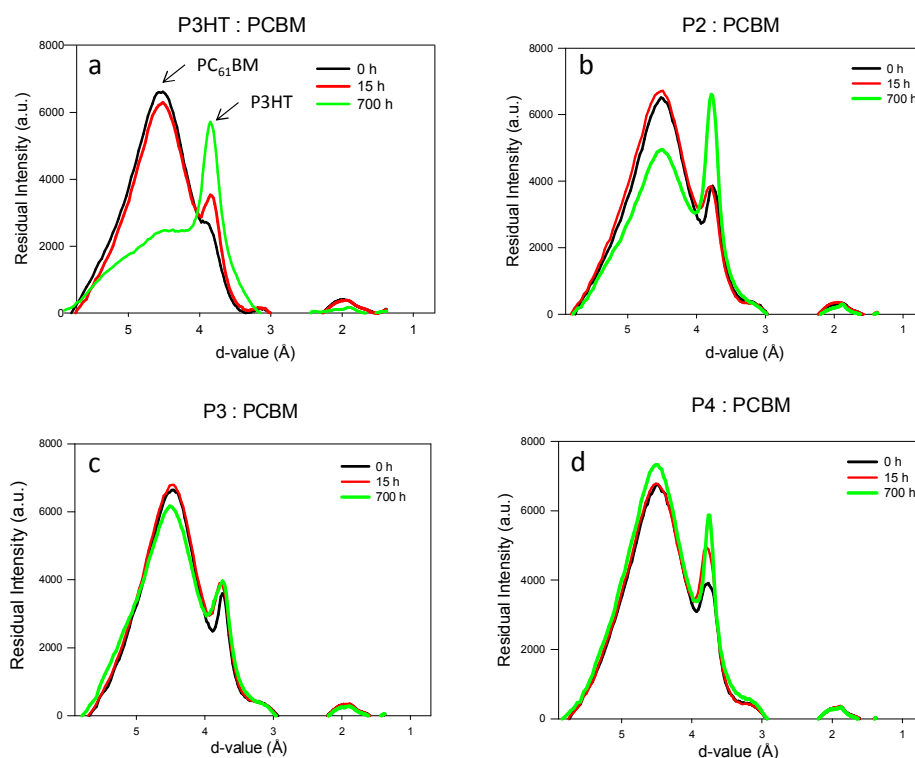


**Figure 9.** Integrated SAED patterns for P3HT:PC<sub>61</sub>BM and the various copolymer:PC<sub>61</sub>BM systems: a) P3HT:PC<sub>61</sub>BM, b) **P2 - 85/15**:PC<sub>61</sub>BM, c) **P3 - 90/10**:PC<sub>61</sub>BM, d) **P4 - 85/15**:PC<sub>61</sub>BM.

Although the glass transition temperatures of the copolymers were not clearly identifiable by regular DSC, previous scattered results (e.g.  $T_g = 30$  °C for **P3** – 90/10 and  $T_g = 19$  °C for **P4** – 90/10)<sup>20h</sup> indicate that these are all in close proximity to the value found for P3HT ( $T_g = 12$  °C). The beneficial effect of the copolymers on blend stability hence does not seem to be merely a  $T_g$  effect causing reduced mobility (which is substantiated by the very similar results obtained upon degradation at various temperatures). Noncovalent interactions (e.g.  $\pi$ - $\pi$ -overlap, hydrogen bonding or dipole-dipole interactions) are probably involved (as well).<sup>14n,34</sup> As there is clearly a change in crystallization kinetics when functionalized P3HT copolymers are blended with PC<sub>61</sub>BM, advanced thermal analysis seems to be well-suited to gain more insight in the underlying principles causing the increased morphological stability.<sup>13</sup> Studies in this direction are currently ongoing within our groups.

### 3.4. Conclusions

In this work, a set of 12 functionalized poly(3-alkylthiophene) random copolymers was efficiently synthesized by the Rieke protocol and analyzed in bulk heterojunction organic solar cell devices with the general aim to increase the thermal stability of the corresponding P3AT:PC<sub>61</sub>BM photoactive layers. Morphology development and phase separation were visualized by TEM (and corresponding SAED patterns) at several stages during the aging process, corroborated by electrical *J-V* testing of devices at increasing annealing times. Even though the functionalization approach might lead to a slight decrease - if any - in initial power conversion efficiency, the overall performance in function of time is considerably enhanced due to the increased thermal stability of (some of) the copolymer:PC<sub>61</sub>BM blends, therefore making this approach a viable option to improve the lifetime of BHJ polymer solar cells.

Further work will be directed toward analysis of the photooxidative sensitivity of the copolymer series and the degradation behavior of encapsulated devices in climate chamber conditions, and in-depth analysis of the mechanism governing the stability improvement by dedicated thermal analysis techniques (crystallization kinetics/dynamics and phase behavior).

### **3.5. Acknowledgments**

We are grateful to Huguette Penxten for UV-Vis, CV and FT-IR measurements. We thank IMEC and Hasselt University for providing the PhD grants of J. K. and S.K. We further acknowledge the OPV-Life project from the IWT (Agentschap voor Innovatie door Wetenschap en Technologie; O&O 080368), the POLYSTAR project from PV ERA-NET, the IWT-SBO project POLYSPEC (Nanostructured POLYmer photovoltaic devices for efficient solar SPECTrum harvesting), and Belspo for supporting the IAP P6/27 and IAP 7/05 networks.

### 3.6. References

<sup>1</sup> a) Thompson, B. C.; Fréchet, J. M. J. *Angew. Chem. Int. Ed.* **2008**, *47*, 58. b) Kippelen, B.; Brédas, J.-L. *Energy Environ. Sci.* **2009**, *2*, 251. c) Brabec, C. J.; Gowrisanker, S.; Halls, J. J. M.; Laird, D.; Jia, S.; Williams, S. P. *Adv. Mater.* **2010**, *22*, 3839. d) Nelson, J. *Mater. Today* **2011**, *14*, 462. e) Service, R.F. *Science* **2011**, *332*, 293. f) Thompson, B. C.; Khlyabich, P. P.; Burkhart, B.; Aviles, A. E.; Rudenko, A.; Shultz, G. V.; Ng, C. F.; Mangubat, L. B. *Green* **2011**, *1*, 29. g) Li, G.; Zhu, R.; Yang, Y. *Nat. Photonics* **2012**, *6*, 153. h) Koster, L. J. A.; Shaheen, S. E.; Hummelen, J. C. *Adv. Energy Mater.* **2012**, *10*, 1246. i) Vandewal, K.; Himmelberger, S.; Salleo, A. *Macromolecules* **2013**, dx.doi.org/10.1021/ma400924b.

<sup>2</sup> a) Green, M. A.; Emery, K.; Hishikawa, Y.; Warta, W.; Dunlop, E. D. *Prog. Photovolt: Res. Appl.* **2012**, *20*, 12. b) He Z.; Zhong C.; Su S.; Xu M.; Wu H.; Cao Y. *Nat. Photonics* **2012**, *6*, 591.

<sup>3</sup> a) Jorgensen, M.; Norrman, K.; Krebs, F. C. *Sol. Energy Mater. Sol. Cells* **2008**, *92*, 686. b) Jorgensen, M.; Norrman, K.; Gevorgyan, S. A.; Tromholt, T.; Andreasen, B.; Krebs, F. C. *Adv. Mater.* **2012**, *24*, 580. c) Grossiord, N.; Kroon, J. M.; Andriessen, R.; Blom, P. W. M. *Org. Electron.* **2012**, *13*, 432. d) Manceau, M.; Rivaton, A.; Gardette, J.-L. Photochemical stability of materials for OPV. In *Stability and Degradation of Organic and Polymer Solar Cells*; Krebs, F.C., Ed.; Wiley, **2012**, 71. e) Lee, J. U.; Jung, J. W.; Jo, J. W.; Jo, W. H. *J. Mater. Chem.* **2012**, *22*, 24265. f) Gupta, S. K.; Dharmalingam, K.; Pali, L. S.; Rastogi, S.; Singh, A.; Garg, A. *Nanomaterials and Energy* **2013**, *2*, 42.

<sup>4</sup> Brabec, C. J. *Sol. Energy Mater. Sol. Cells* **2004**, *83*, 273.

<sup>5</sup> a) Bundgaard, E.; Krebs, F. C. *Sol. Energy Mater. Sol. Cells* **2007**, *91*, 954. b) Heeger, A. J. *Chem. Soc. Rev.* **2010**, *39*, 2354. c) Boudreault, P.-L. T.; Najari, A.; Leclerc, M. *Chem. Mater.* **2011**, *23*, 456. d) Facchetti, A. *Chem. Mater.* **2011**,

---

23, 733. e) Zhou, H.; Yang, L.; You, W.; *Macromolecules* **2012**, *45*, 607. f) Bian, L.; Zhu, E.; Tang, J.; Tang, W.; Zhang, F. *Prog. Polym. Sci.* **2012**, *37*, 1292.

<sup>6</sup> a) Dang, M. T.; Hirsch, L.; Wantz, G. *Adv. Mater.* **2011**, *23*, 3597. b) Marrocchi, A.; Lanari, D.; Facchetti, A.; Vaccaro, L. *Energy Environ. Sci.* **2012**, *5*, 8457. (c) Dang, M. T.; Hirsch, L.; Wantz, G.; Wuest, J. D. *Chem. Rev.* **2013**, *113*, 3734.

<sup>7</sup> a) Ma, W.; Yang, C.; Gong, X.; Lee, K.; Heeger, A. J. *Adv. Funct. Mater.* **2005**, *15*, 1617. b) Li, G.; Shrotriya, V.; Huang, J.; Yao, Y.; Moriarty, T.; Emery, K.; Yang, Y. *Nat. Mater.* **2005**, *4*, 864.

<sup>8</sup> Zimmermann, B.; Würfel, U.; Niggemann, M. *Sol. Energy Mater. Sol. Cells* **2009**, *93*, 491.

<sup>9</sup> Tipnis, R.; Bernkopf, J.; Jia, S.; Krieg, J.; Li, S.; Storch, M.; Laird, D. *Sol. Energy Mater. Sol. Cells* **2009**, *93*, 442.

<sup>10</sup> a) Manceau, M.; Rivaton, A.; Gardette, J.-L.; Guillerez, S.; Lemaitre, N. *Polym. Degrad. Stab.* **2009**, *94*, 898. b) Manceau, M.; Rivaton, A.; Gardette, J.-L.; Guillerez, S.; Lemaitre, N. *Sol. Energy Mater. Sol. Cells* **2011**, *95*, 1315. c) Dupuis, A.; Wong-Wah-Chung, P.; Rivaton, A.; Gardette, J.-L. *Polym. Degrad. Stab.* **2012**, *97*, 366.

<sup>11</sup> a) Yang, X.; van Duren, J. K. J.; Rispens, M. T.; Hummelen, J. C.; Janssen, R. A. J.; Michels, M. A. J.; Loos, J. *Adv. Mater.* **2004**, *16*, 802. b) Yang, X.; van Duren, J. K. J.; Janssen, R. A. J.; Michels, M. A. J.; Loos, J. *Macromolecules* **2004**, *37*, 2151. c) Bertho, S.; Janssen, G.; Cleij, T. J.; Conings, B.; Moons, W.; Gadisa, A.; D'Haen, J.; Goovaerts, E.; Lutsen, L.; Manca, J.; Vanderzande, D. *Sol. Energy Mater. Sol. Cells* **2008**, *92*, 753.

<sup>12</sup> Manceau, M.; Helgesen, M.; Krebs, F. C. *Polym. Degrad. Stab.* **2010**, *95*, 2666.

<sup>13</sup> a) Zhao, J.; Swinnen, A.; Van Assche, G.; Manca, J.; Vanderzande, D.; Van Mele, B. *J. Phys. Chem. B* **2009**, *113*, 1587. b) Demir, F.; Van den Brande, N.; Van Mele, B.; Bertho, S.; Vanderzande, D.; Manca, J.; Van Assche, G. *J. Therm. Anal. Calorim.* **2011**, *105*, 845.

<sup>14</sup> a) Marcos Ramos, A.; Rispens, M. T.; van Duren, J. K. J.; Hummelen, J. C.; Janssen, R. A. J. *J. Am. Chem. Soc.* **2001**, *123*, 6714. b) Sivula, K.; Ball, Z. T.; Watanabe, N.; Fréchet, J. M. J. *Adv. Mater.* **2006**, *18*, 206. c) Zhou, Z.; Chen, X.; Holdcroft, S. *J. Am. Chem. Soc.* **2008**, *130*, 11711. d) Woo, C. H.; Thompson, B. C.; Kim, B. J.; Toney, M. F.; Fréchet, J. M. J. *J. Am. Chem. Soc.* **2008**, *130*, 16324. e) Miyanishi, S.; Tajima, K.; Hashimoto, K. *Macromolecules* **2009**, *42*, 1610. f) Zhang, Y.; Yip, H.-L.; Acton, O.; Hau, S.K.; Huang, F.; Jen, A.K.-Y. *Chem. Mater.* **2009**, *21*, 2598. g) Kim, B. J.; Miyamoto, Y.; Ma, B.; Fréchet, J. M. J. *Adv. Funct. Mater.* **2009**, *19*, 2273. h) Lee, J. U.; Jung, J. W.; Emrick, T.; Russell, T. P.; Jo, W. H. *J. Mater. Chem.* **2010**, *20*, 3287. i) Hsieh, C.-H.; Cheng, Y.-J.; Li, P.-J.; Chen, C.-H.; Dubosc, M.; Liang, R.-M.; Hsu, C.-S. *J. Am. Chem. Soc.* **2010**, *13*, 4887. j) Vandenberg, J.; Conings, B.; Bertho, S.; Kesters, J.; Spoltore, D.; Esiner, S.; Zhao, J.; Van Assche, G.; Wienk, M. M.; Maes, W.; Lutsen, L.; Van Mele, B.; Janssen, R. A. J.; Manca, J.; Vanderzande, D. *J. M. Macromolecules* **2011**, *44*, 8470. k) Lee, U. R.; Lee, T. W.; Hoang, M. H.; Kang, N. S.; Yu, J. W.; Kim, K. H.; Lim, K.-G.; Lee, T.-W.; Jin, J.-I.; Choi, D. H. *Org. Electron.* **2011**, *12*, 269. l) Griffini, G.; Douglas, J. D.; Piliago, C.; Holcombe, T. W.; Turri, S.; Fréchet, J. M. J.; Mynar, J. L. *Adv. Mater.* **2011**, *23*, 1660. m) Kim, H. J.; Han, A.-R.; Cho, C.-H.; Kang, H.; Cho, H.-H.; Lee, M. Y.; Fréchet, J. M. J.; Oh, J. H.; Kim, B. J. *Chem. Mater.* **2012**, *24*, 215. n) Lin, Y.; Lim, J. A.; Wei, Q.; Mannsfeld, S. C. B.; Briseno, A. L.; Watkins, J. J. *Chem. Mater.* **2012**, *24*, 622. o) Yun, H. M.; Kim, J.; Yang, C.; Kim, J. Y. *Sol. Energy Mater. Sol. Cells* **2012**, *104*, 7. p) Nam, C.-Y.; Qin, Y.; Park, Y. S.; Hlaing, H.; Lu, X.; Ocko, B. M.; Black, C. T.; Grubbs, R. B.

---

*Macromolecules* **2012**, *45*, 2338. q) He, D.; Du, X.; Zhang, W.; Xiao, Z.; Ding, L. *J. Mater. Chem. A* **2013**, *1*, 4589. r) Ouhib, F.; Tomassetti, M.; Manca, J.; Piersimoni, F.; Spoltore, D.; Bertho, S.; Moons, H.; Lazzaroni, R.; Desbief, S.; Jerome, C.; Detrembleur, C. *Macromolecules* **2013**, *46*, 785.

<sup>15</sup> a) Peters, C. H.; Sachs-Quintana, I. T.; Kastrop, J. P.; Beaupré, S.; Leclerc, M.; McGehee, M. D. *Adv. Energy Mater.* **2011**, *1*, 491. b) Peters, C. H.; Sachs-Quintana, I. T.; Mateker, W. R.; Heumueller, T.; Rivnay, J.; Noriega, R.; Beiley, Z. M. *Adv. Mater.* **2012**, *24*, 663.

<sup>16</sup> Tournebize, A.; Bussiere, P.-O.; Wong-Wah-Chung, P.; Therias, S.; Rivaton, A.; Gardette, J.-L.; Beaupré, S.; Leclerc, M. *Adv. Energy Mater.* **2013**, *3*, 478.

<sup>17</sup> Mateker, W. R.; Douglas, J. D.; Cabanetos, C.; Sachs-Quintana, I. T.; Bartelt, J. A.; Hoke, E. T.; Labban, A. E.; Beaujuge, P. M.; Fréchet, J. M. J.; McGehee, M. D. *Energy Environ. Sci.* **2013**, *6*, 2529.

<sup>18</sup> a) Li, Z.; Wong, H. C.; Huang, Z.; Zhong, H.; Tan, C. H.; Tsoi, W. C.; Kim, J. S.; Durrant, J. R.; Cabral, J. T. *Nat. Commun.* **2013**, DOI: 10.1038/ncomms3227. b) Piersimoni, F.; Degutis, G.; Bertho, S.; Vandewal, K.; Spoltore, D.; Vangerven, T.; Drijkoningen, J.; Van Bael, M. K.; Hardy, A.; D'Haen, J.; Maes, W.; Vanderzande, D.; Nesladek, M.; Manca, J. *J. Polym. Sci.: Polym. Phys.* **2013**, *51*, 1209.

<sup>19</sup> a) Lutsen, L.; Vanderzande, D.; Campo, B. *PCT Int. Appl.* **2011**, WO 2011069554 A1 20110616. b) Lutsen, L.; Vanderzande, D.; Campo, B. *PCT Int. Appl.* **2010**, WO 2010000504 A1 20100107.

<sup>20</sup> a) Campo, B. J.; Oosterbaan, W. D.; Gilot, J.; Cleij, T. J.; Lutsen, L.; Janssen, R. A. J.; Vanderzande, D. *Proceedings of SPIE*, **2009**, 7416, 74161G. b) Campo, B. J.; Duchateau, J.; Ganivet, C. R.; Ballesteros, B.; Gilot, J.; Wienk, M. M.; Oosterbaan, W. D.; Lutsen, L.; Cleij, T. J.; de la Torre, G.; Janssen, R. A. J.; Vanderzande, D.; Torres, T. *Dalton Trans.* **2011**, *40*, 3979. c) Oosterhout, S. D.

### Chapter 3

---

L.; Koster, J. A.; van Bavel, S. S.; Loos, J.; Stenzel, O.; Thiedmann, R.; Schmidt, V.; Campo, B.; Cleij, T. J.; Lutsen, L.; Vanderzande, D.; Wienk, M. M.; Janssen, R. A. J. *Adv. Energy Mater.* **2011**, *1*, 90. d) Tanenbaum, D. M.; Hermenau, M.; Voroshazi, E.; Lloyd, M. T.; Galagan, Y.; Zimmermann, B.; Hösel, M.; Dam, H. F.; Jørgensen, M.; Gevorgyan, S. A.; Kudret, S.; Maes, W.; Lutsen, L.; Vanderzande, D.; Würfel, U.; Andriessen, R.; Rösch, R.; Hoppe, H.; Lira-Cantu, M.; Rivaton, A.; Uzunoğlu, G. Y.; Germack, D.; Andreasen, B.; Madsen, M. V.; Norrman, K.; Krebs, F. C. *RSC Adv.* **2012**, *2*, 882. e) Rösch, R.; Tanenbaum, D. M.; Jørgensen, M.; Seeland, M.; Bärenklau, M.; Hermenau, M.; Voroshazi, E.; Lloyd, M. T.; Galagan, Y.; Zimmermann, B.; Würfel, U.; Hösel, M.; Dam, H. F.; Gevorgyan, S. A.; Kudret, S.; Maes, W.; Lutsen, L.; Vanderzande, D.; Andriessen, R.; Teran-Escobar, G.; Lira-Cantu, M.; Rivaton, A.; Uzunoğlu, G. Y.; Germack, D.; Andreasen, B.; Madsen, M. V.; Norrman, K.; Hoppe, H.; Krebs, F. C. *Energy Environ. Sci.* **2012**, *5*, 6521. f) Andreasen, B.; Tanenbaum, D. M.; Hermenau, M.; Voroshazi, E.; Lloyd, M. T.; Galagan, Y.; Zimmermann, B.; Kudret, S.; Maes, W.; Lutsen, L.; Vanderzande, D.; Würfel, U.; Andriessen, R.; Rösch, R.; Hoppe, H.; Teran-Escobar, G.; Lira-Cantu, M.; Rivaton, A.; Uzunoğlu, G. Y.; Germack, D.; Hösel, M.; Dam, H. F.; Jørgensen, M.; Gevorgyan, S. A.; Madsen, M. V.; Bundgaard, E.; Krebs, F. C.; Norrman, K. *Phys. Chem. Chem. Phys.* **2012**, *14*, 11780. g) Teran-Escobar, G.; Tanenbaum, D. M.; Voroshazi, E.; Hermenau, M.; Norrman, K.; Lloyd, M. T.; Galagan, Y.; Zimmermann, B.; Hösel, M.; Dam, H. F.; Jørgensen, M.; Gevorgyan, S.; Kudret, S.; Maes, W.; Lutsen, L.; Vanderzande, D.; Würfel, U.; Andriessen, R.; Rösch, R.; Hoppe, H.; Rivaton, A.; Uzunoğlu, G. Y.; Germack, D.; Andreasen, B.; Madsen, M. V.; Bundgaard, E.; Krebs, F. C.; Lira-Cantu, M. *Phys. Chem. Chem. Phys.* **2012**, *14*, 11824. h) Bertho, S.; Campo, B.; Piersimoni, F.; Spoltore, D.; D'Haen, J.; Lutsen, L.; Maes, W.; Vanderzande, D.; Manca, J. *Sol. Energy Mater. Sol. Cells* **2013**, *110*, 69. i)



---

Campo, B.; Kesters, J.; Bevk, D.; Gilot, J.; Bolink, H. J.; Zhao, J.; Bolsée, J.-C.; Oosterbaan, W. D.; Bertho, S.; Ruttens, B.; D'Haen, J.; Manca, J.; Lutsen, L.; Maes, W.; Van Assche, G.; Janssen, R. A. J.; Vanderzande, D. *Org. Electron.* **2013**, *14*, 523.

<sup>21</sup> Kudret, S.; D'Haen, J.; Oosterbaan, W.; Lutsen, L.; Vanderzande, D.; Maes, W. *Adv. Synth. Catal.* **2013**, *355*, 569.

<sup>22</sup> a) Chen, T. A.; Wu, X. M.; Rieke, R. D. *J. Am. Chem. Soc.* **1995**, *117*, 233. b) Oosterbaan, W. D.; Vrindts, V.; Berson, S.; Guillerez, S.; Douhéret, O.; Ruttens, B.; D'Haen, J.; Adriaensens, P.; Manca, J.; Lutsen, L.; Vanderzande, D. *J. Mater. Chem.* **2009**, *19*, 5424.

<sup>23</sup> a) *Organozinc Reagents, A Practical Approach* (Eds.: P. Knochel, P. Jones), Oxford University Press, New York, **1999**. b) *The Chemistry of Organozinc Compounds* (Eds: Z. Rappoport, I. Marek), John Wiley & Sons Ltd, West Sussex, England, **2006**. c) Knochel, P.; Schade, M. A.; Bernhardt, S.; Manolikakes, G.; Metzger, A.; Piller, F. M.; Rohbogner, C. J.; Mosrin, M. *Beilstein J. Org. Chem.* **2011**, *7*, 1261; d) Wu, X.-F. *Chem. Asian J.* **2012**, *7*, 2505; e) Wu, X.-F.; Neumann, H. *Adv. Synth. Catal.* **2012**, *354*, 3141.

<sup>24</sup> The importance of the Rieke zinc synthetic method for the field of organic photovoltaics cannot be underestimated though, as a large number of studies are based on the commercially available 'Rieke P3HT'.

<sup>25</sup> a) Chen, T. A.; O'Brien, R. A.; Rieke, R. D. *Macromolecules* **1993**, *26*, 3462. b) Coppo, P.; Adams, H.; Cupertino, D. C.; Yeates, S. G.; Turner, M. L. *Chem. Commun.* **2003**, 2548.

<sup>26</sup> Bauerle, P.; Pfau, F.; Schlupp, H.; Wurthner, F.; Gaudl, K.-U.; Caro, M. B.; Fischer, P., *J. Chem. Soc. Perkin Trans 2* **1993**, 489.

<sup>27</sup> Kim, S.-H.; Kim, J.-G. *Bull. Korean Chem. Soc.* **2009**, *30*, 2283.

### Chapter 3

---

<sup>28</sup> Lanzi, M.; Costa-Bizzarri, P.; Paganin, L.; Cesari, G. *React. Funct. Polym.* **2007**, *67*, 329.

<sup>29</sup> Iovu, M. C.; Jeffries-El, M.; Sheina, E. E.; Cooper, J. R.; McCullough, R. D. *Polymer* **2005**, *46*, 8582.

<sup>30</sup> a) Babudri, F.; Colangiuli, D.; Di Bari, L.; Farinola, G. M.; Hassan Omar, O.; Naso, F.; Pescitelli, G. *Macromolecules* **2006**, *39*, 5206; b) Vandeleene, S.; Van den Bergh, K.; Verbiest, T.; Koeckelberghs, G. *Macromolecules* **2008**, *41*, 5123.

<sup>31</sup> Lee, J. K.; Ma, W. L.; Brabec, C. J.; Yuen, J.; Moon, J. S.; Kim, J. Y.; Lee, K.; Bazan, G. C.; Heeger, A. J. *J. Am. Chem. Soc.*, **2008**, *130*, 3619.

<sup>32</sup> Voroshazi, E.; Verreet, B.; Aernouts, T.; Heremans, P. *Sol. Energy Mater. Sol. Cells* **2011**, *95*, 1303.

<sup>33</sup> Swinnen, A.; Haeldermans, I.; van de Ven, M.; D'Haen, J.; Vanhoyland, G.; Aresu, S.; D'Olieslaeger, M.; Manca, J. *Adv. Funct. Mater.* **2006**, *16*, 760.

<sup>34</sup> a) Chen, Y.-H.; Huang, P.-T.; Lin, K.-C.; Huang, Y.-J.; Chen, C.-T. *Org. Electron.* **2012**, *13*, 283. b) Lobez, J. M.; Andrew, T. L.; Bulovic, V.; Swager, T. M. *ACS Nano* **2012**, *6*, 3044.

### 3.7. Supporting information

**Table S1.** Electrochemical characterization of the copolymers.

Polymer	HOMO (eV)	LUMO (eV)	$E_g$ opt (eV)
Rieke P3HT	-5.25	-3.37	1.88
<b>P1</b> - 95/5	-5.16	-3.24	1.92
<b>P1</b> - 90/10	-5.26	-3.34	1.92
<b>P1</b> - 85/15	-5.12	-3.20	1.92
<b>P2</b> - 95/5	-5.17	-3.26	1.91
<b>P2</b> - 90/10	-5.16	-3.26	1.90
<b>P2</b> - 85/15	-5.19	-3.26	1.93
<b>P3</b> - 95/5	-5.13	-3.25	1.88
<b>P3</b> - 90/10	-5.21	-3.32	1.89
<b>P3</b> - 85/15	-4.84	-2.93	1.91
<b>P4</b> - 95/5	-5.13	-3.21	1.92
<b>P4</b> - 90/10	-5.17	-3.28	1.89
<b>P4</b> - 85/15	-5.11	-3.22	1.89

**Table S2.** Optimized solar cell efficiencies for BHJ blends based on P3HT and copolymers **P1-P4**.

Donor material	$V_{oc}$	$J_{sc}$	FF	$\eta$
P3HT	0.52	11.86	0.56	3.48
<b>P1</b> - 95/5	0.54	7.97	0.62	2.67
<b>P1</b> - 90/10	0.52	8.39	0.60	2.61
<b>P1</b> - 85/15	0.52	5.70	0.58	1.68
<b>P2</b> - 95/5	0.58	10.20	0.62	3.69
<b>P2</b> - 90/10	0.54	9.26	0.58	2.88
<b>P2</b> - 85/15	0.58	9.18	0.57	3.04
<b>P3</b> - 95/5	0.56	9.33	0.64	3.34
<b>P3</b> - 90/10	0.60	6.39	0.57	2.19
<b>P3</b> - 85/15	0.64	6.11	0.61	2.39
<b>P4</b> - 95/5	0.56	8.72	0.63	3.07
<b>P4</b> - 90/10	0.60	6.71	0.60	2.43
<b>P4</b> - 85/15	0.60	6.61	0.65	2.58

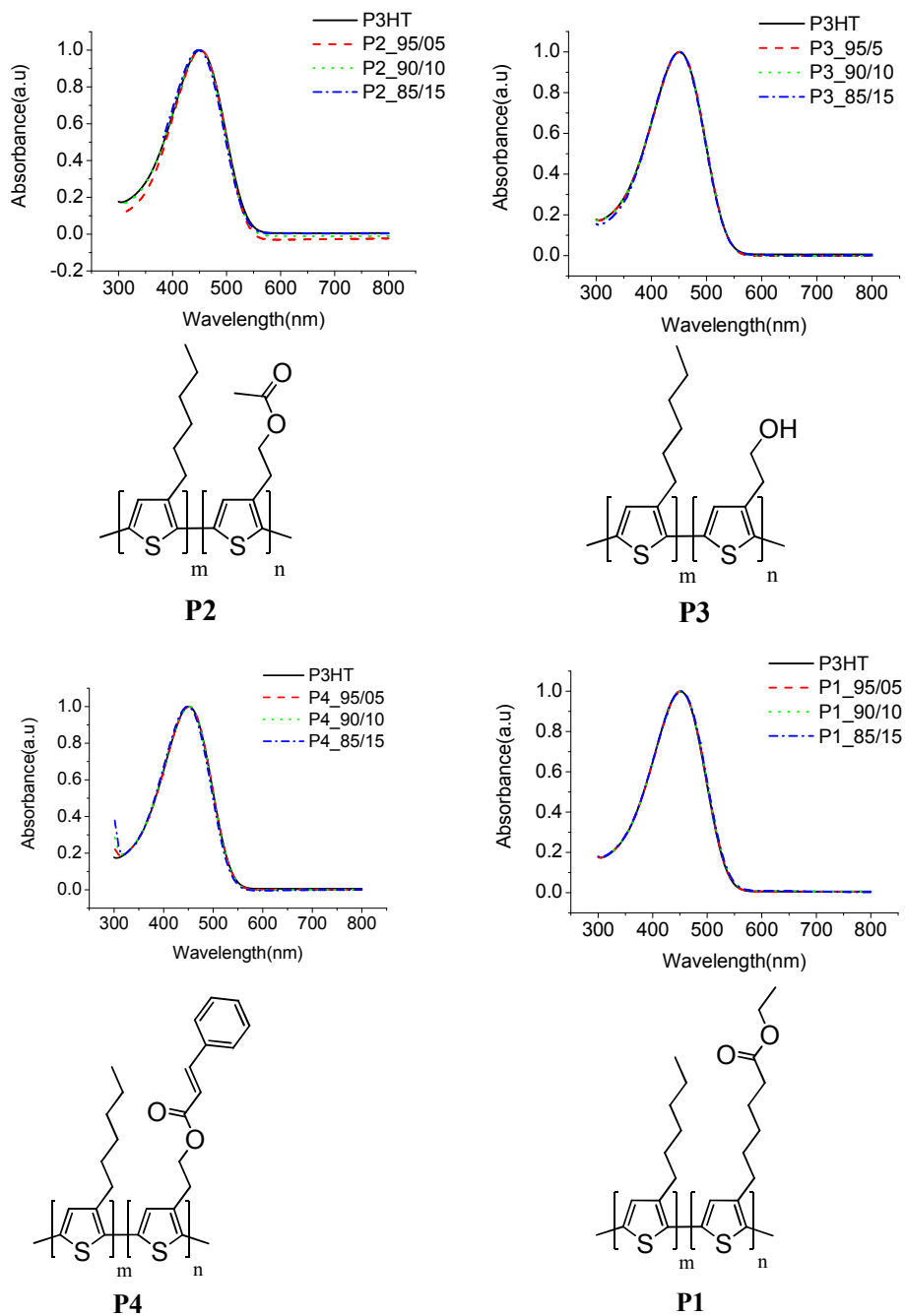


Figure S1. UV-Vis characteristics of the copolymers in chloroform solution.

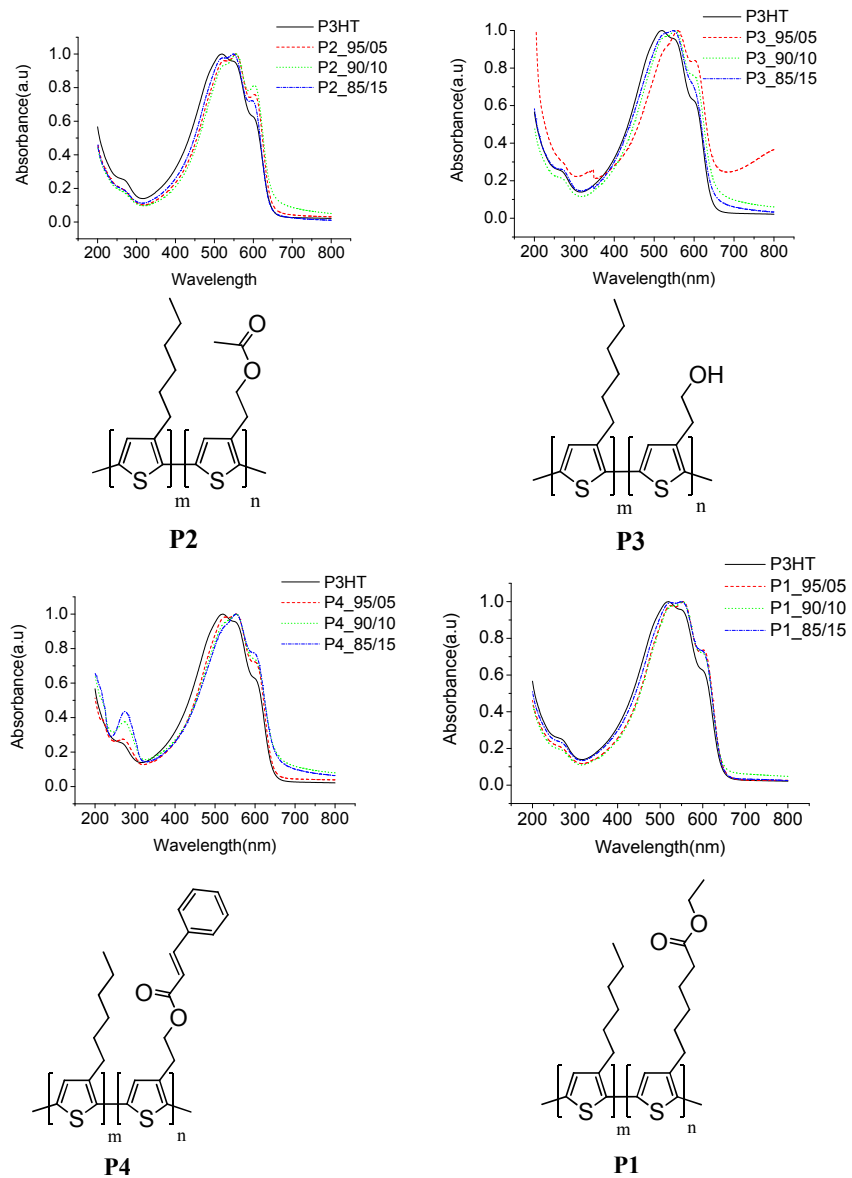


Figure S2. UV-Vis characteristics of the copolymers in thin film.

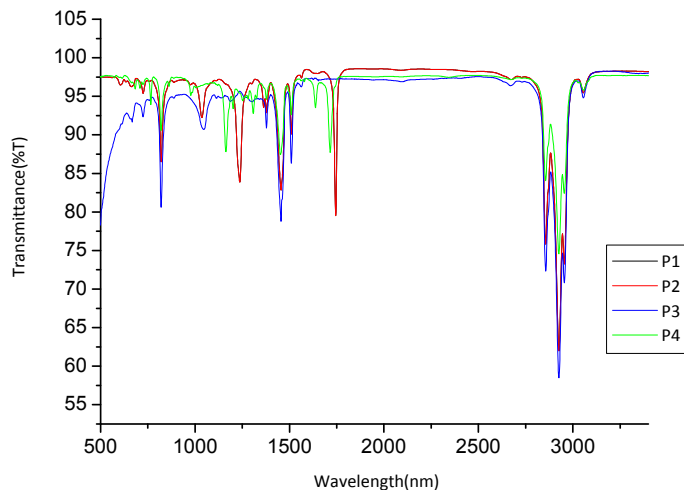


Figure S3. FT-IR spectrum of polymers P1-P4:85/15

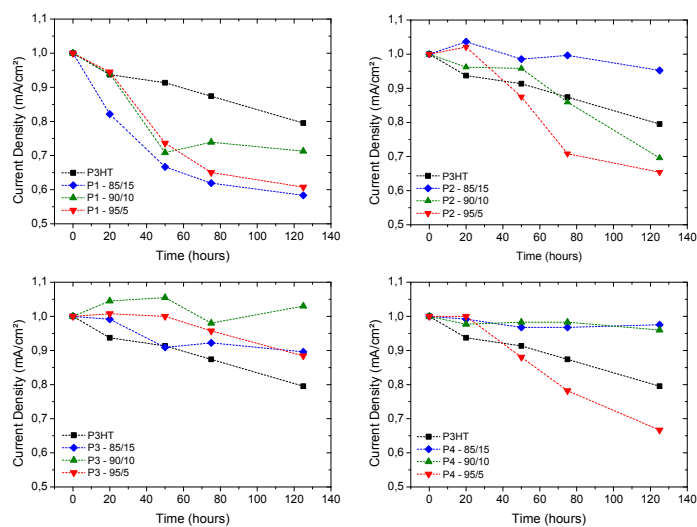
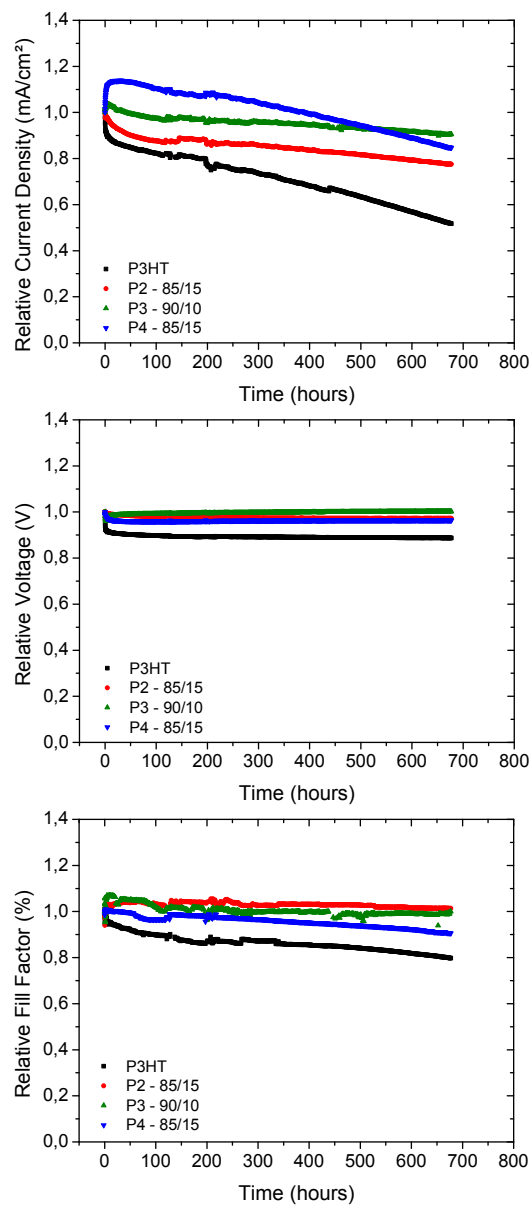


Figure S4. Output characteristics for the 'basic' thermal degradation study at 100 °C (for 140 h) for devices based on P1-P4:PC<sub>61</sub>BM active layers. Dashed lines serve as a guide to the eye only.



**Figure S5.** Degradation curves ( $V_{OC}$ ,  $J_{SC}$  and FF) for BHJ organic solar cells based on P3HT and the best-performing P3AT (**P2-P4**) copolymers (700 h at 85 °C). The curves were normalized to the first measurement point at 85 °C.



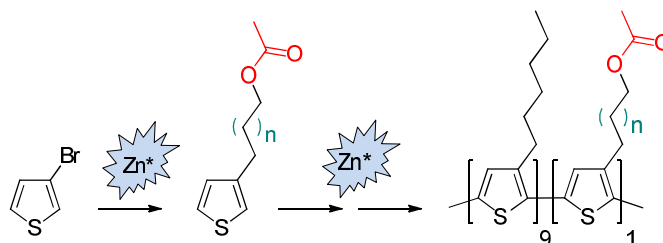


---

# Chapter 4

Facile synthesis of 3-( $\omega$ -acetoxyalkyl)-thiophenes and derived copolythiophenes using Rieke zinc

---



---

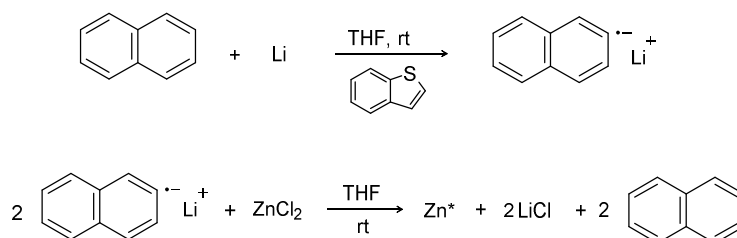
\* Facile synthesis of 3-( $\omega$ -acetoxyalkyl)thiophenes and derived copolythiophenes using Rieke zinc: Kudret, S.; Kesters, J.; Janssen, S.; Van den Brande, N.; Defour, M.; Van Mele, B.; Manca, J.; Lutsen, L.; Vanderzande, D.; Maes, W. to be submitted.

#### 4.1. Introduction

Polymer solar cells have a number of advantages over traditional silicon-based photovoltaics, such as versatility in form factor (flexible, semi-transparent, colored) and better performance in diffuse light, which makes them particularly attractive for portable or wearable electronics and building-integrated photovoltaics.<sup>1</sup> Moreover, solution-processability allows low cost large-area thin film fabrication by e.g. roll-to-roll printing. Hesitations by (photovoltaic) industry to make large investments in OPV are driven by the limited device/module efficiency and lifetime, so far not at the required levels to successfully compete with the existing PV technologies. Among the conjugated polymers applied as electron donor materials in bulk heterojunction (BHJ) organic photovoltaics (OPV), polythiophenes have been the most studied and implemented material class,<sup>2</sup> with P3HT (poly(3-hexylthiophene)) as the most famous representative.<sup>3</sup> Solution processability can be ensured by the introduction of alkyl side chains at the  $\beta$ -position(s) of the aromatic thiophene units.<sup>4,5</sup> It is known that these side chains do not only improve solubility and hence processability, but also alter the polymer's electrical and optical properties.<sup>6-9</sup> It has been reported that poly(3-alkylthiophenes) (P3ATs) with a chain length of more than 10 carbon atoms show characteristics of liquid crystals.<sup>7</sup> In another study by McCullough *et al.*, it was stated that alkyl chains up to 10-12 carbon atoms lead to a consistent increase in mean conjugation length due to a higher planarity of the main polymer chain.<sup>8</sup> On the other hand, Koeckelberghs and co-workers have seen important substituent effects on the chiroptical and magnetic properties of polythiophene materials.<sup>9</sup> The nature of the side chains can also lead to important modifications in the nanomorphology of the polymer:fullerene active layer blends applied in BHJ devices,<sup>1,10,11</sup> a crucial aspect to achieve

highly efficient and stable organic solar cells. A large number of polythiophenes bearing a functional moiety at the end of (some of) the side chains, such as esters,<sup>12</sup> alcohols,<sup>12c</sup> sulfonates,<sup>13</sup> fluoroalkyls,<sup>14</sup> mesogenic groups,<sup>15</sup> and optically active units,<sup>9,16</sup> has been prepared and evaluated in OPV.

The building blocks for P3ATs, 3-substituted dibromothiophene derivatives, are generally prepared via cross-coupling of organomagnesium compounds to 3-bromothiophene. On the other hand, organozinc reagents are also useful synthetic tools as they can readily be prepared by oxidative addition of Rieke zinc to alkyl halides,<sup>17</sup> and, unlike Grignard reagents and organolithium compounds, they tolerate the presence of a wide range of functional groups, such as ketones, nitriles, esters and other halides.<sup>18</sup> The polythiophenes themselves are commonly synthesized via the Grignard metathesis (GRIM) protocol.<sup>2,3,19</sup> The alternative Rieke method,<sup>20</sup> which uses organozinc intermediates, is much less popular,<sup>21</sup> mainly due to difficulties in the (reproducible) preparation of the reactive Rieke zinc.<sup>22</sup> Nevertheless, as for the monomer synthesis, the wide functional group tolerance is an important advantage. Recently, we have developed an optimized method for the preparation of highly reactive Rieke zinc metal (Zn\*) under standard laboratory conditions.<sup>17</sup> This procedure involves the preparation of Zn\* by reduction of the zinc chloride precursor with lithium naphthalenide prepared *in situ* in the presence of a catalytic amount (3 mol%) of benzothiophene (Scheme 1). The active zinc species readily undergoes oxidative addition to alkyl halides and 2,5-dibromothiophenes under mild conditions to yield the corresponding organozinc intermediates.

**Scheme 1.** Optimized procedure for the preparation of Rieke zinc.

In this study, the optimized Rieke zinc method was applied to synthesize ester-functionalized dibromothiophenes with different alkyl chain length, as well as copolymers containing the functional monomers, in a straightforward and efficient way. As recent work<sup>12</sup> has shown that ester-functionalized random copolythiophenes can give similar solar cell efficiencies as regular P3HT, as far as the functionalized side chains are introduced in a moderate ratio, while improving the thermal stability of the BHJ active layer,<sup>1g,23</sup> the synthesized materials allow to analyze the effect of functionalized side chains (length) on BHJ blend nanomorphology formation and evolution, and thereby achieve a more profound fundamental insight in molecular miscibility on a molecular scale. Moreover, further post-polymerization reactions readily afford alternative functionalized polythiophene derivatives.<sup>12c,24</sup>

## 4.2. Results and discussion

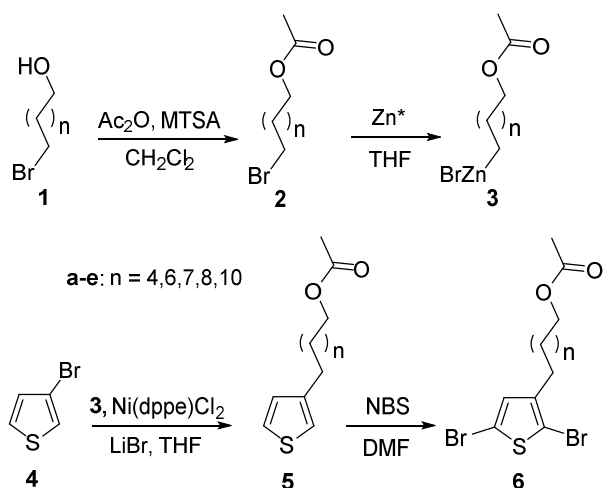
3-Alkylthiophenes bearing a pendant functional group within the alkyl side chain are attractive building blocks for the preparation of functionalized P3ATs.<sup>5,25</sup> Despite the fact that syntheses of 3-substituted alkylthiophenes bearing a terminal carboxylic acid, amide or nitrile functional group have been reported, the synthetic routes leading to these materials after often tedious,

involving multiple steps. Carboxylic acid and sulfonate-functionalized thiophenes were synthesized starting from 3-methylthiophene<sup>26</sup> or 3-(2-hydroxyethyl)thiophene<sup>12,27</sup> by laborious consecutive chain extensions. Bäuerle *et al.* developed a method for the synthesis of 3-substituted thiophenes bearing a terminal halogen substituent on alkyl side chains of length  $n \geq 4$  by reaction of 3-bromothiophene with the Grignard reagents of  $\omega$ -(*p*-methoxyphenoxy)alkyl bromides, followed by removal of the *p*-methoxyphenoxy group with HBr/acetic anhydride to afford 3-( $\omega$ -bromoalkyl)thiophenes.<sup>28</sup> Further functionalization was achieved by reaction with KCN to yield the nitrile derivatives, which were later hydrolyzed to the corresponding carboxylic acids. A similar route for the preparation of carboxylic acid-functionalized thiophenes employed a Grignard coupling reaction with long alkyl chain allylic bromides.<sup>29</sup> This method has, however, not been used for  $\omega$ -(3-thienyl)alkanecarboxylic acids with alkyl chain lengths below  $n = 11$ . Alternatively, Dai *et al.* have prepared thiophene compounds possessing carboxylic acid, carboxamide, imide or amine (hydrochloride) functionalities in two steps utilizing a commercially available organozinc reagent, 4-cyanobutylzinc bromide, in Kumada-type cross coupling reactions.<sup>30</sup> The method was reported to be remarkably more efficient, affording the desired products in fewer synthetic steps.

We have chosen to synthesize dibromothiophene monomers with different alkyl chain lengths, varying from hexyl to dodecyl, and an acetate end group starting from 3-bromothiophene and employing self-prepared Rieke reagents (Scheme 2). For this purpose, the recently optimized Rieke zinc conditions were beneficially applied.<sup>17</sup> The monomers were then used consecutively in polymerization reactions (in combination with regular 2,5-dibromothiophene),

again employing the Rieke zinc protocol, toward the final copolythiophene semiconducting polymers.

**Scheme 2.** Preparation of  $\omega$ -(2,5-dibromothiophen-3-yl)alkyl acetate monomers **6a-e** employing Rieke zinc.



The desired  $\omega$ -(2,5-dibromothiophen-3-yl)alkyl acetate monomers **6a-e** were derived from 3-bromothiophene (**4**) and the respective ( $\omega$ -acetoxyalkyl)zinc bromides **3**, and subsequent bromination. As the required organozinc reagents are not commercially available, they had to be prepared and a simple procedure has been developed for that cause. The synthetic sequence starts from the  $\omega$ -bromoalcohols **1**.<sup>31</sup> Since these derivatives are quite costly, they were synthesized by monobromination of the corresponding  $\alpha,\omega$ -diols. Traditionally, this was done by heating with aqueous HBr and petroleum ether in a continuous extraction apparatus.<sup>32</sup> However, this method is not convenient for large scale synthesis and showed low selectivity, as significant amounts of the dibrominated compounds were formed. In 1985, it was reported that azeotropic water removal with benzene allowed to achieve

monobromination with high selectivity and material purity (>99%).<sup>33</sup> Nevertheless, Chong and co-workers observed variable results under these conditions as well.<sup>31</sup> Therefore, they have used different solvents and found out that toluene was the best choice to obtain pure bromoalkanols. Five different bromoalkanols **1a-e** were synthesized applying this procedure. The materials were obtained in pure form by simple kugelrohr distillation of the crude reaction mixture. Alternatively, column chromatography (silica) could be used as well. Acetylation was then performed with acetic anhydride using melamine trisulfonic acid (MTSA) as a catalyst to yield  $\omega$ -bromoalkyl acetates **2a-e**.<sup>34</sup> MTSA was easily prepared from melamine and neat chlorosulfonic acid at room temperature. The acetylation reactions proceeded smoothly, with very short reaction times (~10 min) and yields over 90%. The heterogeneous nature of the reaction facilitates the work-up. Afterwards, following our recently developed procedure to prepare highly reactive Rieke zinc,<sup>17</sup>  $\omega$ -(thiophene-3-yl)alkyl acetates **5a-e** were prepared from ( $\omega$ -acetoxyalkyl)zinc bromides **3** and 3-bromothiophene (**4**) via nickel-mediated cross coupling reactions. Thus, the  $\omega$ -bromoalkyl acetates **2a-e** were treated with an excess of freshly prepared Rieke zinc. Oxidative addition of Zn\* to **2a-e** at a molar ratio of 1.0-1.2 Zn\*/**2** proceeded at room temperature within 2 hours to afford organozinc reagents **3a-e** in very high conversions (estimated to be >99% according to GC-MS analysis after quenching with iodine). The formed organozinc solutions were allowed to settle for 3 hours to separate the unreacted Zn\*. Then, organozinc reagents **3a-e** were cannulated to another flask containing 3-bromothiophene and 5 mol% of Ni(dppe)Cl<sub>2</sub> ([1,2-bis(triphenylphosphino)ethane]nickel(II) dichloride) catalyst was added to initiate the coupling reaction.<sup>30</sup> Best results were obtained when the reaction

mixture was stirred at room temperature for 2 days. When the coupling reaction was carried out in the presence of lithium bromide, the reaction time could be significantly shortened (from 2 days to 18 h) and the reaction yield strongly enhanced.<sup>17</sup> In all cases, minor amounts of homo-coupled 3,3'-bithiophene were observed as well. Bromination of the obtained  $\omega$ -(thiophene-3-yl)alkyl acetates **5a-e** with an excess of *N*-bromosuccinimide (NBS) under mild conditions yielded the final  $\omega$ -(2,5-dibromothiophen-3-yl)alkyl acetate monomers **6a-e**.<sup>35</sup> Simple distillations afforded the monomers in high purity grades (see SI for <sup>1</sup>HNMR spectra).

Functionalized polythiophenes can be prepared by incorporating the desired functional entities in the reactive thiophene monomers, but this may lead to low conversions and side reactions.<sup>36</sup> Therefore, post-polymerization functionalization is often preferred, as it enables the insertion of the desired functional moiety on a pre-synthesized polymer precursor.<sup>37</sup> An important aspect of the functional groups in substituted alkylthiophenes is their effect on the behavior of the polymerization reaction. Previously, ester-functionalized P3ATs have been prepared via oxidative polymerization with FeCl<sub>3</sub>.<sup>38</sup> In another study it was emphasized that, although the alkylester functionalities render the polymer soluble, they nevertheless suffered from chemical degradation (acidolysis) depending on the polymerization medium.<sup>39</sup> Pomerantz *et al.* have shown that synthesis of poly[3-(6-bromoalkyl)thiophenes] by chemical oxidation yielded regiorandom polymers.<sup>40</sup> However, for most applications in organic electronics, well-defined regioregular (rr) polythiophenes are required (the rr being defined as the percentage of head-to-tail couplings). Both the GRIM<sup>41</sup> and Rieke method<sup>42</sup> afford highly rr P3ATs.



In our case, the optimized Rieke method was employed to prepare rr poly{[3-hexylthiophene-2,5-diyl]-co-[3-( $\omega$ -acetoxyalkyl)thiophene-2,5-diyl]} materials (Scheme 3). It was chosen to limit the functional monomers to 10%, as recent results showed that larger amount of functional entities afford materials with strongly deviating crystallinity behavior and inferior photovoltaic performance.<sup>12c,d</sup> Oxidative addition of Rieke zinc to the mixture of dibromothiophenes (regular 3-hexylthiophene and  $\omega$ -(2,5-dibromothiophen-3-yl)alkyl acetates **6a-e** in a 9:1 feed ratio) afforded the respective 2-bromo-5-(bromozincio)thiophenes. The reaction was completed in 2 h and the regioselectivity was found to be greater than 99% (based on GC-MS analysis of the crude reaction mixture, quenched with a saturated ammonium chloride solution). Polymerization of these organozinc reagents with the aid of Ni(dppe)Cl<sub>2</sub> (0.2 mol%) and quenching of the polymerization with a HCl/MeOH solution then yielded the rr statistical copolythiophenes **P1-P5**. The crude polymers were purified by repetitive soxhlet extractions with methanol, *n*-hexane, acetone, and chloroform. The molar masses of the copolymers were analyzed by size exclusion chromatography (SEC) (Table 1). All copolythiophenes showed reasonable average molar masses ( $M_n = 14.2\text{--}21.6 \times 10^3 \text{ g mol}^{-1}$ ) and rather narrow polydispersities (PDI = 1.41–1.53).

**Scheme 3.** Regiocontrolled synthesis of ester-functionalized P3AT copolymers **P1-P5** employing the optimized Rieke zinc protocol.

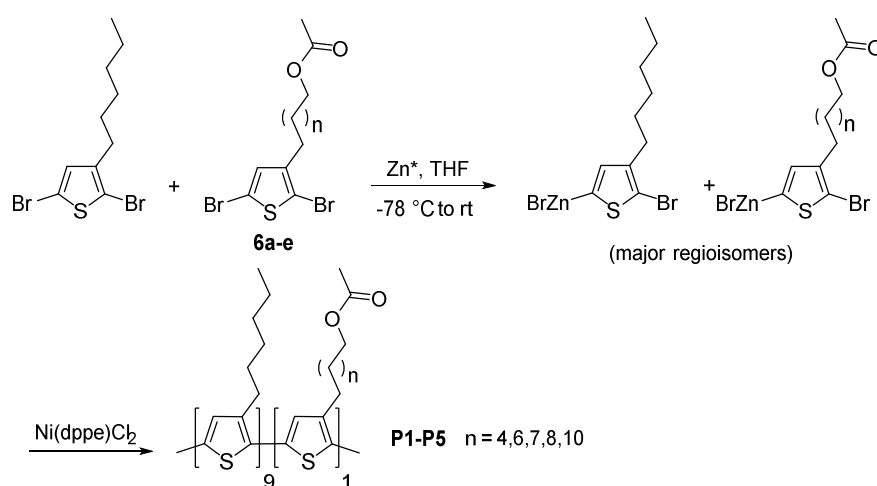


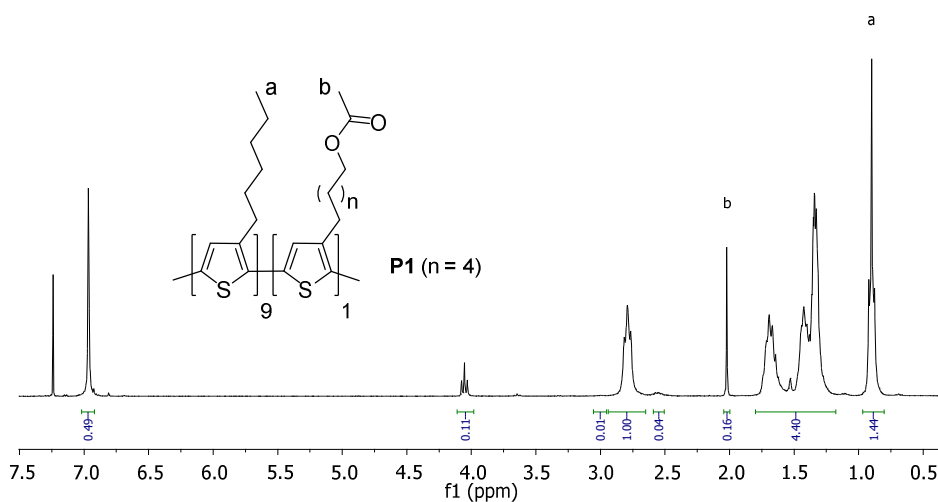
**Table 1.** Molar masses and polydispersities for ester-functionalized copolymers **P1-P5**.

Polymer	$M_n$ ( $\times 10^3$ g mol <sup>-1</sup> )	PDI
<b>P1</b>	18.4	1.53
<b>P2</b>	14.2	1.37
<b>P3</b>	18.4	1.41
<b>P4</b>	17.6	1.42
<b>P5</b>	21.6	1.46

<sup>1</sup>H NMR spectroscopy analysis provided information on the regioregularity and built-in monomer ratio of the synthesized statistical copolymers. As an example, the <sup>1</sup>H NMR spectrum of poly{[3-hexylthiophene-2,5-diyl]-*co*-[3-(6-acetoxyhexyl)thiophene-2,5-diyl]} 9/1 (**P1**) is given in Figure 1 (for other copolymers see SI). The regioregularity of all copolythiophenes synthesized via

this process was found to be at least 94% (as defined by the ratio of the  $\alpha$ -CH<sub>2</sub> triplet signals at  $\delta = 2.80$  and 2.55 ppm). The monomer content in the random copolymers was easily defined by comparing the intensity of the acetoxy (CH<sub>3</sub>) singlet at  $\delta = 2.0$  ppm and the triplet due to the terminal methyl group of the hexylthiophene units at  $\delta = 0.9$  ppm. The ester-functionalized monomers were incorporated in  $\sim 10\%$ , closely matching the feed ratio (Figure 1). The FT-IR spectra of the copolymers were almost identical (see SI) with a strong C=O stretching vibration at  $\sim 1745$  cm<sup>-1</sup>.

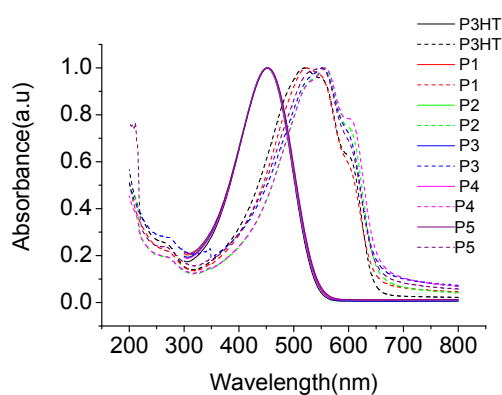
**Figure 1.** <sup>1</sup>H NMR spectrum of poly{[3-hexylthiophene-2,5-diyl]-co-[3-(6-acetoxyhexyl)thiophene-2,5-diyl]} 9/1 (**P1**).



UV-Vis spectroscopic analysis was performed both in chloroform solution and in films spin-coated from chloroform on a glass disk (Figure 2). The absorption spectra from solution showed typical P3AT features with a broad band covering the 300–560 nm range and maximum absorption ( $\lambda_{\text{max}}$ ) at  $\sim 450$  nm. The solid-state spectra were red-shifted, suggesting molecular organization in

the thin films. All copolymers showed a maximum absorption at ~550 nm in film, with a shoulder at ~605 nm representative for the degree of solid-state aggregation. The stacking features of the copolythiophenes seem to increase in the order **P1 < P3HT < P5 < P3 < P2 < P4**.

**Figure 2.** Solution (solid lines) and solid-state (dashed lines) UV-Vis spectra of copolymers **P1-P5**.



The electrochemical characteristics of the copolymers were determined by cyclic voltammetry (CV). Using the  $E_{\text{onset}}$  oxidation and reduction values, the HOMO and LUMO energy levels were calculated (Table 2). The side-chain functionalized copolymers all presented comparable values with respect to standard P3HT, indicating that the length of the functionalized alkyl side chains does not have a major impact on the electrochemical characteristics.

**Table 2.** Electrochemical and optical data of random copolythiophenes **P1-P5**.

Polymer	UV-Vis		Cyclic voltammetry		
	$\lambda_{\max \text{ film}}$ (nm)	$E_g^{\text{opt}}$ (eV)	HOMO (eV)	LUMO (eV) <sup>a</sup>	$E_g^{\text{ec}}$ (eV)
P3HT <sup>b</sup>	520	1.88	-5.25	-3.37	2.55
<b>P1</b>	523	1.88	-5.11	-3.23	2.43
<b>P2</b>	555	1.90	-5.06	-3.16	2.39
<b>P3</b>	552	1.90	-5.16	-3.26	2.47
<b>P4</b>	558	1.89	-5.11	-3.22	2.45
<b>P5</b>	549	1.89	-5.12	-3.23	2.44

<sup>a</sup> Calculated from the HOMO level as derived from CV and the optical bandgap. <sup>b</sup> Mn = 22.9 x 10<sup>3</sup> g.mol<sup>-1</sup>, PDI = 1.6.

Figure 3 shows the DSC thermograms for the series of copolymers prepared. Melting point values and melting enthalpies are summarized in Table 3. All materials are semi-crystalline with a higher melting enthalpy, and probably thus a higher crystallinity, than P3HT prepared by the same Rieke procedure. Their melting peak temperatures, however, are lower than that of P3HT, except for **P1**. Copolymer **P1**, with the shortest side chain and containing the same number of methylene spacing groups as in P3HT, showed the highest melting temperature and melting enthalpy. For copolymers **P2**, **P3**, and **P4** a similar melting point and comparable melting enthalpies were determined. The lowest melting point was seen for **P5**, which has the longest alkyl side chain among the copolymers prepared. No straightforward relation is observed with the stacking properties deduced from the solid-state UV-Vis spectra.

**Figure 3.** DSC thermograms of the second heating at  $20 \text{ K min}^{-1}$  of copolymers **P1-P5**. P3HT is included for comparison. All curves are shifted vertically for clarity.

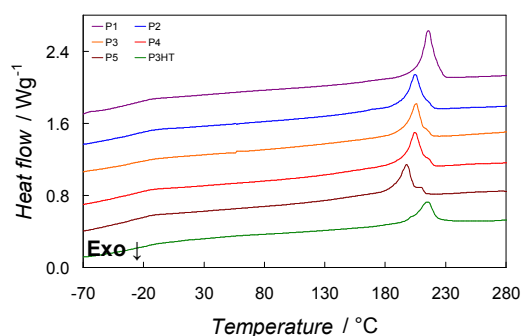


**Table 3.** Summary of the melting points and melting enthalpies determined for copolymers **P1-P5**. Values for P3HT are mentioned for comparison.

Copolymer	$T_m$ ( $^{\circ}\text{C}$ )	$\Delta H_m$ ( $\text{J g}^{-1}$ )
<b>P1</b>	216	22.3
<b>P2</b>	205	19.4
<b>P3</b>	205	16.3
<b>P4</b>	204	20.6
<b>P5</b>	198	18.0
P3HT <sup>a</sup>	215	16.2

<sup>a</sup>  $M_n = 22.9 \times \text{g.mol}^{-1}$ , PDI = 1.6.

The copolymers were applied in polymer:PC<sub>61</sub>BM ([6,6]-phenyl-C<sub>61</sub> butyric acid methyl ester) BHJ organic solar cells to observe the effect of the side chain length on photovoltaic performance. Devices were made based on the standard glass/ITO/PEDOT-PSS/polymer:PC<sub>61</sub>BM/Ca/Ag stack. Processing conditions were identical for all materials, and no further individual optimization was performed so far. As can be observed in Table 4, the resulting device parameters are in close proximity with respect to each other and pristine P3HT. There is a slight increase in open-circuit voltage ( $V_{oc}$ ) for **P1-**

**P5**, combined with a slight decrease in short-circuit current density ( $J_{sc}$ ). The  $J$ - $V$  curves for the best performing cells can be found in the Supporting Information. These results lead to conclude that the alkyl chain length does not have a detrimental effect on device efficiency and the materials are hence attractive candidates as electron donor materials for polymer solar cells. Future efforts will therefore be directed toward individual optimization of the photovoltaic parameters and thorough analysis of the effect of chain length on the thermal stability of the phase-separated BHJ blend.<sup>12c</sup>

**Table 4.** Photovoltaic performance of P3HT and **P1-P5** based polymer solar cells.<sup>a</sup>

Polymer	$V_{oc}$ (V)	$J_{sc}$ (mA/cm <sup>2</sup> )	FF (%)	Average $\eta$ (%)	Best $\eta$ (%)
P3HT	0.55	6.29	0.71	2.47	2.55
<b>P1</b>	0.58	6.02	0.69	2.42	2.72
<b>P2</b>	0.58	5.63	0.70	2.25	2.47
<b>P3</b>	0.57	5.03	0.70	2.00	2.23
<b>P4</b>	0.58	5.81	0.68	2.29	2.41
<b>P5</b>	0.58	5.17	0.70	2.09	2.25

<sup>a</sup> Device architecture: glass/ITO/PEDOT-PSS/polymer:PC<sub>61</sub>BM/Ca/Ag. <sup>b</sup> Mn = 22.9 x 10<sup>3</sup> g.mol<sup>-1</sup>.

### 4.3. Conclusions

Terminal ester-functionalized alkylthiophenes with different alkyl chain lengths were prepared starting from readily available 3-bromothiophene and  $\alpha,\omega$ -diols employing Rieke zinc in the key step, i.e. attachment of the side chains via a Kumada-type cross coupling reaction. The required organozinc reagents were synthesized in excellent yields under common laboratory conditions by treatment of the  $\omega$ -alkylesters with highly reactive Rieke zinc, prepared *in situ* by reduction of zinc chloride with lithium naphthalenide in the presence of benzothiophene, proven to be an essential additive for

stabilization of the Zn\* particles. Polymerization of the functionalized dibromothiophene monomers by the Rieke procedure afforded regioregular poly{[3-hexylthiophene]-*co*-[3-( $\omega$ -acetoxyalkyl)thiophene]} statistical copolymers incorporating 10% of ester-functionalized units. The copolymers were characterized by <sup>1</sup>H NMR, FT-IR and UV-Vis spectroscopy, thermal analysis, and cyclic voltammetry, and they were screened as donor materials in bulk heterojunction polymer solar cells, indicating that the side chains do not jeopardize the photovoltaic efficiency, while providing opportunities toward increasing the lifetime of the resulting devices.

#### 4.4. Experimental

##### Materials and methods

All manipulations were carried out on a dual manifold vacuum/Ar system. Lithium (granular, Acros, 99+%) was stored in a schlenk tube under Ar. Lithium, naphthalene and benzothiophene were weighed in air as needed and transferred to a schlenk tube under a stream of Ar. Naphthalene (Acros, 99+%) and benzothiophene (Sigma-Aldrich, 98%) were stored in a desiccator over phosphorous pentoxide. Zinc chloride (Acros, analysis grade 98.5%) was transferred into small vials in a glove box and stored in a desiccator over phosphorous pentoxide. Zinc chloride was dried by treating it with thionyl chloride and subsequent heating with a Bunsen burner, and removed under a stream of Ar gas. THF was freshly distilled from Na/benzophenone under a N<sub>2</sub> atmosphere at atmospheric pressure prior to use. Brass cannulas were stored in an oven at 110 °C and cleaned immediately after use with acetic acid (in the case of Zn\* remnant), acetone (to clean non-polymeric residues), or hot chloroform and/or chlorobenzene (for polymer-based contaminations). 3-Bromothiophene (99%) was purchased from Fluorchem. 1,6-Hexanediol



(97%), 1,8-octanediol (98+%), 1,9-nonanediol (97%), 1,10-decanediol (97%), and 1,12-dodecanediol (97%) were obtained from Alfa Aesar. Chlorosulfonic acid (97%), melamine (99%), and acetic anhydride (99+%) were obtained from Acros Organics. All chemicals were used as received without any further purification. Melamine trisulfonic acid was prepared according to the procedure reported by Shirini *et al.*<sup>34</sup>

NMR chemical shifts ( $\delta$ , in ppm) were determined relative to the residual  $\text{CHCl}_3$  absorption (7.26 ppm) or the  $^{13}\text{C}$  resonance shift of  $\text{CDCl}_3$  (77.16 ppm). Gas chromatography-mass spectrometry (GC-MS) analysis was carried out with a thermoquest TSQ7000 applying a DB-5MS 30 m x 0.25 mm column and a temperature range of 35–320 °C. Molar masses and distributions were determined relative to polystyrene standards by size exclusion chromatography (SEC). Chromatograms were recorded on a Spectra Series P100 (Spectra Physics) equipped with two mixed-B columns (10  $\mu\text{m}$ , 0.75 cm x 30 cm, Polymer labs) and a refractive index detector (Shodex) at 40 °C. THF was used as the eluent at a flow rate of 1.0 mL  $\text{min}^{-1}$ . The energy levels of the copolythiophenes were determined using cyclic voltammetry and optical band gap analyses. UV-visible spectra were recorded on a Varian Cary 500 spectrometer. Electrochemical measurements were performed with an Eco Chemie Autolab PGSTAT 30 potentiostat/galvanostat using a three-electrode microcell containing a Ag/AgNO<sub>3</sub> reference electrode (silver wire in 0.01 M AgNO<sub>3</sub> and 0.1 M NBu<sub>4</sub>PF<sub>6</sub> in MeCN), a platinum counter electrode and a platinum working electrode, and 0.1 M NBu<sub>4</sub>PF<sub>6</sub> in anhydrous MeCN or CH<sub>2</sub>Cl<sub>2</sub> was used as the electrolyte. To prevent air from entering the system, the buffer solutions were degassed with Ar prior to each measurement and all experiments were carried out under a curtain of Ar. The respective

copolymers were dissolved to their maximum solubility in the electrolyte solution, or coated as a thin film on the working electrode by dipping the electrode in the polymer solution. Cyclic voltammograms were recorded at a scan rate of 100 to 300 mV s<sup>-1</sup>. For the conversion to eV, the onset oxidation and reduction potential were used and referenced to the known standard ferrocene/ferrocenium (0.05 V vs. Ag/AgNO<sub>3</sub>), which in MeCN solution was estimated to have an oxidation potential of -4.98 eV vs. vacuum. To estimate the optical bandgap, the intersection of the tangent line to the absorption spectrum on the low energy side with the X-axis was used. FT-IR spectra were obtained on a Perkin-Elmer spectrophotometer with a resolution of 4 cm<sup>-1</sup> (16 scans) using films drop-casted on a NaCl disk. DSC measurements were performed at 20 K min<sup>-1</sup> in aluminum crucibles on a TA Instruments Q2000 Tzero DSC equipped with a refrigerated cooling system (RCS), using nitrogen (50 mL min<sup>-1</sup>) as purge gas. For all DSC results the second heating was depicted, in order to avoid thermal history effects.

#### **Preparation of $\omega$ -bromoalkanols**

All brominated alcohols were prepared in the same manner from the corresponding diols following literature procedures. Spectral data were in accordance with the literature.<sup>31,33</sup>

#### **Acetylation of the $\omega$ -bromoalkanols with MTSA<sup>34</sup> - General procedure 1**

6-Bromo-1-hexanol (**1a**) (29.3 g, 162 mmol) and MTSA (17.9 g, 49 mmol) were dissolved together in 400 mL of CH<sub>2</sub>Cl<sub>2</sub>. Acetic anhydride (17 mL, 181 mmol) was added and the mixture was stirred at rt. After completion of the reaction, as monitored by thin-layer chromatography, the mixture was filtered. The organic layer was washed with a 5% NaHCO<sub>3</sub> solution and water, and dried over MgSO<sub>4</sub>. Concentration of the organic layer under reduced pressure gave the crude acetylated product with minor impurities. Purification was

---

performed either by kugelrohr distillation or by column chromatography (silica, eluent hexanes-ethyl acetate, 80-20). Kugelrohr distillation (110 °C, 0.079 mbar) afforded a pure colorless liquid of 6-bromohexyl acetate (**2a**) (33.9 g, 94%).

**6-Bromohexyl acetate (2a).**  $^1\text{H}$  NMR ( $\text{CDCl}_3$ , 300 MHz):  $\delta$  = 1.34–1.44 (m, 4H), 1.61 (q,  $J_{\text{H-H}}$  = 7.3 Hz, 2H), 1.83 (q,  $J_{\text{H-H}}$  = 6.7 Hz, 2H), 2.01 (s, 3H), 3.37 (t,  $J_{\text{H-H}}$  = 6.9 Hz, 2H), 4.02 (t,  $J_{\text{H-H}}$  = 6.7 Hz, 2H);  $^{13}\text{C}$  NMR ( $\text{CDCl}_3$ , 75 MHz):  $\delta$  = 171.9, 65.0, 34.4, 33.3, 29.1, 28.4, 25.8, 21.7; FT-IR (NaCl,  $\text{cm}^{-1}$ ):  $\nu_{\text{max}}$  = 2938, 2860, 1740 (CO), 1462, 1438, 1388, 1366, 1244, 1046, 970, 889, 761, 729, 642.

**8-Bromooctyl acetate (2b).** Yield (13.57 g, 95%).  $^1\text{H}$  NMR ( $\text{CDCl}_3$ , 300 MHz):  $\delta$  = 1.25–1.44 (m, 8H), 1.58 (q,  $J_{\text{H-H}}$  = 7.0 Hz, 2H), 1.81 (q,  $J_{\text{H-H}}$  = 6.7 Hz, 2H), 2.01 (s, 3H), 3.37 (t,  $J_{\text{H-H}}$  = 6.9 Hz, 2H), 4.01 (t,  $J_{\text{H-H}}$  = 6.7 Hz, 2H);  $^{13}\text{C}$  NMR ( $\text{CDCl}_3$ , 75 MHz):  $\delta$  = 171.9, 65.2, 34.6, 33.4, 29.7, 29.3, 29.2, 28.7, 26.5, 21.7; FT-IR (NaCl,  $\text{cm}^{-1}$ ):  $\nu_{\text{max}}$  = 2932, 2857, 1740 (CO), 1465, 1438, 1387, 1365, 1244, 1037, 975, 894, 724, 643.

**9-Bromononyl acetate (2c).** Yield (31.17 g, 95%).  $^1\text{H}$  NMR ( $\text{CDCl}_3$ , 400 MHz):  $\delta$  = 1.27–1.41 (m, 10H), 1.58 (q,  $J_{\text{H-H}}$  = 7.3 Hz, 2H), 1.82 (q,  $J_{\text{H-H}}$  = 7.1 Hz, 2H), 2.01 (s, 3H), 3.37 (t,  $J_{\text{H-H}}$  = 6.9 Hz, 2H), 4.01 (t,  $J_{\text{H-H}}$  = 6.8 Hz, 2H);  $^{13}\text{C}$  NMR ( $\text{CDCl}_3$ , 100 MHz):  $\delta$  = 171.6, 65.2, 34.7, 33.4, 29.7, 29.3, 29.2, 28.7, 26.5, 21.7; FT-IR (NaCl,  $\text{cm}^{-1}$ ):  $\nu_{\text{max}}$  = 2930, 2856, 1741 (CO), 1465, 1438, 1387, 1365, 1242, 1039, 971, 890, 757, 723.

**10-Bromodecyl acetate (2d).** Yield (22.73 g, 94%).  $^1\text{H}$  NMR ( $\text{CDCl}_3$ , 300 MHz):  $\delta$  = 1.24–1.39 (m, 12H), 1.56 (q,  $J_{\text{H-H}}$  = 6.7 Hz, 2H), 1.79 (q,  $J_{\text{H-H}}$  = 7.0 Hz, 2H), 1.99 (s, 3H), 3.35 (t,  $J_{\text{H-H}}$  = 6.7 Hz, 2H), 3.99 (t,  $J_{\text{H-H}}$  = 6.7 Hz, 2H);  $^{13}\text{C}$  NMR ( $\text{CDCl}_3$ , 75 MHz):  $\delta$  = 171.8, 65.2, 34.7, 33.4, 30.01, 29.97, 29.8, 29.4, 29.2, 28.8, 26.5,

21.7. FT-IR (NaCl,  $\text{cm}^{-1}$ ):  $\nu_{\text{max}}$  = 2929, 2855, 1741 (CO), 1466, 1438, 1387, 1365, 1244, 1038, 971, 891, 723.

**12-Bromododecyl acetate (2e).** Yield (33.85 g, 93%).  $^1\text{H}$  NMR ( $\text{CDCl}_3$ , 300 MHz):  $\delta$  = 1.24–1.41 (m, 16H), 1.58 (q,  $J_{\text{H-H}}$  = 1.6 Hz, 2H), 1.82 (q,  $J_{\text{H-H}}$  = 7.1 Hz, 2H), 2.01 (s, 3H), 3.37 (t,  $J_{\text{H-H}}$  = 6.9 Hz, 2H), 3.99 (t,  $J_{\text{H-H}}$  = 6.7 Hz, 2H);  $^{13}\text{C}$  NMR ( $\text{CDCl}_3$ , 75 MHz):  $\delta$  = 172.1, 65.3, 34.7, 33.5, 30.14 (3x), 30.07, 29.9, 29.4, 29.2, 28.8, 26.5, 21.7; FT-IR (NaCl,  $\text{cm}^{-1}$ ):  $\nu_{\text{max}}$  = 2854, 1741 (CO), 1466, 1439, 1387, 1365, 1240, 1039, 972, 722.

**Preparation of Rieke Zinc (Zn\*)<sup>17</sup>**

Two 120 mL schlenk vessels, A and B, were dried by heating with a Bunsen burner under reduced pressure and cooled to rt under a stream of Ar. Schlenk vessel A, filled with Ar, was weighed and then reassembled to the schlenk line. Under a stream of Ar,  $\text{ZnCl}_2$  was charged to the vessel. After three Ar/vacuum sequences,  $\text{ZnCl}_2$  was wetted with a small amount of  $\text{SOCl}_2$ . The schlenk vessel was heated with a bunsen burner until the  $\text{ZnCl}_2$  salt melted and a white fume was released, and the schlenk was subsequently cooled down under an Ar flow. Schlenk flask A was weighed again to determine the exact amount of  $\text{ZnCl}_2$  and a stirring bar was added. Dried  $\text{ZnCl}_2$  (1.1 equiv) was dissolved in freshly distilled THF (25 mL/g). Li pellets (2.2 equiv), naphthalene (2.25 equiv) and benzo thiophene (0.04 equiv) were weighted in air and charged into schlenk B under an Ar stream. Dry THF was added (the same amount as added to dissolve  $\text{ZnCl}_2$ ) and the solution (which turned from colorless to dark green within less than 2 min) was stirred for 2 additional h to dissolve the Li pellets. The  $\text{ZnCl}_2$  solution was transferred dropwise via cannula to the lithium naphthalenide solution over 10–15 min. (The resulting black suspension might be stirred for 1 more h to consume the Li that is not dissolved or stirring can be stopped right after the addition.) The highly reactive zinc was allowed to

settle down for a couple of h. The supernatant was siphoned off via cannula leaving the reactive Zn\* powder. Thus prepared Rieke zinc was ready to use.

**Preparation of organozinc halides 3a-e and their Ni-mediated coupling with 3-bromothiophene<sup>43</sup> - General procedure 2**

6-Acetoxyhexyl bromide (**2a**) (7.96 g, 35.7 mmol) was dissolved in dry THF (40 mL) and added via cannula to the active zinc powder (39.3 mmol) at rt. The reaction mixture was stirred for 3 h, after which the solution was allowed to stand for a couple of h to allow the excess of zinc to settle down from the dark brown organozinc bromide solution.

In an 300 mL flame-dried schlenk vessel, LiBr (3.41 g, 39.2 mmol), Ni(dppe)Cl<sub>2</sub> (0.94 g, 1.8 mmol), and 3-bromothiophene (2.5 mL, 26.8 mmol) were dissolved dry THF (150 mL). The organozinc bromide solution was then transferred via cannula over a period of 1 h to this mixture under stirring at rt and the reaction was continued overnight. The reaction was quenched with a saturated NH<sub>4</sub>Cl solution, followed by extraction with diethyl ether, affording 6-(thiophene-3-yl)hexyl acetate (**5a**) (4.54 g, 75%) in relatively pure form (as analyzed by <sup>1</sup>H NMR; more thorough purification was only performed upon subsequent bromination).

**6-(Thiophene-3-yl)hexyl acetate (5a).** <sup>1</sup>H NMR (CDCl<sub>3</sub>, 300 MHz):  $\delta$  = 1.32–1.65 (m, 8H), 2.02 (s, 3H), 2.61 (t,  $J_{H-H}$  = 8.1 Hz, 2H), 4.03 (t,  $J_{H-H}$  = 6.7 Hz, 2H), 6.89–6.92 (m, 2H), 7.22 (dd,  $J_{H-H}$  = 4.8/3.0 Hz, 1H).

**8-(Thiophene-3-yl)octyl acetate (5b).** Yield (27.7 g, 76%). <sup>1</sup>H NMR (CDCl<sub>3</sub>, 300 MHz):  $\delta$  = 1.27–1.35 (m, 8H), 1.57–1.60 (m, 4H), 2.03 (s, 3H), 2.60 (t,  $J_{H-H}$  = 7.5 Hz, 2H), 4.03 (t,  $J_{H-H}$  = 6.7 Hz, 2H), 6.89–6.92 (m, 2H), 7.22 (dd,  $J_{H-H}$  = 4.8/3.0 Hz, 1H).

---

**9-(Thiophene-3-yl)nonyl acetate (5c).** Yield (27 g, 77%).  $^1\text{H}$  NMR ( $\text{CDCl}_3$ , 300 MHz):  $\delta$  = 1.24–1.34 (m, 6H), 1.55–1.64 (m, 6H), 1.83 (q,  $J_{\text{H-H}} = 6.7$  Hz, 2H), 2.02 (s, 3H), 2.60 (t,  $J_{\text{H-H}} = 7.5$  Hz, 2H), 4.03 (t,  $J_{\text{H-H}} = 6.7$  Hz, 2H), 6.89–6.92 (m, 2H), 7.22 (dd,  $J_{\text{H-H}} = 4.8/3.0$  Hz, 1H).

**10-(Thiophene-3-yl)decyl acetate (5d).** Yield (21.7 g, 75%).  $^1\text{H}$  NMR ( $\text{CDCl}_3$ , 300 MHz):  $\delta$  = 1.17–1.34 (m, 10H), 1.52–1.64 (m, 6H), 2.03 (s, 3H), 2.60 (t,  $J_{\text{H-H}} = 7.3$  Hz, 2H), 4.03 (t,  $J_{\text{H-H}} = 6.7$  Hz, 2H), 6.89–6.92 (m, 2H), 7.21 (dd,  $J_{\text{H-H}} = 4.8/3.0$  Hz, 1H).

**12-(Thiophene-3-yl)dodecyl acetate (5e).** Yield (20.2 g, 77%).  $^1\text{H}$  NMR ( $\text{CDCl}_3$ , 300 MHz):  $\delta$  = 1.17–1.34 (m, 14H), 1.56–1.63 (m, 6H), 2.03 (s, 3H), 2.60 (t,  $J_{\text{H-H}} = 7.8$  Hz, 2H), 4.03 (t,  $J_{\text{H-H}} = 6.7$  Hz, 2H), 6.89–6.92 (m, 2H), 7.21 (dd,  $J_{\text{H-H}} = 4.8/3.0$  Hz, 1H).

**Bromination of the  $\omega$ -(thiophen-3-yl)alkyl acetates<sup>35</sup> - General procedure 3**

6-(Thiophene-3-yl)hexyl acetate (**5a**) (3.84 g, 17.9 mmol) was placed in a three-neck round bottom flask and dissolved in DMF (75 mL). *N*-bromosuccinimide (7.80 g, 43.8 mmol) was added portionwise and the resulting mixture was left to stir at rt overnight in the absence of light. The reaction mixture was poured into an ice-cooled 2.5 M NaOH solution and stirred for 5 min, and then extracted with diethyl ether. The organic phase was washed with 2.5 M NaOH,  $\text{H}_2\text{O}$ , and  $\text{NaCl}_{\text{sat}}$ , respectively, dried over  $\text{MgSO}_4$ , and filtered. The solvent was discarded under reduced pressure and the crude product was purified by column chromatography (silica, eluent hexanes:ethyl acetate) to yield a pale yellow liquid (6.40 g, 93%).

**6-(2,5-Dibromothiophene-3-yl)hexyl acetate (6a).**  $^1\text{H}$  NMR ( $\text{CDCl}_3$ , 300 MHz):  $\delta$  = 1.28–1.42 (m, 4H), 1.49–1.66 (m, 4H), 2.03 (s, 3H), 2.49 (t,  $J_{\text{H-H}} = 7.8$  Hz, 2H), 4.03 (t,  $J_{\text{H-H}} = 6.7$  Hz, 2H), 6.75 (s, 1H);  $^{13}\text{C}$  NMR ( $\text{CDCl}_3$ , 100 MHz):  $\delta$  = 171.7, 143.3, 131.5, 111.1, 108.7, 65.1, 30.1, 30.0, 29.3, 29.2, 26.4, 21.7; GC-

MS:  $m/z = 381/383/385 [M^+]$  ( $\geq 98\%$ ); FT-IR (NaCl,  $\text{cm}^{-1}$ ):  $\nu_{\text{max}} = 3091, 2934, 2857, 1738, 1541, 1463, 1418, 1387, 1364, 1241$ .

**8-(2,5-Dibromothiophene-3-yl)octyl acetate (6b).** Yield (5.21 g, 92%).  $^1\text{H}$  NMR ( $\text{CDCl}_3$ , 300 MHz):  $\delta = 1.27\text{--}1.34$  (m, 8H), 1.47–1.60 (m, 4H), 2.00 (s, 3H), 2.46 (t,  $J_{\text{H-H}} = 7.5$  Hz, 2H), 4.01 (t,  $J_{\text{H-H}} = 6.7$  Hz, 2H), 6.73 (s, 1H);  $^{13}\text{C}$  NMR ( $\text{CDCl}_3$ , 100 MHz):  $\delta = 171.8, 143.5, 131.6, 111.0, 108.6, 65.2, 30.2, 30.1, 29.9, 29.8, 29.6, 29.3, 26.5, 21.7$ ; GC-MS:  $m/z = 409/411/413 [M^+]$  ( $\geq 99\%$ ); FT-IR (NaCl,  $\text{cm}^{-1}$ ):  $\nu_{\text{max}} = 3091, 2929, 2855, 1739, 1541, 1464, 1418, 1387, 1364, 1241$ .

**9-(2,5-Dibromothiophene-3-yl)nonyl acetate (6c).** Yield (4.49 g, 93%).  $^1\text{H}$  NMR ( $\text{CDCl}_3$ , 300 MHz):  $\delta = 1.25\text{--}1.35$  (m, 10H), 1.46–1.64 (m, 4H), 2.03 (s, 3H), 2.48 (t,  $J_{\text{H-H}} = 7.5$  Hz, 2H), 4.03 (t,  $J_{\text{H-H}} = 6.7$  Hz, 2H), 6.75 (s, 1H);  $^{13}\text{C}$  NMR ( $\text{CDCl}_3$ , 100 MHz):  $\delta = 171.9, 143.3, 131.6, 110.0, 108.6, 65.3, 30.2, 30.1, 30.04, 29.93, 29.9, 29.7, 29.3, 26.6, 21.7$ ; GC-MS:  $m/z = 423/425/427 [M^+]$  ( $\geq 99\%$ ); FT-IR (NaCl,  $\text{cm}^{-1}$ ):  $\nu_{\text{max}} = 3090, 2927, 2854, 1740, 1542, 1464, 1418, 1387, 1364, 1239$ .

**10-(2,5-Dibromothiophene-3-yl)decyl acetate (6d).** Yield (3.83 g, 92%).  $^1\text{H}$  NMR ( $\text{CDCl}_3$ , 300 MHz):  $\delta = 1.23\text{--}1.35$  (m, 12H), 1.48–1.64 (m, 4H), 2.03 (s, 3H), 2.48 (t,  $J_{\text{H-H}} = 7.5$  Hz, 2H), 4.03 (t,  $J_{\text{H-H}} = 6.7$  Hz, 2H), 6.75 (s, 1H);  $^{13}\text{C}$  NMR ( $\text{CDCl}_3$ , 100 MHz):  $\delta = 171.8, 143.5, 131.5, 111.0, 108.6, 65.3, 30.2, 30.12, 30.10, 30.07, 29.97, 29.9, 29.7, 29.2, 26.5, 21.7$ ; GC-MS:  $m/z = 437/439/441 [M^+]$  ( $\geq 97\%$ ); FT-IR (NaCl,  $\text{cm}^{-1}$ ):  $\nu_{\text{max}} = 3091, 2927, 2855, 1739, 1540, 1463, 1417, 1387, 1364, 1240$ .

**12-(2,5-Dibromothiophene-3-yl)dodecyl acetate (6e).** Yield (4.76 g, 93%).  $^1\text{H}$  NMR ( $\text{CDCl}_3$ , 300 MHz):  $\delta = 1.22\text{--}1.34$  (m, 16H), 1.48–1.62 (m, 4H), 2.03 (s, 3H), 2.48 (t,  $J_{\text{H-H}} = 7.9$  Hz, 2H), 4.03 (t,  $J_{\text{H-H}} = 6.8$  Hz, 2H), 6.75 (s, 1H);  $^{13}\text{C}$  NMR ( $\text{CDCl}_3$ , 400 MHz):  $\delta = 171.9, 144.8, 131.5, 110.6, 108.6, 65.3, 30.22, 30.20$ ,

---

30.16 (2x), 30.1, 30.0, 29.9, 29.7, 29.3, 26.7, 21.7; GC-MS:  $m/z = 466/468/470$  [ $M^+$ ] ( $\geq 97\%$ ); FT-IR (NaCl,  $\text{cm}^{-1}$ ):  $\nu_{\text{max}} = 3090, 2927, 2856, 1740, 1541, 1464, 1418, 1387, 1354, 1239$ .

#### Synthesis of the copolythiophenes - General procedure 4

The monomer mixture, 2,5-dibromo-3-hexylthiophene (4.52 g, 13.9 mmol) and 2,5-dibromo-3-(6-acetoxyhexyl)thiophene (**6a**) (0.59 g, 1.5 mmol), was added via cannula to freshly prepared  $\text{Zn}^*$  (16.9 mmol), as made by the optimized Rieke method,<sup>17</sup> at  $-78\text{ }^\circ\text{C}$ . The mixture was stirred for 1 h at this temperature and then allowed to warm to  $0\text{ }^\circ\text{C}$  gradually. The unreacted  $\text{Zn}^*$  was allowed to settle down overnight and the formed organozinc supernatant was filtered via a  $0.45\text{ }\mu\text{m}$  acrodisc filter into a flame-dried schlenk flask.  $\text{Ni}(\text{dppe})\text{Cl}_2$  (0.016 g, 0.031 mmol, 0.2 mol%) was added via a cannula to the ice-cooled organozinc solution and the schlenk vessel was immersed into a preheated oil bath at  $60\text{ }^\circ\text{C}$ . The mixture was stirred at this temperature overnight. It was then poured into a MeOH-HCl (2M) solution, and the resulting dark precipitate was filtered off and washed several times with MeOH. The crude polymer was transferred into an extraction thimble and purification was performed by sequential soxhlet extractions using MeOH, acetone and *n*-hexane. The polymer was finally collected with chloroform and the solvent was removed under reduced pressure. The polymer was redissolved in chloroform and reprecipitation was performed upon addition of MeOH. Filtration and drying under high vacuum afforded the pure polymer material (in  $\sim 60\%$  yield for all copolymers).

**Poly{[3-hexylthiophene-2,5-diyl]-co-[3-(6-acetoxyhexyl)thiophene-2,5-diyl]}**  
**9/1 (P1).**  $^1\text{H}$  NMR (300 MHz,  $\text{CDCl}_3$ ):  $\delta = 6.97$  (s, 2H), 4.06 (t, 4H), 2.79/2.55 (t, 4H), 2.02 (s, 3H), 1.77–1.60 (m, 4H), 1.51–1.25 (m, 12H), 0.90 (t, 3H);  $^{13}\text{C}$  NMR ( $\text{CDCl}_3$ , 100 MHz):  $\delta = 171.9, 140.6, 134.4, 131.2, 129.3, 65.3, 30.2, 30.0, 29.3$ ,



26.6, 23.4, 21.7, 14.8; FT-IR (NaCl,  $\text{cm}^{-1}$ ):  $\nu_{\text{max}} = 3055, 2955, 2927, 2856, 1745, 1509, 1456, 1378, 1235, 820$ .

**Poly{[3-hexylthiophene-2,5-diyl]-co-[3-(8-acetoxyoctyl)thiophene-2,5-diyl]}**

**9/1 (P2).**  $^1\text{H}$  NMR (400 MHz,  $\text{CDCl}_3$ ):  $\delta = 6.96$  (s, 2H), 4.03 (t, 4H), 2.80/2.56 (t, 4H), 2.02 (s, 3H), 1.75–1.64 (m, 4H), 1.48–1.29 (m, 16H), 0.90 (t, 3H);  $^{13}\text{C}$  NMR ( $\text{CDCl}_3$ , 100 MHz):  $\delta = 171.9, 140.6, 134.4, 131.2, 129.3, 65.2, 32.4, 31.2, 30.2, 30.0, 29.3, 26.7, 23.4, 21.7, 14.8$ ; FT-IR (NaCl,  $\text{cm}^{-1}$ ):  $\nu_{\text{max}} = 3055, 2955, 2926, 2856, 1744, 1509, 1455, 1377, 1237, 820$ .

**Poly{[3-hexylthiophene-2,5-diyl]-co-[3-(9-acetoxynonyl)thiophene-2,5-diyl]}**

**9/1 (P3).**  $^1\text{H}$  NMR (300 MHz,  $\text{CDCl}_3$ ):  $\delta = 6.97$  (s, 2H), 4.03 (t, 4H), 2.79/2.55 (t, 4H), 2.02 (s, 3H), 1.80–1.60 (m, 4H), 1.50–1.25 (m, 18H), 0.90 (t, 3H);  $^{13}\text{C}$  NMR ( $\text{CDCl}_3$ , 100 MHz):  $\delta = 171.9, 140.6, 134.3, 131.2, 129.3, 65.3, 32.4, 31.2, 30.2, 30.0, 29.3, 26.6, 23.4, 21.7, 14.8$ ; FT-IR (NaCl,  $\text{cm}^{-1}$ ):  $\nu_{\text{max}} = 3055, 2955, 2926, 2856, 1744, 1509, 1455, 1377, 1237, 819$ .

**Poly{[3-hexylthiophene-2,5-diyl]-co-[3-(10-acetoxydecyl)thiophene-2,5-diyl]}**

**9/1 (P4).**  $^1\text{H}$  NMR ( $\text{CDCl}_3$ , 300 MHz):  $\delta = 6.97$  (s, 2H), 4.03 (t, 4H), 2.79/2.55 (t, 4H), 2.02 (s, 3H), 1.80–1.60 (m, 4H), 1.50–1.25 (m, 20H), 0.90 (t, 3H);  $^{13}\text{C}$  NMR (100 MHz,  $\text{CDCl}_3$ ):  $\delta = 171.9, 140.6, 134.4, 131.2, 129.3, 65.2, 32.4, 31.2, 30.2, 30.0, 29.3, 26.6, 23.4, 21.7, 14.8$ ; FT-IR (NaCl,  $\text{cm}^{-1}$ ):  $\nu_{\text{max}} = 3055, 2955, 2926, 2856, 1744, 1510, 1455, 1378, 1237, 820$ .

**Poly{[3-hexylthiophene-2,5-diyl]-co-[3-(12-acetoxydodecyl)thiophene-2,5-**

**diyl]} 9/1 (P12).**  $^1\text{H}$  NMR (300 MHz,  $\text{CDCl}_3$ ):  $\delta = 6.97$  (s, 2H), 4.02 (t, 4H), 2.80/2.56 (t, 4H), 2.02 (s, 3H), 1.77–1.55 (m, 4H), 1.50–1.22 (m, 24H), 0.90 (t, 3H);  $^{13}\text{C}$  NMR ( $\text{CDCl}_3$ , 400 MHz):  $\delta = 171.9, 140.6, 134.4, 131.2, 129.3, 65.5, 32.4, 31.2, 30.3, 30.2, 30.2, 30.0, 29.3, 26.6, 23.4, 21.7, 14.8$ ; FT-IR (NaCl,  $\text{cm}^{-1}$ ):  $\nu_{\text{max}} = 3055, 2955, 2926, 2856, 1744, 1509, 1456, 1378, 1238, 820$ .

---

### **Solar cell device fabrication**

The BHJ organic solar cells were constructed using the traditional glass/ITO/PEDOT-PSS/active layer/Ca/Ag architecture. Prior to device processing, the indium tin oxide (ITO, Kintec, 100 nm, 20 Ohm/sq) containing substrates were cleaned using soap, demineralized water, acetone, isopropanol and a UV/O<sub>3</sub> treatment. Subsequently, the ITO substrates were covered by a ~30 nm thick layer of PEDOT-PSS [poly(3,4-ethylenedioxythiophene)-poly(styrenesulfonic acid), Heraeus Clevios] by spin-coating. Further processing was performed under nitrogen atmosphere in a glove box, starting off with an annealing step at 130 °C for 15 min to remove any residual water. The active layer consisting of polymer:PC<sub>61</sub>BM ([6,6]-phenyl-C<sub>61</sub> butyric acid methyl ester, Solenne) was spin-coated with a thickness of ~80 nm (as confirmed by DEKTAK). Blend solutions were prepared in a 1:1 ratio, with polymer concentrations of 10 mg/mL, using chlorobenzene as a solvent. Finally, the devices were finished off with Ca and Ag as the top electrodes, with thicknesses of 20 and 100 nm, respectively. In the standard cell configuration, an active area of 8 mm<sup>2</sup> was obtained.

### **4.5. Acknowledgements**

We thank IMEC and Hasselt University for providing the PhD grant of S.K. We acknowledge the OPV-Life project from the IWT (Agentschap voor Innovatie door Wetenschap en Technologie; O&O 080368), the POLYSTAR project from PV ERA-NET, the IWT-SBO project POLYSPEC (Nanostructured POLYmer photovoltaic devices for efficient solar SPECTrum harvesting), and Belspo for supporting the IAP P6/27 and IAP 7/05 networks. We are also thankful to Huguette Penxten for the UV-Vis and CV measurements.

#### 4.6. References

1. (a) Brabec, C. J.; Gowrisanker, S.; Halls, J. J. M.; Laird, D.; Jia, S.; Williams, S. P. *Materials Today* **2011**, *14* (10), 462-470. (b) Nelson, J., Polymer:fullerene bulk heterojunction solar cells. *Materials Today* **2011**, *14* (10), 462-470. (c) Boudreault, P.-L. T.; Najari, A.; Leclerc, M. *Chemistry of Materials* **2011**, *23* (3), 456-469. (d) Koster, L. J. A.; Shaheen, S. E.; Hummelen, J. C. *Advanced Energy Materials* **2012**, *2* (10), 1246-1253. (e) Kumar, P.; Chand, S. *Progress in Photovoltaics: Research and Applications* **2012**, *20* (4), 377-415. (f) Gang, I.; Rui, Z.; Yang, Y. *Nature Photonics* **2012**, *6* (3), 153-161. (g) Jørgensen, M.; Norrman, K.; Gevorgyan, S. A.; Tromholt, T.; Andreasen, B.; Krebs, F. C. *Advanced Materials* **2012**, *24* (5), 580-612. (h) Van Mierloo, S.; Kesters, J.; Hadipour, A.; Spijkman, M.-J.; Van den Brande, N.; D'Haen, J.; Van Assche, G.; de Leeuw, D. M.; Aernouts, T.; Manca, J.; Lutsen, L.; Vanderzande, D.; Maes, W. *Chemistry of Materials* **2012**, *24*, 587-593.
2. Marrocchi, A.; Lanari, D.; Facchetti, A.; Vaccaro, L. *Energy & Environmental Science* **2012**, *5*, 8457-8474.
3. (a) Dang, M. T.; Hirsch, L.; Wantz, G., P3HT:PCBM, Best Seller in Polymer Photovoltaic Research. *Advanced Materials* **2011**, *23* (31), 3597-3602. (b) Dang, M. T.; Hirsch, L.; Wantz, G.; Wuest, J. D. *Chemical Reviews* **2013**, *113*, 3734-3765.
4. Elsenbaumer, R. L.; Jen, K. Y.; Oboodi, R. *Synthetic Metals* **1986**, *15* (2-3), 169-174.
5. Osaka, I.; McCullough, R. *Accounts of Chemical Research* **2008**, *41* (9), 1202-1214.
6. McCullough, R. D. *Advanced Materials* **1998**, *10* (2), 93-116.

7. (a) Thobie-Gautier, C.; Bouligand, Y.; Gorgues, A.; Jubault, M.; Roncali, J. *Advanced Materials* **1994**, *6* (2), 138-142. (b) Corish, J.; Morton-Blake, D. A. *Synthetic Metals* **2005**, *151* (1), 49-59.
8. McCullough, R. D.; Tristram-Nagle, S.; Williams, S. P.; Lowe, R. D.; Jayaraman, M. *Journal of the American Chemical Society* **1993**, *115* (11), 4910-4911.
9. (a) Van den Bergh, K.; Cosemans, I. *Macromolecules* **2010**, *43*(8), 3794-3800. (b) Vandeleene, S.; Jivanescu, M.; Stesmans, A.; Cuppens, J.; Van Bael, M. J. *Macromolecules* **2011**, *44*(12), 4911-4919. (c) Verswyvel, M. *Macromolecules* **2011**, *44*(24), 9489-9498.
10. Oosterbaan, W. D.; Vrindts, V.; Berson, S.; Guillerez, S.; Douheret, O.; Ruttens, B.; D'Haen, J.; Adriaensens, P.; Manca, J.; Lutsen, L.; Vanderzande, D. *Journal of Materials Chemistry* **2009**, *19* (30), 5424-5435.
11. Uy, R. L.; Price, S. C.; You, W. *Macromolecular Rapid Communications* **2012**, *33* (14), 1162-1177.
12. (a) Andreasen, B.; Tanenbaum, D. M.; Hermenau, M.; Voroshazi, E.; Lloyd, M. T.; Galagan, Y.; Zimmermann, B.; Kudret, S.; Maes, W.; Lutsen, L.; Vanderzande, D.; Wurfel, U.; Andriessen, R.; Rösch, R.; Hoppe, H.; Teran-Escobar, G.; Lira-Cantu, M.; Rivaton, A.; Uzunoglu, G. Y.; Germack, D. S.; Hosel, M.; Dam, H. F.; Jorgensen, M.; Gevorgyan, S. A.; Madsen, M. V.; Bundgaard, E.; Krebs, F. C.; Norrman, K. *Physical Chemistry Chemical Physics* **2012**, *14* (33), 11780-11799. (b) Rösch, R.; Tanenbaum, D. M.; Jorgensen, M.; Seeland, M.; Barenklau, M.; Hermenau, M.; Voroshazi, E.; Lloyd, M. T.; Galagan, Y.; Zimmermann, B.; Wurfel, U.; Hosel, M.; Dam, H. F.; Gevorgyan, S. A.; Kudret, S.; Maes, W.; Lutsen, L.; Vanderzande, D.; Andriessen, R.; Teran-Escobar, G.; Lira-Cantu, M.; Rivaton, A.; Uzunoglu, G. Y.; Germack, D.; Andreasen, B.; Madsen, M. V.; Norrman, K.; Hoppe, H.; Krebs, F. C. *Energy & Environmental*

- Science* **2012**, *5* (4), 6521-6540. (c) Bertho, S.; Campo, B.; Piersimoni, F.; Spoltore, D.; D'Haen, J.; Lutsen, L.; Maes, W.; Vanderzande, D.; Manca, J. *Solar Energy Materials and Solar Cells* **2013**, *110* (0), 69-76. (d) Campo, B. J.; Bevk, D.; Kesters, J.; Gilot, J.; Bolink, H. J.; Zhao, J.; Bolsée, J.-C.; Oosterbaan, W. D.; Bertho, S.; D'Haen, J.; Manca, J.; Lutsen, L.; Van Assche, G.; Maes, W.; Janssen, R. A. J.; Vanderzande, D. *Organic Electronics* **2013**, *14* (2), 523-534.
13. Patil, A. O.; Ikenoue, Y.; Wudl, F.; Heeger, A. J. *Journal of the American Chemical Society* **1987**, *109* (6), 1858-1859.
14. Yamada, I.; Takagi, K.; Hayashi, Y.; Soga, T.; Shibata, N.; Toru, T. *International Journal of Molecular Sciences* **2010**, *11* (12), 5027-5039.
15. Soto, J. P.; Díaz, F. R.; del Valle, M. A.; Núñez, C. M.; Bernède, J. C. *European Polymer Journal* **2006**, *42* (4), 935-945.
16. Saito, F.; Takeoka, Y.; Rikukawa, M.; Sanui, K. *Synthetic Metals* **2005**, *153* (1-3), 125-128.
17. Kudret, S.; Oosterbaan, W.; D'Haen, J.; Lutsen, L.; Vanderzande, D.; Maes, W. *Advanced Synthesis & Catalysis* **2013**, *355* (2-3), 569-575.
18. (a) Rieke, R. D. *Science* **1989**, *246* (4935), 1260-1264. (b) Knochel, P., Preparation and Applications of Functionalized Organozinc Reagents. In *Active Metals*, Wiley-VCH Verlag GmbH: 2007; pp 191-236. (c) Knochel, P.; Schade, M. A.; Bernhardt, S.; Manolikakes, G.; Metzger, A.; Piller, F. M.; Rohbogner, C. J.; Mosrin, M. *Beilstein J. Org. Chem.* **2011**, *7*, 1261-1277. (d) Wu, X.-F.; Neumann, H. *Advanced Synthesis & Catalysis* **2012**, *354* (17), 3141-3160. (e) Wu, X.-F. *Chemistry - An Asian Journal* **2012**, *7*, 2502-2509.
19. Iovu, M. C.; Sheina, E. E.; Gil, R. R.; McCullough, R. D. *Macromolecules* **2005**, *38* (21), 8649-8656.

20. Chen, T.-A.; Wu, X.; Rieke, R. D. *Journal of the American Chemical Society* **1995**, *117* (1), 233-244.
21. (a) Chen T. A.; O'Brien R. A.; Rieke R. D. *Macromolecules* **1993**, *26*, 3462. (b) Coppo P.; Adams H.; Cupertino D. C.; Yeates S. G.; Turner M. L. *Chemical Communications* **2003**, 2548.
22. The importance of the Rieke zinc synthetic method for the field of organic photovoltaics cannot be underestimated though, as a large number of studies are based on the commercially available "Rieke P3HT".
23. (a) Miyanishi, S.; Tajima, K.; Hashimoto, K. *Macromolecules* **2009**, *42* (5), 1610-1618. (b) Kim, B. J.; Miyamoto, Y.; Ma, B.; Fréchet, J. M. J. *Advanced Functional Materials* **2009**, *19* (14), 2273-2281; (c) Vandenberg, J.; Conings, B.; Bertho, S.; Kesters, J.; Spoltore, D.; Esiner, S.; Zhao, J.; Van Assche, G.; Wienk, M. M.; Maes, W.; Lutsen, L.; Van Mele, B.; Janssen, R. A. J.; Manca, J.; Vanderzande, D. J. M. *Macromolecules* **2011**, *44* (21), 8470-8478. (d) Nam, C.-Y.; Qin, Y.; Park, Y. S.; Hlaing, H.; Lu, X.; Ocko, B. M.; Black, C. T.; Grubbs, R. B. *Macromolecules* **2012**, *45* (5), 2338-2347. (e) Ouhib, F.; Tomassetti, M.; Manca, J.; Piersimoni, F.; Spoltore, D.; Bertho, S.; Moons, H.; Lazzaroni, R.; Desbief, S.; Jerome, C.; Detrembleur, C. *Macromolecules* **2013**, *46*, 785-795.
24. Campo B.; Oosterbaan W. D.; Gilot J.; Cleij T. J.; Lutsen L.; Janssen, R. A. J.; Vanderzande D. *Proc. SPIE* **2009**, *7416*, 74161G.
25. Higgins, S. J. *Chemical Society Reviews* **1997**, *26* (4), 247-257.
26. Cagniant, P.; Merle, G.; Cagniant, D. *Bull. Soc. Chim. France* **1970**, *1*, 308.
27. Ikenoue, Y.; Outani, N.; Patil, A. O.; Wudl, F.; Heeger, A. J. *Synthetic Metals* **1989**, *30* (3), 305-319.
28. Bäuerle, P.; Würthner, F.; Heid, S. *Angewandte Chemie International Edition in English* **1990**, *29* (4), 419-420.

29. Bäuerle, P.; Gaudl, K.-U.; Würthner, F.; Sariciftci, N. S.; Mehring, M.; Neugebauer, H.; Zhong, C.; Doblhofer, K. *Advanced Materials* **1990**, *2* (10), 490-494.
30. Dai, J.; Sellers, J. L.; Nofle, R. E. *Synthetic Metals* **2003**, *139* (1), 81-88.
31. Chong, J. M.; Heuft, M. A.; Rabbat, P. *The Journal of Organic Chemistry* **2000**, *65* (18), 5837-5838.
32. Pattison, F. L. M.; Stothers, J. B.; Woolford, R. G. *Journal of the American Chemical Society* **1956**, *78* (10), 2255-2259.
33. Kang, S.-K.; Kim, W.-S.; Moon, B.-H. *Synthesis* **1985**, *1985* (12), 1161,1162.
34. Shirini, F.; Zolfigol, M. A.; Aliakbar, A.-R.; Albadi, J. *Synthetic Communications* **2010**, *40* (7), 1022-1028.
35. Bauerle, P.; Pfau, F.; Schlupp, H.; Würthner, F.; Gaudl, K.-U.; Caro, M. B.; Fischer, P. *Journal of the Chemical Society, Perkin Transactions 2* **1993**, (3), 489-494.
36. Wu, X.; Chen, T.-A.; Rieke, R. D. *Macromolecules* **1995**, *28* (6), 2101-2102.
37. Zhai, L.; Pilston, R. L.; Zaiger, K. L.; Stokes, K. K.; McCullough, R. D. *Macromolecules* **2002**, *36* (1), 61-64.
38. Casa, C. D.; Bizzarri, P. C.; Salatelli, E.; Bertinelli, F. *Advanced Materials* **1995**, *7* (12), 1005-1009.
39. Casa, C. D.; Andreani, F.; Bizzarri, P. C.; Salatelli, E. *Journal of Materials Chemistry* **1994**, *4* (7), 1035-1039.
40. Pomerantz, M.; Liu, M. L. *Synthetic Metals* **1999**, *101* (1-3), 95.
41. McCullough, R. D.; Lowe, R. D. *Journal of the Chemical Society, Chemical Communications* **1992**, (1), 70-72.

## Chapter 4

---

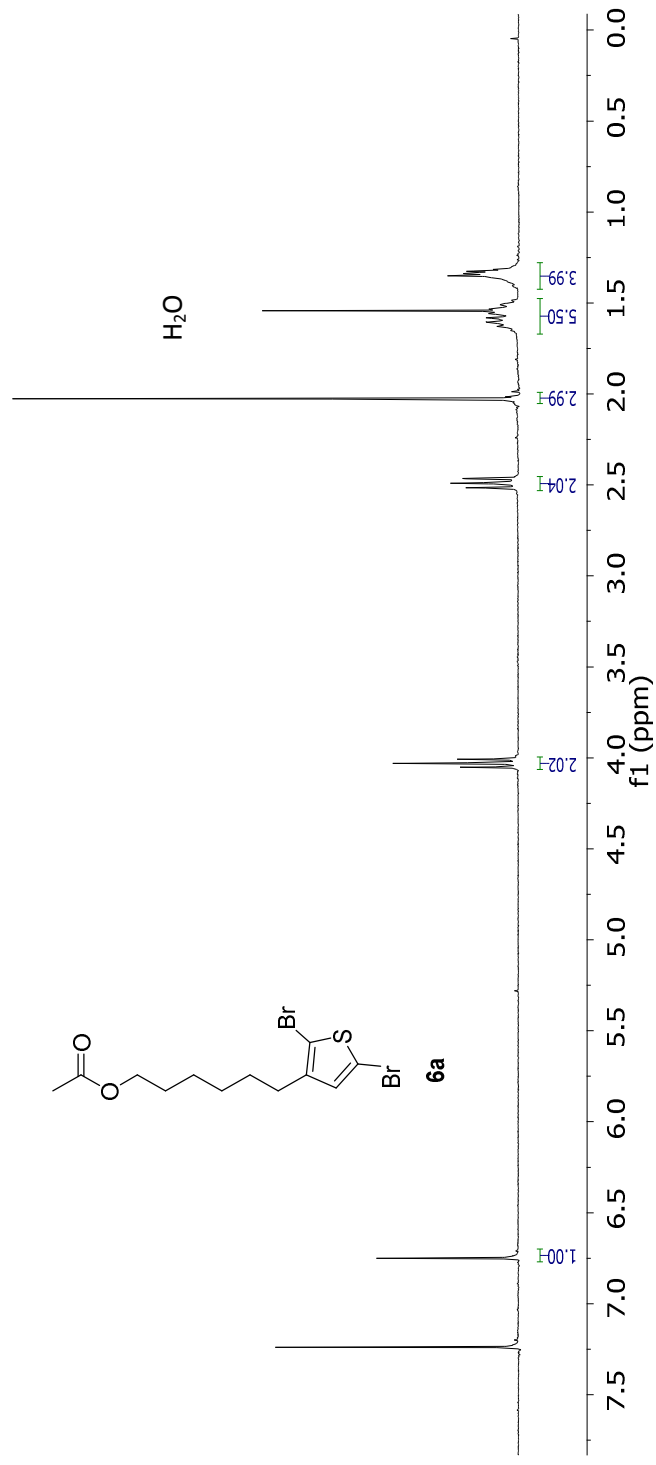
42. Chen, T. A.; Rieke, R. D. *Journal of the American Chemical Society* **1992**, *114* (25), 10087-10088.

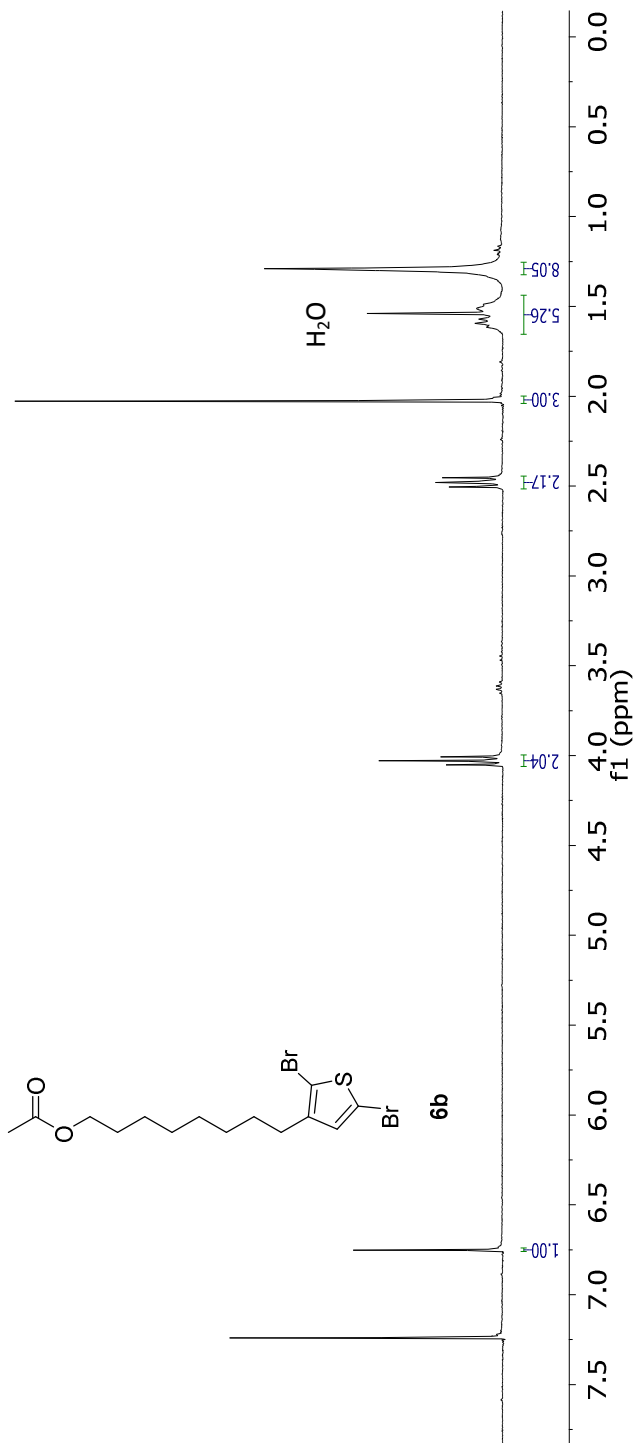
43. (a) Zhu, L.; Wehmeyer, R. M.; Rieke, R. D. *The Journal of Organic Chemistry* **1991**, *56* (4), 1445-1453. (b) Kim S.-H.; Kim, J.-G. *Bull. Korean Chem. Soc.* **2009**, *30* (10), 2283-2286.

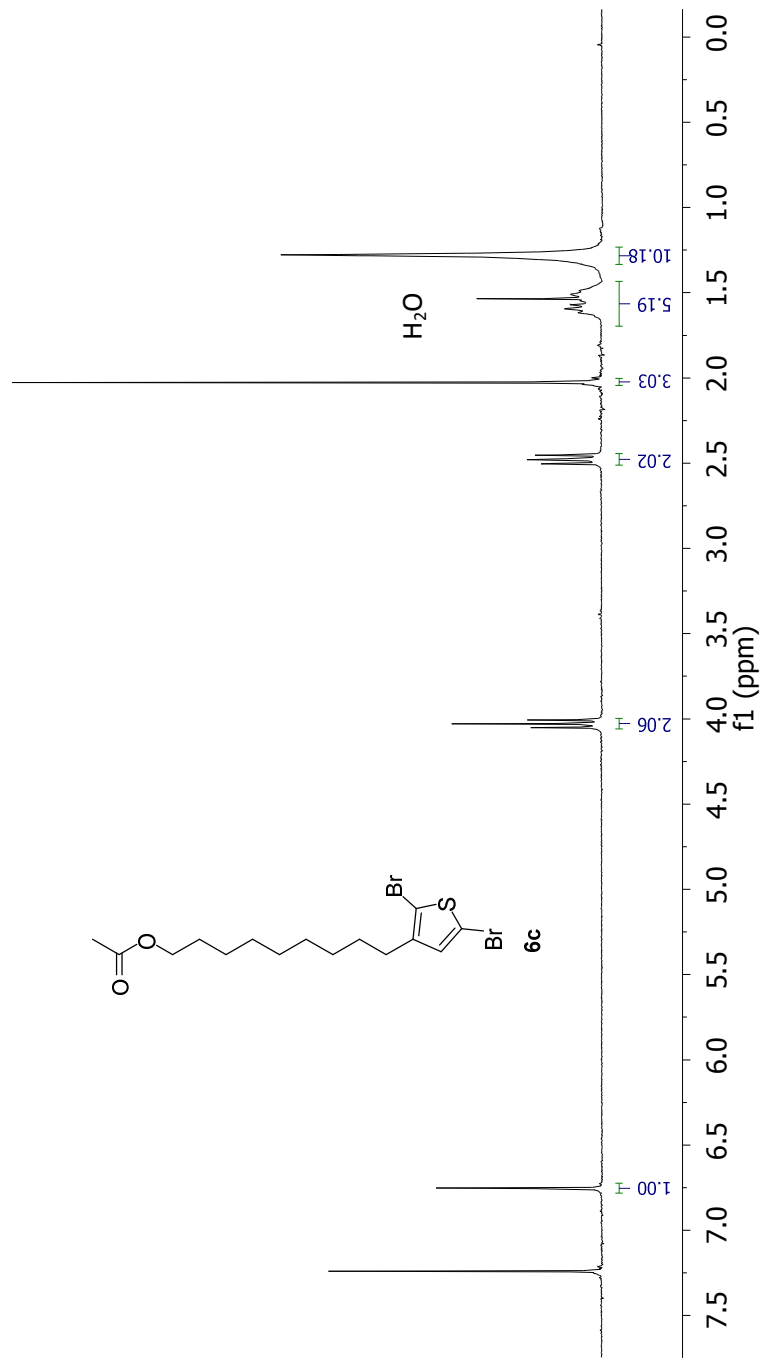


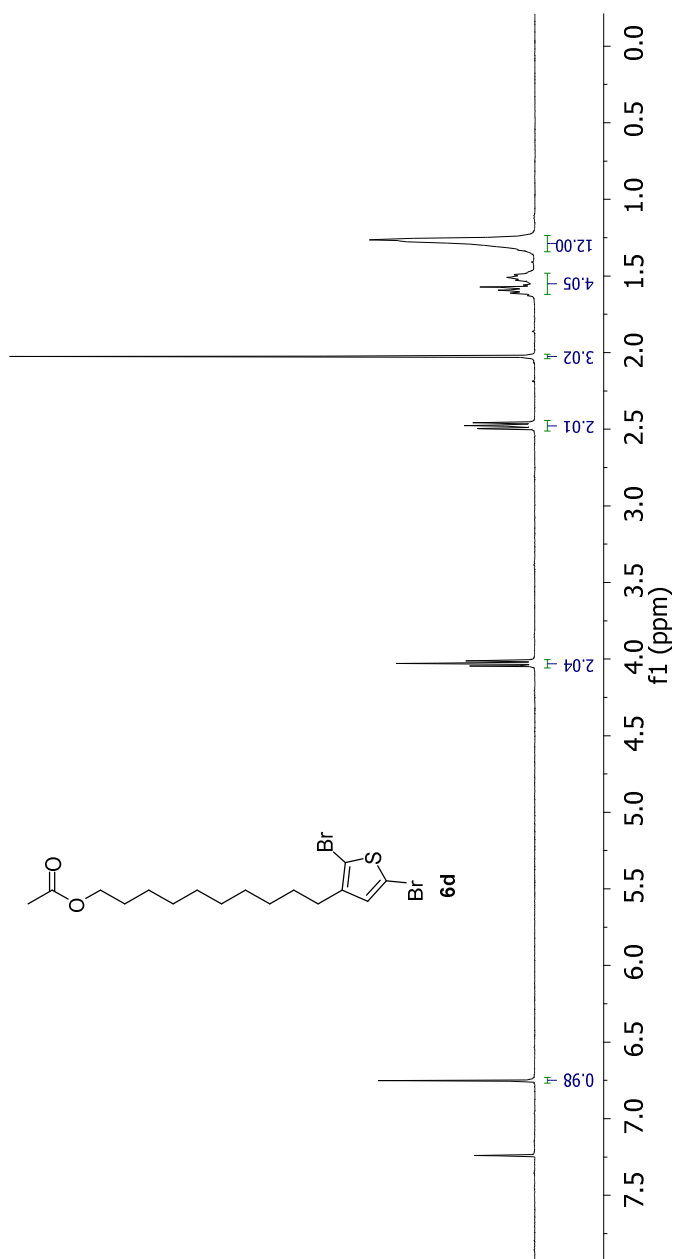
#### 4.7. Supporting information

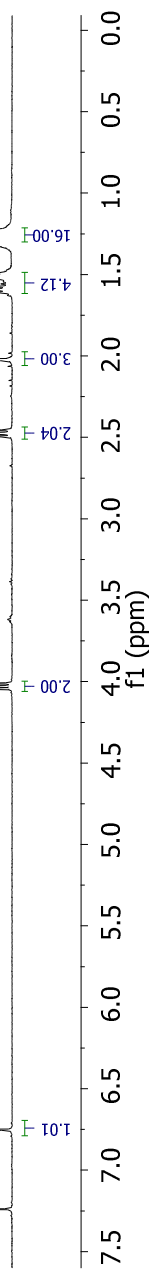
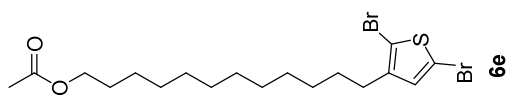
##### 1. <sup>1</sup>H NMR spectra of the ω-(2,5-dibromothiophene-3-yl)alkyl acetate monomers 6a-e and copolythiophenes P1-P5

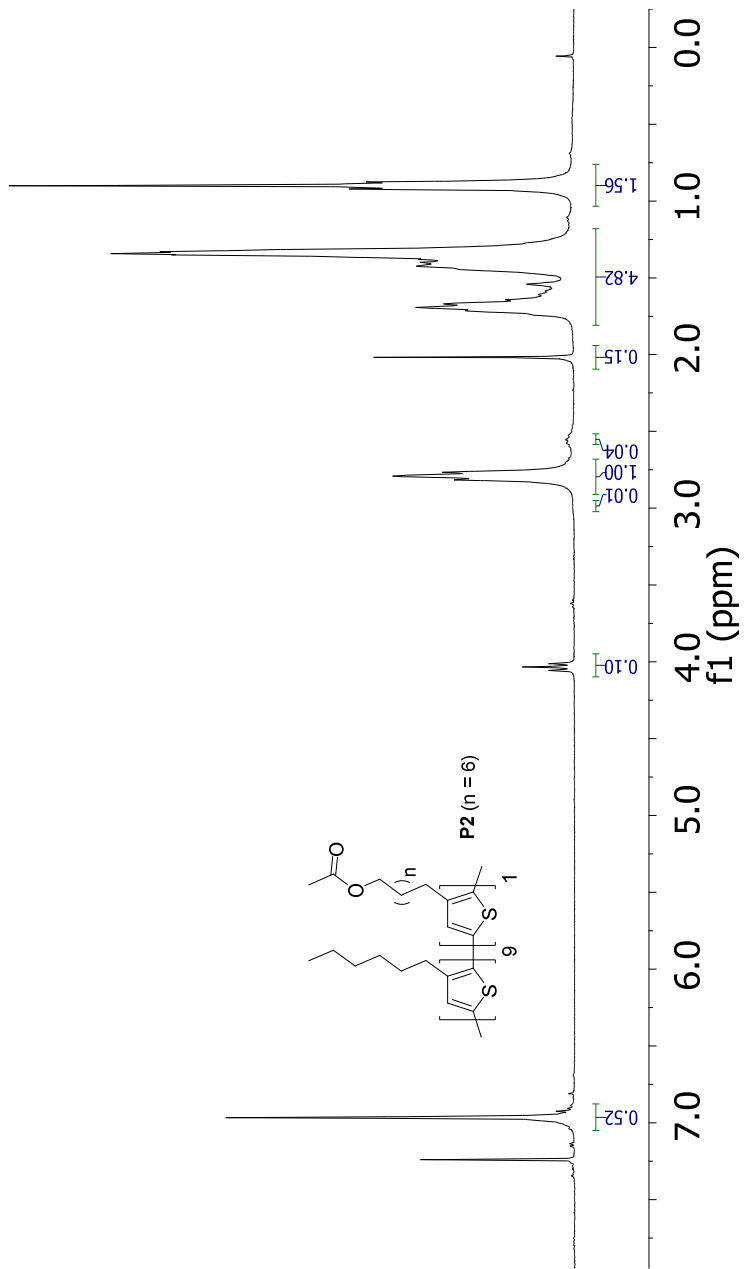


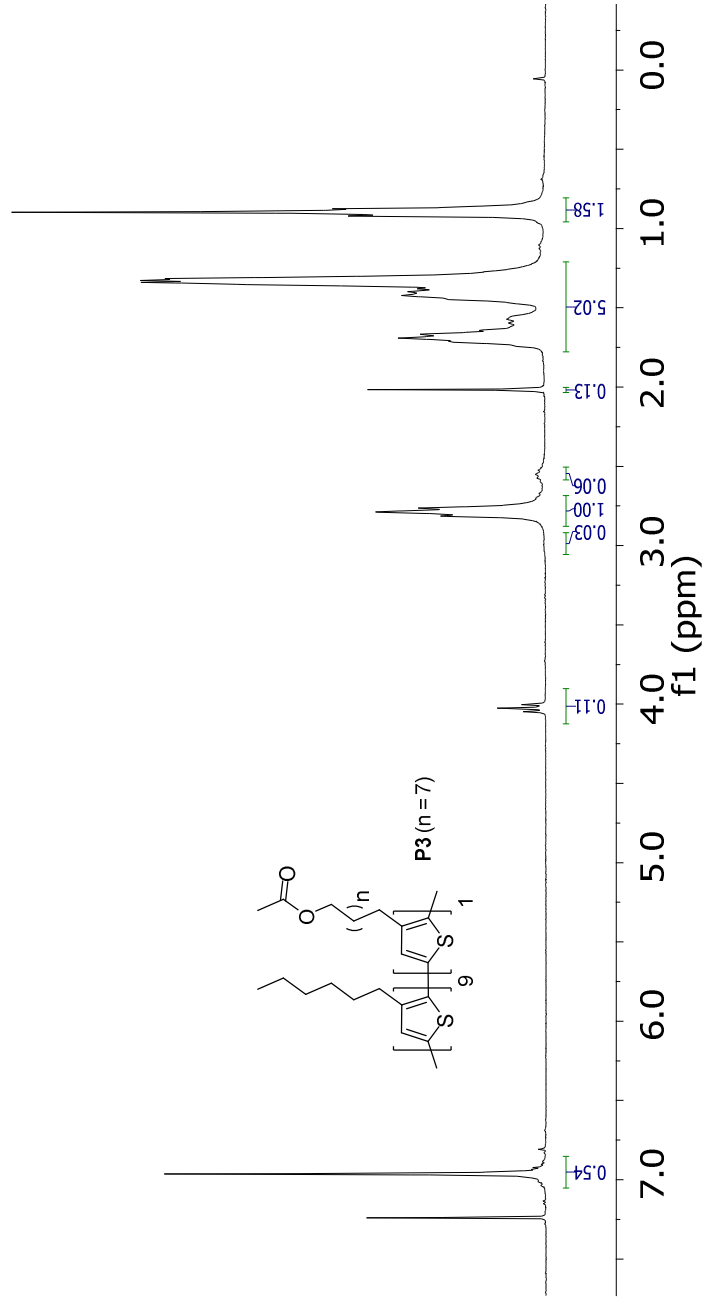


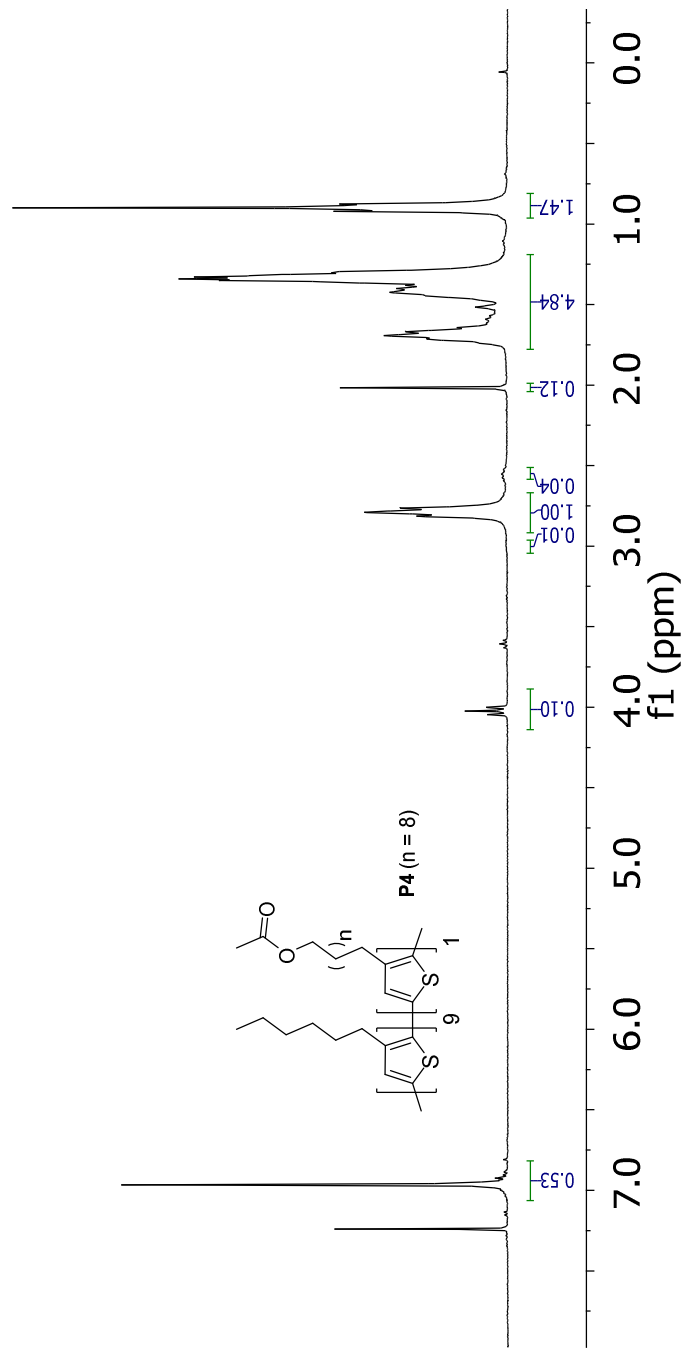




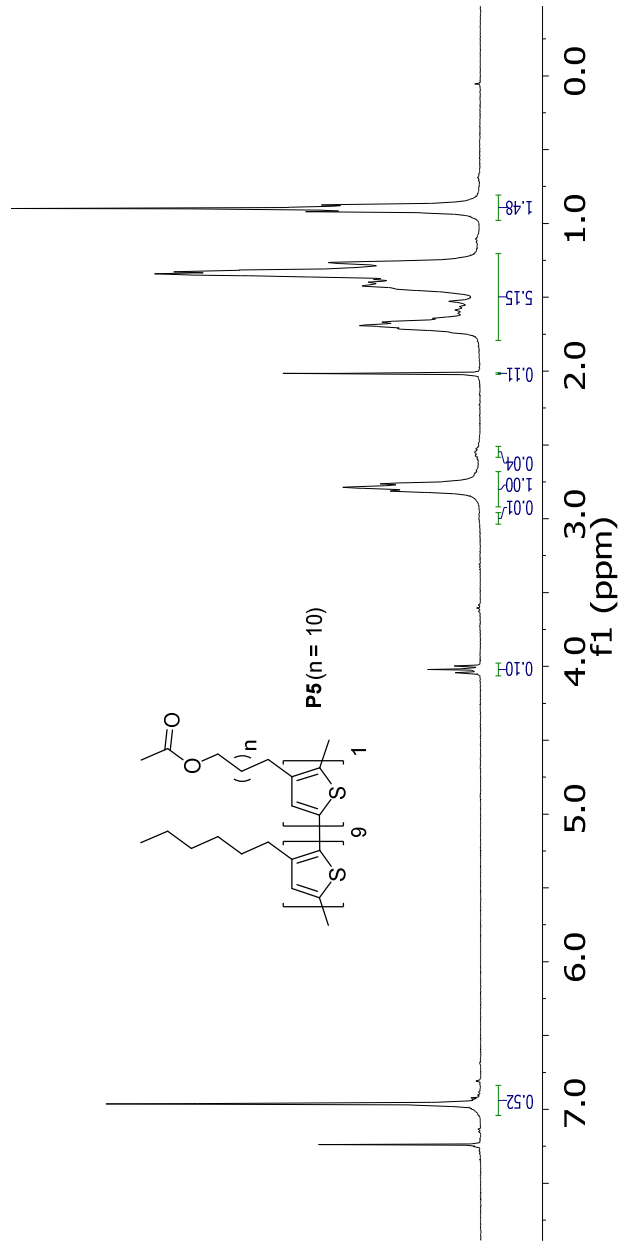




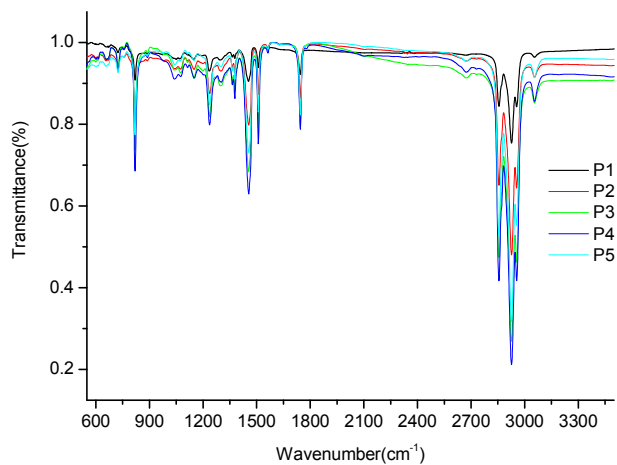




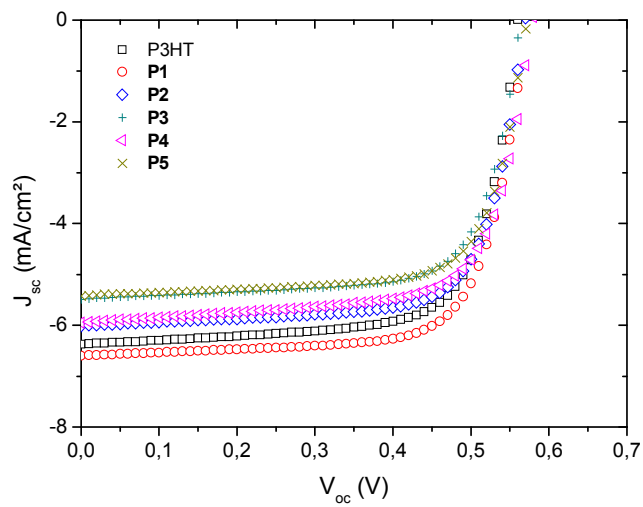




**2. FT-IR spectra of the copolythiophenes (as cast on NaCl disks)**



**3. J-V curves for the best performing polymer(P1-P5):PC<sub>61</sub>BM solar cells**

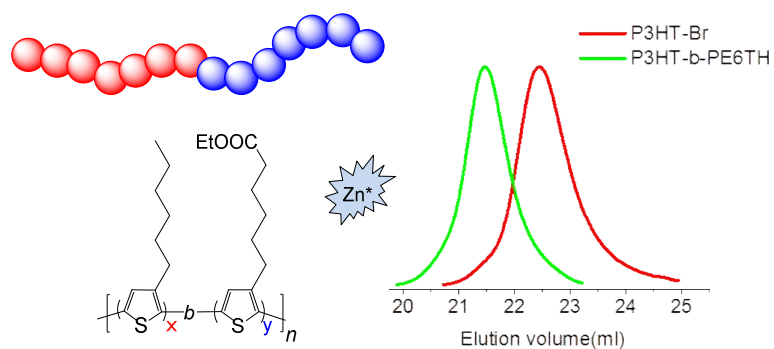


---

# Chapter 5

## Synthesis of ester side-chain functionalized diblock copolythiophenes via the Rieke method

---



---

\* Synthesis of ester side-chain functionalized diblock copolythiophenes via the Rieke method: Kudret, S.; Van den Brande, N.; Defour, M.; Van Mele, B.; Lutsen, L.; Vanderzande, D.; Maes, W. to be submitted.

### 5.1. Introduction

Since the discovery of electrical conductivity in organic polymers in the late 1970's,<sup>1</sup> these materials have found many applications. Polythiophenes show good conductivity, stability, and processability and have therefore been one of the most popular classes of conjugated polymers,<sup>2</sup> widely studied in organic field-effect transistors (OFETs),<sup>3</sup> light-emitting diodes (OLEDs),<sup>4</sup> solar cells,<sup>5</sup> and chemical sensors.<sup>6</sup> Organic photovoltaics (OPVs) based on conjugated polymers, as an alternative to the traditional silicon-based solar cells, have received large attention over the last decade due to the eminent interest in low cost energy production employing renewable resources.<sup>7</sup> Polymer-based bulk heterojunction (BHJ) organic solar cells have extensively been studied for the benchmark P3HT:PCBM (poly(3-hexylthiophene):[6,6]-phenyl C<sub>61</sub> butyric acid methyl ester) combination.<sup>7,8</sup> It is apparent from this research that the donor-acceptor composite active layer governs all aspects of the energy conversion mechanism. The morphology of the conjugated polymer:fullerene blend is one of the important properties that control the function within these devices, and is a key issue to improve both the power conversion efficiency and the long term stability of the devices.<sup>9</sup> This nanomorphology can be optimized toward an ideal phase-separated structure, enabling efficient charge transfer and percolation pathways for the charge carriers, by varying the blend composition, processing from different solvents, the use of additives or thermal/solvent annealing.<sup>10,11</sup> Even when an optimal morphology can be achieved, the blend components tend to phase-separate over time, creating individual polymer and fullerene regions, rendering the device less efficient. This decline in photovoltaic performance proceeds considerably faster at higher (operational) temperatures. It has been shown that the stability of the blend morphology can be significantly improved by utilization

of high  $T_g$  conducting polymers,<sup>12</sup> side chain functionalization<sup>13</sup> or crosslinkable<sup>14</sup> polymers and/or fullerenes.

Another way to achieve control over the blend morphology when using conjugated polymers is the implementation of block copolymers.<sup>15-17</sup> Due to their well-defined sequences, ordered chain architectures, and capability of self-assembly, block copolymers tend to phase-separate into well-ordered domains.<sup>18</sup> Block copolythiophenes composed of two different polythiophene blocks have been prepared for several optoelectronic applications, such as FETs,<sup>19</sup> polymer solar cells (either as active or hole transporting layers),<sup>20,21</sup> and memory devices.<sup>22</sup> Block copolythiophenes have generally been prepared by the Grignard metathesis (GRIM) polymerization, taking advantage of the quasi-living nature of the system.<sup>8,23</sup> The 'Rieke method' has also been used for the synthesis of polythiophenes, but block copolymers were only mentioned in a single patent.<sup>24</sup> The Rieke method uses highly reactive Rieke zinc metal powder ( $Zn^*$ ) which undergoes selective oxidative addition to 2,5-dibromo-3-alkylthiophenes at cryogenic temperature to afford the organozinc intermediate in a regio-controlled way. This organozinc compound then undergoes regioselective polymerization affording highly regioregular (rr) polymers.<sup>25</sup> In contrast to the GRIM method, the procedure is compatible with numerous side chain patterns, including ketones, nitriles, esters and other halides, making it a very useful synthetic protocol.<sup>26</sup> Nevertheless, the Rieke polymerization has only scarcely been used or elaborated, apart from some notable exceptions,<sup>27</sup> mainly due to difficulties in preparation of the Rieke zinc ( $Zn^*$ ) and (as a result) reproducibility problems. Recently, we have developed an optimized method which enables the preparation of Rieke zinc in an efficient and reproducible way and we have successfully applied this improved

procedure for the synthesis of regular P3HT.<sup>28</sup> It was shown that the benzothiophene impurity, present in commercial naphthalene in small quantities, has a crucial effect on the physical properties and reactivity of the formed active zinc powder. Therefore, addition of 3 mol% of benzothiophene (with regard to ZnCl<sub>2</sub>) to the lithiumnaphthalenide precursor solution (prepared *in situ*) is crucial to prevent agglomeration of the resulting Zn\* particles. In this study, we report that this optimized procedure also allows to prepare ester side-chain functionalized block copolythiophenes. To the best of our knowledge, this is the first time that block copolythiophenes were effectively made by the Rieke method (apart from the patent by Rieke et al.<sup>24</sup>).

## 5.2. Results and discussion

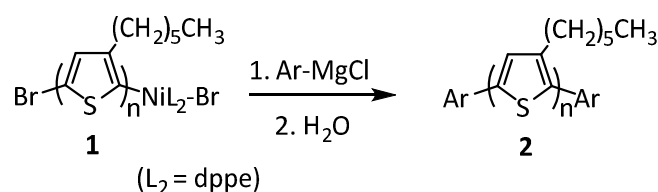
### 5.2.1. Living character of the Rieke polymerization

The GRIM and Rieke polymerization methods toward regioregular poly(3-alkylthiophenes) (P3ATs) are transition metal (Ni) catalyzed cross-coupling reactions, proceeding via a catalytic cycle of three sequential steps, i.e. oxidative addition, transmetalation, and reductive elimination.<sup>8,29</sup> It is formally accepted that this reaction is a polycondensation reaction and therefore it should follow a step-growth mechanism. Nevertheless, it was proposed by Yokozawa *et al.* that the GRIM and McCullough Ni-catalyzed cross-coupling polymerizations proceed via a chain-growth mechanism.<sup>23a</sup> Moreover, McCullough and co-workers suggested that the polymerization is not only chain-growth, but it is also a 'living' system.<sup>23b</sup> Since the polymerization is considered living, the addition of Grignard reagents (RMgX) at the end of the polymerization leads to end-capped *rr*-P3ATs.<sup>30</sup> The same group has also observed that addition of a new portion of 2-bromo-5-chloro-magnesium-3-alkylthiophene monomer to the nickel-terminated P3AT resulted in increase

of the molar mass, which gave rise to formation of a polythiophene polymer composed of two different blocks.<sup>23b</sup>

The high chemoselectivity and functional group tolerance and stability of organozinc compounds<sup>31</sup> render the Rieke zinc protocol attractive for more advanced polymer architectures as well. To be able to synthesize block copolythiophenes via the Rieke method, the propagating chain has to maintain its reactivity over a sufficient period of time, enabling sequential addition of different monomers. To analyze the living nature of the Rieke polymerization, some initial end-capping trials were performed. In general, an arylmagnesium chloride solution was added to reaction samples, withdrawn from the polymerization mixture via a syringe at different time intervals, to confirm the living character of the system and identify the propagating group in the polymerization (Scheme 1). If the propagating group is the Ni complex **1**, this will react with the arylmagnesium chloride and the coupling reaction occurs, followed by liberation of the Ni(0) catalyst by reductive elimination. In the resulting product, the remaining C-Br bond undergoes oxidative addition to this Ni(0) species, followed by the same coupling reaction, and quenching with water then gives rise to rr-P3AT **2** with two aryl end groups (Scheme 1).<sup>32</sup>

**Scheme 1.** Analysis of the living character of the Rieke polymerization by end-capping.



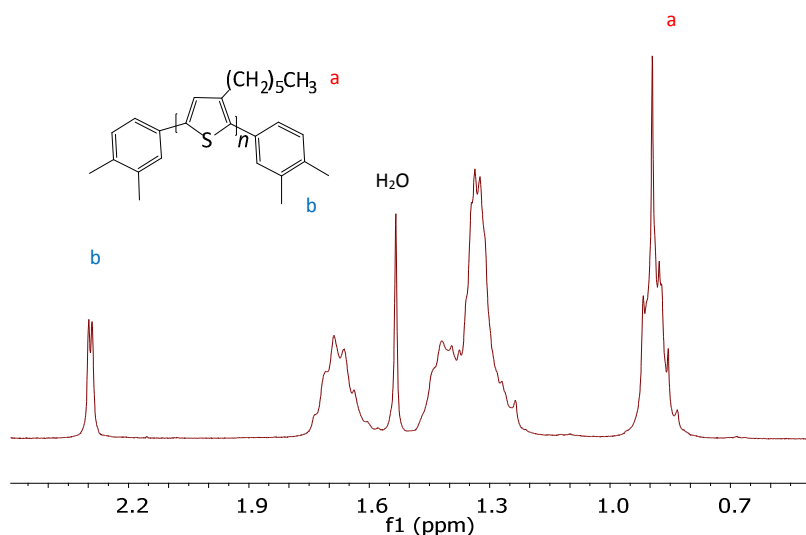
The polymerization of 2-bromo-5-(bromozincio)-3-hexylthiophene, prepared by treatment of 2,5-dibromo-3-hexylthiophene (**M1**) with 1.1 equivalent Rieke zinc (Zn\*) at -78 °C for 1 hour according to our previously optimized

---

protocol,<sup>28</sup> was conducted with 4 mol% Ni(dppe)Cl<sub>2</sub> in tetrahydrofuran (THF) at 40 °C for 60 minutes ( $M_n$  4.8 x 10<sup>3</sup> g mol<sup>-1</sup>,  $D$  1.18). During the course of the polymerization aliquots were withdrawn at different time intervals (15, 30, and 60 min) and quenched by the addition of an excess of 3,4-dimethylphenylmagnesium chloride (3,4-Me<sub>2</sub>C<sub>6</sub>H<sub>3</sub>MgCl), which was specifically chosen to facilitate end group analysis by <sup>1</sup>H NMR and to avoid side reactions (as reported for *tert*-butylmagnesium chloride<sup>32</sup>). The reaction mixture was stirred further for 3 hours and then water was added.<sup>32</sup> Based on the <sup>1</sup>H NMR spectra, number-average molar masses ( $M_n$ ) and polymerization degrees ( $DP_n$ ) could be determined. In the <sup>1</sup>H NMR spectrum of rr-P3HT end-capped with 3,4-Me<sub>2</sub>C<sub>6</sub>H<sub>3</sub>, the methyl proton signals at the two ends appear at 2.29 and 2.30 ppm (Figure 1). Consequently, based on the integral ratio of the methyl proton signals (**a**) of the hexyl side chains and the methyl proton signals (**b**) of the dimethylphenyl end groups, the  $DP_n$  and  $M_n$  were determined to be ~23 and 4.2 x 10<sup>3</sup> g mol<sup>-1</sup>, respectively. These results were in accordance with the monomer to catalyst feed ratio (which was ~23 as well), assuming that one Ni catalyst molecule forms one polymer chain. The conversion of the monomers seemed to be completed already after 15 minutes. The results revealed that the polymer was successfully end-capped, hence confirming the living character of the system.



**Figure 1.**  $^1\text{H}$  NMR spectrum of rr-P3HT obtained by polymerization of **M1** with 4 mol% Ni(dppe) $\text{Cl}_2$  in THF at rt for 60 minutes, followed by addition of 3,4-dimethylphenylmagnesium chloride (full spectrum in Figure S4).

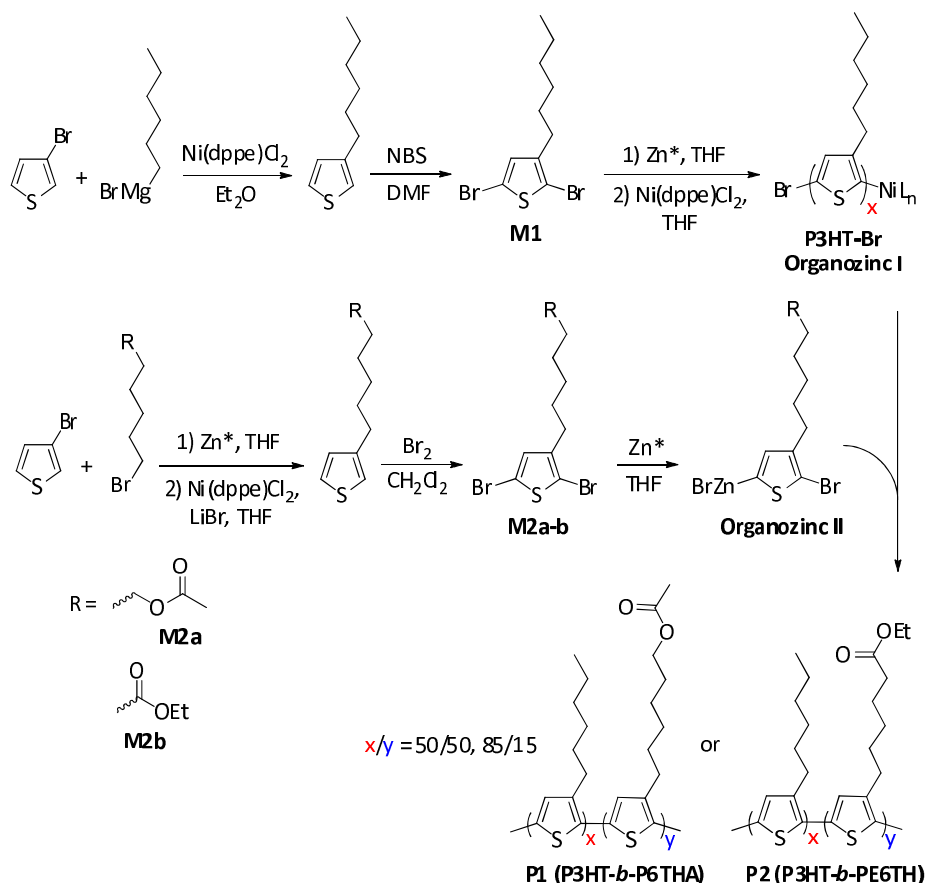


### 5.2.2. Block copolymer synthesis and characterization

For the block copolymer synthesis, dibrominated thiophenes with ester-functionalized side chains were used as the second monomer units, besides regular 2,5-dibromo-3-hexylthiophene, for several reasons. First of all, such monomers are not applicable in the standard GRIM procedures due to incompatibility of the ester moieties with the applied Grignard reagents, nicely illustrating the benefits of the activated Zn approach. The ester functions can also smoothly be converted to other functional groups (acids, alcohols, etc.) by postpolymerization reactions. Moreover, we have recently shown that ester-functionalized random copolymers can be beneficially applied to increase the thermal stability of BHJ organic solar cell active layer blends.<sup>13</sup>

The synthetic strategies employed for the preparation of the 2,5-dibromothiophene monomers and the ester-functionalized block copolymers are outlined in Scheme 2. 2,5-Dibromo-3-hexylthiophene (**M1**) was prepared according to the standard literature procedure via Kumada coupling of 3-bromothiophene and hexylmagnesium bromide and subsequent dibromination with an excess of *N*-bromosuccinimide (NBS) in DMF.<sup>33</sup> A similar route was used to prepare the ester-functionalized monomers (**M2a-b**). Nonetheless, in the first step, an organozinc compound was employed instead of the normal organomagnesium reagent. Following our optimized procedure to prepare Rieke zinc in highly reactive form,<sup>28</sup> the alkylester bromide precursors were treated with an excess of Rieke zinc at room temperature to afford the organozinc reagents in excellent yields (> 99%, as determined by GC-MS analysis after quenching an aliquot of the reaction mixture with a saturated ammonium chloride solution). The coupling reaction with 3-bromothiophene was performed in the presence of a Ni(dppe)Cl<sub>2</sub> catalyst with addition of LiBr to shorten the reaction time.<sup>34</sup> Dibromination was performed with bromine in dichloromethane as described in the literature.<sup>34</sup>

**Scheme 2.** Synthetic routes employed toward ester side-chain functionalized block copolythiophenes **P1** and **P2**.



The synthetic approach for the preparation of the block copolymers then consisted of two steps. The first step involved the synthesis of the monobromo-terminated poly(3-hexylthiophene) (**P3HT-Br**) (prepolymer) block, requiring oxidative addition of Rieke zinc to 2,5-dibromo-3-hexylthiophene (**M1**) in a regiospecific manner, yielding 2-bromo-5-(bromozincio)-3-hexylthiophene as the major and 2-(bromozincio)-5-bromo-3-hexylthiophene as the minor regioisomer.<sup>28</sup> Polymerization of the organozinc

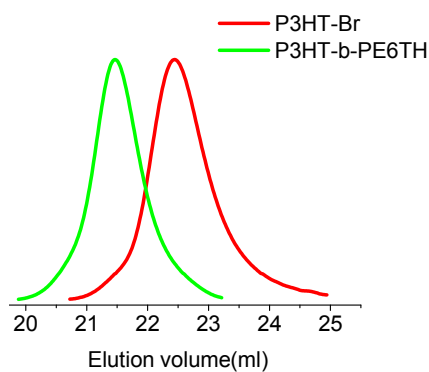
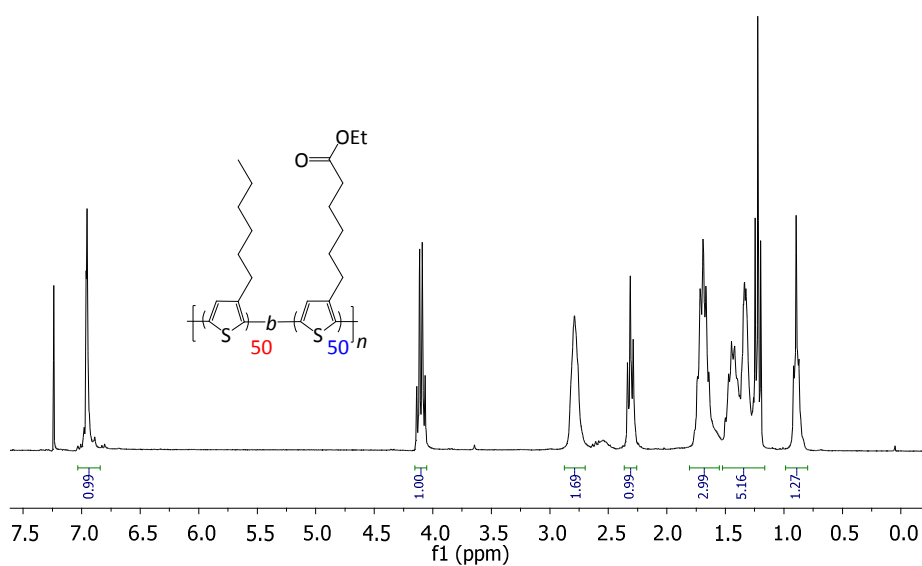
monomer was performed by addition of a catalytic amount (*vide infra*) of Ni(dppe)Cl<sub>2</sub> catalyst at 40 °C for 15 minutes. In the second step, the organozinc solution (**organozinc II**) of the respective ester-functionalized thiophene monomer **M2a-b**, prepared in the same manner in a separate schlenk tube, was transferred dropwise to the polymerization mixture. This was only done after complete conversion of 2,5-dibromo-3-hexylthiophene (**M1**) was confirmed by <sup>1</sup>H NMR and size exclusion chromatography (SEC) analysis. The polymerization was allowed to continue for an additional 30 minutes and then quenched with a 2M HCl solution. The polymers were precipitated in methanol, followed by sequential soxhlet extractions with methanol, hexanes and chloroform, respectively. The chloroform fractions were concentrated to afford the purified block copolymers in around 65% yield. The resultant diblock copolythiophenes were readily soluble in organic solvents. The polymerization was performed for the two different ester-functionalized monomers **M2a-b** with monomer feed ratios of 50/50 and 85/15. The results obtained are summarized in Table 1. The amount of catalyst was adjusted to 3 (**P2**) or 1 mol% (**P1**) with respect to the total amount of monomer. The monomer concentration was 0.1 M for the **P2** polymers, whereas it was 0.015 M for the **P1** block copolythiophenes. The high dilution was applied to prevent possible precipitation of the resultant polymers. Despite the fact that a lower amount of Ni catalyst (1 mol%) was employed, aiming to achieve the **P1** polymers in higher molar masses, the resulting materials had almost the same average molar masses as the **P2** polymers (Table 1), which can probably be related to the non-optimized polymerization conditions.

**Table 1.** Summary of polymer synthesis and characterization results.

polymer	monomer:catalyst ratio (mol:mol)	molar ratio (%) <sup>a</sup>	$M_n$ ( $\times 10^3$ g mol <sup>-1</sup> )	$D$
<b>P2-85/15</b>	100:3	87/13	8.3	1.10
<b>P2-50/50</b>	100:3	46/54	10.6	1.18
<b>P1-85/15</b>	100:1	86/14	8.8	1.49
<b>P1-50/50</b>	100:1	56/44	10.2	1.29

<sup>a</sup> As analyzed by <sup>1</sup>H NMR.

Figure 2 shows the size exclusion chromatograms of the bromine-terminated **P3HT-Br** prepolymer and the **P3HT-*b*-PE6TH 50/50 (P2-50/50)** block copolymer resulting thereof. The chromatogram clearly shifted to higher molar mass, while maintaining a narrow dispersity ( $D$  1.18), confirming the formation of a block copolymer through chain extension of the Ni-terminated **P3HT-Br** prepolymer. The successful addition of the second block and the built-in molar ratios were also confirmed by <sup>1</sup>H NMR. The built-in ratios closely respond to the monomer feed ratios (Table 1). Figure 3 shows the <sup>1</sup>H NMR spectrum of the **P2-50/50** block copolymer (the other ones can be found in the Supporting Information). The ester-functionalized **M2b** monomer can be identified by the appearance of a quadruplet and a triplet at 4.10 and 2.31 ppm, respectively, arising from the methylene protons closest to the ester moiety. The monomer incorporation ratio was determined by integrating either of these signals and the triplet arising from the methyl protons of the hexyl side chains.

**Figure 2.** SEC profiles of **P3HT-Br** and **P3HT-*b*-PE6TH 50/50 (P2 50/50)**.**Figure 3.**  $^1\text{H}$  NMR spectrum of **P3HT-*b*-PE6TH (P2) 50/50**.

Rapid heat-cool (RHC) DSC thermograms for the different copolymers are presented in Figure 4 and the values of the melting peak temperatures and enthalpies are gathered in Table 2. Glass transition temperatures were hard to define for all materials studied. Both the **P1** and **P2** block copolymers show

semi-crystalline behavior. For the **P1** materials, this behavior is most pronounced in the **50/50** composition, where a melting peak temperature (174 °C) is found that is very similar to that of the **P3HT-Br** precursor (177 °C). The lower melting enthalpy, about 58% of that of **P3HT-Br**, is a possible indication that this melting can be entirely attributed to the P3HT block in the copolymer, as this corresponds well to the molar ratio (56/46) found by <sup>1</sup>H NMR. For the 85/15 composition a very small melting peak can be found at reduced temperature, despite the larger amount of P3HT present. The **P2 50/50** copolymer shows the clearest indication of block copolymer behavior, exhibiting a double melting peak, which may be attributed to both blocks forming a separate crystalline phase (confirming the melting temperature of 177 °C for the P3HT block). The **P2-85/15** copolymer exhibits one pronounced melting peak at a higher temperature than for the **P3HT-Br** precursor. This is a striking change in thermal characteristics as compared to the **50/50** composition as well as the precursor polymer. When comparing the **P2 85/15** copolymer with the analogous random copolymer ( $T_m$  207 °C,  $\Delta H_m$  19.8 J g<sup>-1</sup>;  $M_n$  15.4 x 10<sup>3</sup> g mol<sup>-1</sup>,  $D$  1.67),<sup>13d</sup> the statistical monomer distribution seems to improve the melting temperature to a larger extent, although this may also be related to the higher  $M_n$  for this material. All in all it is quite hard to draw any conclusions from this limited data set regarding actual trends.

**Figure 4.** RHC thermograms of the second heating at  $500 \text{ K min}^{-1}$  of both **P1** and **P2** copolymers. The **P3HT-Br** precursor was included for comparison. The curves were shifted vertically for clarity.

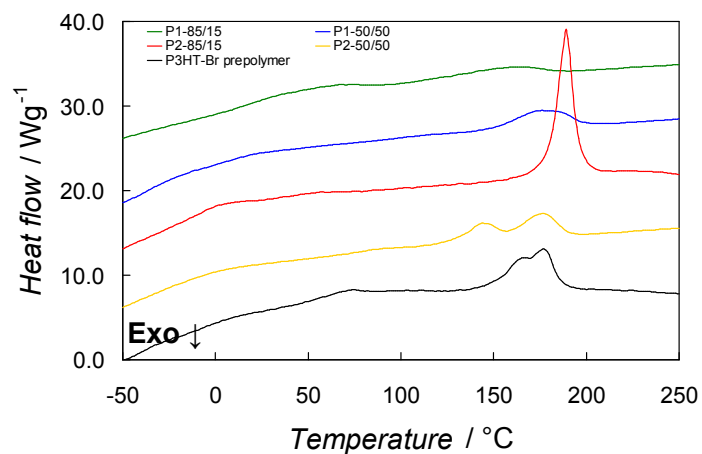


**Table 2.** Summary of the results from RHC thermal analysis.

Polymer	$T_m$ (°C)	$\Delta H_m$ (J g <sup>-1</sup> )
<b>P2-85/15</b>	189	23.9
<b>P2-50/50</b> <sup>a</sup>	143 & 177	13.4
<b>P1-85/15</b>	158	4.7
<b>P1-50/50</b>	174	9.4
<b>P3HT-Br</b>	177	16.1

<sup>a</sup> Two overlapping melting peaks were present for this polymer, indicated by the two peak maxima given here. The melting enthalpy is a combined value.



### 5.3. Conclusions

In conclusion, we have successfully synthesized ester-functionalized diblock copolythiophenes via the Rieke method, in an efficient way and under common laboratory conditions. The living nature of the Rieke polymerization was demonstrated by quenching the reaction mixture with 3,4-dimethylphenylmagnesium chloride, affording rr-P3HT with well-defined end groups and molar mass, and narrow dispersity. The formation of block copolymers by sequential organozinc monomer addition was confirmed by SEC and  $^1\text{H}$  NMR analysis, and further substantiated by RHC thermal analysis. The polymerization conditions have to be further optimized to achieve higher molar mass block copolythiophenes and efforts in this direction, including addition of other types of monomers, are currently ongoing, as is the application of the block copolythiophenes in organic solar cells.

### 5.4. Acknowledgements

We thank IMEC and Hasselt University for providing the PhD grant of S.K. We acknowledge the OPV-Life project from the IWT (Agentschap voor Innovatie door Wetenschap en Technologie; O&O 080368), the POLYSTAR project from PV ERA-NET, the IWT-SBO project POLYSPEC (Nanostructured POLYmer photovoltaic devices for efficient solar SPECTrum harvesting), and Belspo for supporting the IAP P6/27 and IAP 7/05 networks.

## 5.5. Experimental section

### Materials and methods

All manipulations were carried out on a dual manifold vacuum/Ar system. Lithium (granular, 99+%) from Acros was stored in a schlenk tube under Ar. Lithium, naphthalene and benzothiophene were weighed in air as needed and transferred to a schlenk tube under a stream of Ar. Naphthalene (Acros, 99+%) and benzothiophene (Sigma-Aldrich, 98%) were stored in a desiccator over phosphorous pentoxide. Zinc chloride (Acros, analysis grade 98.5%) was transferred into small vials inside a glove box and stored in a separate desiccator over phosphorous pentoxide. Zinc chloride was dried by treating it with thionyl chloride and heating with a Bunsen burner, and subsequently removed under a stream of Ar gas. THF was freshly distilled from Na/benzophenone under a N<sub>2</sub> atmosphere at atmospheric pressure prior to use. Brass cannulas were stored in an (air) oven at 110 °C and cleaned immediately after use with acetic acid (in the case of Zn\* remnant), acetone (to clean non-polymeric residues), or hot chloroform and/or chlorobenzene (for polymer-based contaminations).

NMR chemical shifts ( $\delta$ , in ppm) were determined relative to the residual CHCl<sub>3</sub> absorption (7.26 ppm) or the <sup>13</sup>C resonance shift of CDCl<sub>3</sub> (77.16 ppm). Polymer molar masses and distributions were determined relative to polystyrene standards by size exclusion chromatography (SEC). Chromatograms were recorded on a Spectra Series P100 (Spectra Physics) equipped with two mixed-B columns (10  $\mu$ m, 0.75 cm x 30 cm, Polymer labs) and a UV detector at 40 °C. THF was used as the eluent at a flow rate of 1.0 mL min<sup>-1</sup>. IR spectra were obtained on a Perkin-Elmer spectrophotometer with a resolution of 4 cm<sup>-1</sup> (16 scans) using films drop-casted on a NaCl disk. UV-Vis absorption measurements were performed with a scan rate of 600 nm min<sup>-1</sup> in

a continuous run from 200 to 800 nm. Rapid Heat-Cool Calorimetry (RHC) experiments were performed on a prototype RHC of TA Instruments, equipped with liquid nitrogen cooling and specifically designed for operation at high scanning rates.<sup>35</sup> RHC measurements were performed at 500 K min<sup>-1</sup> in aluminum crucibles, using neon (6 mL min<sup>-1</sup>) as a purge gas.

**Standard preparation of Rieke Zinc (Zn\*)**<sup>28</sup>

Two 120 mL schlenk vessels, A and B, were dried by heating with a Bunsen burner under reduced pressure and cooled down to rt under a stream of Ar. Schlenk vessel A, filled with Ar, was weighed and then reassembled to the schlenk line. Under a stream of Ar, ZnCl<sub>2</sub> was charged to the vessel. After three Ar/vacuum cycles, ZnCl<sub>2</sub> was wetted with a small amount of SOCl<sub>2</sub>. The schlenk vessel was heated by a Bunsen burner until the ZnCl<sub>2</sub> salt melted and a white fume was released, and the schlenk was then cooled down again under an Ar flow. Schlenk flask A was weighed again to determine the exact amount of ZnCl<sub>2</sub> and a stirring bar was added. Dried ZnCl<sub>2</sub> (1.1 equiv) was dissolved in freshly distilled THF (25 mL/g). Li pellets (2.2 equiv), naphthalene (2.25 equiv) and benzothiophene (0.04 equiv) were weighted in air and charged into schlenk flask B under an Ar stream. Dry THF (the same amount as added to dissolve ZnCl<sub>2</sub>) was added (the solution turned from colorless to dark green within less than 2 min) and the mixture was stirred further for 2 h to dissolve the Li pellets. The ZnCl<sub>2</sub> solution was transferred dropwise via cannula to the lithium naphthalenide solution over 10-15 min. The resulting black suspension might be stirred for 1 more h to consume the Li that was not dissolved before or stirring can be stopped right after the addition. The highly reactive zinc powder obtained was allowed to settle down for a couple of

---

hours. The supernatant was siphoned off via cannula leaving the Zn\* powder. Thus prepared reactive Rieke zinc was ready to use.

**2,5-Dibromo-3-hexylthiophene (M1)** was prepared according to a literature method.<sup>33</sup>

**6-(2,5-Dibromothiophen-3-yl)hexyl acetate (M2a).** 6-Acetoxyhexyl bromide (21.95 g, 98.4 mmol) was added neat, via a syringe, to freshly prepared Zn\* (120.5 mmol) in THF (150 mL) at rt, and the reaction mixture was stirred for 3 h at rt. Stirring was stopped and the solution was allowed to stand for a couple of hours to allow the excess of the zinc to settle from the dark brown organozinc bromide solution. In a second 500 mL flame-dried 3-neck round bottom flask, LiBr (8.54 g, 98.4 mmol), Ni(dppe)Cl<sub>2</sub> (1.7 g, 3.3 mmol), and 3-bromothiophene (6.22 mL, 66.4 mmol) were dissolved in dry THF (100 mL). The organozinc bromide solution was then transferred via cannula over a period of 30 min to that mixture under stirring at rt, and the mixture was allowed to stir further overnight. The reaction was quenched by the addition of a saturated NH<sub>4</sub>Cl solution, followed by extraction with Et<sub>2</sub>O, and simple distillation afforded 6-(thiophene-3-yl)hexyl acetate (11.27 g, 75%) in pure form. Dibromination with bromine (2.0 equiv) in CH<sub>2</sub>Cl<sub>2</sub> for 10 min at rt yielded the corresponding dibrominated compound **M2a** (Scheme 2). The resulting mixture was quenched with a NaHSO<sub>3</sub> solution and then neutralized by washing with a saturated NaHCO<sub>3</sub> solution. The crude product was distilled under high vacuum to afford a light-yellow oil (17.79 g, 93%). <sup>1</sup>H NMR (CDCl<sub>3</sub>, 300 MHz): δ 1.28–1.42 (m, 4H), 1.49–1.66 (m, 4H), 2.03 (s, 3H), 2.49 (t, *J*<sub>H-H</sub> = 7.8 Hz, 2H), 4.03 (t, *J*<sub>H-H</sub> = 6.7 Hz, 2H), 6.75 (s, 1H); <sup>13</sup>C NMR (CDCl<sub>3</sub>, 400 MHz): δ 171.7, 143.3, 131.5, 111.1, 108.7, 65.1, 30.1, 30.0, 29.3, 29.1, 26.4, 21.7; GC-MS: *m/z* 381/383/385 [M<sup>+</sup>] (≥ 98%); FT-IR (NaCl, *ν*<sub>max</sub> cm<sup>-1</sup>): 3091, 2934, 2857, 1738, 1541, 1463, 1418, 1387, 1364, 1241.

---

**Ethyl 6-(2,5-dibromothiophene-3-yl)hexanoate (M2b).**<sup>13d,34</sup> Ethyl 6-bromohexanoate (28.5 mL, 160 mmol) was added, via a syringe, to a freshly prepared Zn\* (195.6 mmol) solution in THF (250 mL) at rt, and the reaction mixture was stirred for 3 h at rt. Stirring was stopped and the solution was allowed to stand for a couple of hours to allow the excess of zinc to settle from the dark brown (6-ethoxy-6-oxohexyl)zinc(II) bromide solution. In a second 500 mL flame-dried 3-neck round bottom flask, LiBr (13.9 g, 160 mmol), Ni(dppe)Cl<sub>2</sub> (4.81 g, 8.9 mmol), and 3-bromothiophene (12.5 mL, 133.3 mmol) were dissolved in dry THF (150 mL). The organozinc bromide solution was then transferred via a cannula over a period of 45 min to that mixture under stirring at rt, and the reaction mixture was allowed to stir further overnight. The reaction was quenched with a saturated NH<sub>4</sub>Cl solution, followed by extraction with Et<sub>2</sub>O. Kugelrohr distillation of the crude product afforded ethyl 6-(thiophene-3-yl)hexanoate in pure form (22.02 g, 73%). Dibromination with bromine (2.0 equiv) in CH<sub>2</sub>Cl<sub>2</sub> for 10 min at rt yielded the corresponding dibrominated compound **M2b** (Scheme 2). Work-up and purification of the crude product was performed according to the literature procedure (34.76 g, 93%).<sup>34</sup> Material purity and identity were confirmed by NMR and MS.

**Reaction of the propagating group with a Grignard reagent (end-capping procedure).** A solution of 2,5-dibromo-3-hexylthiophene (**M1**) (4.08 g, 12.5 mmol) in THF (50 mL) was added via cannula to freshly prepared Rieke Zn\* (13.8 mmol) at -78 °C. The mixture was stirred for 1 h at this temperature and then allowed to warm to 0 °C gradually. The unreacted Zn\* was left to settle down overnight and the formed organozinc supernatant was then transferred by cannula via a 0.45 µm acrodisc filter into a flame-dried schlenk tube. Via a

---

cannula, 0.2 mol% of Ni(dppe)Cl<sub>2</sub> (0.013 g, 0.025 mmol) suspended in THF (5 mL) was added to the ice-cooled organozinc solution. The schlenk vessel was immersed into a preheated oil bath at 40 °C and the mixture was further stirred at this temperature. During the reaction, a part of the polymerization mixture was withdrawn at different time intervals and to these aliquots 3,4-dimethylphenylmagnesium chloride (0.5 M solution in THF) was added via a syringe. The reaction samples were stirred for another 3 h and then water was added, and the mixtures were extracted with CHCl<sub>3</sub>. The organic phases were washed with water, dried over anhydrous MgSO<sub>4</sub>, and concentrated under reduced pressure. The residues were dissolved in a minimum amount of CHCl<sub>3</sub>, precipitated in methanol and collected by suction filtration to yield rr-P3HT samples with Me<sub>2</sub>C<sub>6</sub>H<sub>3</sub> end groups.

**Poly(3-hexylthiophene)-*block*-poly[6-(thiophene-3-yl)hexyl acetate] (P3HT-*b*-P6THA or P1).**

The feed molar ratio of **M1** and **M2a** was either 50:50 or 85:15. The synthesis procedure for the **P3HT-*b*-P6THA** diblock copolymers (illustrated for the 50:50 feed molar ratio) was as follows: 2,5-Dibromo-3-hexylthiophene (**M1**) (1.010 g, 3.10 mmol) in THF (6 mL) was added via a cannula to freshly prepared Rieke Zn\* (3.72 mmol) at -78 °C. The mixture was stirred for 1 h at this temperature and then allowed to warm to 0 °C gradually. The unreacted Zn\* was allowed to settle down overnight and the formed organozinc supernatant was then transferred by cannula via a 0.45 µm acrodisc filter into a flame-dried schlenk tube and further diluted to 0.015 M by the addition of fresh THF. Organozinc solution I was heated up to 40 °C and 1 mol% of Ni(dppe)Cl<sub>2</sub> (0.028 g, 0.053 mmol) was added in one portion. After stirring at this temperature for 15 min, the conversion of the monomer and the molar mass of the polymer formed were evaluated by taking a small aliquot of the reaction mixture (0.927 mmol),

---

which was withdrawn via a syringe, quenched with 2M HCl, and extracted with CHCl<sub>3</sub>. Organozinc solution II, prepared by reacting 6-(2,5-dibromothiophene-3-yl)hexyl acetate (**M2a**) (0.833 g, 2.17 mmol) with Rieke Zn\* (2.60 mmol) in the same manner as for organozinc I, was added via a syringe to the first solution, and the resulting mixture was stirred for an additional 30 min. The reaction was quenched by pouring 2M HCl aq. into the solution and the mixture was extracted with CHCl<sub>3</sub>. The organic layer was washed with water, dried over MgSO<sub>4</sub>, filtered, and concentrated under reduced pressure. The residue was added to methanol to give a black precipitate, which was filtered off and washed several times with methanol. The crude polymer was purified via sequential soxhlet extractions with methanol and hexanes, respectively. Polymer **P1 85/15** was synthesized in the same manner.

**P1 50/50**: UV-Vis (film,  $\lambda_{\max}$ , nm): 549, 605sh; SEC (THF):  $M_n$   $10.2 \times 10^3$  g mol<sup>-1</sup>,  $D$  1.29; <sup>1</sup>H NMR (300 MHz, CDCl<sub>3</sub>):  $\delta$  6.96 (s, 2H), 4.05 (t, 2H), 2.77/2.55 (t, 4H), 2.02 (s, 3H), 1.85–1.14 (m, 16H), 0.89 (t, 3H); <sup>13</sup>C NMR (CDCl<sub>3</sub>, 100 MHz): 171.2, 139.9, 130.4, 128.6, 64.5, 31.7, 30.5, 30.4, 29.4, 29.3, 29.2, 28.6, 25.8, 22.6, 21.0, 14.1; FT-IR (NaCl,  $\nu_{\max}$  cm<sup>-1</sup>): 3054, 2953, 2928, 2857, 1740, 1510, 1456, 1365, 1240, 1049, 820.

**P1 85/15**: UV-Vis (film,  $\lambda_{\max}$ , nm): 515, 600; SEC (THF):  $M_n$  =  $8.8 \times 10^3$  g mol<sup>-1</sup>,  $D$  1.49; <sup>1</sup>H NMR (300 MHz, CDCl<sub>3</sub>):  $\delta$  6.96 (s, 2H), 4.04 (t, 2H), 2.78/2.55 (t, 4H), 2.01 (s, 3H), 1.86–1.13 (m, 16H), 0.89 (t, 3H); <sup>13</sup>C NMR (CDCl<sub>3</sub>, 100 MHz): 171.2, 139.9, 133.7, 130.4, 128.6, 64.6, 31.7, 30.5, 30.4, 29.4, 29.3, 28.5, 25.7, 22.7, 21.0, 14.1; FT-IR (NaCl,  $\nu_{\max}$  cm<sup>-1</sup>): 3055, 2955, 2927, 2856, 1740, 1510, 1457, 1364, 1238, 1048, 822.

---

**Poly(3-hexylthiophene)-*block*-poly[ethyl 6-(thiophene-3-yl)hexanoate]**

**(P3HT-*b*-PE6TH or P2).** The feed molar ratio of **M1** and **M2b** was either 50:50 or 85:15. The synthesis procedure for the **P3HT-*b*-PE6TH** diblock copolymers (illustrated for the feed molar ratio of 50:50) was as follows: 2,5-Dibromo-3-hexylthiophene (**M1**) (3.587 g, 11.0 mmol) in THF (22 mL) was added via a cannula to freshly prepared Rieke Zn\* (13.2 mmol) at -78 °C. The mixture was stirred for 1 h at this temperature and then allowed to warm to 0 °C gradually. The unreacted Zn\* was allowed to settle down overnight and the formed organozinc supernatant was then transferred by cannula via a 0.45 µm acrodisc filter into a flame-dried schlenk tube and further diluted to 0.1 M by addition of fresh THF. Organozinc solution I was heated up to 40 °C and 3 mol% of Ni(dppe)Cl<sub>2</sub> (0.332 g, 0.63 mmol) was added in one portion. After stirring at this temperature for 15 min, the conversion of the monomer and the molar mass of the polymer formed were evaluated by taking a small aliquot of the reaction mixture (1.0 mmol), which was withdrawn via a syringe, quenched with 2M HCl, and extracted with CHCl<sub>3</sub>. Organozinc solution II, prepared by reacting ethyl 6-(2,5-dibromothiophene-3-yl)hexanoate (**M2b**) (3.841 g, 10.0 mmol) with Rieke Zn\* (12.0 mmol) in the same manner as for organozinc I, was added via syringe to the first solution, and the resulting mixture was stirred for an additional 30 min. The reaction was quenched by pouring 2M HCl aq. into the solution and the mixture was extracted with CHCl<sub>3</sub>. The organic layer was washed with water, dried over MgSO<sub>4</sub>, filtered, and concentrated under reduced pressure. The residue was added to methanol to give a black precipitate, which was filtered off and washed several times with methanol. The crude polymer was purified via sequential soxhlet extractions with methanol and hexanes, respectively. Polymer **P2 85/15** was synthesized in the same manner.



**P2 50/50:** UV-Vis (film,  $\lambda_{\max}$ , nm): 550, 605sh; SEC (THF):  $M_n$   $10.6 \times 10^3$  g mol<sup>-1</sup>,  $D$  1.18; <sup>1</sup>H NMR (300 MHz, CDCl<sub>3</sub>):  $\delta$  6.95 (s, 2H), 4.10 (q, 2H), 2.79/2.55 (t, 4H), 2.31 (t, 2H), 1.76–1.18 (m, 14H), 0.90 (t, 6H); <sup>13</sup>C NMR (CDCl<sub>3</sub>, 100 MHz):  $\delta$  174.4, 140.5, 140.2, 134.3, 131.3, 131.1, 129.3, 60.9, 35.0, 32.4, 31.2, 31.0, 30.1, 30.0, 29.8, 25.5, 23.3, 15.0, 14.8; FT-IR (NaCl,  $\nu_{\max}$  cm<sup>-1</sup>): 3055, 2952, 2928, 2857, 1736, 1510, 1456, 1349, 1214, 1033, 820.

**P2 85/15:** UV-Vis (film,  $\lambda_{\max}$ , nm): 556, 605sh; SEC (THF):  $M_n$   $8.3 \times 10^3$  g mol<sup>-1</sup>,  $D$  1.10; <sup>1</sup>H NMR (300 MHz, CDCl<sub>3</sub>):  $\delta$  6.96 (s, 2H), 4.10 (q, 2H), 2.78/2.55 (t, 4H), 2.31 (t, 2H), 1.78–1.20 (m, 14H), 0.90 (t, 6H); <sup>13</sup>C NMR (CDCl<sub>3</sub>, 100 MHz):  $\delta$  174.4, 140.55, 134.3, 131.2, 129.3, 77.3, 60.9, 35.0, 32.3, 31.1, 30.9, 30.04, 29.9, 29.7, 25.5, 23.3, 14.93, 14.81; FT-IR (NaCl,  $\nu_{\max}$  cm<sup>-1</sup>): 3055, 2955, 2927, 2857, 1737, 1510, 1455, 1350, 1214, 820.

### 5.6. References

1. Shirakawa, H.; Louis, E. J.; MacDiarmid, A. G.; Chiang, C. K.; Heeger, A. J. *Journal of the Chemical Society, Chemical Communications* **1977**, 0 (16), 578-580.
2. McCullough, R. D. *Advanced Materials* **1998**, 10 (2), 93-116.
3. Sirringhaus, H.; Tessler, N.; Thomas, D. S.; Brown, P. J.; Friend, R. H., High-mobility conjugated polymer field-effect transistors. In *Advances in Solid State Physics 39*, Kramer, B., Ed. Springer Berlin Heidelberg: 1999; Vol. 39, pp 101-110.
4. Andersson, R. M.; Thomas, O.; Mammo, W.; Svensson, M.; Theander, M.; Inganäs, O. *Journal of Materials Chemistry* **1999**, 9 (9), 1933-1940.
5. Blom, P. W. M.; Mihailetschi, V. D.; Koster, L. J. A.; Markov, D. E. *Advanced Materials* **2007**, 19 (12), 1551-1566.
6. McQuade, D. T.; Pullen, A. E.; Swager, T. M. *Chemical Reviews* **2000**, 100 (7), 2537-2574.
7. (a) Brabec, C. J.; Gowrisanker, S.; Halls, J. J. M.; Laird, D.; Jia, S.; Williams, S. P. *Advanced Materials* **2010**, 22 (34), 3839-3856; (b) Nelson, J. *Materials Today* **2011**, 14 (10), 462-470; (c) Boudreault, P.-L. T.; Najari, A.; Leclerc, M. *Chemistry of Materials* **2011**, 23 (3), 456-469; (d) Koster, L. J. A.; Shaheen, S. E.; Hummelen, J. C. *Advanced Energy Materials* **2012**, 2 (10), 1246-1253; (e) Kumar, P.; Chand, S. *Progress in Photovoltaics: Research and Applications* **2012**, 20 (4), 377-415; (f) Gang, I.; Rui, Z.; Yang, Y. *Nature Photonics* **2012**, 6 (3), 153-161; (g) Jørgensen, M.; Norrman, K.; Gevorgyan, S. A.; Tromholt, T.; Andreasen, B.; Krebs, F. C. *Advanced Materials* **2012**, 24 (5), 580-612.
8. (a) Marrocchi, A.; Lanari, D.; Facchetti, A.; Vaccaro, L. *Energy & Environmental Science* **2012**, 5, 8457-8474; (b) Dang, M. T.; Hirsch, L.; Wantz,

G. *Advanced Materials* **2011**, *23* (31), 3597-3602; (c) Dang, M. T.; Hirsch, L.; Wantz, G.; Wuest, J. D. *Chemical Reviews* **2013**, *113*, 3734-3765.

9. Yang, X.; Loos, J. *Macromolecules* **2007**, *40* (5), 1353-1362.

10. Savenije, T. J.; Kroeze, J. E.; Yang, X.; Loos, J. *Advanced Functional Materials* **2005**, *15* (8), 1260-1266.

11. Yao, Y.; Hou, J.; Xu, Z.; Li, G.; Yang, Y. *Advanced Functional Materials* **2008**, *18* (12), 1783-1789.

12. Vandenberg, J.; Conings, B.; Bertho, S.; Kesters, J.; Spoltore, D.; Esiner, S.; Zhao, J.; Van Assche, G.; Wienk, M. M.; Maes, W.; Lutsen, L.; Van Mele, B.; Janssen, R. A. J.; Manca, J.; Vanderzande, D. J. M. *Macromolecules* **2011**, *44* (21), 8470-8478.

13. (a) Rösch, R.; Tanenbaum, D. M.; Jorgensen, M.; Seeland, M.; Barenklau, M.; Hermenau, M.; Voroshazi, E.; Lloyd, M. T.; Galagan, Y.; Zimmermann, B.; Wurfel, U.; Hosel, M.; Dam, H. F.; Gevorgyan, S. A.; Kudret, S.; Maes, W.; Lutsen, L.; Vanderzande, D.; Andriessen, R.; Teran-Escobar, G.; Lira-Cantu, M.; Rivaton, A.; Uzunoglu, G. Y.; Germack, D.; Andreasen, B.; Madsen, M. V.; Norrman, K.; Hoppe, H.; Krebs, F. C. *Energy & Environmental Science* **2012**, *5* (4), 6521-6540; (b) Tanenbaum, D. M.; Hermenau, M.; Voroshazi, E.; Lloyd, M. T.; Galagan, Y.; Zimmermann, B.; Hosel, M.; Dam, H. F.; Jorgensen, M.; Gevorgyan, S. A.; Kudret, S.; Maes, W.; Lutsen, L.; Vanderzande, D.; Wurfel, U.; Andriessen, R.; Rösch, R.; Hoppe, H.; Teran-Escobar, G.; Lira-Cantu, M.; Rivaton, A.; Uzunoglu, G. Y.; Germack, D.; Andreasen, B.; Madsen, M. V.; Norrman, K.; Krebs, F. C. *RSC Advances* **2012**, *2* (3), 882-893; (c) Bertho, S.; Campo, B.; Piersimoni, F.; Spoltore, D.; D'Haen, J.; Lutsen, L.; Maes, W.; Vanderzande, D.; Manca, J. *Solar Energy Materials and Solar Cells* **2013**, *110* (0), 69-76; (d) Campo, B. J.; Bevk, D.; Kesters, J.; Gilot, J.;

Bolink, H. J.; Zhao, J.; Bolsée, J.-C.; Oosterbaan, W. D.; Bertho, S.; D'Haen, J.; Manca, J.; Lutsen, L.; Van Assche, G.; Maes, W.; Janssen, R. A. J.; Vanderzande, D. *Organic Electronics* **2013**, *14* (2), 523-534.

14. (a) Miyanishi, S.; Tajima, K.; Hashimoto, K. *Macromolecules* **2009**, *42* (5), 1610-1618; (b) Kim, B. J. *Advanced Functional Materials* **2009**, *19* (14), 2273-2281; (c) Gholamkhash, B.; Holdcroft, S. *Chemistry of Materials* **2010**, *22* (18), 5371-5376; (d) Kim, H. J.; Han, A. R.; Cho, C.-H.; Kang, H.; Cho, H.-H.; Lee, M. Y.; Fréchet, J. M. J.; Oh, J. H.; Kim, B. J. *Chemistry of Materials* **2011**, *24* (1), 215-221; (e) Nam, C.-Y.; Qin, Y.; Park, Y. S.; Hlaing, H.; Lu, X.; Ocko, B. M.; Black, C. T.; Grubbs, R. B. *Macromolecules* **2012**, *45* (5), 2338-2347; (f) He, D.; Du, X.; Zhang, W.; Xiao, Z.; Ding, L. *Journal of Materials Chemistry A* **2013**, *1* (14), 4589-4594; (g) Ouhib, F.; Tomassetti, M.; Manca, J.; Piersimoni, F.; Spoltore, D.; Bertho, S.; Moons, H.; Lazzaroni, R.; Desbief, S.; Jerome, C.; Detrembleur, C. *Macromolecules* **2013**, *46*, 785-795.

15. de Cuendias, A.; Hiorns, R. C.; Cloutet, E.; Vignau, L. *Polymer International* **2010**, *59* (11), 1452-1476.

16. Lin, Y.; Lim, J. A.; Wei, Q.; Mannsfeld, S. C. B.; Briseno, A. L.; Watkins, J. J. *Chemistry of Materials* **2012**, *24* (3), 622-632.

17. Higashihara, T.; Ohshimizu, K.; Ryo, Y.; Sakurai, T.; Takahashi, A.; Nojima, S.; Ree, M.; Ueda, M. *Polymer* **2011**, *52* (17), 3687-3695.

18. (a) Zhang, Y.; Tajima, K.; Hirota, K.; Hashimoto, K. *Journal of the American Chemical Society* **2008**, *130* (25), 7812-7813; (b) Wu, P.-T.; Ren, G.; Li, C.; Mezzenga, R.; Jenekhe, S. A. *Macromolecules* **2009**, *42* (7), 2317-2320; (c) Wu, P.-T.; Ren, G.; Kim, F. S.; Li, C.; Mezzenga, R.; Jenekhe, S. A. *Journal of Polymer Science Part A: Polymer Chemistry* **2010**, *48* (3), 614-626; (d) Verswyvel, M.; Verstappen, P.; De Cremer, L.; Verbiest, T.; Koeckelberghs, G. *Journal of Polymer Science Part A: Polymer Chemistry* **2011**, *49* (24), 5339-

- 5349; (e) Lee, E.; Hammer, B.; Kim, J.-K.; Page, Z.; Emrick, T.; Hayward, R. C. *Journal of the American Chemical Society* **2011**, *133* (27), 10390-10393; (f) Hollinger, J.; DiCarmine, P. M.; Karl, D.; Seferos, D. S. *Macromolecules* **2012**, *45* (9), 3772-3778.
19. Chueh, C.-C.; Higashihara, T.; Tsai, J.-H.; Ueda, M.; Chen, W.-C. *Organic Electronics* **2009**, *10* (8), 1541-1548.
20. Yamada, I.; Takagi, K.; Hayashi, Y.; Soga, T.; Shibata, N.; Toru, T. *International Journal of Molecular Sciences* **2010**, *11* (12), 5027-5039.
21. Yao, K.; Chen, L.; Chen, X.; Chen, Y. *Chemistry of Materials* **2013**, *25*, 897-904.
22. Lai, Y.-C.; Ohshimizu, K.; Lee, W.-Y.; Hsu, J.-C.; Higashihara, T.; Ueda, M.; Chen, W.-C. *Journal of Materials Chemistry* **2011**, *21* (38), 14502-14508.
23. (a) Yokoyama, A.; Miyakoshi, R.; Yokozawa, T. *Macromolecules* **2004**, *37* (4), 1169-1171; (b) Iovu, M. C.; Sheina, E. E.; Gil, R. R.; McCullough, R. D. *Macromolecules* **2005**, *38* (21), 8649-8656.
24. Rieke, R. D. (6133 Heide Lane, Lincoln, Nebraska, 68512, US) PROCESS FOR PREPARATION OF REGIOREGULAR CONDUCTING BLOCK COPOLYMERS. 2009.
25. Chen, T.-A.; Wu, X.; Rieke, R. D. *Journal of the American Chemical Society* **1995**, *117* (1), 233-244.
26. Rieke, R. D. *Science* **1989**, *246* (4935), 1260-1264.
27. (a) Chen, T. A.; O'Brien, R. A.; Rieke, R. D. *Macromolecules* **1993**, *26*, 3462; (b) Coppo, P.; Adams, H.; Cupertino, D. C.; Yeates, S. G.; Turner, M. L. *Chemical Communications* **2003**, 2548.
28. Kudret, S.; Oosterbaan, W.; D'Haen, J.; Lutsen, L.; Vanderzande, D.; Maes, W. *Advanced Synthesis & Catalysis* **2013**, *355* (2-3), 569-575.

29. (a) Negishi, E.; Takahashi, T.; Baba, S.; Van Horn, D. E.; Okukado, N. *Journal of the American Chemical Society* **1987**, *109* (8), 2393-2401; (b) Yamamoto, T.; Morita, A.; Miyazaki, Y.; Maruyama, T.; Wakayama, H.; Zhou, Z. H.; Nakamura, Y.; Kanbara, T.; Sasaki, S.; Kubota, K. *Macromolecules* **1992**, *25* (4), 1214-1223.
30. Jeffries-El, M.; Sauvé, G.; McCullough, R. D. *Advanced Materials* **2004**, *16* (12), 1017-1019.
31. a) *Organozinc Reagents, A Practical Approach* (Eds.: Knochel, P.; Jones, P.), Oxford University Press, New York, **1999**; b) *The Chemistry of Organozinc Compounds* (Eds: Rappoport, Z.; Marek, I.), John Wiley & Sons Ltd, West Sussex, England, **2006**; c) Knochel, P.; Schade, M. A.; Bernhardt, S.; Manolikakes, G.; Metzger, A.; Piller, F. M.; Rohbogner, C. J.; Mosrin, M. *Beilstein J. Org. Chem.* **2011**, *7*, 1261-1277; d) Wu, X.-F. *Chemistry - An Asian Journal* **2012**, *7*, 2502-2509; e) Wu, X.-F.; Neumann, H, *Advanced Synthesis & Catalysis* **2012**, *354* (17), 3141-3160.
32. Miyakoshi, R.; Yokoyama, A.; Yokozawa, T. *Journal of the American Chemical Society* **2005**, *127* (49), 17542-17547.
33. Bauerle, P.; Pfau, F.; Schlupp, H.; Wurthner, F.; Gaudl, K.-U.; Caro, M. B.; Fischer, P. *Journal of the Chemical Society, Perkin Transactions 2* **1993**, (3), 489-494.
34. Kim, S.-H.; Kim, J.-G. *Bull. Korean Chem. Soc.* **2009**, *30* (10), 2283-286.
35. (a) Danley, R. L.; Caulfield, P. A.; Aubuchon, S. R. *Am. Lab.* **2008**, *40*, 9-11; (b) Wouters, S.; Demir, F.; Beenaerts, L.; Van Assche, G. *Thermochimi Acta* **2012**, *530*, 64-72.

## 5.7. Supporting information

### 1. Size exclusion chromatograms of the block copolymers and respective precursor polymers

**Figure S1.** SEC profiles of **P3HT-Br** and **P3HT-*b*-PE6TH (P2-85/15)**.

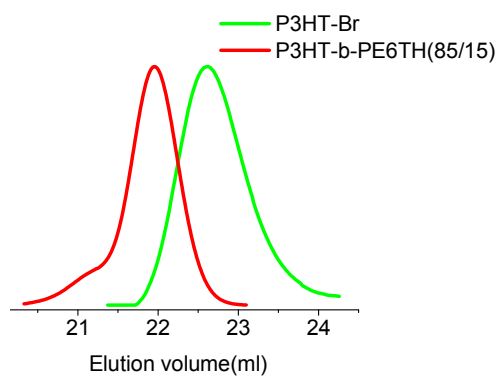


**Figure S2.** SEC profiles of **P3HT-Br** and **P3HT-*b*-P6THA 85/15 (P1-85/15)**.

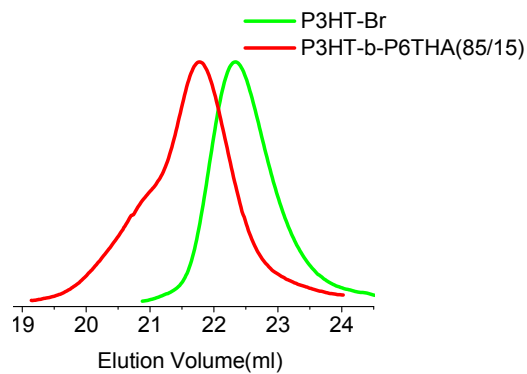
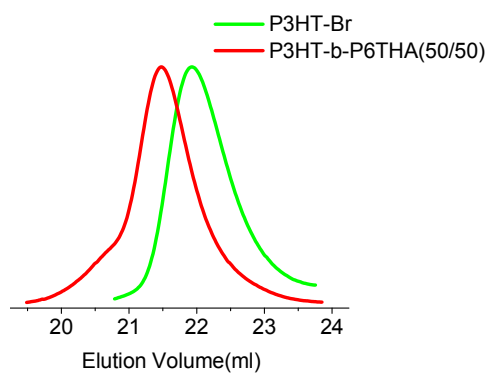


**Figure S3.** SEC profiles of **P3HT-Br** and **P3HT-*b*-P6THA 50/50 (P1-50/50)**.





## 2. <sup>1</sup>H NMR spectra of the block copolythiophenes and the end-capped P3HT

**Figure S4.** <sup>1</sup>H NMR spectrum (full range) of rr-P3HT obtained by polymerization of M1 with 4 mol% Ni(dppe)Cl<sub>2</sub> in THF at rt for 60 minutes, followed by addition of 3,4-dimethylphenylmagnesium

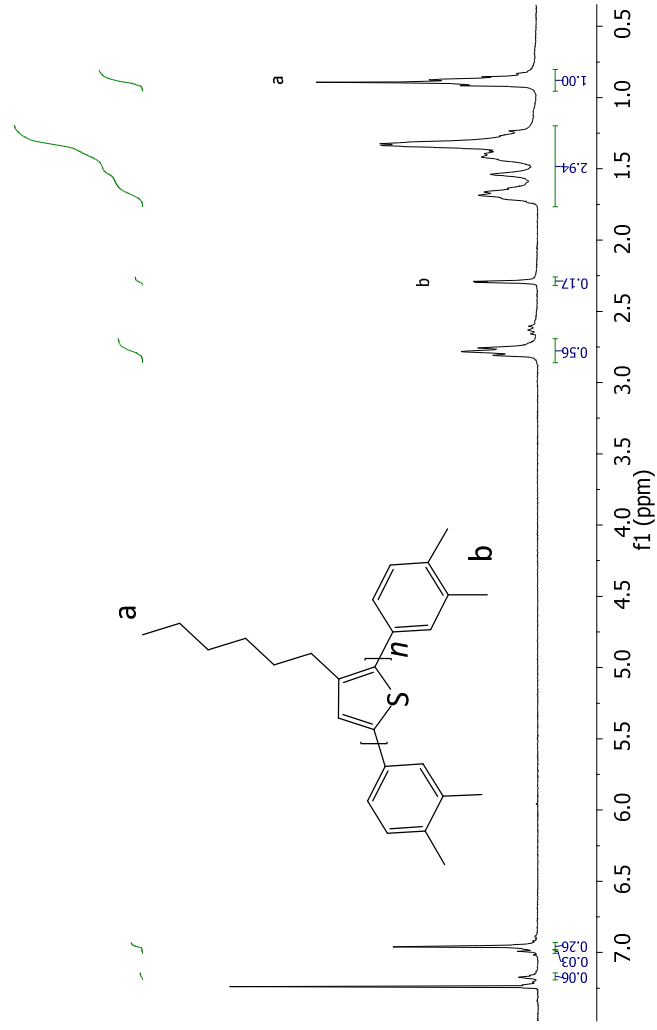


Figure S5.  $^1\text{H}$  NMR spectrum of P3HT-*b*-PE6TH 85/15 (P2-85/15).

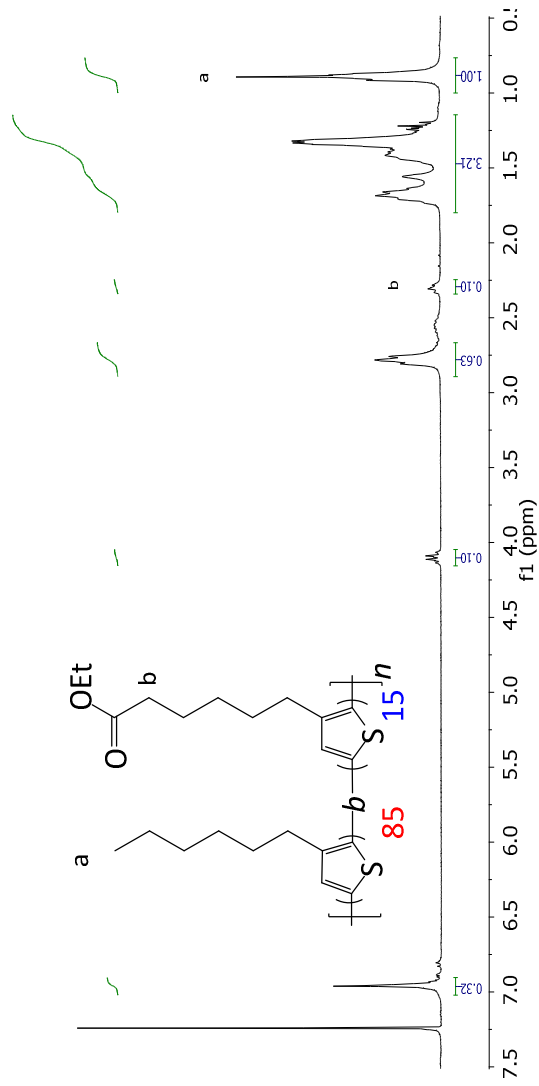


Figure S6.  $^1\text{H}$  NMR spectrum of P3HT-*b*-P6THA 85/15 (P1-85/15).

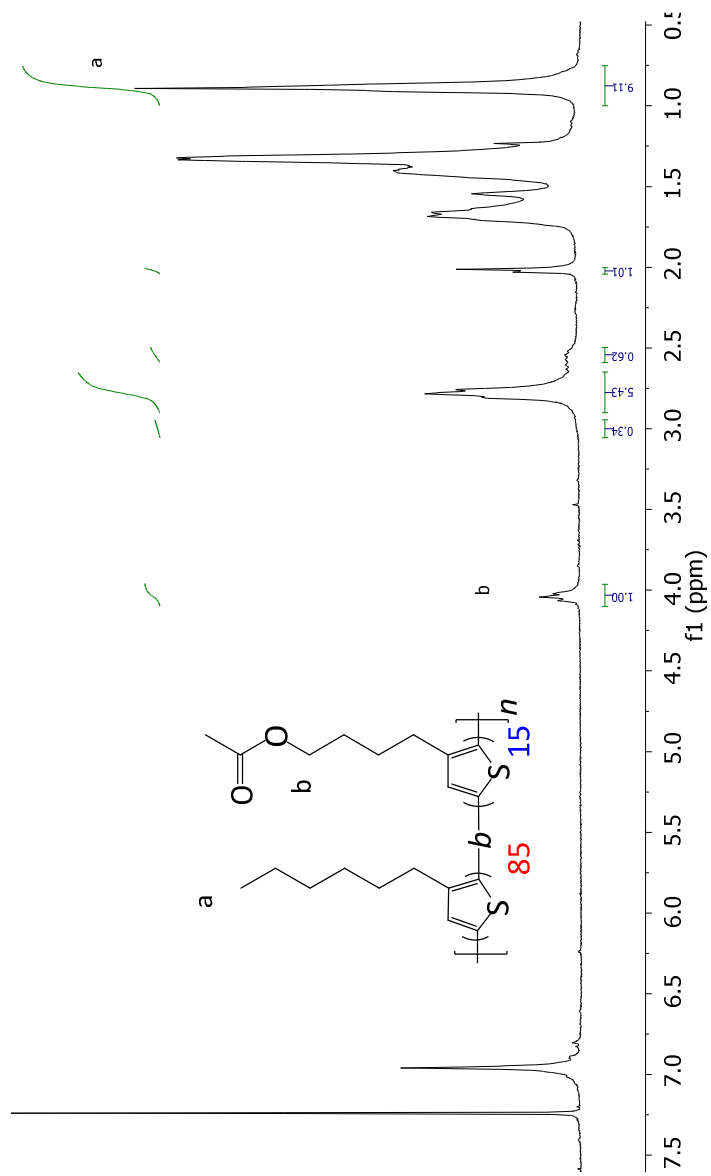
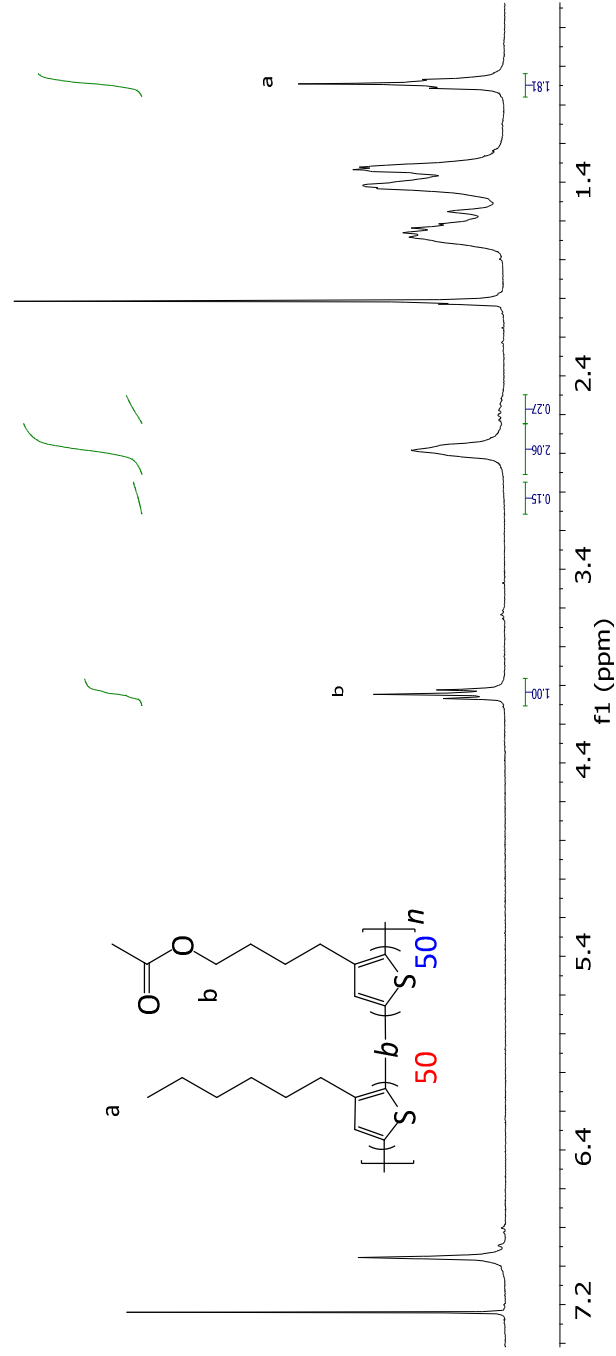


Figure S7.  $^1\text{H}$  NMR spectrum of P3HT-*b*-P6THA 50/50 (P1-50/50)





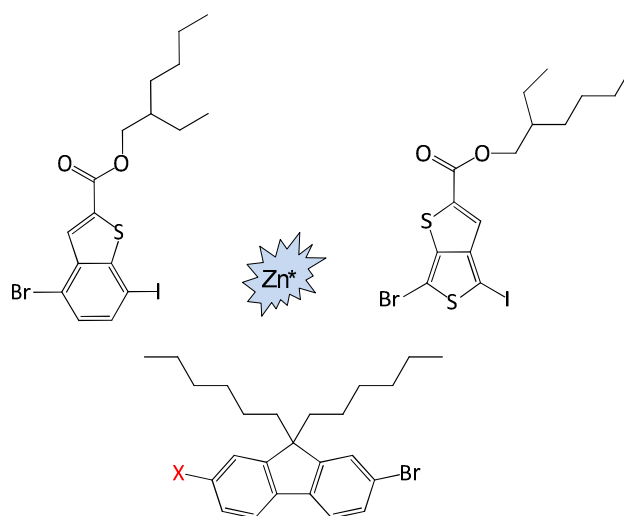


---

# Chapter 6

Applying the Rieke zinc method to the synthesis of alternative poly(hetero)arylenes

---



### 6.1. Introduction

Since the discovery of conductivity in conjugated polymer systems, they have increasingly been prepared and investigated for applications in organic electronics. Polythiophenes – with P3HT or poly(3-hexylthiophene) as the most famous representative – have been widely studied, notably in the field of organic photovoltaics.<sup>1,2</sup> A particular synthetic approach to prepare regioregular (RR) poly(3-alkylthiophenes) (P3ATs) was introduced by Rieke in 1992.<sup>3</sup> The ‘Rieke method’ uses highly reactive Rieke zinc metal powder (Zn\*), which undergoes regioselective oxidative addition to 2,5-dibromo-3-alkylthiophenes at cryogenic temperatures to afford the respective organozinc intermediates, which then polymerize in a regiospecific manner giving highly RR polymers.

According to our knowledge, this method was so far only successfully applied toward polythiophenes<sup>4,5</sup> and poly(cyclopentadithiophenes),<sup>6,7</sup> mostly due to the synthetic difficulties inherent to the Rieke zinc procedure. As a matter of fact, even standard polythiophene synthesis by the Rieke protocol has only been performed by a limited number of groups, despite the obvious benefits compared to more common Grignard metathesis (GRIM) protocols.

In general, the synthesis of polyarylenes is performed through metal-catalyzed polycondensation reactions, such as Yamamoto, Suzuki, or Stille cross-coupling reactions. Polymerization using any one of these methods often requires 2-3 days and high temperatures (> 100 °C). Employing the Rieke method can shorten the polymerization times and lower the reaction temperatures, facilitating the preparation of several (hetero)aryl-based conjugated polymers. Moreover, the Rieke protocol is compatible with a wide range of functional groups, diminishing the need for post-polymerization modifications. As we recently developed an efficient and more reliable



procedure for the preparation of Rieke zinc,<sup>8</sup> attempting to apply this protocol to some other polyarylenes is an evident next step.

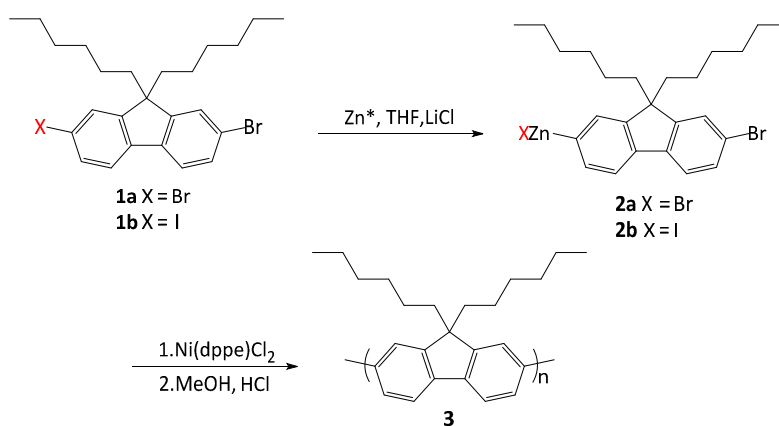
## 6.2. Results and discussion

### 6.2.1. Polyfluorenes

Polyfluorenes are intensively being studied, especially in the field of organic light-emitting diodes (OLEDs), due to their exceptional electro-optical properties.<sup>9,10,11</sup> For this reason, polymerization of two fluorene derivatives, 2,7-dibromo-9,9-dihexylfluorene (**1a**) and 2-bromo-7-iodo-9,9-dihexylfluorene (**1b**) (Scheme 1), was attempted using the optimized Rieke conditions. Oxidative addition of 1.2 equiv of Rieke zinc to 2,7-dibromo-9,9-dihexylfluorene was unsuccessful, even after 24 h. When LiCl was added to the mixture, organozinc formation did take place. This observation has also been done by Stefan *et al.* during formation of the organomagnesium intermediates of dibrominated fluorenes.<sup>12</sup> Moreover, Rieke and co-workers reported that addition of 10-20 % LiCl to Rieke zinc facilitated the preparation of pyridylzincbromide dramatically.<sup>13</sup> The conversion was studied by taking samples periodically from the supernatant and quenching them with saturated NH<sub>4</sub>Cl. GC-MS analysis of the aliquots showed that after 4 h reaction only 25% of the starting material had reacted and also ~0.5% of the bis(organozinc) was formed. Even after 16 h stirring at room temperature, only 45% of the starting material was converted into the required mono(organozinc) compound **2a**, while 2.8% bis(organozinc) was observed. From these observations it can be concluded that Rieke zinc is apparently not reactive enough toward dibrominated fluorene **1a** to allow fast and full conversion to the mono(organozinc) derivative. Polymerization was anyway

performed at 60 °C for 4 h in the presence of Ni(dppe)Cl<sub>2</sub> catalyst. The reaction mixture was precipitated in methanol and according to molecular weight analysis by size exclusion chromatography, polymer **3** had an  $M_n = 3.1$  kDa and  $M_w = 7.5$  kDa, which corresponds to ~10 monomer units only. Moreover, polymerization yield was very low (around 20%).

**Scheme 1** Synthesis of polyfluorenes via the Rieke method.



As a higher reactivity of the iodo derivative toward Rieke zinc can be expected, 2-bromo-7-iodo-9,9-dihexylfluorene (**1b**) was also employed as a substrate for the Rieke zinc synthesis (Scheme 1). As predicted, better conversion to the organozinc intermediates was achieved. Treatment of **1b** with 1.5 equiv Zn\* at reflux temperature for 3 h gave at least 90% conversion to mono(organozinc) compound **2b**, in a regioselective manner, with less than 1% of bis(organozinc) product. Polymerization of the formed organozinc derivative was performed at 60 °C for 3 h by addition of a catalytic amount of Ni(dppe)Cl<sub>2</sub> and polyfluorene **3** was obtained, again in a low yield (around 20%) though, with  $M_n = 4$  kDa and  $M_w = 9$  kDa. The most probable cause for the low yield and molecular weight is the non-settled zinc, which can further

react with the bromine atom leading to formation of the bis(organozinc) species, which hinders polymerization. From these initial trials it is clear that, although the Rieke zinc protocol can be applied for polyfluorenes, optimization is still required to enhance the molecular weight and the polymerization yield.

### 6.2.2. Thieno[3,4-*b*]thiophenes

Conjugated polymers containing thieno[3,4-*b*]thiophene units have recently received considerable attention because organic photovoltaic devices fabricated with these materials have reached top power conversion efficiencies over 7%.<sup>14</sup> Thieno[3,4-*b*]thiophene contains a thiophene ring fused with another thiophene moiety in a specific way, making it capable of stabilizing the quinoid form of the resulting polymer backbone, which leads to a lower band gap.<sup>15</sup> The first synthesis of unsubstituted thieno[3,4-*b*]thiophene was performed by Zwanenburg in 1967.<sup>16</sup> In 1990, another route was developed by Brandsma.<sup>17</sup> The polymers obtained from this monomer were insoluble in common organic solvents and polymerization was only performed electrochemically.<sup>15</sup> In 1994, Hawkins *et al.* reported a short and simple procedure for the preparation of ethyl thieno[3,4-*b*]thiophene-2-carboxylate in low yield (20%).<sup>18</sup> An improved method using a catalytic amount of CuO nanoparticles, which gave rise to an increase in the yield up to 85%, was reported by Lee and co-workers in 2010.<sup>19</sup> Coughlin *et al.* recently prepared soluble low band gap thieno[3,4-*b*]thiophene polymers with various alkyl side chains via Grignard methathesis (GRIM) and studied the photophysical properties of these materials.<sup>20</sup>

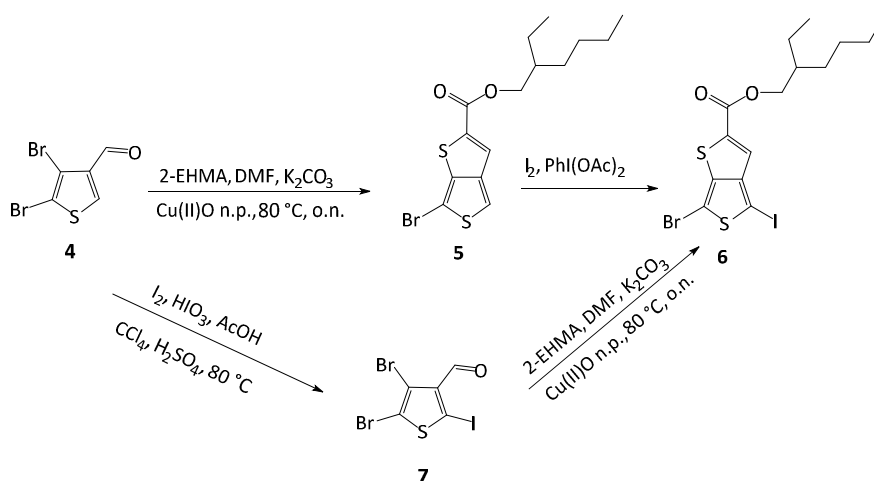
Our idea was to synthesize dibromo and bromo-iodo-thieno[3,4-*b*]thiophenes to investigate their reactivity toward Rieke zinc and, if possible, polymerize

---

these derivatives by the Rieke method. Dibrominated thieno[3,4-*b*]thiophene was prepared according to the procedure described by Baek *et al.*<sup>19a</sup> 2-Ethylhexyl-6-bromo-4-iodothieno[3,4-*b*]thiophene (**6**) was prepared for the first time (Scheme 2). The synthesis started with the preparation of 4,5-dibromothiophene-3-carbaldehyde (**4**). The synthesis of precursor **4** has extensively been studied by Gronowitz *et al.*<sup>21</sup> Throughout this work, halogenations of 3-formylthiophene in the presence of aluminum trichloride were investigated. Aluminum trichloride complexes with the formyl group, which renders the second carbon atom more deactivated, therefore first halogenating the fifth position. Afterwards, the second halogen rather goes to the fourth position rather than the deactivated second carbon atom. Depending on the amount of bromine used, an appreciable amount of tribrominated compound is formed as well, which is hard to remove from the product. 2-Ethylhexyl-6-bromothiopheno[3,4-*b*]thiophene-2-carboxylate (**5**) was then prepared via nucleophilic displacement of the bromine atom by 2-ethylhexyl mercaptoacetate (2-EHMA) and spontaneous intramolecular aldol condensation (Scheme 2).<sup>22</sup> Monobrominated thieno[3,4-*b*]thiophene **5** was found to be very unstable in air in the presence of light, as it oxidizes very fast. Even when kept in the fridge overnight, it completely decomposed and became insoluble. Monobrominated thieno[3,4-*b*]thiophene, as a mixture of 4-bromo and 6-bromo isomers, was also prepared by Carsten *et al.* by very slow addition of 1 equiv *N*-bromosuccinimide (NBS) to thieno[3,4-*b*]thiophene.<sup>23</sup> In this paper, the stability issue is not discussed. Due to the instability of monobrominated thieno[3,4-*b*]thiophene **5**, iodination was performed *in situ* with iodine and iodobenzene diacetate as iodination agents (Scheme 2). Unfortunately, the iodination was unsuccessful. In an alternative route, the iodination of 4,5-dibromo-3-thiophenecarbaldehyde (**4**) to yield

4,5-dibromo-2-iodothiophene-3-carbaldehyde (**7**) was performed first,<sup>24</sup> and reaction with 2-ethylhexyl mercaptoacetate afterwards. This attempt was, however, also unsuccessful.

**Scheme 2** Synthesis of thieno[3,4-*b*]thiophene-2-carboxylate **6**.



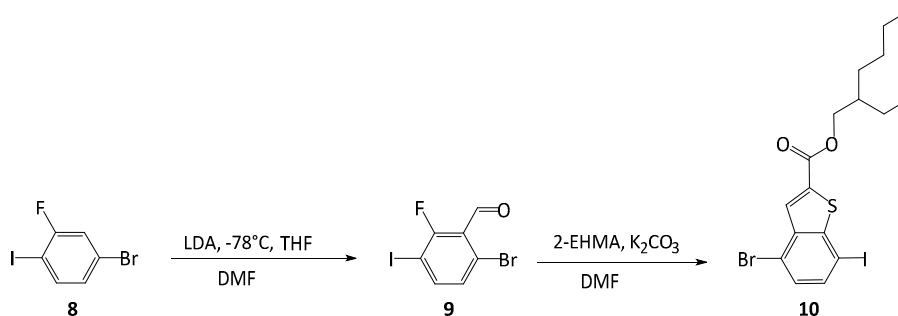
Dodecyl 4,6-dibromothiopheno[3,4-*b*]thiophene-2-carboxylate was reacted with Zn\*. Unfortunately, the formation of the organozinc intermediates was not regioselective, due to the similar reactivity of the bromine atoms at the 4- and 6-positions. Nickel catalyst (2% mol) was anyway added to the formed organozinc solution (full conversion was not achieved due to the non-selectivity of the zinc) and the mixture was stirred overnight at 60 °C. The resulting mixture was precipitated in methanol and filtered to give a black solid in 20% yield. UV-Vis spectra showed an absorption maximum around 800 nm, and according to SEC the number average molecular weight was around 5000 g/mol.

---

### 6.2.3. Benzo[*b*]thiophenes

One of the main pathways to obtain  $\pi$ -conjugated polymers with high conductivity is the preparation of low band gap polymers. A possible way to lower the band gap is the use of ring-fused thiophene units in the conjugated polymer backbone, which exhibit an extended  $\pi$ -conjugation and more rigid structure compared to regular thiophenes.<sup>25</sup> The first ring-fused thiophene-based polymer was synthesized by electrochemical polymerization of benzo[*c*]thiophene or isothianaphthene.<sup>26</sup> Studies on poly(benzo[*c*]thiophene) have demonstrated that fusion of the benzene ring to the thiophene ring stabilizes the quinoid character of the thiophene ring, lowering the band gap, due to the larger resonance energy of the benzene ring.<sup>25b</sup> Substituted poly(benzo[*c*]thiophenes) were also prepared. Nonetheless, these chemical modifications did not cause any remarkable changes in the band gap.<sup>27</sup>

For this study we intended to prepare substituted poly(benzo[*b*]thiophene)s, another class of benzothiophenes, starting from 2-ethylhexyl 7-bromo-4-iodobenzo[*b*]thiophene (**10**) (Scheme 3) employing the Rieke polymerization protocol. Monomer **10** was prepared by a simple two-step procedure.<sup>28</sup> In the first step, regioselective lithiation of 4-bromo-2-fluoro-1-iodobenzene (**8**) using lithium diisopropylamide (LDA), followed by formylation with dimethylformamide (DMF), lead to formation of 6-bromo-2-fluoro-3-iodobenzaldehyde (**9**).<sup>29</sup>

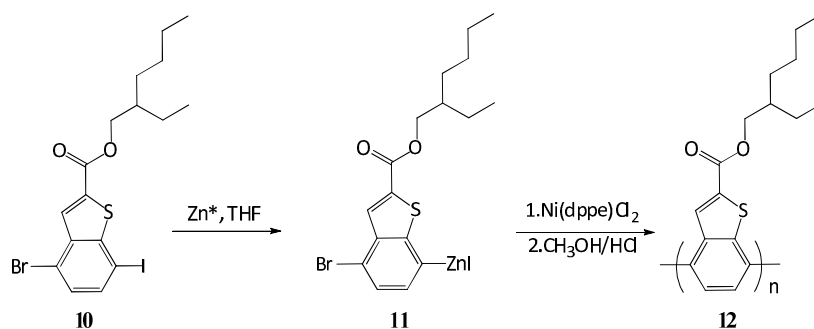
**Scheme 3** Synthesis of alkyl benzo[*b*]thiophene-2-carboxylate **10**.

The second step involves treatment of **9** with 2-EHMA to obtain 2-ethylhexyl 7-bromo-4-iodobenzo[*b*]thiophene (**10**). Based on the rate of the nucleophilic displacement ( $F > NO_2 > Cl > Br$ ) and the activating effect of the carboxaldehyde function, the substitution was accomplished under mild conditions.<sup>22</sup>

It was then attempted to synthesize poly(2-ethylhexyl benzo[*b*]thiophene-2-carboxylate) (**12**) via the Rieke method (Scheme 4). First, 2-ethylhexyl 7-bromo-4-iodobenzo[*b*]thiophene (**10**) was treated with 1.0 equiv of Rieke zinc in THF. Oxidative addition of the Zn\* to the carbon-iodine bond took place at room temperature within less than 10 min to form the organozinc intermediate **11** in a regioselective manner. The regioselectivity was determined by quenching an aliquot of **11** with saturated ammonium chloride and was found to be >99% based on GC-MS analysis. The polymerization was then accomplished by addition of a catalytic amount of Ni(dppe)Cl<sub>2</sub> catalyst. Unfortunately, the polymerization did not occur, as GPC analysis of the quenched mixture revealed that there was only formation of dimers and trimers, and many unreacted monomer was still present. This could be related to the high stability of the formed nickel complex, which will prevent the

release of nickel during the transmetalation step during the course of the polymerization.<sup>30</sup> Therefore, to be able to perform this polymerization, the kinetics of the reaction have to be studied more profoundly.

**Scheme 4** Synthesis of poly(2-ethylhexyl benzo[*b*]thiophene-2-carboxylate) **12** via the Rieke method.



### 6.3. Conclusions

In conclusion, different (hetero)aromatic dibromo and/or bromo-iodo compounds were polymerized through the Rieke polymerization protocol. Oxidative addition of the Rieke zinc to the carbon-halogen bond to form the organozinc intermediates, which is the key step of the Rieke method, could successfully be performed in most cases, sometimes by addition of a catalytic amount of LiCl salt. However, the polymers were not obtained in high yields nor high molecular weights, as in the case of poly(3-hexylthiophene). Accordingly, the Rieke method has to be further fine-tuned for every specific case to be applicable toward alternative poly(hetero)arylenes and copolymers of these heteroatoms and thiophenes.



#### 6.4. Experimental part

All manipulations were carried out with the aid of a dual manifold vacuum/Ar system. Lithium (Acros, 99+%) was stored in a schlenk tube under Ar. Lithium, naphthalene and benzothiophene (Sigma-Aldrich, 98%) were weighed in air as needed and transferred to the schlenk tube under a stream of Ar. Naphthalene was stored in a separate dessiccator together with benzothiophene over P<sub>2</sub>O<sub>5</sub>. Zinc chloride (Acros, analysis grade 98.5%) was transferred into small vials in the glove box and stored in a dessiccator over P<sub>2</sub>O<sub>5</sub>. Zinc chloride was dried by treating it with thionyl chloride and heating with a Bunsen burner, and subsequently removed under a stream of Ar. THF was freshly distilled from Na/benzophenone under a N<sub>2</sub> atmosphere at atmospheric pressure prior to use. Brass cannulas were stored in an oven at 110 °C and cleaned immediately after use with acetic acid (in the case of Zn\* remnant), acetone (to clean non-polymeric residues), or hot chloroform and/or chlorobenzene (for polymer-based contaminations). Rieke zinc formation and polymerization was achieved according to our recently published method.<sup>8</sup> 2,7-Dibromo-9,9-dihexylfluorene and 2-bromo-7-iodo-9,9-dihexylfluorene were prepared following literature procedures.<sup>31</sup> 4,5-Dibromo-3-formylthiophene was prepared according to the Gronowitz procedure.<sup>21</sup>

#### 4,5-Dibromo-2-iodothiophene-3-carbaldehyde (7)

4,5-Dibromothiophene-3-carbaldehyde (1.0 g, 3.70 mmol), iodine (0.432 g, 1.70 mmol), carbon tetrachloride (5 mL), iodic acid (0.14 g, 0.8 mmol), deionized water (3.75 mL), acetic acid (10 mL) and H<sub>2</sub>SO<sub>4</sub> (0.15 mL) were stirred at 80 °C for 2h. Afterwards, the reaction mixture was poured into a NaHSO<sub>3</sub> solution to neutralize the excess of iodine. The solution was then

extracted with chloroform and the combined organic layers were washed with saturated  $\text{NaHCO}_3$ , dried over anhydrous  $\text{MgSO}_4$  and filtered. Removal of the solvent under reduced pressure afforded a yellowish solid. The crude product was purified by column chromatography (silica) using a solvent mixture of hexanes and ethyl acetate (95:5) to afford pure **7** as yellowish crystals (0.58 g, 1.48 mmol, 40%).  $^1\text{H}$  NMR (300 MHz,  $\text{CDCl}_3$ ):  $\delta$  9.70 (s, 1H);  $^{13}\text{C}$  NMR (300 MHz,  $\text{CDCl}_3$ ):  $\delta$  184.9 (CHO), 135.4, 117.4, 114.3, 84.8; GC-MS:  $m/z$  393.72 (>99%).

#### **2-Ethylhexyl 6-bromothieno[3,4-*b*]thiophene-2-carboxylate (5)**

2-Ethylhexyl thieno[3,4-*b*]thiophene-2-carboxylate was prepared by refluxing copper(II)oxide nanoparticles (0.29 g, 0.55 mmol), potassium carbonate (3.84 g, 27.8 mmol), 4,5-dibromothiophene-3-carbaldehyde (5.0 g, 18.5 mmol) and 2-EHMA (4.16 g, 20.4 mmol) in dry DMF at 80 °C overnight. The mixture was then extracted with  $\text{Et}_2\text{O}$ , washed with water, dried over  $\text{MgSO}_4$ , filtered and evaporated to dryness. The crude product was purified by column chromatography (silica) using a solvent mixture hexanes/dichloromethane (80/20) and a pale yellow oil was obtained. Due to product instability, only half of the product was recovered (2.1 g, 5.59 mmol, 30%). The reaction was done again over the weekend and right after work-up the whole product already degraded, confirming the instability of the monobrominated thieno[3,4-*b*]thiophene.  $^1\text{H}$  NMR (300 MHz,  $\text{CDCl}_3$ ):  $\delta$  7.64 (s, 1H), 7.50 (s, 1H), 4.22 (dd, 2H), 1.78–1.58 (m, 2H), 1.49–1.22 (m, 8H), 0.91 (t, 6H); GC-MS:  $m/z$  374.0 ( $\geq$  97%).

#### **6-Bromo-2-fluoro-3-iodobenzaldehyde (9)**

To 1-bromo-3-fluoro-4-iodobenzene (**8**) (15.0 g, 49.9 mmol), dissolved in dry THF (200 mL), lithium diisopropylamide (28.3 mL, 54.83 mmol) was added slowly at  $-78$  °C over 30 min. After complete addition, the mixture was left to stir for another 30 min at the same temperature. Then DMF (4.0 mL, 52.0

---

mmol) was added dropwise while maintaining the temperature at  $-78\text{ }^{\circ}\text{C}$ . The resulting solution was stirred for another 15 min and then quenched with diluted sulfuric acid. The organic and water phase were separated and the water phase was extracted with diethyl ether and dried over  $\text{Na}_2\text{SO}_4$ . The solvent was discarded at the rotary evaporator to leave the crude product as a yellow-brown solid. Recrystallization from cyclohexane afforded flaky brown crystals (15.14 g, 46.03 mmol, 92%). mp:  $129.5\text{--}131.2\text{ }^{\circ}\text{C}$ ;  $^1\text{H}$  NMR (400 MHz,  $\text{CDCl}_3$ ): $\delta$  10.25 (s, 1H), 7.77 (dd, 1H), 7.26 (dd, 2H);  $^{13}\text{C}$  NMR (75 MHz,  $\text{CDCl}_3$ ): $\delta$  188.2, 164.3, 160.8, 144.7, 132.0, 125.9, 123.7, 82.8, 82.4; GC-MS:  $m/z$  327.84 ( $\geq 99\%$ ).

#### **2-Ethylhexyl 7-bromo-4-iodobenzo[*b*]thiophene-2-carboxylate (10)**

6-Bromo-2-fluoro-3-iodobenzaldehyde (**9**) (13.0 g, 39.5 mmol) and potassium carbonate (8.19 g, 59.3 mmol) were mixed in DMF (20 mL). To this mixture, 2-ethylhexyl mercaptoacetate (8.88 g, 43.5 mmol) was added via a syringe in one shot at rt. The mixture was stirred overnight and then poured into water. The organic material was extracted with diethyl ether, dried over magnesium sulfate and removal of the solvent yielded a very viscous yellow oil. The crude product was purified by column chromatography (silica) using pure hexanes as the eluent, affording a very viscous yellow oil (18.0 g, 36.3 mmol, 92%).  $^1\text{H}$  NMR (300 MHz,  $\text{CDCl}_3$ ): $\delta$  8.36 (s, 1H), 7.60 (d, 1H), 7.29 (d, 1H), 4.27 (d, 2H), 1.73 (dt, 1H), 1.51–1.27 (m, 9H), 0.94 (t, 3H);  $^{13}\text{C}$  NMR (75 MHz,  $\text{CDCl}_3$ ): $\delta$  161.8, 148.6, 137.6, 136.3, 134.3, 131.0, 128.9, 119.1, 85.5, 68.0, 38.4, 30.1, 28.6, 23.5, 22.6, 13.7, 10.7; GC-MS:  $m/z$  493.94 ( $\geq 99\%$ ).

### 6.5. References

1. Dang, M. T.; Hirsch, L.; Wantz, G. *Advanced Materials* **2011**, *23* (31), 3597-3602.
2. Marrocchi, A.; Lanari, D.; Facchetti, A.; Vaccaro, L. *Energy & Environmental Science* **2012**, *5*, 8457-8474.
3. Chen, T. A.; Rieke, R. D. *Journal of the American Chemical Society* **1992**, *114* (25), 10087-10088.
4. Chen, T. A.; O'Brien, R. A.; Rieke, R. D. *Macromolecules* **1993**, *26* (13), 3462-3463.
5. Chen, T.-A.; Wu, X.; Rieke, R. D. *Journal of the American Chemical Society* **1995**, *117* (1), 233-244.
6. Coppo, P.; Cupertino, D. C.; Yeates, S. G.; Turner, M. L. *Macromolecules* **2003**, *36* (8), 2705-2711.
7. Coppo, P.; Adams, H.; Cupertino, D. C.; Yeates, S. G.; Turner, M. L. *Chemical Communications* **2003**, (20), 2548-2549.
8. Kudret, S.; D'Haen, J.; Oosterbaan, W., Lutsen, L.; Vanderzande, D.; Maes, W. *Advanced Synthesis & Catalysis* **2013**, *355* (2-3), 569-575.
9. Ranger, M.; Rondeau, D.; Leclerc, M. *Macromolecules* **1997**, *30* (25), 7686-7691.
10. Scherf, U.; List, E. J. W. *Advanced Materials* **2002**, *14* (7), 477-487.
11. Liedtke, A.; O'Neill, M.; Wertmüller, A.; Kitney, S. P.; Kelly, S. M. *Chemistry of Materials* **2008**, *20* (11), 3579-3586.
12. Stefan, M. C.; Javier, A. E.; Osaka, I.; McCullough, R. D. *Macromolecules* **2008**, *42* (1), 30-32.
13. Kim, S.-H.; Rieke, R. D. *Molecules* **2010**, *15* (11), 8006-8038.
14. Liang, Y.; Xu, Z.; Xia, J.; Tsai, S.-T.; Wu, Y.; Li, G.; Ray, C.; Yu, L. *Advanced Materials* **2010**, *22* (20), E135-E138.

15. Lee, K.; Sotzing, G. A. *Macromolecules* **2001**, *34* (17), 5746-5747.
16. Wynberg, H.; Zwanenburg, D. J. *Tetrahedron Letters* **1967**, *8* (9), 761-764.
17. Brandsma, L.; Verkruijsse, H. *Synthetic Communications* **1990**, *20* (15), 2275-2277.
18. Hawkins, D. W.; Iddon, B.; Longthorne, D. S.; Rosyk, P. J. *Journal of the Chemical Society, Perkin Transactions 1* **1994**, (19), 2735-2743.
19. (a) Baek, M.-J.; Lee, S.-H.; Zong, K.; Lee, Y.-S. *Synthetic Metals* **2010**, *160* (11–12), 1197-1203; (b) Park, J. H.; Seo, Y. G.; Yoon, D. H.; Lee, Y.-S.; Lee, S.-H.; Pyo, M.; Zong, K. *European Polymer Journal* **2010**, *46* (8), 1790-1795.
20. Bae, W. J.; Scilla, C.; Duzhko, V. V.; Ho Jo, W.; Coughlin, E. B. *Journal of Polymer Science Part A: Polymer Chemistry* **2011**, *49* (15), 3260-3271.
21. Gronowitz, S.; Ander, I. *Tetrahedron* **1976**, *32* (12), 1403-1406.
22. Beck, J. R. *The Journal of Organic Chemistry* **1972**, *37* (21), 3224-3226.
23. Carsten, B.; Szarko, J. M.; Son, H. J.; Wang, W.; Lu, L.; He, F.; Rolczynski, B. S.; Lou, S. J.; Chen, L. X.; Yu, L. *Journal of the American Chemical Society* **2011**, *133* (50), 20468-20475.
24. Wu, L.-H.; Chu, C.-S.; Janarthanan, N.; Hsu, C.-S. *Journal of Polymer Research* **2000**, *7* (2), 125-134.
25. (a) Roncali, J. *Chemical Reviews* **1997**, *97* (1), 173-206; (b) Kertesz, M.; Choi, C. H.; Yang, S. *Chemical Reviews* **2005**, *105* (10), 3448-3481.
26. Wudl, F.; Kobayashi, M.; Heeger, A. J. *The Journal of Organic Chemistry* **1984**, *49* (18), 3382-3384.
27. (a) van Asselt, R.; Hoogmartens, I.; Vanderzande, D.; Gelan, J.; Froehling, P. E.; Aussems, M.; Aagaard, O.; Schellekens, R. *Synthetic Metals*

## Chapter 6

---

**1995**, 74 (1), 65-70; (b) Paulussen, H.; Vanderzande, D.; Gelan, J. *Synthetic Metals* **1997**, 84 (1-3), 415-416.

28. (a) Bridges, A. J.; Lee, A.; Maduakor, E. C.; Schwartz, C. E. *Tetrahedron Letters* **1992**, 33 (49), 7499-7502; (b) J. Bridges, A.; Lee, A.; Maduakor, E. C.; Schwartz, C. E. *Tetrahedron Letters* **1992**, 33 (49), 7495-7498.

29. Luliński, S.; Serwatowski, J. *The Journal of Organic Chemistry* **2003**, 68 (13), 5384-5387.

30. Yamamoto, T.; Morita, A.; Miyazaki, Y.; Maruyama, T.; Wakayama, H.; Zhou, Z. H.; Nakamura, Y.; Kanbara, T.; Sasaki, S.; Kubota, K. *Macromolecules* **1992**, 25 (4), 1214-1223.

31. Peterson, J. J.; Werre, M.; Simon, Y. C.; Coughlin, E. B.; Carter, K. R. *Macromolecules* **2009**, 42 (22), 8594-8598.

### General conclusions

This dissertation has investigated side chain functionalized random and block copolythiophenes synthesized through an optimized Rieke polymerization protocol, which uses highly reactive Rieke zinc ( $Zn^*$ ) for the preparation of the organozinc intermediates. The major goal was to optimize the synthetic procedure for the active Rieke zinc metal and later on to employ this protocol for the synthesis of small molecules and polymers, more in particular functionalized thiophene building blocks and poly(3-alkylthiophenes).

Rieke zinc is generally prepared by the reduction of zinc chloride with lithium employing a stoichiometric amount of naphthalene. We have found out that the 'quality' of the resulting zinc metal particles is strongly dependent upon the naphthalene source. When we started to perform the preparation of Rieke zinc with a new source of naphthalene, the *in situ* formed zinc particles agglomerated to chunky metal clusters, unlike upon application of the 'old' naphthalene source, which gave Rieke zinc as a finely distributed black slurry. Based on these findings, it was postulated that the old naphthalene batch had to contain something that helps to stabilize the zinc particles. ICP-MS analysis of the naphthalene samples and the Rieke zinc powder showed that sulfur was present in both naphthalene sources. Furthermore, HPLC-FLD analysis was conducted, indicating that both samples contained the same contaminant with a signal around 230 nm. However, the amount of the contaminant was found to be nine times higher in the old naphthalene. In addition, GC-MS analysis performed on different naphthalene batches revealed that the main contaminant has a molar mass of 134 g/mol, in accordance with the spectrum of benzothiophene under the same circumstances. Apparently, the old naphthalene was contaminated with benzothiophene to a larger extent, which

## General conclusions

---

has tremendous implications on the stabilization of the Rieke zinc in THF solution. It was also found that the amount of benzothiophene is very important, with an optimum of 3 mol% (with respect to zinc chloride), to prevent coagulation of the zinc particles, as confirmed by SEM-EDX analysis of the Rieke metal powder. Therefore, from that moment on, Rieke zinc was readily prepared from zinc chloride by adding 3 mol% of benzothiophene into the lithium naphthalenide solution.

Employing the Rieke zinc obtained with this enhanced procedure, several regioregular copolythiophenes were synthesized. First of all, a series of ester functionalized random copolythiophenes was prepared and the appended ester moieties were subsequently converted into different functions by postpolymerization reactions. The polymers were fully characterized and applied in bulk heterojunction organic solar cell devices as donor materials (in polymer:PC<sub>61</sub>BM active layer blends). Accelerated lifetime measurements showed that, although side chain functionalization might lead to a small decrease (if any) in the initial power conversion efficiency, the lifetimes of the photovoltaic devices were considerably prolonged due to the enhanced thermal stability of the active layer blends.

The optimized Rieke zinc protocol was also applied to prepare ester functionalized dibromothiophene monomers with different alkyl side chain lengths from commercially available 3-bromothiophene and  $\alpha,\omega$ -diols in a straightforward way. Regioregular poly{[3-hexylthiophene]-co-[3-( $\omega$ -acetoxylalkyl)thiophene]} polymers were prepared from these monomers and they were applied as donor materials in bulk heterojunction solar cells. The side chain length seems to have a minor effect on the efficiencies of the photovoltaic devices, which have to be evaluated further on in reliability tests.



We have also synthesized block copolythiophenes by sequential addition of two organozinc monomers. The formation of diblock structures was confirmed by SEC, NMR and DSC analysis. Further optimization is still needed to obtain higher molar mass polymers.

Finally, it was also tried to extend the applicability of the Rieke protocol to different (hetero)aromatic units apart from thiophenes. Accordingly, dibromo and/or bromo-iodo compounds were polymerized through the Rieke method. It was seen that in some cases addition of LiCl was required for complete oxidative addition of Rieke zinc to the carbon-halogen bond. However, this protocol has to be studied in more detail to allow smooth synthesis of (hetero)arylenes, since so far only polymers with low molar masses could be obtained in low yields.

The findings from this study add several (important) contributions to the current literature. First, the optimized procedure enables the preparation of Rieke zinc in a convenient and reproducible manner in large quantities without significant batch to batch variations. Secondly, we believe that this new procedure will definitely increase the application of Rieke zinc in both general organozinc chemistry and functionalized conjugated polymer synthesis as organozinc reagents show excellent chemoselectivity and good functional group tolerance and stability compared to the more reactive Grignard reagents.

Finally, the most important limitation so far lies in the fact that the Rieke procedure has only been proven its effectiveness toward polythiophene-based (co)polymers. Therefore, further experimental investigations are needed to be able to extend the versatility of the method to other

## General conclusions

---

(hetero)arylenes. A reasonable approach to tackle this issue would be to study the kinetics of the coupling reaction for different catalyst/ligand variations.

---

**List of publications**

- Role of structural order on optical properties, film morphology and hole transport of Poly(3-hexylthiophene) (P3HT) and P3HT/PbS blends": Firdaus, Y.; Kudret, S.; Khetubol, A.; Maes, W.; Lutsen, L.; Li, B.; Frederickx, W.; Flamee, S.; Vanderlinden, W.; Hens, Z.; De Feyter, S.; Vanderzande, D.; Van der Auweraer, M., manuscript in progress.
- Synthesis of ester Side-chain functionalized block copolythiophenes via the Rieke method: Kudret, S.; Van den Brande, N.; Defour, M.; Van Mele, B.; Lutsen, L.; Vanderzande, D.; Maes, W. to be submitted.
- Facile synthesis of 3-( $\omega$ -acetoxyalkyl)thiophenes and derived copolythiophenes using Rieke zinc: Kudret, S.; Kesters, J.; Janssen, S.; Van den Brande, N.; Defour, M.; Van Mele, B.; Manca, J.; Lutsen, L.; Vanderzande, D.; Maes, W. to be submitted.
- Enhanced intrinsic stability of bulk heterojunction polymer solar cells by varying the side chain pattern of the polythiophene donor polymer: Kesters, J.; Kudret, S.; Bertho, S.; Van den Brande, N.; Defour, M.; Van Mele, B.; Lutsen, L.; Manca, J.; Vanderzande, D.; Maes, W. to be submitted.
- An efficient and reliable procedure for the preparation of highly reactive Rieke zinc (Zn\*): Kudret, S.; D'haen, J.; Oosterbaan, W.; Lutsen, L.; Vanderzande, D.; Maes, W. *Adv. Synth. Catal.* **2013**, 355 (2-3), 569-575.

## List of publications

---

- TOF-SIMS investigation of degradation pathways occurring in a variety of organic photovoltaic devices - the ISOS-3 inter-laboratory collaboration: Andreasen, B.; Tanenbaum, D. M.; Hermenau, M.; Voroshazi, E.; Lloyd, M. T.; Galagan, Y.; Zimmermann, B.; Kudret, S.; Maes, W.; Lutsen, L.; Vanderzande, D.; Wurfel, U.; Andriessen, R.; Rösch, R.; Hoppe, H.; Teran-Escobar, G.; Lira-Cantu, M.; Rivaton, A.; Uzunoglu, G. Y.; Germack, D. S.; Hosel, M.; Dam, H. F.; Jorgensen, M.; Gevorgyan, S. A.; Madsen, M. V.; Bundgaard, E.; Krebs, F. C.; Norrman, K. *Phys. Chem. Chem. Phys.* **2012**, *14* (33), 11780-11799.

- On the stability of a variety of organic photovoltaic devices by IPCE and in situ IPCE analyses - the ISOS-3 inter-laboratory collaboration: Teran-Escobar, G.; Tanenbaum, D. M.; Voroshazi, E.; Hermenau, M.; Norrman, K.; Lloyd, M. T.; Galagan, Y.; Zimmermann, B.; Hosel, M.; Dam, H. F.; Jorgensen, M.; Gevorgyan, S.; Kudret, S.; Maes, W.; Lutsen, L.; Vanderzande, D.; Wurfel, U.; Andriessen, R.; Rösch, R.; Hoppe, H.; Rivaton, A.; Uzunoglu, G. Y.; Germack, D.; Andreasen, B.; Madsen, M. V.; Bundgaard, E.; Krebs, F. C.; Lira-Cantu, M. *Phys. Chem. Chem. Phys.* **2012**, *14* (33), 11824-11845.

- Investigation of the degradation mechanisms of a variety of organic photovoltaic devices by combination of imaging techniques-the ISOS-3 inter-laboratory collaboration: Rösch, R.; Tanenbaum, D. M.; Jorgensen, M.; Seeland, M.; Barenklau, M.; Hermenau, M.; Voroshazi, E.; Lloyd, M. T.; Galagan, Y.; Zimmermann, B.; Wurfel, U.; Hosel, M.; Dam, H. F.; Gevorgyan, S. A.; Kudret, S.; Maes, W.; Lutsen, L.; Vanderzande, D.; Andriessen, R.; Teran-Escobar, G.; Lira-Cantu, M.; Rivaton, A.; Uzunoglu, G. Y.; Germack, D.; Andreasen, B.; Madsen, M. V.; Norrman, K.; Hoppe, H.; Krebs, F. C. *Energy Environ. Sci.* **2012**, 5 (4), 6521-6540
  
- The ISOS-3 inter-laboratory collaboration focused on the stability of a variety of organic photovoltaic devices: Tanenbaum, D. M.; Hermenau, M.; Voroshazi, E.; Lloyd, M. T.; Galagan, Y.; Zimmermann, B.; Hosel, M.; Dam, H. F.; Jorgensen, M.; Gevorgyan, S. A.; Kudret, S.; Maes, W.; Lutsen, L.; Vanderzande, D.; Wurfel, U.; Andriessen, R.; Rösch, R.; Hoppe, H.; Teran-Escobar, G.; Lira-Cantu, M.; Rivaton, A.; Uzunoglu, G. Y.; Germack, D.; Andreasen, B.; Madsen, M. V.; Norrman, K.; Krebs, F. C. *RSC Adv.* **2012**, 2 (3), 882-893.

**Acknowledgements**

First of all, I would like to express my gratitude to Prof. Wouter Maes for being my promoter and his friendly advising during my dissertation work.

I am also grateful to Prof. Dirk Vanderzande and Dr. Laurence Lutsen for giving me the opportunity to carry out a PhD at UHasselt.

I would also like to thank Prof. Laurence Vignau, Prof. Bruno Van Mele, Prof. Peter Adriaensens, and Prof. Thomas Junkers for accepting to be part of the jury and reading my thesis.

Finally, I would like to thank the members of Organic & Bio-(Polymer) chemistry group for the nice atmosphere to work together.



